Hijacking *Pseudomonas aeruginosa* active transporters across the outer membrane: Challenges and opportunities for drug transport

Inauguraldissertation

zur

Erlangung der Würde eines Doktors der Philosophie

vorgelegt der

Philosophisch-Naturwissenschaftlichen Fakultät

der Universität Basel

von

Pamela Saint Auguste

aus Frankreich

Basel, 2019

Genehmigt von der Philosophisch-Naturwissenschaftlichen Fakultät auf Antrag von

Prof. Dr. Dirk Bumann

Prof. Dr. Urs Jenal

Basel, den 18.04.2017

Prof. Dr. Martin Spiess
Dekan der Philosophisch- Naturwissenschatlichen Fakultät

Biology is the only science where multiplication and division mean the same thing.
Anonymous

Pamela Saint Auguste
Hijacking Pseudomonas aeruginosa active transporters across the outer membrane: Challenges and opportunities for drug transport
Thesis, 2019
Supervisor: Prof. Dr. Dirk Bumann
PhD Committee members: Prof. Dr. Urs Jenal, Dr. Thilo Köhler

Basel Universität
Bumann group
Focal Area Infection Biology
Biozentrum
Klingerbergstrasse 50/70
4056 Basel

Abstract

Antimicrobial resistance is a serious public health threat worldwide. The emergence of multi-drug resistance bacteria challenges the development of novel antibiotics. *Pseudomonas aeruginosa* (*P. aeruginosa*) is an Gram-negative opportunistic pathogen that infects burn, wound and cystic fibrosis (CF) patients. *P. aeruginosa* is intrinsically resistant to many antibiotics, and further acquired resistance limits treatment options. The high level of resistance to antibiotics arises mainly from the tight control of *P. aeruginosa* over influx and efflux of molecules across its outer membrane. *P. aeruginosa* outer membrane includes a large number of different types of porins and efflux pumps that enable nutrient acquisition and antibiotic resistance.

Among them, *P. aeruginosa* UCBPP-PA14 encodes 35 TonB-dependent transporters (TBDTs), which are defined as high-affinity active transporters and permit the transport of siderophores, heme, heavy metals and carbohydrates. Several studies showed high levels of TBDTs expression under iron deprivation and their importance for *P. aeruginosa* growth *in vivo*, but, except for the high-affinity siderophores and heme transporters, few have determined the contribution of single TBDT *in vivo*. In a Trojan horse approach, mimetics of essential substrates complexed to drugs, including siderophore-antibiotics conjugates and non-iron metalloporphyrins, are employed to induce the expression of associated TBDT(s) and to increase the antibiotic transport through TBDTs, hijacking the bacterial transport machinery. In spite of promising antibacterial activity *in vitro*, *P. aeruginosa* was able to rapidly develop resistance against the Trojan horse conjugates by facile inactivation of the TBDT involved in their transport. To circumvent this resistance mechanism, basic research on the processes associated with *P. aeruginosa* transport capabilities and substrate specificities *in vivo* is seriously needed to guide rational development of novel and effective therapeutics.

In order to prevent facile inactivation of TBDT, we aim at identifying essential *P. aeruginosa* TBDTs that contribute to the bacterial fitness *in vivo*. We addressed this aim (i) by quantifying the abundance of TBDTs *in vitro*, in preclinical and human patients samples and (ii) by evaluating the relevance of TBDTs *in vivo*. We thus developed an ultra-sensitive targeted proteomic approach to determine absolutely the abundance of TBDTs *in vitro* and in various hosts. Proteomic analyses revealed a clear disctinction between

TBDTs expression *in vitro* and *in vivo*, suggesting that there is a urgent need for suitable *in vitro* medium that more faithfully reflects the *in vivo* reality. Expression data also highlighted a subset of TBDTs, including endogenous siderophore, heme, non-iron metal and some xenosiderophore transporters, that was highly abundant among the different *in vivo* conditions. Based on these data, we generated different mutants of the abundant TBDTs and evaluated them in competitive fitness assays *in vivo*. Overall, these data suggested that *P. aeruginosa* primarily used its high-affinity siderophore pyoverdine for iron scavenging, whereas uptake capabilities for its other endogenous siderophores, xenosiderophores, heme-associated substrates and possibly copper and zinc uptake were all dispensable for *in vivo* fitness in an intranasal model. In conclusion, implications of these results in the development of future compounds implementing the Trojan horse approach were discussed.

Graphical abstract

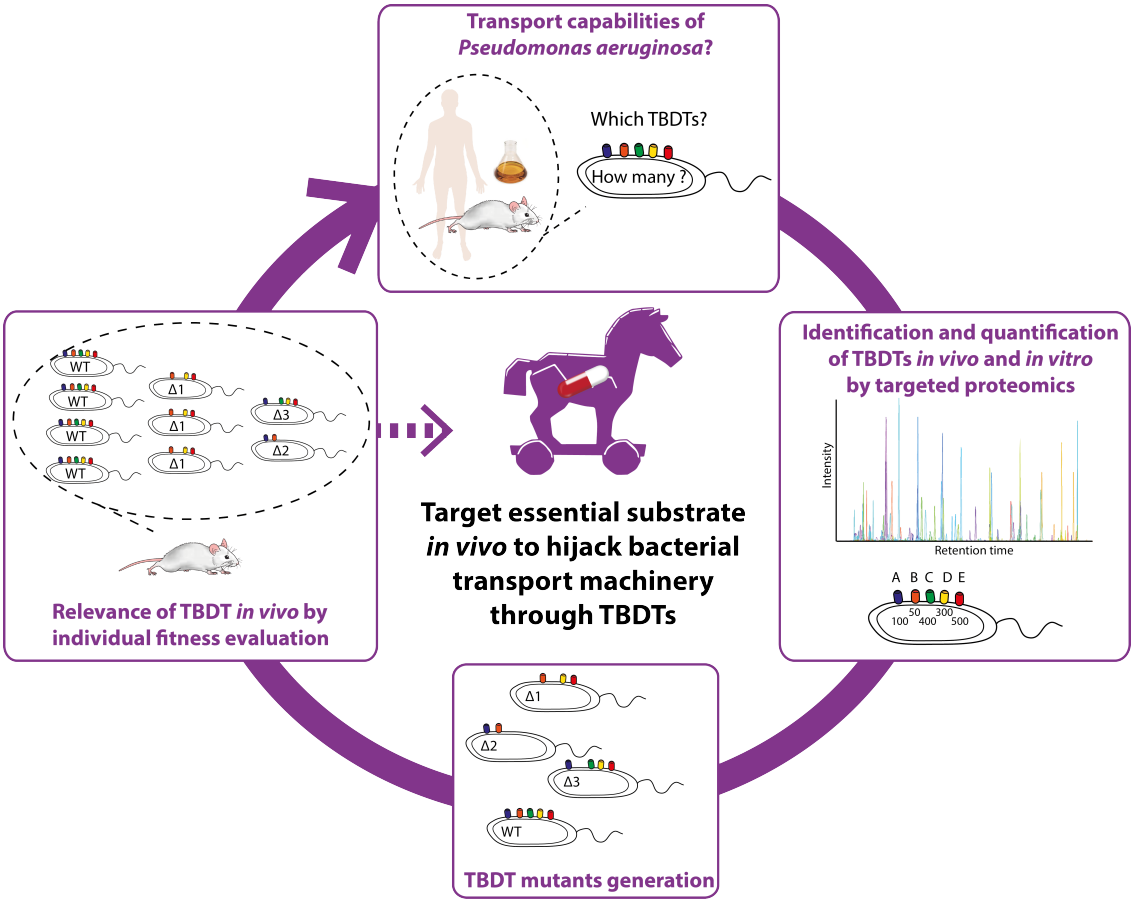

Acknowledgement

I would like to thank Professor Dirk Bumann for his guidance, enthusiasm and continued support throughout the four years of my PhD. I am mostly grateful for the chance and the trust you gave me to work on this fascinating project. You were so inspiring and had this never ending imagination that sometimes I wished to be in your head to see how fast the connections were made. Thank you for your valuable discussions and your patience, you helped me grow professionally and personally and I'm glad our paths have crossed.

I would like to thank Professor Urs Jenal for his constant support along the years. Thank you for being there when I needed to talk, and thank you for your understanding and your advise. Same thanks go to Dr. Thilo Köhler. Thank you for your support, your encouraging notes and your kindness. In times of doubt and high level of pressure, you always had reassuring words. I thank both of you for being part of my PhD committee.

The realisation of the project would not have been possible without the great mentoring of Christian. Literally. You taught me everything and your strong teaching and looong explanations allowed me to work independently when you left. I would also like to thank Julien for the support and the great times we had in the lab. I will definetely miss the post-apocalyptic bench full of piles of 96-well plates. Thanks to Tamara that did her master project with us and generated some important strains. Thank you for your perseverance and your positive attitude. Big thanks go to Sandra for her great help with the proteomic analyses and my thesis. Now, You represent the *Pseudomonas* team, be awesome!

Thank you Olivier for your support in this project. You helped me developing another way of thinking and your explanations have thoroughly enlightened me when I was stuck. I will also miss your sarcasm and your unique way of slamming doors. I wish we had more time to get to know each other, because I think that you are a kind and great person (and I will never tell you this). I would like to thanks Bea for her help and support with the animal experimentations and FACS. Thank you for coaching me during these late nights and for helping me anytime of the day. Literally! Of course, I thanks all the past and current members of the group for the support you showed me during my PhD and the moments we shared together. Thank you for making the four years of my PhD awesome.

A huge thanks to the Proteomic Core Facility: Alex, Timo, Manu, Tom and Erik. Thank you for your constant support and help. Merci Manu d'avoir pris soin de tes bébés, ils m'ont été très utiles. Thank you Alex and Tom for valuable discussions. I would also like to take this opportunity to thank all the people from the Biozentrum and elsewhere that helped me in the project through fruitful collaborations or discussions.

Pauline ma coupine, je ne vais pas te remercier d'être mon amie... mais plutôt pour tous les bons moments qu'on a passés toutes les deux durant cette thèse. Rien que d'y penser j'en rigole encore. Je suis très heureuse d'avoir fait ta connaissance, je ne sais pas comment j'aurai tenu ces quatre ans sans tes maladresses, ta tchatche et les milliers de litres de vin blanc qu'on a partagé. Bah oui, jveux dire... Merci à la French Connection (Selma nah, Vincent, Manu, Etienne, Simon, Clement...) pour toutes nos soirées de ouf à Saint Louis downtown!

Soumi, Priya et Mandj, merci d'avoir toujours été là pour me soutenir. Je suis très fière d'être votre soeur. Chacune d'entres vous a contribué à faire de moi la personne que je suis aujourd'hui. Ces mercis s'adressent aussi à la extended family que je ne peux citer ici, sans quoi ma thèse ferait des milliers de pages. Merci pour tout...

உங்கள் அன்புக்கும் , உங்களது உதவிக்கும் எனது மனமார்ந்த நன்றிகள். நீங்க இல்லை என்றால் நான் இப்பொழுது இல்லை. எனது கனவை எட்டுவதற்கு நீங்கள் குடத்த தயரியமும் , ஊக்கமும் பெரும் பங்கு வகித்தது. இந்த பட்டம் தங்களை பெருமை படுத்தியிருக்கம் என்று நம்புகிறேன். நன்றி...

An Damian meinen Seelenverwandten. Es gibt nicht genug Platz um dir für alles zu danken was du für mich getan hast und noch immer tust. Du bist der einzige, der meine dunkelste Seite in den schweren Momenten während meines Doktors gesehen hat... Danke, dass du trotzdem bei mir bleibst, mich unterstützt und liebst.

Contents

List of Figures

List of Tables

Part I

Context

1 Fighting *Pseudomonas aeruginosa* from inside

> *We are approaching the pre-antibiotic era prior to the 1940s when we didn't have antibiotics. Essentially people will start dying from simple infections because they will be infected by bacteria that are resistant to all antibiotics.*
>
> — **Dr. Hans Wildschutte**
> (Bowling Green State University assistant professor)

1.1 Antibiotic crisis due to the emergence of MDR pathogens

Antimicrobial resistance is a serious public health threat worldwide. There is an urgent need to close the gap between the increasing number of multidrug resistant (MDR) bacteria and the decreasing number of novel antibiotics launched by the pharmaceutical industries (ECDC., 2017). Last resort antibiotics are failing, threatening patients and the healthcare systems. Developing new antibiotics is a considerable challenge because of the rapid emergence of resistance in bacteria through the genetic changes upon antibiotics exposure and the misuses of antibiotic treatment by hospitals. The European Center for Disease Prevention and Control (ECDC) classified *Pseudomonas aeruginosa* (*P. aeruginosa*) among the seven pathogens of major public health importance (ECDC., 2017) and it has also been labelled as ESKAPE pathogens (together with *Enterococcus faecium*, *Staphylococcus aureus*, *Klebsiella pneumoniae*, *Acinetobacter baumannii* and *Enterobacter* species) that are the primary causative agents of nosocomial infections (Rice, 2008).

P. aeruginosa is a Gram-negative bacteria that is able to live in diverse niches (Nikel et al., 2014). *P. aeruginosa* is an environmental bacteria, mostly found in soil and water, but also commonly found in plants, animals and humans (Nikel et al., 2014). *P. aeruginosa* is an opportunistic pathogen that causes infections in burn and wound or cystic fibrosis (CF) patients (Obritsch et al., 2005). The pathogen is also frequently associated with nosocomial infections such as bloodstream, respiratory and urinary tract infections and can cause in patients both acute and chronic infections, characterized by different lifestyles (Obritsch et al., 2005). Acute infections are characterized by a motile state of *P. aeruginosa*

that causes severe damages in a short period of time (Turner et al., 2014). They can then turn into chronic infections, which are characterized by the formation of biofilms, facilitating infections that can persist for months or even years (Turner et al., 2014; Kramer et al., 2006). Like most Gram-negative bacteria, *P. aeruginosa* is difficult to eradicate because of the rapid emergence of multi-drug resistance. It remains one of the leading causes of morbidity and mortality in CF patients. *P. aeruginosa* is intrinsically resistant to many antibiotics (sulfonamides, trimethoprim, tetracycline, and chloramphenicol)(Mesaros et al., 2007), and further acquired resistance limits treatment options (Lister et al., 2009). To date, several classical classes of antibiotics have been used to treat *P. aeruginosa* and decrease its colonization. A first combination is penicillin/cephalosporin with aminoglycoside, and a second is carbapenems with fluoroquinolone and aminoglycoside (Tängdén, 2014). Figure 1.1 recapitulates the different classical classes of antibiotics and their use for specific infections caused by *P. aeruginosa*.

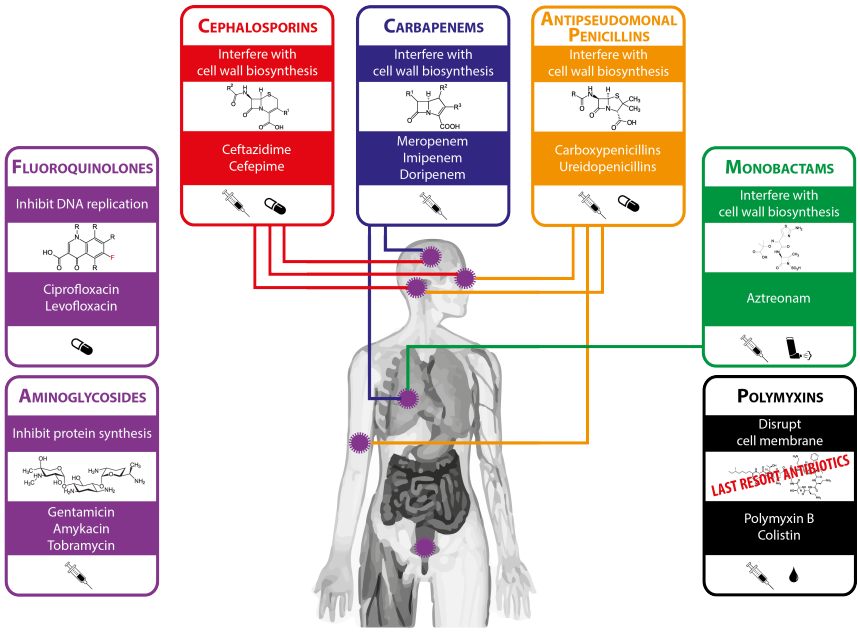

Figure 1.1: Different antibiotics classes used to treat various *Pseudomonas aeruginosa* infections.

Since the last decade, there has been a growing interest in finding solutions to eradicate MDR pathogens because of the huge economical burden they cause, due to the huge economical burden represented by the expenses of the treatment, medical personal care and hospital stay of patients (ECDC., 2017). The high rate of mortality in humans due to infections with MDR bacteria is also a serious problem (ECDC., 2017). Every antibiotic that has been launched, has been followed by the development of resistance in the targeted bacteria. Carbapenems are an efficient antibiotic class against MDR bacteria infections, however their use remains uncertain because of the emergence of carbapenemase-producing strains, e.g. *P. aeruginosa* and *A. baumannii* (Baumgart et al., 2010; Liu et al., 2015).

The ECDC estimated that, in 2007, 25'000 patients died in Europe from bloodstream, tissue, lower respiratory and urinary tract infections due to MDR bacteria, two third of which were Gram-negative bacteria (ECDC., 2017).

1.2 Overcome the first line of bacterial defence: the outer membrane

Gram-negative bacteria possess a bacterial envelope composed of an outer membrane, a peptidoglycan layer and an inner membranes that delimit a periplasmic space. The outer membrane's composition and fluidity is clearly distinct from that of the inner membrane. It displays a unique asymmetric lipid bilayer composed of phospholipids in its inner leaflet and of lipopolysaccharides (LPS) in its outer leaflet. Also, the outer membrane is 15- to 100-fold less permeable than the inner membrane for hydrophobic molecules (Cohen, 2011). The outer membrane plays a crucial role thanks to its dual function. First of all as a protective layer against toxic compounds and secondly, as an interface for nutrient exchange with the environment. The outer membrane includes a large number of protein channels involved in the transport, uptake and efflux of a large variety of compounds, nutrients and toxic molecules (Galdiero et al., 2012). The asymmetric lipid bilayer of the outer membrane is therefore the first line of bacterial defence. Hence, it can prevent rapid permeation of hydrophobic antibiotic molecules such as tetracyclines, fluoroquinolones or macrolides (Delcour, 2009; Galdiero et al., 2012).

1.2.1 Hydrophilic molecules diffuse through simple porins

Nutrient influx is largely enabled through open water-filled channels called porins. Porins play an important role in the transport of sugars, amino acids, phosphates and cations across the outer membrane (Hancock and Brinkman, 2002). Porins are pores of 6-15 Å diameters formed by 16 to 18-stranded β-barrels (Galdiero et al., 2012). This structural motif allows the formation of hydrophilic pores within the outer membrane. The pore is constricted by an inward folded extracellular loop (often the loop 3, L3), so-called the eyelet or the constriction zone (Figure 1.2) (Welte et al., 1995). The constriction zone affects the size exclusion limit and other permeation properties of the barrel (Delcour, 2009). An electrostatic field is created by the interaction of acidic amino acid residues located in the loop and basic amino acid residues located in the opposite β-strand (Fernández and Hancock, 2012). This field plays an important role in the selectivity of the pore for the size and charge of permeating molecules (Fernández and Hancock, 2012). Two main types of porins exist, the general porins, which are non-selective such as *E. coli* OmpC or OmpF (Cowan et al., 1992; Baslé et al., 2006) and the specific porins, which are highly selective such as OprD in *P. aeruginosa* with a loop that makes the pore more narrow (see Figure 1.2) (Delcour, 2009).

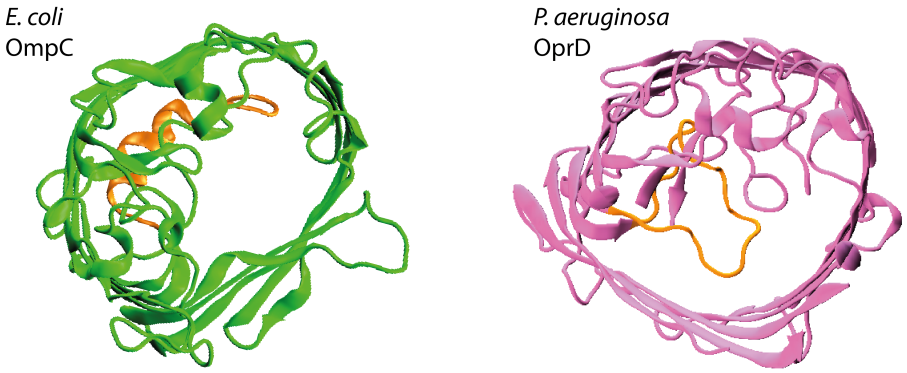

Figure 1.2: Constriction zones difference between OmpC from *E. coli* (2J1N) (Baslé et al., 2006) and OprD from *P. aeruginosa* (4FOZ) (Eren et al., 2013a). The constriction zone is represented in orange in each porin. We can thus clearly observe a narrower pore in the case of OprD. *Structure generated with visual molecular dynamics (VMD)* (Humphrey et al., 1996).

As a result, the outer membrane of *P. aeruginosa* is 12- to 100-fold less permeable than the outer membrane of *E. coli* (Tamber and Hancock, 2006). However, a decrease in outer membrane permeability does not correlate with a decrease in porins exclusion limits. Hence, *P. aeruginosa* takes up nutrients with a molecular weight of up to 3,000 Da thanks to its large number of highly selective porins (Nikaido and Hancock, 2012). On the other hand, *E. coli* harbours several general porins but few specific porins, i.e. lacking selectivity, which restricts the pathogen to an exclusion limit of 600 Da (see Table 1.1 (Hancock and Brinkman, 2002; Keseler et al., 2013). Porin synthesis is regulated by envelope stress response systems, post-transcriptional regulations by small regulatory RNAs and other possible, yet unknown, mechanisms (Masi et al., 2013).

	General porins	Specific porins	Gated porins
***E. coli* K12**	7	4	7
***P. aeruginosa* UCBPP-PA14**	1	39	35

Table 1.1: Predicted porin types for *E. coli* K12 (Keseler et al., 2013) and *P. aeruginosa* UCBPP-PA14 (Lee et al., 2006; Winsor et al., 2016). The gated porins will be described later on (Section 1.2.3).

1.2.2 Efflux pumps decrease intracellular antibiotic concentration

Bacterial efflux pumps are multiple-component systems that include an outer membrane channel, a periplasmic adaptor protein and an inner membrane transporter/pump (Figure 1.3) (Hancock and Brinkman, 2002). They are thus localized in the outer membrane and anchored in the inner membrane. The tripartite composition allows the expulsion

of compounds from the cytoplasm and the periplasm to the extracellular environment (Amaral et al., 2014). Efflux pumps are involved in the secretion of molecules produced by the bacteria and are able to recognize harmful compounds that managed to penetrate the cell wall and reach the periplasm or cytoplasm, and to expel these compounds before they reach their intended targets (Amaral et al., 2014). This process does not involve the alteration or degradation of the antibiotics (Fernández and Hancock, 2012).

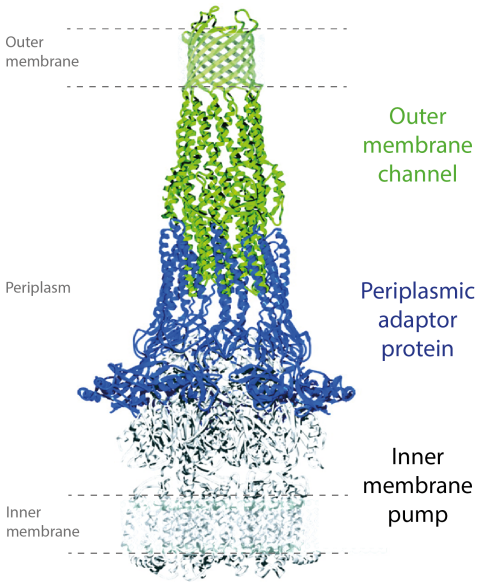

Figure 1.3: Tripartite structure of efflux pump: a qualitative model adapted from the hybrid complex TolC-MexA-AcrB (Higgins et al., 2004). It includes an outer membrane channel, a periplasmic adaptor protein and an inner membrane transporter/pump.

The pumps are classified as five different families, the Resistance-Nodulation-Division (RND) efflux pumps family is the most important class because they are present only in Gram-negative bacteria and they are associated with clinical significant antibiotic resistance (Sun et al., 2014). RND pumps have been extensively studied because they are able to transport a wide range of antibiotics but also toxins, dyes, detergents, lipids, and molecules involved in quorum sensing (Puzari and Chetia, 2017). The best studied multiple drug resistance (MDR) pumps are AcrAB-TolC in *E. coli* and MexAB-OprM in *P. aeruginosa* (Sun et al., 2014).

RND efflux pumps are involved in a complex regulatory network where they are regulated by both local and global regulators (Fernández and Hancock, 2012). Efflux pumps seem to play a major role during infection by expelling host antimicrobials and secreting virulence factors in order to damage host cells (Sun et al., 2014). RND efflux pumps have been discovered as being essential for the survival, colonization and virulence of the bacteria during infection (Puzari and Chetia, 2017). Interestingly, defects in the efflux

pump activity impairs biofilm formation in *P. aeruginosa*, *E. coli* and *Salmonella enterica serovar Typhimurium* (Rosenberg et al., 2003).

1.2.3 Gated porins enable energized substrate-specific transports

For nutrients present in low bioavailability in the extracellular environment, passive diffusion is no longer efficient enough and transport occurs via substrate-specific and active transporters, the so-called gated porins (Galdiero et al., 2012). The gated porins are characterized by 22-stranded β-barrels forming the pore that accommodates a 4-stranded β-sheet domain forming a gate in the center (Figure 1.4) (Koebnik et al., 2000; Hancock and Brinkman, 2002). This gate is described as a plug domain that occludes the barrel and thus completely obstructs unspecific molecules to pass through gated porins. Some TBDTs can harbour a signalling domain when they are involved in cell-surface signalling (CSS) (Llamas et al., 2014).

Nutrient acquisition is achieved upon specific ligand recognition by the transporter, which induces a signal transduction across the outer membrane (Schalk et al., 2004). This results in a conformational change of the plug domain that releases the so-called TonB box (Noinaj et al., 2010), a semi-conserved sequence of five to eight amino acid residues located on the N-terminal of the plug (Gudmundsdottir et al., 1989; Kadner, 1990). The TonB box is stretched into the periplasm and interacts with the TonB machinery in the inner membrane (Noinaj et al., 2010). The TonB machinery is composed of TonB, ExbB and ExbD (1:2:7 stoichiometry) and uses the proton motive force to open the transporter, which can then enable the translocation of the ligand substrate (Noinaj et al., 2010). Because the gated porins require the TonB machinery to energize their ligand substrate transport, they are also called TonB-Dependent Transporters (TBDTs). These transporters are able to acquire a large variety of specific substrates such as heme, vitamins, heavy metals and carbohydrates (Schauer et al., 2008). The most studied transporters are those involved in the uptake of iron through secretion and acquisition of strong iron chelators called siderophores. The synthesis of TBDTs is regulated in multiple ways, involving metal-dependent regulators, σ/ anti-σ factors and possibly other mechanisms not yet detected (Noinaj et al., 2010).

1.2.3.1 The battle for iron

Iron is one of the most abundant element on Earth (Quintero-Gutiérrez et al., 2008), and plays an important role in biology (Abbaspour et al., 2014). Thanks to its redox activity, iron is at the center of the most fundamental enzymatic processes such as DNA and RNA synthesis, oxygen metabolism and electron transfer. Iron has two common oxidation states (Abbaspour et al., 2014): ferrous iron Fe^{2+} and ferric iron Fe^{3+}. Ferrous iron Fe^{2+} is quite soluble in water and can be oxidized to ferric iron Fe^{3+}, which is insoluble. At physiological pH, ferrous iron Fe^{2+} is rapidly oxidized (Abbaspour et al., 2014) and the

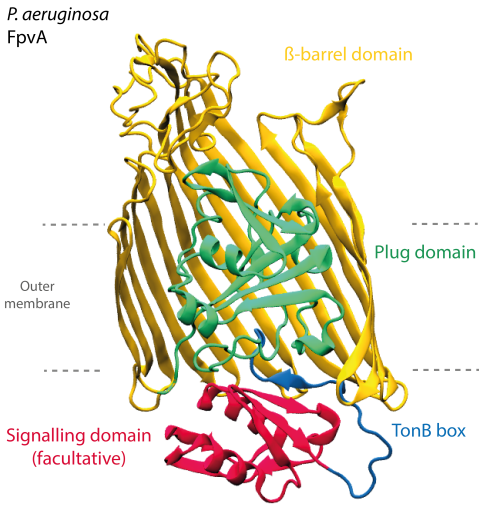

Figure 1.4: Characteristic TBDT structure: example of FpvA, pyoverdine transporter (2W16) (Greenwald et al., 2009). A β-barrel is occluded by a plug domain. A semi-conservative sequence called the TonB box is located at the N-terminus of the protein. Some TBDTs can harbour a signalling domain when they are involved in cell-surface signalling (CSS). *Structure generated with Visual Molecular Dynamics (VMD)* (Humphrey et al., 1996).

concentration of bioavailable Fe^{3+} is 10^{-9} M (Mislin and Schalk, 2014). Bacteria require Fe^{3+} concentrations between 10^{-6} M and 10^{-7} M for optimal growth (Mislin and Schalk, 2014). In host environment, access of iron is restricted by the host by strong complexation of host proteins to iron, such as transferrin, lactoferrin or hemoproteins, through a process called nutritional immunity (Hood and Skaar, 2012). The concentration of the available iron is consequently extremely low in the host, about 10^{-24} M (Hancock and Brinkman, 2002; Raymond et al., 2003).

Iron acquisition through heme

Heme is a cofactor of hemoproteins. The molecule has a porphyrin structure that covalently binds iron in its center (Figure 1.5). High concentration of heme is toxic because heme is highly hydrophobic and can pass through cell membranes, impair lipid bilayers and destabilize the cellular cytoskeleton (Schmitt et al., 1993; Jarolim et al., 1990; Anzaldi and Skaar, 2010). In the case of erythrocyte lysis, released hemoglobin is captured by the plasma protein haptoglobin to prevent the oxidative damage triggered by hemoglobin (Abbaspour et al., 2014). The haptoglobin-hemoglobin complex is recognized by macrophages, which removed it from the plasma (Abbaspour et al., 2014). Any free heme that is released from hemoglobin is rapidly bound by another plasma protein known as hemopexin (Abbaspour et al., 2014). Intracellular concentration of heme is hence tightly controlled by the host in order to limit the toxicity associated with these molecules, ensure iron homeostasis, and prevent microbial growth (Pishchany and Skaar, 2012).

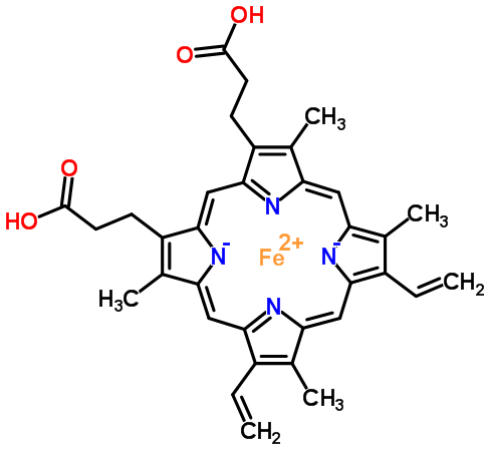

Figure 1.5: Heme structure. The molecule has a porphyrin structure that covalently binds iron in its center.

Hemoglobin is the most abundant reservoir of iron in humans and is thus an attractive nutrient and iron source for invading pathogens (Abbaspour et al., 2014). Numerous bacterial species have evolved systems to extract iron from host hemoglobin (Cornelis and Andrews, 2010). Under iron-limiting conditions, bacteria secrete toxins that lyse erythrocytes in order to release hemoglobin from red blood cells (Skaar, 2010). Released hemoglobin is then bound by specific transporters that are anchored in the cell surface of the bacteria (Skaar, 2010). Upon binding of hemoglobin, these transporters remove the heme moiety from hemoglobin and further translocate it across the outer membrane (Cornelis and Dingemans, 2013). Pathogens are also able to secrete a heme extractor protein called the hemophore, that would then pass the heme moiety to heme transporters (Cornelis and Dingemans, 2013).

Iron acquisition through siderophores

Bacteria have evolved strategies to acquire iron through strong chelator molecules called siderophores (Skaar, 2010). Siderophores are low-molecular-weight chelating agents (200–2000 Da), produced by bacteria to facilitate the uptake of iron (Mislin and Schalk, 2014). They bind iron with very high affinity defined by binding constants (Ka) ranging from 10^{30} M^{-1} to 10^{52} M^{-1} (Schalk and Cunrath, 2016). Fungi and plants are also able to produce siderophores (Mislin and Schalk, 2014). In the soil, the concentration of siderophore is about 10^{-3} to 10^{-7} M, which contributes considerably in extracting insoluble iron from minerals in order to facilitate its mobilization and to maintain intracellular iron reservoirs (Schalk et al., 2011). In the host, siderophores confer a remarkable advantage to bacteria because they can efficiently compete with plasma proteins lactoferrin and transferrin (binding constants of 10^{22}-10^{24} M^{-1} and 10^{20}-10^{21} M^{-1} respectively) (Majka et al., 2013). Siderophores also have the ability to function as metallophores for a variety of other metals (Schalk and Cunrath, 2016). They can also act as toxins or signalling

molecules for quorum sensing, regulate oxidative stress, and provide antibacterial activity (Johnstone and Nolan, 2015).

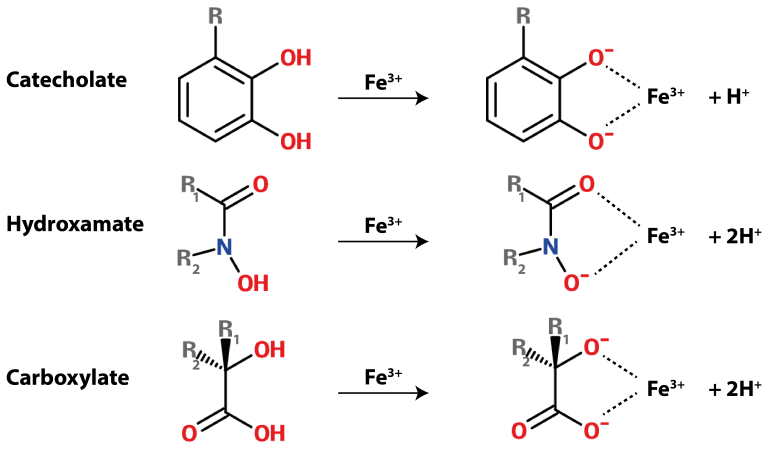

Figure 1.6: Structural classes of siderophores: Catecholate, hydroxamate and carboxylate.

Siderophores can have a variety of chemical structures and they form a family of at least 500 different compounds (Hider and Kong, 2010; Schalk et al., 2011). According to their structures, they are divided into four main classes: the catecholates mostly found in bacteria, the hydroxamates, the carboxylates mostly found in fungi and, a forth class that includes mixed-types structures (Figure 1.6) (Mislin and Schalk, 2014). Ferrisiderophores, i.e. iron Fe^{3+} bound to siderophores, are transported across the outer membrane through dedicated specific TBDTs (Imperi et al., 2009). The ferrisiderophore is then efficiently delivered to the cell through inner membrane ABC transporters (Miethke and Marahiel, 2007). In some case, dissociation of the ferrisiderophore occurs in the periplasm and the siderophore is recycled by an efflux pump, in order to scavenge more iron (Imperi et al., 2009; Guillon et al., 2013).

1.2.3.2 Trojan horse strategy based on sideromycins

Sideromycins are natural antibiotics covalently linked to siderophores, which are produced by various microorganisms (Mislin and Schalk, 2014). Several families of sideromycins have been discovered and characterized in the last decades. The sideromycins identified to date include albomycins produced by *Actinomyces subtropicus* (Bickel et al., 1960; Benz et al., 1982), ferrimycins (Bickel et al., 1965), danomycins (Tsukiura et al., 1964), and salmycins (Vértesy et al., 1995) produced by *Streptomyces* strains, as well as certain microcins (De Lorenzo and Pugsley, 1985; Destoumieux-Garzón et al., 2006; Nolan and Walsh, 2008; Thomas et al., 2004) produced by *Enterobacteriaceae* (Möllmann et al., 2009).

These natural siderophore–antibiotic conjugates can chelate Fe^{3+} and are transported into the bacterium via siderophore-dependent iron uptake pathways (Mislin and Schalk, 2014). This energy-coupled transport across the bacterial membranes greatly increases the antibiotic efficacy of sideromycins (Mislin and Schalk, 2014). The minimum inhibitory concentration (MIC) represents the lowest concentration of an antibiotic required to inhibit the growth of an organism. Sideromycin MICs are often at least two orders of magnitude lower than that of the antibiotic moiety without the siderophore (Mislin and Schalk, 2014).

The Trojan horse approach bases its strategy on these natural compounds in order to increase antibiotic uptake by the bacteria themselves (Carvalho and Fernandes, 2014). The concept is the same as for the sideromycin: a bacterial substrate moiety is associated with an antibiotic moiety (Carvalho and Fernandes, 2014). During infection, bacteria use iron uptake systems in an environment that is poor in iron (Skaar, 2010). Therefore, sideromycins coupled with iron have a high chance to be taken up by the bacteria. The affinities of siderophore coupled-antibiotics with their transporters is high due to their siderophore moiety (Figure 1.7) (Carvalho and Fernandes, 2014). Hijacking iron bacterial transports in order to deliver actively antibiotics is hence a propitious strategy to cross the outer membrane, using bacterial machinery (Möllmann et al., 2009).

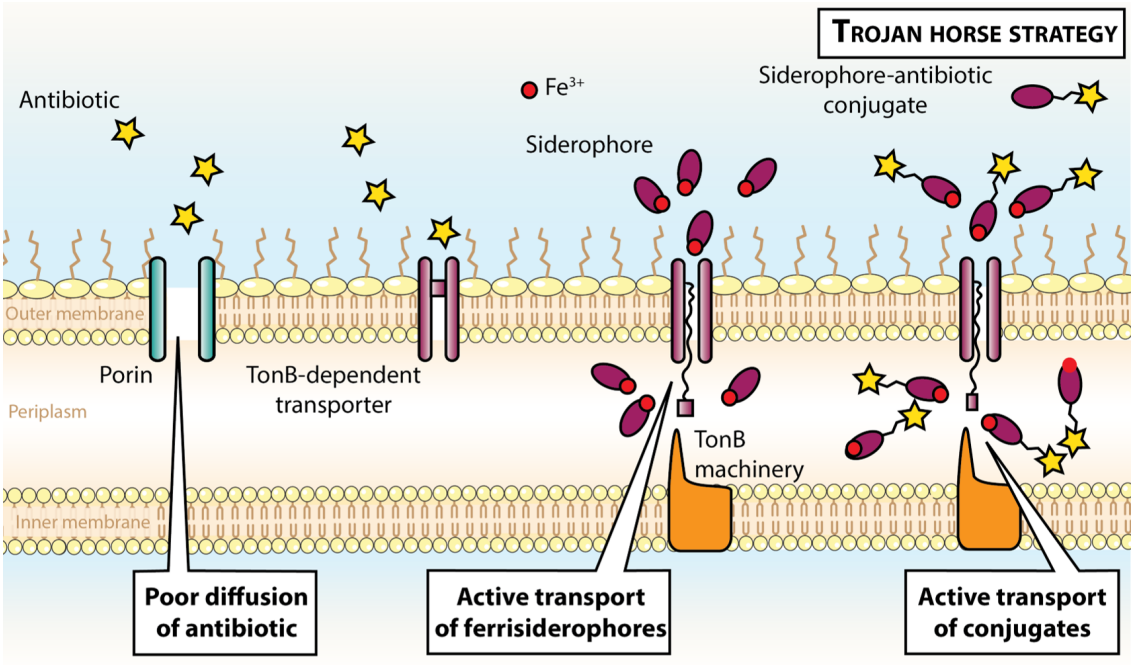

Figure 1.7: Exploiting bacterial active transporters. Example of a Trojan horse strategy, where a siderophore is coupled to an antibiotic moiety in order to increase antibiotic uptake by the dedicated TBDT. Transport of conjugates through the TBDT is more efficient than diffusion of the antibiotic alone.

In order to synthesize a successful siderophore-drug candidate, the compound should fulfill two important properties: it should exhibit a good antibiotic activity and present a high affinity to the bacterial transporter (Mislin and Schalk, 2014). Three major hurdles exist in the synthesis of conjugates:

- The choice of the antibiotic: the translocation of a drug through both the outer and the inner membrane is challenging, because the drug should be able to cross both membranes and still be active. The most used antibiotic class in the Trojan horse strategy are derivatives of the β-lactams, because they directly act in the periplasm by blocking cell wall biosynthesis (Mislin and Schalk, 2014);
- The choice of the arm linker, i.e. in order to associate the antibiotic moiety to the siderophore, the ideal linker should stay stable during the translocation across the outer membrane but should be easily cleaved once inside the bacteria (in the periplasm or in the cytoplasm depending on the drug) (Mislin and Schalk, 2014);
- The choice of the siderophore: the siderophore should be able to reach a wide spectrum of pathogens.

Due to the complexity of the outer membrane envelope, overcoming the bacterial first line of defence is difficult. The outer membrane confers *P. aeruginosa* a higher intrinsic resistance due to its low permeability and the pathogen benefit from sophisticated efflux mechanisms that expel intruding antibiotics (Nikaido and Hancock, 2012). These two major bacterial strategies make the development of new therapeutic approaches even more challenging. In this context, the Trojan horse approach seems promising.

1.3 Acquired resistance of *P. aeruginosa* challenges antibiotic development

In addition to intrinsic resistance, bacteria can acquire or develop resistance to antibiotics. The resistance can be mediated by three major mechanisms (Dever and Dermody, 1991):

- decrease of the intracellular concentration of antibiotics by controlling influx and efflux;
- modification of the antibiotics target by genetic mutations;
- inactivation of antibiotics by hydrolysis or chemical modification.

Porins allow the entry of key nutrients but together with efficient efflux systems, seem to play an important role in restricting the influx of numerous antibiotics (Hancock, 1987; Ochs et al., 1999b; Ruiz, 2003; Olesky et al., 2006). Understanding the mechanisms by which pathogens control their influx and efflux is of particular importance for developing new therapeutic options.

1.3.1 *Pseudomonas aeruginosa* UCBPP-PA14, our model organism

P. aeruginosa have the remarkable ability to colonize diverse environments and infect a wide range of organisms, from plants to humans (Rahme et al., 2000). This environmental and pathogenic promiscuity is in part due to the large and genetically diverse *P. aeruginosa* genome. The common *P. aeruginosa* laboratory strain is PAO1 (Stover et al., 2000). This strain was isolated from an infected burn/wound of a patient in Melbourne, Australia (American Type Culture Collection ATCC 15692) (Hare et al., 2012). PAO1 is a moderately virulent strain (Lee et al., 2006) and belongs to a relatively rare clonal group (Wiehlmann et al., 2007). In contrast, UCBPP-PA14 is a highly virulent strain isolated from a burn wound patient in the United States (Rahme et al., 1995) and represents the most common clonal group worldwide (Figure 1.9) (Wiehlmann et al., 2007).

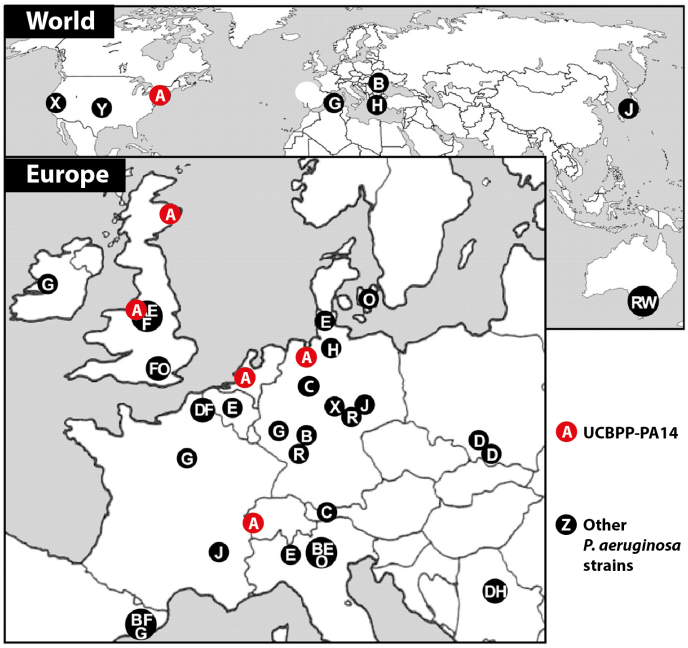

Figure 1.8: Widespread geographic distribution of major *P. aeruginosa* clones. UCBPP-PA14 represents the most common clonal group worldwide. Clones are depicted by uppercase letters and are arranged by decreasing frequency in alphabetical order. Adapted from (Wiehlmann et al., 2007).

The UCBPP-PA14 genome shows a high degree of conservation compared to PAO1, the difference in virulence seems to arise from two pathogenicity islands (PAPI-1 and PAPI-2) that are absent in the PAO1 genome (Harrison et al., 2010). Harrisson and coworkers showed that the deletion of one or both pathogenicity islands impacts the virulence of PA14 in acute pneumonia and bacteremia murine models (Harrison et al., 2010). The two pathogenicity islands were related to virulence factors that might promote pathogen attachment to epithelial cells (He et al., 2004), and hence establish a successful colonization of the host. The UCBPP-PA14 genome was sequenced ten years ago by

Lee and coworkers and they predicted that the genome encodes 40 simple porins, 20 efflux pumps and 35 TBDTs (Table 1.1) (Lee et al., 2006; Winsor et al., 2016).

1.3.2 Porin-mediated resistance to antibiotics

P. aeruginosa UCBPP-PA14 encodes 40 simple porins, among which 19 belong to the OprD family (Hancock and Brinkman, 2002). β-lactams carbapenems, such as imipenem and meropenem, are antibiotics that interfere with the cell wall biosynthesis in the periplasm and, exhibit high resistance against bacterial defence β-lactamases (Figure 1.1). Carbapenems have been shown to pass across *P. aeruginosa* outer membrane through OprD (Trias and Nikaido, 1990a). Additionally, the porin has been described to facilitate the diffusion of basic amino acids and small peptides, which is not surprising as basic amino acids share structural similarities with carbapenem molecules (Trias and Nikaido, 1990b; Lister et al., 2009).

Consequently, the loss of OprD significantly decreases the susceptibility of the pathogen to carbapenems as shown by Sakyo and coworkers for imipenem, meropenem and doripenem (Sakyo et al., 2006). Susceptibility of a strain is measured by changes in MIC. OprD is a highly regulated protein at transcriptional and post-transcriptional levels by some trace metals (Perron et al., 2004; Caille et al., 2007), amino acids (Ochs et al., 1999a), and efflux pump regulators (Köhler et al., 1999; Muller et al., 2011). It has been shown that OprD porin inactivation occurs via mutations that create frameshifts and premature stop codons (Pirnay et al., 2002) and via disruption of the *oprD* structural gene by the insertion of large insertion sequence (IS) elements (Evans and Segal, 2007; Wolter et al., 2004).

Two intriguing studies revealed discordance between *oprD* expression and susceptibility to imipenem. Imipenem-resistant strains showed a low level of *oprD* expression, or none at all, as expected (Lister et al., 2009). However isogenic mutants, derived from the parental imipenem-resistant strains, exhibited lower level of *oprD* expression, or still none at all, but susceptibility to imipenem reverted back due to a not yet known mechanism (Wolter et al., 2005; Wolter, 2008a; Lister et al., 2009). These two studies highlighted the dynamic regulation and remarkable genetic versatility of *P. aeruginosa*, which makes *P. aeruginosa* one of our greatest therapeutic challenges.

1.3.3 Efflux-mediated Resistance to Antibiotics

Decreasing the intracellular concentration of antibiotics can also be achieved through active export by membrane-associated pumps. Efflux pump expression has been associated with increased MIC values to antibiotics in clinical isolates (Sun et al., 2014). *P. aeruginosa* is able to express ten RND pumps: MexAB-OprM, MexCD-OprJ, MexEF-OprN,

MexXY, MexJK, MexGHI-OpmD, MexVW, MexPQ-OpmE, MexMN, and TriABC. Mex is an acronym for *M*ultiple *e*fflu*x*. Four RND efflux pumps have been discovered to be essential for the survival, colonization and virulence of the bacteria during infection: MexXY–OprM, MexCD–OprJ, MexEF–OprN and MexXY (Puzari and Chetia, 2017).

MexAB-OprM was the first multidrug efflux pump to be discovered (Poole et al., 1993). MexAB-OprM is able to export several different classes of antibiotics (Li et al., 1995), including fluoroquinolones, tetracyclines, chloramphenicol, β-lactams and β-lactamase inhibitors (Li et al., 1998), macrolides, novobiocin, trimethoprim and sulfonamides (Köhler et al., 1996; Lister et al., 2009). MexAB-OprM has the broadest substrate profile for the β-lactam class (Srikumar et al., 1998). The pump is also constitutively expressed, thus participating in the intrinsic resistance (Poole and Srikumar, 2001). Maximum expression of the pump was reported in the late log phase/early stationary phase of bacterial growth (Evans and Poole, 1999). As a result, the growth-phase-dependent expression was suggested to participate in quorum sensing (Evans and Poole, 1999). The expression of the pump is repressed by the negative transcriptional regulators MexR, NalC and NalD.

MexCD-OprJ is able to export a variety of antimicrobial agents (Gotoh et al., 1998; Masuda et al., 1996), including fluoroquinolones, β-lactams (Srikumar et al., 1998), chloramphenicol, tetracycline, novobiocin, trimethoprim (Köhler et al., 1996) and macrolides (Lister et al., 2009). Despite the high homology with MexAB-OprM (Poole et al., 1996), MexCD-OprJ preferentially export the fourth-generation cephalosporins (Poole et al., 1996; Masuda et al., 1996). MexCD-OprJ is present at very low levels in wild-type *P. aeruginosa*, suggesting that this pump does not contribute to intrinsic resistance (Morita et al., 2001). However, an increased expression of *mexCD-oprJ* is observed in a Δ*mexAB-*Δ*oprM* mutant (Li et al., 2000). *mexCD-oprJ* expression was not shown to be inducible by clinically relevant antibiotics (Morita et al., 2001). Overexpression of MexCD-OprJ leads to hypersusceptibility to aminoglycosides (Poole et al., 1996; Masuda et al., 1996) and other β-lactams, including sulbenicillin, cefpodoxime, ceftriaxone, imipenem and biapenem (Masuda et al., 2001), due to an unknown mechanism. Hypersusceptibility is defined as an increase in susceptibility of fourfolds or more (Lister et al., 2009). Like MexAB-OprM, MexCD-OprJ is negatively regulated by the negative transcriptional regulator NfxB.

MexEF-OprN is able to export fluoroquinolones, chloramphenicol, and trimethoprim, but none of the currently available β-lactams (Michéa-Hamzehpour et al., 1997). Low levels of *mexEF-oprN* expression was reported in wild-type (Li et al., 2000) and the disruption of the pump did not affect the susceptibility of *P. aeruginosa* (Michéa-Hamzehpour et al., 1997). This suggests that MexEF-OprN does not play a role in intrinsic resistance of the pathogen. In contrast to MexAB-OprM and MexCD-OprJ, MexEF-OprN is positively regulated by the global regulator MexT (Köhler et al., 1999), which also seems to have a role in *oprD* regulation (Ochs et al., 1999b).

MexXY can be associated with OprM, as well as with other outer membrane proteins, such as OpmB, OpmG, OpmH, and OpmI (Mine et al., 1999; Chuanchuen et al., 2005) and is able to export fluoroquinolones, specific β-lactams, aminoglycosides, tetracycline, chloramphenicol, and erythromycin (Poole, 2002; Schweizer, 2003). *mexXY* expression is induced by tetracycline, erythromycin, and gentamicin and, the pump was found to contribute to intrinsic resistance of *P. aeruginosa* (Masuda et al., 2000; Morita et al., 2001). MexXY is negatively regulated by the transcriptional regulator MexZ (Matsuo et al., 2004).

Extensive efforts are made to discover efflux pumps inhibitors, i.e. agents that can inhibit efflux by (i) altering the regulation of their expression, (ii) altering the functional assembly of the efflux components, (iii) obstructing the outer membrane channels, (vi) destroying the efflux energy and (v) inhibiting affinity sites of the efflux pumps with non-antibiotic molecules (Puzari and Chetia, 2017). Two classes of inhibitors (the peptidomimetics and the pyridopyrimidines) exhibited promising inhibitory activity against MexAB-OprM when they were applied with ciprofloxacin and levofloxacin (Askoura et al., 2011; Sun et al., 2014; Venter et al., 2015; Puzari and Chetia, 2017). Efflux pump inhibitors successfully compete with the antibiotics for efflux, thus increasing the intracellular antibiotic concentration (Hirakata et al., 2009).

The development of antibiotic resistance is a complex process that involves several mechanisms, which are co-regulated in an uncharacterised manner. *P. aeruginosa* carbapenem resistance involves downregulation of OprD, utilization of multiple efflux systems and overproduction of the chromosomal AmpC β-lactamase (Lister et al., 2009). Therefore, it is important to understand the contribution of efflux pumps to antibiotic resistance during infection in order to assess the therapeutic success of their inhibitors.

1.3.4 Exploiting TBDTs for conjugates transport

P. aeruginosa UBCPP-PA14 genome encodes 35 TonB-dependent transporters (Table 1.1). A comprehensive list of all TBDTs present in UPCBB-PA14 is presented in Table 1.2 (Winsor et al., 2016). These transporters are classified in different groups according to their substrates:

- endogenous siderophore transporters, i.e. transporters of siderophore produced by the pathogen;
- exogenous siderophore transporters, i.e. transporters of siderophore produced by others microorganisms;
- heme transporters, i.e. transporters of heme or heme derivatives;
- metal transporters, i.e. transporters of heavy metals;
- others transporters, e.g. transporters of carbohydrates;
- unknown transporters, i.e. uncharacterized transport systems so far.

Subclass	PA14_loci	PAO1_loci	Name	Substrate
Siderophores	PA14_09340	PA4221	FptA	Ferripyochelin
	PA14_09970	PA4168	FpvB, OptB	Type I and II Ferripyoverdine
	PA14_33680	PA2398	FpvA	Type I Ferripyoverdine
	PA14_63960	PA4837	OptC	Nicotianamine
Xenosiderophores	PA14_58570	PA4514	PiuA	Trojan horse siderophore conjugates
	PA14_52230	PA0931	PirA	Ferri-enterobactin, Trojan horse siderophore conjugates
	PA14_05640	PA0434	OptJ	Trojan horse siderophore conjugates
	PA14_29350	PA2688	FepA, PfeA	Ferri-enterobactin
	PA14_39650	PA1922	CirA, OptT	Ferri-catocholates siderophores
	PA14_10200	PA4156	FvbA, OptV	Ferri-vibriobactin
	PA14_39820	PA1910	FemA, UfrA	Ferrimycobactin and -carboxymycobactin
	PA14_61850	PA4675	OptH, ChtA, LutA	Ferri-aerobactin And Rhizobactin 1021 And Shizokinen
	PA14_06160	PA0470	FiuA	Ferrioxamine/Ferrichrome
	PA14_32740	PA2466	FoxA, OptS	Ferrioxamine/Ferrichrome
	PA14_46640	PA1365	AleB, OptN	Ferri-Aerobactin
	PA14_13430	PA3901	FecA	Fe(Iii) Dicitrate
	PA14_21730	PA3268	OptR	Fe(Iii) Dicitrate
	PA14_34990	PA2289	OptQ	Ferri-siderophore
	PA14_26420	PA2911	OptE	Siderophore
	PA14_01870	PA0151		Siderophore
	PA14_37490	PA2089	OptL	Siderophore
	PA14_37900	PA2057	SppR, OptK	Siderophore
Heme	PA14_20010	PA3408	HasR	Heme via hemophore
	PA14_47380	PA1302	HxuC	Heme
	PA14_62350	PA4710	PhuR	Heme/Hemoglobin
	PA14_64710	PA4897	OptI	
Metal-Cu **Metal-Co** **Metal-Zn**	PA14_15070	PA3790	OprC	Copper
	PA14_47800	PA1271	BtuB, OptG	Cobalamine, Vitamin B12
	PA14_54180	PA0781	OmR, ZnuD	Zinc
	PA14_37730	PA2070	OptM	Metal uptake
Carbohydrate	PA14_47140	PA1322	PfuA	Sugar
Unknown	PA14_02410	PA0192	OptP	
	PA14_30590	PA2590	OptF	Quorum sensing
	PA14_43650	PA1613		
	PA14_55050			Potential endogenous siderophore

Table 1.2: Comprehensive list of the 35 TBDTs present in *P. aeruginosa* UCBPP-PA14. Most of the functional associations are based on predictions because of the lack of experimental evidence for most TBDTs (Ghysels et al., 2005; Schalk and Cunrath, 2016).

In vivo studies in mice (Takase et al., 2000a), clinical and transcriptomic data (Son et al., 2007; Bielecki et al., 2013; Ochsner et al., 2002; Schulz et al., 2015) have agreed on an expression of TBDTs, which involved them in iron uptake, due to iron restriction in infected tissues. Most of these TBDTs are associated with siderophores-mediated iron or heme uptake. Several studies have suggested crucial roles of the TonB-dependent siderophores and heme receptors during *P. aeruginosa* infection (Takase et al., 2000b; Nguyen et al., 2014), but few have characterized the complete set of relevant TBDTs *in vivo* (Schauer et al., 2008).

In contrast to efflux pumps or simple porins, the use of TBDTs as drug delivery systems has two advantages:

- the transporters enable active transport, more powerful for an efficient drug delivery than a passive diffusion;
- the transporters seem to play a major role during infection, especially those involved in iron uptake.

Designing siderophore-antibiotic conjugates for relevant *in vivo* TBDT might be an efficient way to circumvent the rapid development of antibiotic resistance.

So far, there have been three endogenous siderophores described in *P. aeruginosa* UCBPP-PA14. The high-affinity siderophore systems pyoverdine and pyochelin have been extensively studied *in vitro* and *in vivo* for over 50 years. Recently, a third endogenous siderophore/metallophore, staphylopine (Ghssein et al., 2016) /nicotianamine was discovered in *P. aeruginosa* and seems to have an important role in artificial lung conditions (Gi et al., 2014).

1.3.4.1 Pyoverdine is the main siderophore of *P. aeruginosa*

Pyoverdine is the high-affinity siderophore of *P. aeruginosa* (10^{32} M^{-1}) and is the reason for the characteristic green fluorescence of *P. aeruginosa* (Hoegy et al., 2014). *P. aeruginosa* can produce three different types of pyoverdine in a strain-specific fashion: type I, type II and type III (Briskot et al., 1986; Meyer et al., 1997). Each one is characterized by a different peptide chain. UCBPP-PA14 produces type I pyoverdine (Briskot et al., 1986; Meyer et al., 1997). Pyoverdine biosynthesis is a complex process that starts in the cytoplasm and ends in the periplasm with the maturation of the fluorescent pyoverdine (Figure 1.10) (Hannauer et al., 2012a).

Pyoverdine production is regulated by the Ferric uptake regulator Fur and PvdS that is in turn also regulated by Fur (Leoni et al., 1996). When the iron concentration is high, Fur is bound to iron and represses the expression of pyoverdine biosynthesis (Leoni et al., 1996). Upon iron starvation, Fur releases the sigma factor PvdS that initiates pyoverdine biosynthesis (Leoni et al., 1996). Pyoverdine synthesis starts in the cytoplasm

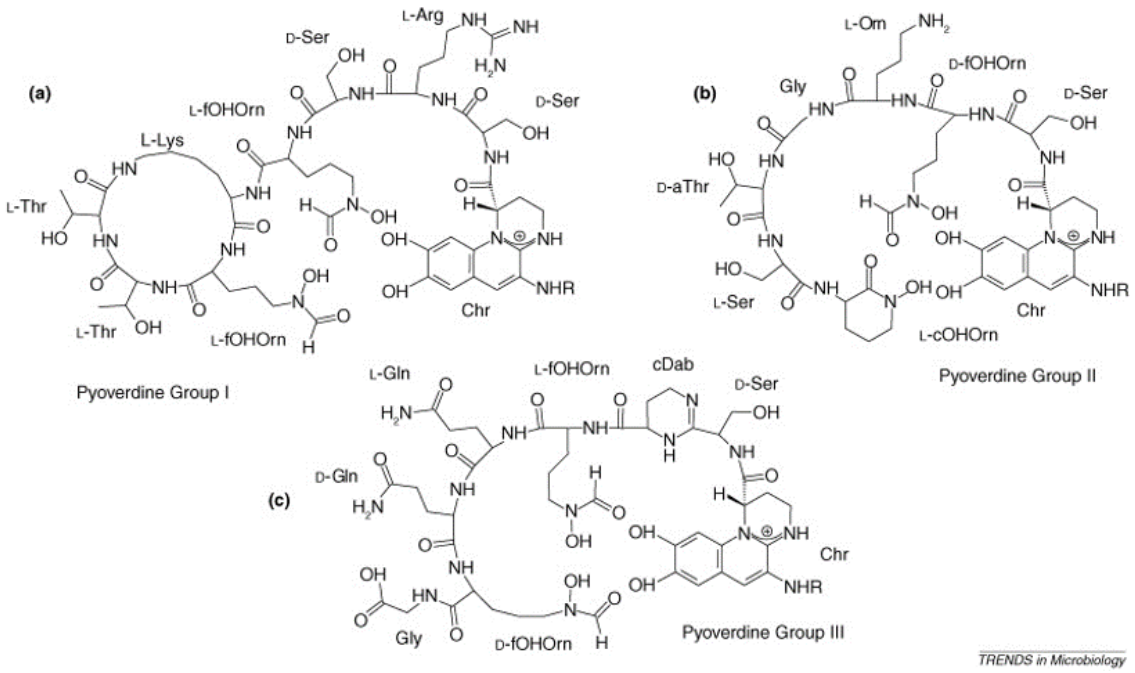

Figure 1.9: Pyoverdine type I, II and III structures (Visca et al., 2007). Each one is characterized by a different peptide chain.

with the assembly of the peptide backbone in a multistep reaction done by four non-ribosomal peptide synthetases (NRPSs) PvdL, PvdI, PvdJ and PvdD (Hannauer et al., 2012a). NRPSs are very large enzymes organized in modules, where each module catalyses the incorporation of one specific amino acid substrate into the peptide product (Crosa and Walsh, 2002; Finking and Marahiel, 2004). Several enzymes produce the necessary substrates for the assembly, such as the ornithine hydroxylase PvdA (Ge and Seah, 2006), the hydroxyornithine transformylase PvdF (McMorran et al., 2001) and the aminotransferase PvdH (Vandenende et al., 2004). Formation of the precursors occurs at the siderophore-specific multi-enzymatic complexes, called siderosome, that is associated with the inner leaflet of the inner membrane (Gasser et al., 2015). It was suggested that this localization prevents the precursor from filling the periplasm and binding free iron (Gasser et al., 2015). It also facilitates rapid secretion of pyoverdine (Imperi and Visca, 2013). The precursors are also bound to the inner membrane through a fatty acid chain (myristoleic acid chain) during its assembly (Hannauer et al., 2012a).

The resulting peptide precursor is non-fluorescent and is transported across the inner membrane and into the periplasm by PvdE, which is an ABC transporter specific to pyoverdine (Yeterian et al., 2010b). The maturation of pyoverdine starts with the removal of the myristoleic acid by the acylase PvdQ prior to the maturation of the chromophore (Hannauer et al., 2012a). The generated precursor is called ferribactin. PvdM, PvdN, PvdO and the tyrosinase PvdP are involved in the ferribactin maturation into pyoverdine by a mechanism that remains unknown (Nadal-Jimenez et al., 2014; Ringel et al., 2016).

PvdP and PvdN have been shown to be essential for pyoverdine production (Nadal-Jimenez et al., 2014; Ringel et al., 2016). The newly synthesized pyoverdines are secreted by the ATP-dependent efflux pump PvdRT-OpmQ (Figure 1.10) (Yeterian et al., 2010a; Hannauer et al., 2012b; Schalk and Guillon, 2013). PvdRT-OpmQ is the second siderophore efflux pump to be described (Hannauer et al., 2012b), AcrAB-TolC from *E. coli* being the first (Sun et al., 2014).

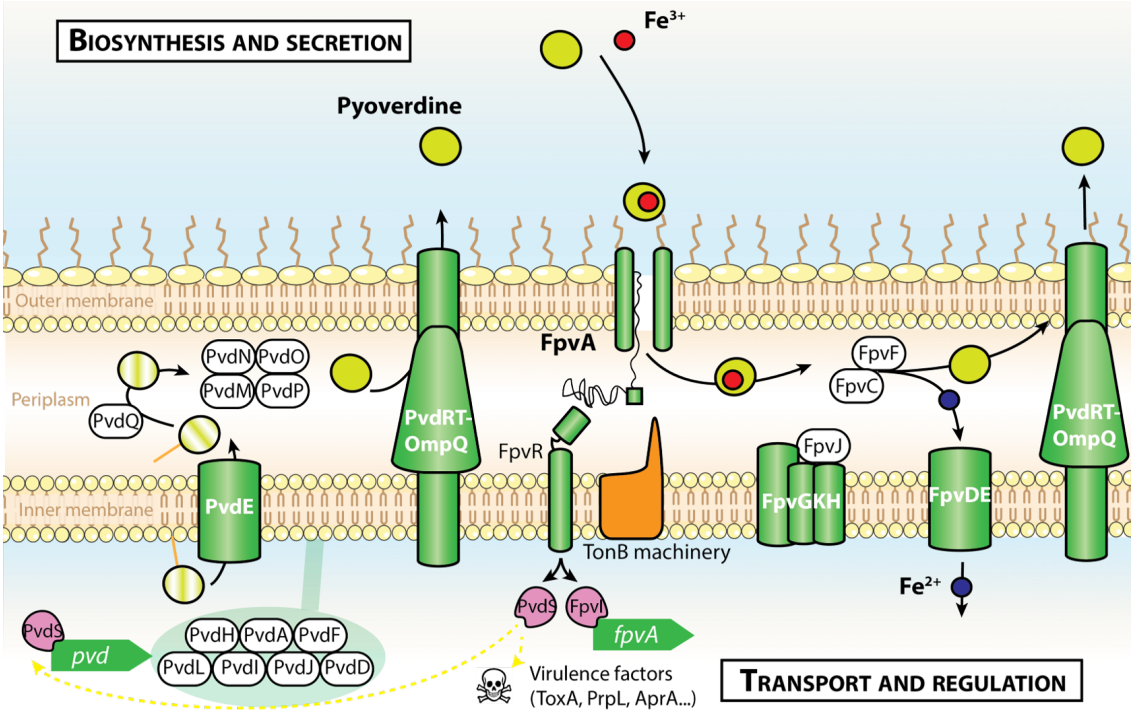

Figure 1.10: Pyoverdine biosynthesis, secretion, transport and regulation.

Once iron Fe^{3+} has been chelated in the extracellular medium, ferripyoverdine is transported across the outer membrane via its two dedicated TBDTs: FpvA (Schalk et al., 1999) and FpvB (Ghysels et al., 2004). The binding site of FpvA is highly specific for the ferripyoverdine, with an affinity of 0.5 nM (Hannauer et al., 2012b). FpvB has been identified as a ferripyoverdine transporter but its exact role remains unknown (Ghysels et al., 2004). In the periplasm, the iron reductase FpvG releases iron from the siderophore by reduction (Greenwald et al., 2007; Imperi et al., 2009). FpvH, FpvJ, and FpvK proteins probably act as partners of FpvG by transferring iron to a chaperon protein FpvC (Ganne et al., 2017b). FpvC has a higher affinity for Fe^{2+} than pyoverdine (Ganne et al., 2017b). FpvC, together with another chaperon protein FpvF possibly bring Fe^{2+} to the ABC transporter FpvDE for its translocation into the cytoplasm (Brillet et al., 2012). The apo-siderophore is then recycled into the extracellular medium by PvdRT-OpmQ (Figure 1.10) (Schalk et al., 2002; Imperi et al., 2009).

Depending on the strain, *P. aeruginosa* produces large amounts of pyoverdine: its concentration is between 15 and 37 mM under iron-depleted culture conditions (Mislin and Schalk,

2014). Pyoverdine is also able to efficiently chelate other metals: Ag^{+},Al^{3+},Cd^{2+},Co^{2+} ,Cu^{2+} ,Fe^{3+} ,Ga^{3+} ,Hg^{2+} ,Mn^{2+} ,Ni^{2+} and Zn^{2+}, but its highest affinity is for Fe^{3+} (Schalk and Guillon, 2013). In contrast to Fe^{3+}, these other metal ions are not released from pyoverdine, but rather directly pumped out of the cell by PvdRT-OpmQ (Schalk and Guillon, 2013). The process has been proposed as a detoxification mechanism of the environment in order to maintain metal homeostasis in *P. aeruginosa* and to prevent high intracellular heavy metal concentration, carried by simple porin diffusion (Schalk and Guillon, 2013).

FpvA has been associated with a cell surface signalling (CSS) pathways (Llamas et al., 2014). The binding of ferripyoverdine to FpvA initiates a signalling cascade through the interaction between the signalling domain present on FpvA N-terminal domain and the anti-sigma factor FpvR (Llamas et al., 2014). FpvR controls the activity of two extracytoplasmic function (ECF) alternative sigma factors: PvdS and FpvI (Llamas et al., 2014). The FpvI sigma factor recruits RNA polymerase to promote the expression of *fpvA*, while PvdS promotes the expression of genes involved in pyoverdine biosynthesis (*pvd*) and virulence factors such as exotoxin A (ToxA), proteases PrpL and AprA, and others (Figure 1.10) (Beare et al., 2003; Tiburzi et al., 2008). Pyoverdine triggers a positive feedback loop of its own expression and acts as a signalling molecule that controls the production of virulence factors (Lamont et al., 2002; Minandri et al., 2016).

For decades, pyoverdine has been described as important for *in vivo* infections (Meyer et al., 1996; Takase et al., 2000a; Takase et al., 2000b). Lately, a meta-analysis on pyoverdine effects *in vivo* showed that different experimental conditions can lead to divergent outcomes (Granato et al., 2016). A pyoverdine-deficient mutant showed lower virulence in a wide range of hosts (Meyer et al., 1996; Takase et al., 2000a; Takase et al., 2000b; Imperi et al., 2013; Lopez-Medina et al., 2015), potentially because of the absence of pyoverdine-related virulence factors. This mutant showed reduced growth *in vivo* compared to the wild-type, but was still able to colonize the host and trigger an infection in the various infection models (Granato et al., 2016). Moreover, the mutation of pyoverdine enyzme biosynthesis, PvdA, in clinical *P. aeruginosa*, associated with chronic lifestyle of *P. aeruginosa*, is frequent in CF patients (De Vos et al., 2001; Jiricny et al., 2014; Andersen et al., 2015). However the strains maintain the ability to take up pyoverdine (De Vos et al., 2001; Jiricny et al., 2014; Andersen et al., 2015).

As a Trojan horse candidate, pyoverdine-antibiotic conjugates are challenging because the structure of the pyoverdine is composed of a polycyclic moiety with asymmetric centers of unnatural amino acids. Most of the Trojan horse pyoverdine-drugs that have been developed, have been synthesized by hemisynthesis, i.e starting from chromopeptides that were extracted from *P. aeruginosa* culture broth (Mislin and Schalk, 2014), making it difficult to scale up to an industrial production level. Budzikiewicz and coworkers developed two pyoverdine drug conjugates from pyoverdine that was isolated from *P. aeruginosa*

ATCC 27853 and *Pseudomonas fluorescens* ATCC 13525 complexed with ampicillin (PaTSebAmp and Pv9446SebAmp) (Kinzel et al., 1998; Kinzel and Budzikiewicz, 1999). These pyoverdine-conjugates showed increased levels of antibacterial activity with very low MIC, compared to ampicillin alone *in vitro* (Kinzel et al., 1998; Kinzel and Budzikiewicz, 1999). However, to our knowledge, there has been no follow up *in vivo*. Abdallah and coworkers developed conjugates from pyoverdine that was extracted from *P. aeruginosa* ATCC 15692 and fluoroquinolones (norfloxacin) (Hennard et al., 2001). The conjugates showed antibacterial activity against *E. coli*, however when tested against several *P. aeruginosa* strains, the compounds failed to exhibit any killing, presumably because the fluoroquinolone moiety could not cross *P. aeruginosa* inner membrane (Fluoroquinolones inhibit bacterial DNA gyrase) (Hennard et al., 2001). This study also highlighted the complexity that arises from the three different types of pyoverdine, which would restrict the spectrum of treatable *Pseudomonas* pathogens. (Mislin and Schalk, 2014).

1.3.4.2 Pyochelin is the second main *P. aeruginosa* siderophore

P. aeruginosa second main siderophore is pyochelin. Pyochelin is binding Fe^{3+} with a lower affinity than pyoverdine ($10^{-28.8}$ M^{-2} compared to 10^{-32} M^{-1}) (Brandel et al., 2012). The pyochelin molecule is smaller than pyoverdine (Figure 1.11) and the biosynthesis is less energy-costly than the pyoverdine biosynthesis because it involves fewer steps and enzymes. Pyochelin biosynthesis occurs in the cytoplasm (Serino et al., 1997). Two operons, *pchDCBA* and *pchEFGHI*, are responsible for pyochelin biosynthesis (Gaille et al., 2003). The first step involves the modification of the precursor salicylate by two cytoplasmic enzymes: the isochorismate synthetase PchA (Gaille et al., 2003; Serino et al., 1995) and the isochorismate pyruvate-lyase PchB (Gaille et al., 2002). The precursor is then activated by PchD and further assembled by two NRPSs PchE and PchF. The reduction of the precursor by the reductase PchG forms pyochelin (Figure 1.12) (Gasser et al., 2015).

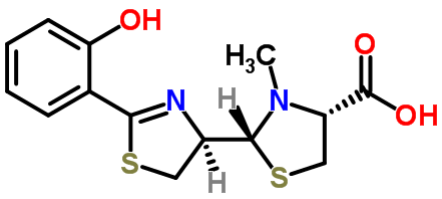

Figure 1.11: Pyochelin structure.

The regulatory gene PchR and the operon *fptABCX* that is responsible for the pyochelin transport, are located next to the operons for pyochelin biosynthesis *pchDCBA* and *pchEFGHI* (Reimmann, 2012). These three operons are repressed by Fur in the presence of iron and activated by PchR complexed to ferripyochelin and pyochelin itself when iron is scarce (Reimmann, 2012). The complexe ferripyochelin induces the expression

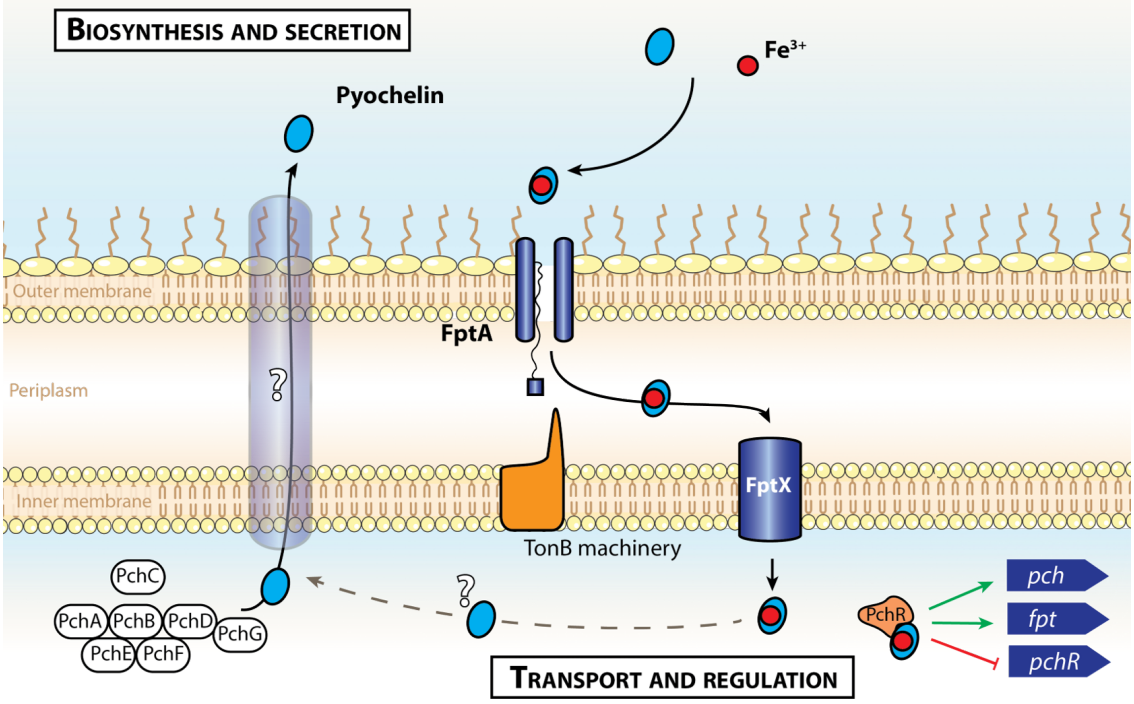

Figure 1.12: Pyochelin biosynthesis, transport and regulation.

of pyochelin synthesis and transporters and represses the expression of *pchR* (Reimmann, 2012). FptA is the transporter involved in ferripyochelin transport across the outer membrane (Ankenbauer and Quan, 1994). Once in the periplasm, the complex ferripyochelin is transported across the inner membrane via the permease FptX (Cuív et al., 2004). The mechanisms of the dissociation of the complex in the periplasm and the secretion/potential recycling of pyochelin are not yet understood (Reimmann, 2012). Like pyoverdine, pyochelin is able to bind to a wide spectrum of metals: Ag^{+}, Al^{3+}, Cd^{2+}, Co^{2+}, Cr^{2+}, Cu^{2+}, Eu^{3+}, Ga^{3+}, Hg^{2+}, Mn^{2+}, Ni^{2+}, Pb^{2+}, Sn^{2+}, Tb^{3+}, Tl^{+}, and Zn^{2+} but its affinity for iron is the highest (Braud et al., 2009). When iron availability decreases, there is a switch in *P. aeruginosa* that goes from pyochelin to pyoverdine production (Dumas et al., 2013). This switch can also be triggered by changes in temperature and pH (Dumas et al., 2013).

Pyochelin could be a promising candidate for the Trojan horse strategy because the molecule is smaller than pyoverdine. Several groups tried to developed pyochelin conjugates and failed because of the lack of conjugate solubility under physiological conditions and hydrolysis problem of the spacer arm in the extracellular medium (Mislin and Schalk, 2014). Furthermore, pyochelin has been shown to cause oxidative damages and inflammation, especially in the presence of the pyocyanin toxin (Britigan et al., 1994). Pyochelin production was increased in a synthetic CF sputum medium (Hare et al., 2011). However, a contradictory study measured the concentration of pyochelin in 148 sputum samples from 36 CF patients and could not detect any pyochelin (Martin et al., 2011). In chronic in-

fections, such as in CF lungs, the production of pyochelin might contribute to the on-going inflammatory response which is known to occur and cause damage to tissues (Cornelis and Dingemans, 2013). Pyochelin is consequently not a good candidate for the Trojan horse approach.

1.3.4.3 *P. aeruginosa* produces an endogenous metallophore

Recently, a third endogenous siderophore was reported in *P. aeruginosa* PAO1 (Gi et al., 2014). In this study, they found that PA4834 (PA14_63910 in UCBPP-PA14) has an important role in iron uptake in an artificial lung medium (Gi et al., 2014). PA4834 encodes a putative nicotianamine synthase (Winsor et al., 2016). Nicotianamine is a metabolite that is essential in the homeostasis of iron, copper, nickel, and zinc (Curie et al., 2009; Walker and Waters, 2011) in plants. Nicotianamine is the first precursor of phytosiderophores, a family of molecules that shares functional characteristics with siderophores (Hell and Stephan, 2003). Nicotianamine was first identified in leaves of tobacco plants and was found, subsequently, in all naturally occurring plants (Noma et al., 1971). Nicotianamine is present at varying concentrations, up to 400 µmol g^{-1} fresh mass has been reported in growing tissues (Stephan et al., 1996). It forms strong complexes with heavy metals (Beneš et al., 1983; Callahan et al., 2007; Ghssein et al., 2016; Zhou et al., 2013), including Fe^{2+} and Fe^{3+} (Wirén et al., 1999) (Table 1.3). In the presence of both Fe^{2+} and Fe^{3+}, nicotianamine chelates preferentially Fe^{2+}, suggesting that the complex nicotianamine-Fe^{2+} is kinetically stable under aerobic conditions (Wirén et al., 1999). By binding to Fe^{2+}, the complex prevents the cell from oxidative damages (Wirén et al., 1999).

PA4834 is organized in an operon that includes three other gene members: the two hypothetical proteins PA4835 and PA4836, and one TBDT transporter PA4837 (respectively PA14_63960) (Winsor et al., 2016). Gi and coworkers showed that the mutant Δ*PA4834* exhibited growth defects in artificial lung sputum. These defects in growth were restored by the addition of 100 µM iron or 100 µM nicotianamine, thus suggesting an iron scavenging role for nicotianamine (Gi et al., 2014). Another recent study revealed the presence of biosynthesis and trafficking pathways of a structurally related nicotianamine, staphylopine, in *Staphylococcus aureus* (Figure 1.13) (Ghssein et al., 2016). Bioinformatic analyses revealed that *P. aeruginosa* nicotianamine operon presents genes for putative biosynthetic enzymes and transport proteins that are homologous to genes of the *cnt* cluster, responsible for staphylopine synthesis (Ghssein et al., 2016; Neumann et al., 2017). Ghessein and coworkers also confirmed the broad-spectrum of heavy metal substrates for staphylopine as shown in previous studies (Callahan et al., 2007).

Nicotianamine synthase, the enzyme responsible for the biosynthesis of nicotianamine, is conserved in *P. aeruginosa*, but the functions of the others genes present in the

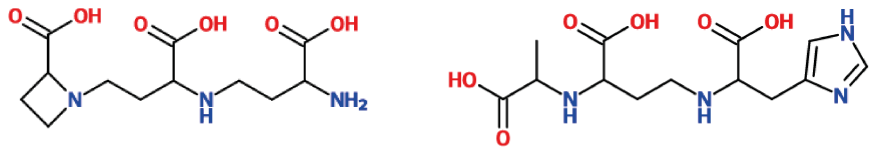

Figure 1.13: Nicotianamine vs. staphylopine structure.

K_a	Ni^{2+}	Zn^{2+}	Fe^{3+}	Fe^{2+}	Cu^{2+}	Co^{2+}
Nicotianamine	16.1	14.7, 15.4	20.6	12.1–12.8	18.6	14.8

Table 1.3: Nicotianamine affinity constant K_a to different metals. Adapted from (Callahan et al., 2007)

operon, need to be investigated. Applications of nicotianamine in plants and agriculture have been widely exploited (Jones and Wildermuth, 2011). The molecule serves as an antihypertensive substance in humans (Hayashi and Kimoto, 2007; Usuda et al., 2009). Hence, it would be interesting to synthesize nicotianamine-based antibiotic conjugates as Trojan horse.

1.3.4.4 *P. aeruginosa* benefits from host iron reservoir

P. aeruginosa can extract heme from hemoproteins via two TBDT-related systems Has and Phu (Figure 1.14) (Ochsner et al., 2000). UCBPP-PA14 encodes for two other potential heme uptake systems: HxuC (PA14_47380) which is similar to the transporter involved in hemopexin utilisation of *H. influenzae* (Cope et al., 1994), and OptI (PA14_64710), which is annotated as extracellular heme binding protein on UCBPP-PA14 (Winsor et al., 2016). These last two candidates have not yet been studied in *P. aeruginosa*.

Pseudomonas heme uptake (Phu) system

The *Pseudomonas* heme uptake (Phu) system was identified in a screen for iron regulated genes by Ochsner and coworkers (Ochsner and Vasil, 1996). PhuR is the TBDT that is responsible for direct heme uptake (Ochsner et al., 2000). PhuS has been described as the intracellular heme trafficking protein (Kaur et al., 2009). PhuR is negatively regulated by Fur and *phuSTUVW* by three regulatory sRNA under the control of Fur (Oglesby-Sherrouse and Vasil, 2010). Under iron-deficient conditions, heme is directly extracted by PhuR from hemoglobin, haptoglobin-hemoglobin, hemopexin and myoglobin (Tong and Guo, 2009).

Heme acquisition system (Has)

P. aeruginosa has an alternative system, which involves the secreted extracellular

hemophore HasA, which captures free or haemoglobin-bound heme (Létoffé et al., 1999). The hemophore-heme complex is then shuttled by another specific TBDT HasR (Létoffé et al., 1999). HasR is able to transport free heme but this transport is less efficient than the transport of the complexe heme-HasA. Indeed, the hemophore HasA has a higher affinity for heme (10^{-11} M) than HasR (10^{-6} M) (Létoffé et al., 2001; Létoffé et al., 2004; Tong and Guo, 2009).

Once in the periplasm, heme is bound by PhuT, a periplasmic binding protein (Tong and Guo, 2007) and is then internalized through the inner membrane by the ATP-dependent permeases PhuUVW, which transfer heme to PhuS, a cytoplasmic heme-binding protein (Lansky et al., 2006). Afterwards, heme is delivered to the heme oxygenase HemO, where it is degraded to form biliverdin, CO, and Fe^{2+}(Cornelis and Dingemans, 2013). PhuR and HasR might not be redundant, because it was suggested that HasR predominantly plays a role in sensing heme in the environment, while PhuR achieves the heme uptake and utilisation (Anzaldi and Skaar, 2010; Smith and Wilks, 2015).

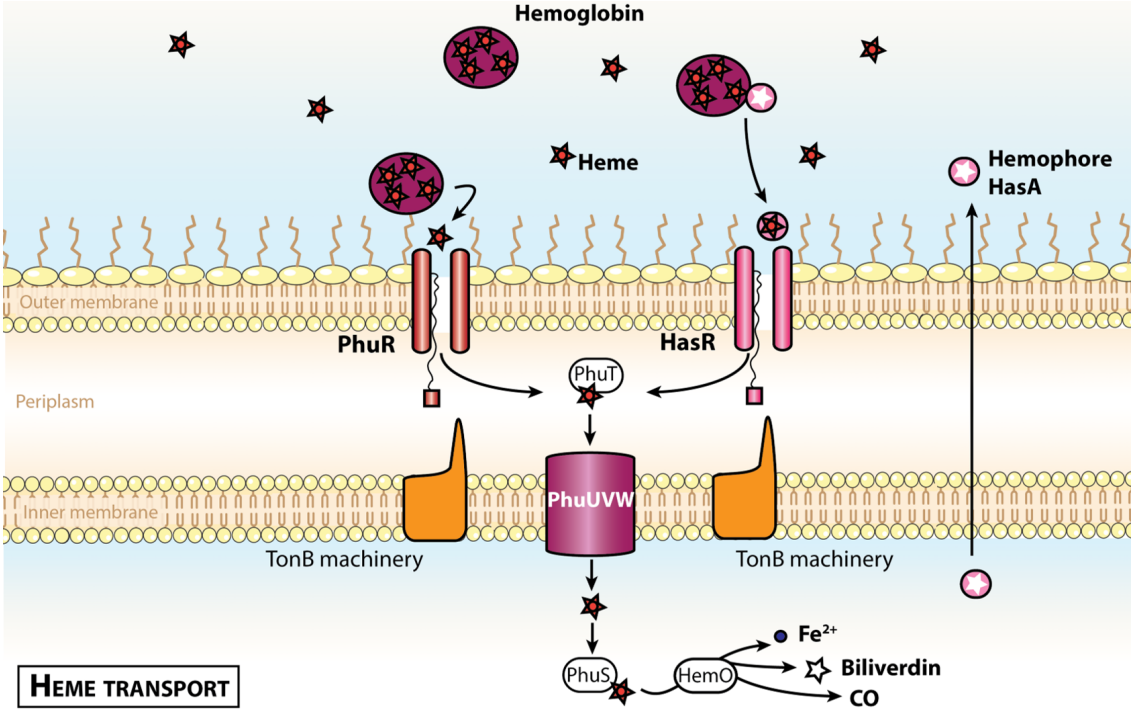

Figure 1.14: Heme transport systems Phu and Has.

There has been research conducted on the use of the so-called non-iron metalloporphyrins, e.g. heme-mimetics. Some metalloporphyrins severely impaired the growth of Gram-positive and Gram-negative pathogenic bacteria such as *A. baumannii* (Moriwaki et al., 2011). The porphyrin coupled with gallium showed promising *in vitro* results, as the Ga^{3+} ligand chemistry shares similarity with that of the Fe^{3+} for the metalloprophyrin (Moriwaki et al., 2011). The compound inhibited the growth of a range of pathogens (Stojiljkovic et al., 1999; Moriwaki et al., 2011). The compound is thought to exploit

the heme uptake pathway of the pathogens, generating reactive oxygen species in the cell, which lead to toxicity and cell death (Stojiljkovic et al., 1999; Moriwaki et al., 2011). Few studies have investigated these non-iron metalloporphyrins as drug delivery targets (Stojiljkovic et al., 1999; Moriwaki et al., 2011).

Following the example of metallo-conjugates, Trojan horse studies have been carried on heme-mimetics. A recent example of this approach is GaPPIX [i.e., Ga^{3+} coupled with the heme precursor protoporphyrin IX (Anzaldi and Skaar, 2010; Hijazi et al., 2017). This compound showed good antibacterial activity against several bacterial species, including *Staphylococcus aureus* and *A. baumannii* (Hijazi et al., 2017). GaPPIX was shown to mainly exploit the Phu uptake pathway in order to enter bacterial cells, where it could then substitute heme in heme-containing enzymes, including cytochromes, catalases, and peroxidases, therefor resulting in the perturbation of bacterial respiration (Anzaldi and Skaar, 2010; Hijazi et al., 2017). Clinical strains were sensitive to GaPPIX *in vitro* and studies on human cell lines showed no cytotoxicity (Hijazi et al., 2017). *In vivo* investigation should be carried out in order to conclude on the efficacy of this approach.

1.3.4.5 *P. aeruginosa* is involved in siderophore piracy

P. aeruginosa is able to utilize siderophores that are produced by other micro-organisms, called the xenosiderophores (Cornelis and Dingemans, 2013). This siderophore piracy confers to the pathogen a fitness advantage over its competitors in the environment (Luján et al., 2015). *P. aeruginosa* saves the biosynthesis cost of producing siderophores and it deprives its competitors from their iron source (Luján et al., 2015). *P. aeruginosa* metabolic diversity allows the pathogen to colonize a wide range of niches with dynamic microbial diversity. Consequently, the xenosiderophores play an important role in its iron acquisition (Cornelis and Dingemans, 2013). Twelve transporters have been described in UCBPP-PA14 (directly or inferred from homology) to transport xenosiderophore (Table 1.2).

Most of the TBDTs, including FepA, PiuA, PirA and BfrG, that are involved in xenosiderophore uptake, have been studied *in vitro*, as part of the predicted translocation pathways for drug transport using the Trojan horse approach (Köhler et al., in prep). Catecholates are among the most common iron-chelating compounds used in synthetic siderophore-antibiotic conjugates (Gasser et al., 2016). Several studies have reported *in vitro* antibacterial activity of the catechol-antibiotic conjugates, showing lower MIC than the antibiotic alone (Ghosh and Miller, 1996; Poras et al., 1998; Heinisch et al., 2002; Ji et al., 2012; Fardeau et al., 2014; Paulen et al., 2015; Gasser et al., 2016; Nairn et al., 2017). These studies reported also that the antibacterial activity was measured under iron-deficient conditions, highlighting the crucial role of xenosiderophore TBDTs in the uptake of the conjugates, particularly of the enterobactin-related pathways such as PiuA and PirA. Enterobactin, produced by *E. coli* is the tricatechol siderophore with the highest affinity for iron 10^{52} M^{-1} (Raymond

et al., 2003). This value is even larger than pyoverdine 10^{32} M^{-1} or the strong synthetic metal chelator EDTA (10^{25} M^{-1}) (Walsh et al., 1990). For most of these conjugates, potent *in vivo* antibacterial activity needs to be demonstrated.

Another interesting alternative that was proposed is the use of metallo-complex to increase toxicity in bacteria. In this approach, metal properties are exploited instead of antibiotics (Banin et al., 2008). Banin and coworkers attempted to replace Fe^{3+} by Ga^{3+} in the ferriferrioxmine B siderophore, because Ga^{3+} shares similar properties with Fe^{3+} and could interfere with iron metabolism. The galliferrioxamine complex acts by a "push and pull" mechanism, releasing gallium in the cell and immediately sequestering iron at iron binding sites of proteins (Banin et al., 2008). This compound showed inhibition of *P. aeruginosa* growth and decrease in biofilm formation *in vitro* (Banin et al., 2008). *In vivo* applications were not successful because the gallium complex seemed to reduce formation of reactive oxygen species in *P. aeruginosa*, therefor contributing to the expansion of the infection (Banin et al., 2008).

1.4 Motivation and problem statement

1.4.1 Failures of the Trojan horse approach

Hurdles associated with the development of new drugs arise from the remarkable versatility of *P. aeruginosa*. Numerous siderophore-antibiotic conjugates based on the Trojan horse strategy have been developed for over 50 years by both pharmaceutical industries and academics (Page, 2013; Mislin and Schalk, 2014). These past five years, five promising siderophore-antibiotics conjugates were developed by different pharmaceutical companies: the siderophore-conjugated monocarbam MC-1 (McPherson et al., 2012a) and the siderophore-conjugated monobactam MB-1 (Tomaras et al., 2013) by Pfizer, the siderophore monosulfactam BAL30072 by Basilea Pharmaceutica (Livermore, 2009), the siderophore-conjugated monocarbam SMC-3176 by AstraZeneca (Kim et al., 2015a) and the catechol-substituted siderophore cephalosporin S-649266 (Cefiderocol) by Shionogi Pharmaceuticals (Kohira et al., 2016) (Figure 1.15). Out of these five conjugates, only S-649266 and BAL30072 conjugates reached clinical trials (Tillotson, 2016). However, Basilea Pharmaceutica recently announced that BAL30072 development program has terminated (*Basilea reports 2016 half-year results*).

The four conjugates (MC-1, MB-1, SM-3176 and BAL30072) exhibited high *in vitro* antibacterial activity measured by MIC changes for various clinical strains (McPherson et al., 2012a; Tomaras et al., 2013; Kim et al., 2015a; Tillotson, 2016). The antibacterial activity of the conjugates was increased under iron-deficient conditions, therefore MIC studies were determined on iron-deficient media such as chelated MHB with subsequent addition of essential non-iron metals (McPherson et al., 2012a; Tomaras et al., 2013; Kim

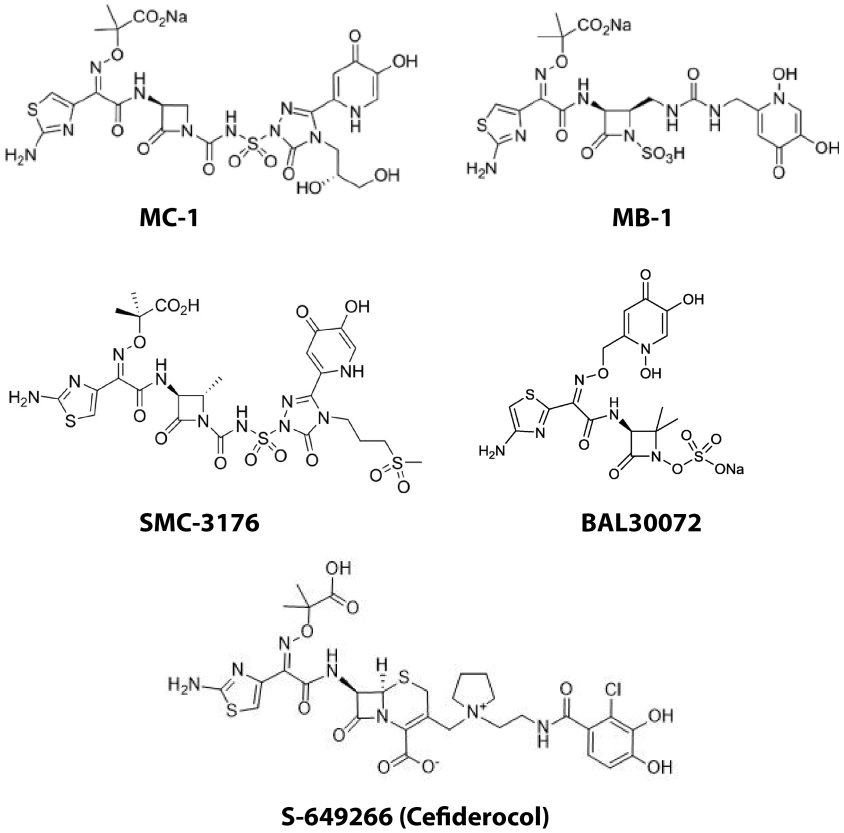

Figure 1.15: Synthetic siderophore-drug conjugates. Molecular structures of the siderophore-conjugated monocarbam MC-1 (McPherson et al., 2012a) and the siderophore-conjugated monobactam MB-1 (Tomaras et al., 2013) by Pfizer, the siderophore monosulfactam BAL30072 by Basilea Pharmaceutica (Livermore, 2009; Page et al., 2010), the siderophore-conjugated monocarbam SMC-3176 by AstraZeneca (Kim et al., 2015a) and the catechol-substituted siderophore cephalosporin S-649266 (Cefiderocol) by Shionogi Pharmaceuticals (Kohira et al., 2016).

et al., 2015a; Tillotson, 2016). These studies also highlighted that the susceptibility of *P. aeruginosa* (and *A. baumannii* for BAL30072) is mediated through PiuA and alternatively PirA (to a lesser extent) which is not surprising because of the chemical similarities of the four conjugates (McPherson et al., 2012a; Tomaras et al., 2013; Kim et al., 2015a; Tillotson, 2016). Despite these encouraging *in vitro* results, the different studies exposed a lack of correlation between *in vitro* MIC measurements and *in vivo* antibacterial efficacy of the conjugates using neutropenic and septicemia mouse models (McPherson et al., 2012a; Tomaras et al., 2013; Kim et al., 2015a). In the case of BAL30072, *in vivo* data supported part of the *in vitro* antibacterial activity in *A. baumannii* (Moynié et al., 2017). It was reported that the *in vitro* conditions were not predictive of the *in vivo* efficacy of the conjugates against multiple strains of *P. aeruginosa* (McPherson et al., 2012a; Tomaras et al., 2013; Kim et al., 2015a). Native siderophores such as pyoverdine or enterobactin could attenuate the antibacterial efficacy by competing with the conjugates for iron. It

was thus proposed to inactivate the biosynthesis of these siderophores in order to avoid potentially adaptation-based resistance mechanism to conjugates (Kim et al., 2015a). However, despite the development of new *in vitro* assays, none of the four conjugates reached clinical trials (McPherson et al., 2012a; Tomaras et al., 2013; Kim et al., 2015a; Tillotson, 2016).

In contrast, S-649266 has demonstrated potent *in vitro* and *in vivo* activity against carbapenemase-producing MDR isolates (Ito et al., 2016; Kohira et al., 2016). S-649266 is also thought to exploit the bacterial iron active transport (Ito et al., 2016; Kohira et al., 2016). However, the transporter involved in the translocation of the drug has not yet been identified but PiuA, PirA and PfeA are suspected to transport this compound (Ito et al., 2016; Kohira et al., 2016).

1.4.2 Problem Statement

Extensive research has been done on the development of new classes of antibiotics that could target surface exposed proteins. The Trojan horse approach, targeting the bacterial active transporters, seems to be a propitious approach to increase the antibiotics uptake in the bacteria. However, the recent failures of the Trojan horse approach highlighted two main issues:

(i) **the gap of knowledge on *P. aeruginosa* physiology *in vivo***. In order to prevent the rapid development of resistance, we need to have a broader understanding of how porins are modulated according to their environment. Therefore, a better understanding of bacterial transport specificities and of its importance in infected hosts should guide a rational drug design for novel therapeutic approach to eradicate *P. aeruginosa*.

(ii) **the lack of correlation between *in vitro* and *in vivo***. We need better *in vitro* conditions that can mimic *in vivo* situations for further conjugate developments in order to prevent the attenuation of conjugates efficacy *in vivo* and the development of resistance.

1.4.3 Goals of my PhD

This PhD project was part of the Translocation project, an Innovative Medicines Initiatives (IMI) antimicrobial resistance (AMR) program called New Drugs for Bad Bugs (ND4BB). Translocation aims to increase the overall understanding of antibiotics translocation and efflux mechanisms in multi-resistant Gram-negative bacteria such as the ESKAPE pathogens (*Enterococcus faecium*, *Staphylococcus aureus*, *Klebsiella pneumoniae*, *Acinetobacter baumannii*, *Pseudomonas aeruginosa*, and *Enterobacter* species).

This PhD project aims to strengthen the knowledge on porins expression and functions during infection, with a main focus on TonB-Dependent Transporters (TBDTs). Understanding the contribution of porins during infection could bring insights on *P. aeruginosa* physiology *in vivo* and could establish a basis for the development of rational therapeutic options. To achieve the aim of my PhD, I addressed three specific questions:

1. Which TonB-dependent transporters are expressed *in vivo*, i.e. in different animal models and human patients?
2. Which TonB-dependent transporters are essential for *P. aeruginosa in vivo* fitness?
3. What could be the implications of my results for the Trojan horse approach and the development of future specific siderophore conjugates?

To accomplish this aim, we combined (i) ultrasensitive quantitative methods to determine the absolute *in vivo* expression of *Pseudomonas aeruginosa* TBDTs in different hosts; and (ii) competitive infections to assess individual TBDT mutant fitness against the wild-type,

allowing for a better representation of the disease dynamic and the emergence of the resistant clones.

1.5 Thesis Structure

This thesis is written in cumulative form. It includes a general introduction to introduce the goals of my thesis, followed by a paper in preparation on my main project, and additional papers to which I contributed: one paper in preparation, one submitted paper and two published papers. The results are further discussed and brought into perspectives at the end of the thesis.

Part I: Context

Chapter 1 Fighting *Pseudomonas aeruginosa* from inside

Part II: Main Paper

Chapter 2: Exploiting bacterial iron transport for antibiotic delivery

Part III: Additional Papers

Chapter 3: Role of *Pseudomonas aeruginosa* porins in nutrient uptake and antimicrobial killing

Chapter 4: Limited impact of efflux on clinical multi-drug resistance of *Escherichia coli* and *Pseudomonas aeruginosa*

Chapter 5: Catechol siderophores repress the pyochelin pathway and activate the enterobactin pathway in *Pseudomonas aeruginosa*: an opportunity for siderophore-antibiotic conjugates development

Chapter 6: TonB-Dependent Receptor Repertoire of *Pseudomonas aeruginosa* for Uptake of Siderophore-Drug Conjugates

Part VI: Discussion and Perspectives

Chapter 7: Discussion

Chapter 8: Conclusions and perspectives

Part II

Main paper

2 Exploiting bacterial iron transport for antibiotic delivery

Pamela Saint Auguste[1*], Christian Schleberger[1*], Tamara Schmid[1], Sandra Söderholm[1], Thomas Bock[2], Scott Sucoloski[3], Jennifer Hoover[3], Josh West[3], Klaus Gebhardt[4], Malcolm Page[4], Michael Hogardt[5], Dominik Vogt[6], Olivier Cunrath[1], Adrian Egli[6], Thilo Köhler[7], Dirk Bumann[1]

[1] Infection Biology, [2] Proteomics Core Facility, Biozentrum, University Basel, CH-4056 Basel, Switzerland; [3] Antibacterial Discovery Performance Unit, GlaxoSmithKline, Collegeville, PA, USA; [4] Basilea, CH-4056 Basel, Switzerland; [5] University Hospital, Frankfurt, Germany; [6] University Hospital Basel; [7] Department of Microbiology and Molecular Medicine, University of Geneva, CH-1211 Genève, Switzerland

* These authors contributed equally to the work.

State of the paper: Manuscript in preparation

2.1 Abstract of the paper

Poor compound penetration into bacteria is a key challenge for developing novel antibiotics. The most advanced strategy to overcome this challenge exploits bacterial active uptake of chelated iron, by coupling substrate analogs to bacterial inhibitors ("Trojan horse" antimicrobials). However, incomplete understanding of bacterial iron transport in infected tissues hampers further development. Here, we used ultra sensitive mass spectrometry and extensive mutagenesis to comprehensively determine *in vivo* absolute abundance and function of iron transporters of two key pathogens, *Pseudomonas aeruginosa* and *Acinetobacter baumannii*. This analysis revealed similar *P. aeruginosa* iron transporter patterns during pneumonia in human patients and rodent models, but clear discrepancies to common *in vitro* conditions. Both pathogens primarily scavenged iron with endogenous siderophores, but also expressed transporters for many other substrates including current drug candidates. However, a *P. aeruginosa* mutant lacking 25 such transporters retained wild-type *in vivo* fitness suggesting resistance risks. Together, the data reveal opportunities and challenges for rational development of effectively penetrating antimicrobials, and establish a reverse paradigm for antimicrobial development that starts with pathogen

properties in human patients, validates animal infection models, and then uses these data to establish suitable *in vivo*-like screening conditions.

2.2 Statement of my work

- Design of all the experiments;
- Development of the mutagenesis protocol that allows the generation of markerless deletions in UCBPP-PA14;
- *In vitro* growth in different media;
- Development of the targeted proteomic methods (SRM mainly done by Dr. Christian Schleberger and the PCF): Contribution in the peptides panel creation and set-up of the PRM assay (together with Dr. Sandra Söderholm and the PCF);
- Proteomic sample preparation and data analysis;
- Development of an optimized intranasal model for UCBPP-PA14;
- Animal experimentation and data analysis.

2.3 Draft paper

Exploiting Bacterial Iron Transport for Antibiotic Delivery

Pamela Saint Auguste[1*], Christian Schleberger[1*], Tamara Schmid[1], Sandra Söderholm[1], Thomas Bock[2], Scott Sucoloski[3], Jennifer Hoover[3], Josh West[3], Klaus Gebhardt[4], Malcolm Page[4], Michael Hogardt[5], Dominik Vogt[6], Alexander Schmidt[2], Olivier Cunrath[1], Adrian Egli[6], Thilo Köhler[7], Dirk Bumann[1]

[1]Infection Biology, [2]Proteomics Core Facility, Biozentrum, University Basel, CH-4056 Basel, Switzerland; [3]Antibacterial Discovery Performance Unit, GlaxoSmithKline, Collegeville, PA, USA; [4]Basilea, CH-4056 Basel, Switzerland; [5]University Hospital, Frankfurt, Germany; [6]University Hospital Basel, CH-4056 Basel, Switzerland; [7]Department of Microbiology and Molecular Medicine, University of Geneva, CH-1211 Genève, Switzerland

Correspondence and requests for materials should be addressed to dirk.bumann@unibas.ch.

Dirk Bumann

Biozentrum

Klingelbergstrasse 50/70

CH-4056 Basel

Phone: +41 61 207 2382

Abstract

Poor compound penetration into bacteria is a key challenge for developing novel antibiotics. The most advanced strategy to overcome this challenge exploits bacterial active uptake of chelated iron, by coupling substrate analogs to bacterial inhibitors ("Trojan horse" antimicrobials). However, incomplete understanding of bacterial iron transport in infected tissues hampers further development. Here, we used ultrasensitive mass spectrometry and extensive mutagenesis to determine *in vivo* absolute abundance and fitness contribution of iron transporters of two key pathogens, *Pseudomonas aeruginosa* and *Acinetobacter baumannii*. This analysis revealed similar *P. aeruginosa* iron transporter capabilities during pneumonia in human patients and rodent pneumonia models, but clear discrepancies to common *in vitro* conditions. Both pathogens primarily scavenged iron with endogenous siderophores, but also expressed transporters for many other substrates including current drug candidates. However, a *P. aeruginosa* mutant lacking 25 such transporters retained wild-type fitness *in vivo* suggesting resistance risks. Together, the data reveal opportunities and challenges for rational development of effectively penetrating antimicrobials, and establish a reverse paradigm for antimicrobial development that starts with pathogen properties in human patients, and uses this to benchmark pre-clinical animal infection models and to establish suitable *in vitro* assay conditions.

Multi-drug resistant pathogens are a major threat to human health worldwide [1]. Novel drugs are urgently required, but their development has been difficult, especially for Gram-negative bacteria [2]. These bacteria have outer membranes with low permeability, which hampers access of many inhibitors to their intracellular targets. On the other hand, Gram-negative bacteria actively transport nutrients such as iron siderophore complexes across the outer membrane using TonB-dependent transporters (TBDTs). Natural and synthetic siderophore analogs that are conjugated to antimicrobials can hijack these TBDTs, thereby boosting antimicrobial translocation and efficacy ('Trojan horse' strategy) [3,4]. Based on extensive efforts in pharmaceutical companies and academia, two conjugate drug candidates have already entered human clinical trials making this the most advanced strategy to overcome the crucial outer membrane permeability barrier [2]. However, conjugate efficacy depends on the respective TBDT abundance, and differential TBDT expression can cause inconsistencies between drug activities *in vitro* and in animal infection models [5-7]. TBDT patterns might deviate even more in human patients due to difference in host genetics and siderophore-producing microbiota, which could put the whole strategy at risk. Yet a systematic characterization of iron transport of key pathogens in infected host tissues is currently lacking.

As part of the Innovative Medicines Initiative project ND4BB-TRANSLOCATION, we focus on two pathogens with largely impermeable outer membranes, *Acinetobacter baumannii* and *Pseudomonas aeruginosa,* which WHO ranked first and second among the twelve bacteria that pose the greatest antimicrobial resistance threat to human health [8]. These pathogens encode a large diversity of TBDTs, most of which are involved in iron uptake (Pseudomonas aeruginosa 35 TBDTs, Acinetobacter baumannii 22 TBDTs; Tab. S1, S2). Almost all P. aeruginosa TBDTs are highly conserved among completely sequenced diverse clinical isolates (Tab. S1) suggesting that each of them confers fitness advantages in some relevant environments. However, in a particular mammalian host tissue probably only a TBDT subset is expressed [9], and this subset will determine if a specific Trojan horse antimicrobial is effectively transported. Analysis of bacterial gene expression in infected host tissues is

challenging because of low numbers of bacteria (often 10^6 cells/ml or less) in a large excess of host proteins [10]. To address these issues, we established ultrasensitive methods to determine absolute *in vivo* quantities of all potentially relevant TBDTs in *P. aeruginosa* and *A. baumannii*, using parallel reaction monitoring (PRM) on a high resolution and accurate mass instrument [11] (Fig. 1A; Tables S1, S2). We achieved attomole sensitivity indicating that in a sample containing 10^5 *P. aeruginosa* or *A. baumannii* cells, we could detect and quantify TBDTs that were present at only 10-50 molecules per cell, even in highly complex human sputum samples with an estimated 1millionfold excess of host proteins (Fig. 1A). We used these methods to quantify *P. aeruginosa* TBDTs in various samples directly taken from acutely infected human patients (urine, tracheal/broncheal secretions, bronchioalveolar lavage, sputum) (Fig. 1B).

P. aeruginosa in urine from patients with urinary tract infections (UTI) had largely homogeneous TBDT patterns indicating that differences in host and *P. aeruginosa* genetics, or individual bladder microbiota, had limited impact on this aspect of *P. aeruginosa* physiology. *P. aeruginosa* expressed transporters for its endogenous siderophores pyoverdine (FpvA/FpvB, our methods detected FpvA I but not variants FpvA II and FpvA III that are present in many clinical isolates [12]) and pyochelin (FptA), as well as heme (especially PhuR, but also HasR and HxuC). *P. aeruginosa* had low and variable levels of transporters for siderophores produced by other microbes ("xenosiderophores"), and commonly expressed the ferri-citrate transporter FecA consistent with high citrate content of urine in most patients [13]. Besides these iron transporters, *P. aeruginosa* had moderate levels of the putative copper transporter OprC [14], but no detectable zinc transporter ZnuD although zinc might be limiting for other UTI pathogens [15]. A recent proteome study of *P. aeruginosa* biofilms on urine catheters from three patients also detected the endogeneous siderophore receptors FpvA, FpvB, and FptA, the heme receptors PhuR, HasR, the citrate transporter FecA, and the putative copper transporter OprC, while ZnuD were undetectable [16]. Although absolute transporter abundances were not determined, these data were generally consistent with our

findings, supporting rather homogeneous *P. aeruginosa* iron transport capabilities during UTI in human patients.

Acute pneumonia is a major indication for current antimicrobial development against Gram-negative bacterial pathogens. Compared to UTI samples, lung secretions are much more challenging for *P. aeruginosa* analysis because of the typically low bacterial loads during acute infection (in contrast to chronic infection in cystic fibrosis patients) combined with a very large excess of host material. As a consequence, no data have been available for TBDT expression, and even in cystic fibrosis patients only very few TBDT transcripts could be detected [17,18]. We found that ultrasensitive PRM methods could partially overcome this issue, at least for samples containing more than about 100'000 *P. aeruginosa* CFU per ml of secretion. Altogether, we could obtain seven such samples from acute pneumonia patients in two hospitals in Switzerland and Germany, respectively. The data revealed largely consistent TBDT patterns indicating that differences in host and *P. aeruginosa* genetics [19,20], or individual airway microbiota [21], had limited impact on this aspect of *P. aeruginosa* physiology. In lung *P. aeruginosa* expressed transporters for its endogenous siderophores pyoverdine (FpvB, the lack of FpvA I might be due to expression of variants FpvA II or III) and pyochelin (FptA), and in contrast to UTI, especially the mucin-inducible transporter OptC for the recently discovered third endogenous siderophore nicotianamine [22]. *P. aeruginosa* had substantial levels of the heme transporter PhuR, and mostly low and variable numbers of transporter molecules for siderophores produce by other microbes ('xensiderophores'), but not FecA in contrast to UTI. Besides these iron uptake systems, *P. aeruginosa* had moderate levels of the putative copper transporter OprC [14] and, again in contrast to UTI, high levels of the zinc transporter ZnuD consistent with zinc starvation [23]. Together, the UTI and pneumonia data showed largely homogeneous, but tissue-specific *P. aeruginosa* TBDT patterns in human patients.

For antimicrobial development, efficacy testing of drug candidates in pre-clinical animal infection models (usually rodent hosts) is mandatory prior to proceeding to human clinical trials. However, it has been unclear if rodent hosts are appropriate for testing Trojan horse

antibiotics, which would require similar *P. aeruginosa* iron transport capabilities as in humans in spite of differences in innate immunity and airway microbiota [24] that might compete with *P. aeruginosa* for heavy metal uptake. To address this issue, we determined TBDT patterns of the virulent strain *P. aeruginosa* UCBPP-PA14 [25] in three different rodent infection models (mouse/rat intratracheal instillation [26]; mouse septicemia [27]) with demonstrated predictive power for standard antibiotics. Both rodent pneumonia models showed good overall agreement with TBDT patterns in human pneumonia, while reproducing differences to human UTI (high OptC and ZnuD, but low FecA). By contrast, blood samples from the septicemia model showed generally lower TBDT levels and particularly less abundant transporters for endogenous siderophores, heme, and zinc, possibly reflecting higher heavy metal availability in this model. These animal model data suggest rather homogeneous, but lung-specific *P. aeruginosa* heavy metal physiology across different host species irrespective of host and *P. aeruginosa* genetics or competing airway microbiota, and support the use of rodent pneumonia models for efficacy testing of Trojan horse antibiotics.

In contrast, commonly used *in vitro* conditions poorly reproduced TBDT patterns in human pneumonia or UTI (Fig. 1B). In iron-replete media, all TBDTs had rather low levels as expected. At low iron levels in CAA and chelexed CAA media many xenosiderophore transporter and particularly the potentially quorum sensing-associated [28] TBDT OptF were abnormally high, while TBDTs with substantial in vivo levels such as the dominant endogenous siderophore transporter OptC and the zinc transporter ZnuD were still poorly expressed. Human serum resulted in a TBDT pattern with similarities to *P. aeruginosa* in blood in the mouse septicemia model. Together, these data suggested that slightly increasing iron concentration in CAA, scavenging of zinc, addition of mucus for OptC induction [22], and lowering *P. aeruginosa* densities, might result in a medium more closely mimicking relevant conditions during human (and rodent) pneumonia.

The discrepancies between *in vitro* and *in vivo* TBDT patterns also suggest an important change to current methods for drug efficacy testing in animal infection models. In

such experiments, all Trojan horse candidates are administered already 1 to 2 hours post infection [5-7,29]. TBDTs turnover strictly depends on bacterial growth and at least two divisions are required to deplete previously present TBDTs in at least half of the daughter cells [30]. *P. aeruginosa* TBDT patterns early after infection will thus largely reflect the *in vitro* conditions that were used to grow the *P. aeruginosa* inoculum, instead of the quite different, but more relevant (and often less favorable) TBDT patterns that appear after the pathogen has fully adapted to the new *in vivo* conditions. Early drug administration thus exploits partially *in vitro* TBDT patterns and is not a realistic test for real *in vivo* efficacy, and should therefore be avoided in future studies.

We also determined *A. baumannii* ATCC-19606 TBDT levels in the rodent pneumonia models that appeared to mimic human pneumonia based on our *P. aeruginosa* data (Fig. 2). *A. baumannii* expressed particularly transporters for its endogenous siderophores baumannoferrin (BfnH and possibly A1S_1667 encoded in close vicinity to the baumannoferrin gene cluster) and acinetobactin (BauA). In addition, multiple TBDTs for xenosiderophores were consistently expressed, often with higher levels in the rat model. The zinc transporter ZnuD had also high abundance, again consistent with zinc starvation in lung. In contrast to *P. aeruginosa*, heme transport capabilities were low based on poor A1S_1606 expression (A1S_1607 has been annotated as another heme-TBDT but its protein sequence is too short for a functional TBDT). Again, various in vitro media poorly reproduced *A. baumannii* in vivo TBDT patterns. Baseline conditions resulted in poor BauA expression, whereas iron depletion led to exaggerated TBDT abundances. Fine tuning of iron concentration and zinc scavenging in Iso-Sensitest broth at low *A. baumannii* densities, might enable more closely mimicking relevant *in vivo* conditions.

Our data suggested *in vivo* presence of several TBDTs that might be exploitable for Trojan horse strategies. However, mutational inactivation of a specific TBDT can rapidly lead to resistance development [31], unless TBDT loss is associated with a fitness disadvantage, or multiple co-expressed TBDTs transport the same compound. Previous studies found a

moderate, but consistent *in vivo* fitness defect in *P. aeruginosa* strains incapable of using pyoverdine [32-35], while data for heme uptake are contradicting [18,34,36]. Individual studies reported large fitness contributions of nicotianamine transporter OptC [22], the ferrichrome/ferioxamine transporter FiuA [37], and the zinc transporter ZnuD [18], but these have not yet been confirmed. To comprehensively determine *in vivo* fitness contributions of potentially redundant TBDTs, we generated a series of strains lacking single, or up to 25 different TBDT genes in the virulent strain *P. aeruginosa* UCBPP-PA14 (Fig. 3A). We tested these strains for *in vivo* fitness in an acute intranasal mouse pneumonia model (Fig. 3B). In contrast to previous studies, which all employed single-strain infections, we used mixed infections to assess mutant fitness in presence of competing wild-type, a scenario more closely mimicking emergence of resistant clones among wild-type bacteria. Under these conditions deletion of *fpvA* (strain "1"), but not the alternative pyoverdine TBDT gene *fpvB* ("2"), resulted in a significant fitness drop. A *fpvA fpvB* double mutant ("3") showed no synergism arguing against an *in vivo* backup function of FpvB for pyoverdine uptake, consistent with low FpvB levels in rodent pneumonia (Fig. 1B). Additional inactivation of pyoverdine biosynthesis by deleting *pvdA* ("4") ameliorated the fitness defect, which could reflect saving of futile biosynthesis costs and/or less local iron deprivation by its own ferri-pyoverdine complexes (which the uptake mutant ("3") generates but cannot scavenge). In contrast to pyoverdine, inactivation of uptake of pyochelin ("5"), or both uptake and synthesis of pyochelin ("6"), or uptake and synthesis of the nicotianamine-related compound ("8") did not decrease *in vivo* fitness in our model, partially in agreement with previous observations [33,34]. However, simultaneous inactivation of uptake and synthesis of all three endogeneous siderophores ("9") diminished in vivo fitness to levels below the pyoverdine-defective mutant ("4"). Additional deletion of *feoB* encoding an inner membrane transporter for ferrous iron ("10"), or another putative siderophore biosynthesis cluster present in a few *P. aeruginosa* strains including UCBPP-PA14 ("11"), had no further fitness effect. These data confirm the primary importance of pyoverdine, and partial compensation by pyochelin [33,34] and/or nicotianamine. To determine the fitness contributions of other in vivo expressed TBDTs, we

deleted nine additional genes (“11”) but this did also not result in further fitness defects indicating that these TBDTs were unable to compensate for blocked utilization of endogenous siderophores. Finally, we constructed a *P. aeruginosa* strain lacking 25 different TBDT genes (but still carrying functional TBDTs for the endogenous siderophores) (“12”). This strain had wild-type *in vivo* fitness, indicating dispensability of transporters for heme and xenosiderophores, at least in this in pneumonia model. Together, these data suggested that *P. aeruginosa* primarily used its high-affinity siderophore pyoverdine for iron scavenging, whereas uptake capabilities for its other endogenous siderophores, xenosiderophores, heme-associated substrates and possibly copper and zinc uptake were all dispensable for *in vivo* fitness in our acute pneumonia model. Low fitness contributions of xenosiderophore receptors might reflect limited delivery of microbiota-produced siderophores to *P. aeruginosa* infection foci in the lung.

The only available data for *A. baumannii* [38] indicate that inactivation of the TBDT BauA specific for the endogenous siderophore acinetobactin, decreased *in vivo* fitness in strain ATCC-19606 (which is defective for biosynthesis of the other, possibly more potent endogenous siderophore baumannoferrin [39]). These data suggest that *A. baumannii* ATCC-19606 cannot compensate blocked uptake of endogenous siderophores using its abundantly expressed ferri-xenosiderophore TBDTs (Fig. 2, data shown were obtained with the same strain) suggesting at most supportive roles for these TBDTs.

The *in vivo* expression and fitness data could provide a rational basis to guide further development of Trojan horse antibiotics for treating Pseudomonas and Acinetobacter infections (Fig. 4; Supplemental Text). Xenosiderophore TBDTs are especially attractive for the Trojan horse strategy because of the extended pathogen spectrum compared to species-specific siderophores. Indeed, all four most advanced siderophore conjugates exploit *P. aeruginosa* TBDTs PirA, PiuA (or its paralog PiuD), and BfrG (also called OptJ; Köhler et al. in prep.), or *A. baumannii* TBDTs PirA and PiuA [40]. *P. aeruginosa* all three relevant TBDTs had rather low abundance compared to other TBDTs in human patients and rodent infection

models, and this might in part explain the variable *in vivo* efficacy of these compounds [5,6]. Siderophores can induce the expression of their transporters [41], and this is also true for PirA induction by the advanced drug candidate BAL30072 (Köhler et al., in prep.). However, induction ratios are typically moderate (less than 10fold), and this does not always substantially increase susceptibility (e.g., PirA-dependent activity of BAL30072 is still weak [42]).

P. aeruginosa expresses at least two or all three TBDTs PiuA, PirA, and BfrG in all tested common *in vitro* conditions including cation-adjusted Müller Hinton broth (MHB), the favored medium for antimicrobial testing and development. This homogeneous expression might contribute to the promising activity and slow resistance development *in vitro* [42] (and *in vivo* efficacy when administrating drug candidates early after infection, see above). Pathogens often encounter severe iron starvation in mammalian tissues [43], but common methods for iron depletion to mimic such conditions *in vitro* lead to overshooting *P. aeruginosa* TBDT abundances well above levels observed in vivo (Fig. 1B). Under such condition, all three crucial TBDTs PiuA, PirA, and BfrG are present in levels of at least a few hundred molecules, which could explain the increased activity of drug candidates [7,44]. However, these attractive properties might not always translate to *in vivo* conditions where *P. aeruginosa* often expresses only one, and sometimes none, of these TBDTs at detectable levels.

In contrast to *P. aeruginosa*, *A. baumannii* consistently expressed low to moderate levels of both PirA and PiuA in the rat model (and low but consistent levels in the mouse model), suggesting a potentially more reliable efficacy of these compounds against *A. baumannii*. Again, iron-depleted in vitro conditions might be exaggerating drug efficacy due to untypically high PiuA and PirA levels.

Both *P. aeruginosa* and *A. baumannii* expressed additional xenosiderophore TBDTs but except for the *A. baumannii* receptors A1S_1725 and A1S_3339 with unknown ferri-siderophore substrates, abundance levels of these TBDTs were rather variable.

TBDT expression and fitness contributions would favor employment of endogenous siderophores that are required for *in vivo* fitness such as pyoverdine, baumannoferrin and acinetopbactin, but challenging chemistry and small potential spectrum would limit their utility. All other substrates for *P. aeruginosa* showed a risk for facile resistance development. Either only a single specific TBDT with no detectable fitness contribution transports such a substrate; or multiple TBDTs could transport the same substrate, but their low-level, scattered expression and low fitness contribution fail to provide robust redundancy for preventing resistance development. Based on these considerations, no TBDT substrate appeared to pass stringent suitability criteria as a basis for mono-therapy against *P. aeruginosa*. However, Trojan horse conjugates to heme analogs targeting PhuR, respectively, might be suitable for combination therapy with another antimicrobial (as previously proposed for BAL30072 [29]). If both small spectrum and combination therapy would be acceptable, pyochelin and nicotianamine transporters FptA and OptC could also be attractive choices.

All these considerations were based on our data for acute infections. The issue is even more complex for chronic *Pseudomonas* infections in cystic fibrosis patients in which TBDT diversifies and changes over time [45-47]. In contrast to these challenging conditions in *P. aeruginosa*, current advanced compounds exploiting *A. baumannii* PirA and PiuA appear to target already the most suitable TBDT targets in this pathogen.

In conclusion, comprehensive *in vivo* analysis of TBDT abundance and fitness contributions provides a rational basis to prioritize specific strategies for implementing the Trojan horse approach. More generally, our study shows how current antimicrobial development paradigms that optimize drug candidates under *in vitro* conditions and in animal infection models with unknown relevance for conditions in human patients, might cause subsequent failures. Instead, we propose a reverse paradigm for antimicrobial development that first determines relevant pathogen properties in human patients, uses these data as benchmark to validate and improve testing methods in animal infection models, and then employs *in vitro* assay conditions that most closely reproduce the relevant pathogen *in vivo*

properties. Ultrasensitive, high-resolution direct analysis of infected patient material as used in this study, might pave the way for broad application of this reverse paradigm to better control human infections.

ACKNOWLEDGEMENTS

This study received support from the Innovative Medicines Initiative Joint Undertaking under Grant Agreement no 115525, resources, which are composed of financial contribution from the European Union's seventh framework program (FP7/2007–2013) and from EFPIA companies in kind contribution, as part of the Project TRANSLOCATION (http://www.imi.europa.eu/content/translocation).

The authors declare no competing financial interests.

Author contributions

P.S.A., C.S., T.S, S.S., T.B., S.S., J.W., K.G., D.V., O.C., T.K. and D.B. performed experiments and analyzed the data; J.H., M.P., M.H., A.S., A.E., and D.B. designed experiments; and P.S.A. and D.B. wrote the paper with input from all authors.

Methods

Bacterial strains, growth conditions, and mutagenesis

For all animal infections and *in vitro* work with *Pseudomonas aeruginosa*, we used strain UBCPP-PA14 [25]. *P. aeruginosa* was routinely grown on lysogeny broth (Lennox-LB) or cation-adjusted Müller-Hinton broth. Clean gene deletions were generated by two-step allelic exchange using gentamicin and sucrose for positive and negative selection respectively [48], and confirmed by sequencing. Strains with multiple deletions were confirmed for all atered loci using PCR.

For all animal infections and *in vitro* work with *Acinetobacter baumannii*, we used strain ATCC 19606 [49]. This strain was routinely grown on cation-adjusted Müller-Hinton broth.

Human samples

Urine, sputum, tracheal secretions, and bronchioalveolar lavage samples from infected patients were obtained from material obtained for medical microbiology diagnostics. All samples were anonymized and freshly processed upon arrival at the in-house diagnostic laboratory (irrespective of having culture confirmation for *P. aeruginosa*). Samples not containing *P. aeruginosa* were subsequently discarded.

Animal infection models

Intratracheal instillation model: specific pathogen free (SPF) immunocompetent male Sprague-Dawley rats weighing 100 - 120 g or male CD-1 mice weighing 20 - 25 g were infected by depositing an agar bead containing around 10^7 colony-forming units *P. aeruginosa* UCBPP-PA14 or *Acinetobacter baumannii* ATCC 19606, deep into the lung via nonsurgical

intratracheal intubation [26]. At 24 h post infection, animals were sacrificed and lung was homogenized in sterile saline using a lab blender. All procedures are in accordance with protocols approved by the GSK Institutional Animal Care and Use Committee (IACUC), and meet or exceed the standards of the American Association for the Accreditation of Laboratory Animal Care (AAALAC), the United States Department of Health and Human Services and all local and federal animal welfare laws.

Septicemia model: male CD-1 mice were infected by intraperitoneal injection of around 10^5 colony-forming units *P. aeruginosa* UCBPP-PA14 in 750 µl 0.9 % NaCl, 3.3% porcine stomach mucin (Sigma, M-2378) [27]. Animals were observed carefully and euthanized when the surface body temperature dropped under 25°C and/or the general health score reached predefined termination criteria. The animals were killed with pentobarbital (200 mg/kg) and the blood was taken via heart puncture in heparine coated vials. All procedures were approved (license 1927, Kantonales Veterinäramt Basel) and performed according to local guidelines (Tierschutz-Verordnung, Basel) and the Swiss animal protection law (Tierschutz-Gesetz).

Intranasal model: Female BALB/c mice were exposed to 2.5% isoflurane delivered in O_2 (2 l/min) within a 1 liter induction chamber until a state of areflexia was reached. Mice were then removed from the induction chamber and instillation was performed immediately by pipetting by pipetting 25 µl of PBS containing $5x10^6$ colony-forming units *P. aeruginosa* UCBPP-PA14 from exponentially growing cultures [50] onto the outer edge of each nare of the mice [51]. Mice were euthanized at 10 h post infection by intraperitoneal injection of 300 µl water containing 6 mg xylazine and 15 mg ketamine. The lungs were recovered and homogenized in 2 ml PBS using a cell strainer. For competitive fitness determination, various mutants were mixed with wild-type *P. aeruginosa* and administrated together. Lungs from sacrificed mice were plated on LB plates. Colonies were typed using multiplex PCR. Competitive indices were calculated as $(output_{mutant}/output_{wild\text{-}type})/(input_{mutant}/input_{wild\text{-}type})$. Competitive indices were log-normally distributed permitting parametric testing for statistical significance after log-transformation. All procedures were approved (license 2746, Kantonales Veterinäramt Basel) and performed

according to local guidelines (Tierschutz-Verordnung, Basel) and the Swiss animal protection law (Tierschutz-Gesetz).

Sample workup for proteomics

The sample workup protocol was optimized to deplete host material while maintaining *P. aeruginosa* viability until lysis. All buffers and equipment were used at 0 to 4°C to minimize proteome changes during sample workup. The sample volume (maximum of 1 ml) was estimated and an equal volume of 1% Tergitol in PBS was added followed by vigorous vortexing for 30 s. After centrifugation at 500xg for 5 min, the supernatant was transferred to a fresh tube, and the pellet was extracted again with 2 ml 0.5% Tergitol in PBS. The supernatant was combined with the first supernatant and centrifuged at 18'000xg for 5 min. The pellet was washed with 2 ml and again centrifuged at 18'000xg for 5 min.

The supernatant was removed, and the pellet was resuspended in 100 µL 5% sodium deoxycholate, 5 mM Tris(2-carboxyethyl)phosphine hydrochloride, 100 mM NH_4HCO_3. The sample was incubated at 90°C for 1 min. and then stored at -80 °C. Samples were thawed and sonicated for 2x20 s (1 s interval, 100% power). Proteins were alkylated with 10 mM iodoacetamide for 30 min in the dark at room temperature. Samples were diluted with 0.1M ammonium bicarbonate solution to a final concentration of 1% sodium deoxycholate before digestion with trypsin (Promega) at 37°C overnight (protein to trypsin ratio: 50:1). After digestion, the samples were supplemented with TFA to a final concentration of 0.5% and HCl to a final concentration of 50 mM. Precipitated sodium deoxycholate was removed by centrifugation at 4°C and 14'000 rpm for 15 min. Peptides in the supernatant were desalted on C18 reversed phase spin columns according to the manufacturer's instructions (Macrospin, Harvard Apparatus), dried under vacuum, and stored at −80°C until further processing.

Parallel reaction monitoring

Heavy proteotypic peptides (JPT Peptide Technologies GmbH) were chemically synthesized for *P. aeruginosa* and *A. baumannii* TBDTs and *P. aeruginosa* OprF (Tables S1, S2). Peptides were chosen dependent on their highest detection probability and their length ranged between 7 and 20 amino acids. Heavy proteotypic peptides were spiked into each sample as reference peptides at a concentration of 20 fmol of heavy reference peptides per 1 µg of total endogenous protein mass. For spectrum library generation, we generated parallel reaction-monitoring (PRM) assays [11] from a mixture containing 500 fmol of each reference peptide. The setup of the µRPLC-MS system was as described previously [52]. Chromatographic separation of peptides was carried out using an EASY nano-LC 1000 system (Thermo Fisher Scientific) equipped with a heated RP-HPLC column (75 µm x 37 cm) packed in-house with 1.9 µm C18 resin (Reprosil-AQ Pur, Dr. Maisch). Peptides were separated using a linear gradient ranging from 97% solvent A (0.15% formic acid, 2% acetonitrile) and 3% solvent B (98% acetonitrile, 2% water, 0.15% formic acid) to 30% solvent B over 60 minutes at a flow rate of 200 nl/min. Mass spectrometry analysis was performed on Q-Exactive HF mass spectrometer equipped with a nanoelectrospray ion source (both Thermo Fisher Scientific). Each MS1 scan was followed by high-collision-dissociation (HCD) of the 10 most abundant precursor ions with dynamic exclusion for 20 seconds. Total cycle time was approximately 1 s. For MS1, 3e6 ions were accumulated in the Orbitrap cell over a maximum time of 100 ms and scanned at a resolution of 120,000 FWHM (at 200 m/z). MS2 scans were acquired at a target setting of 1e5 ions, accumulation time of 50 ms and a resolution of 30,000 FWHM (at 200 m/z). Singly charged ions and ions with unassigned charge state were excluded from triggering MS2 events. The normalized collision energy was set to 35%, the mass isolation window was set to 1.1 m/z and one microscan was acquired for each spectrum.

The acquired raw-files were converted to the mascot generic file (mgf) format using the msconvert tool (part of ProteoWizard, version 3.0.4624 (2013-6-3)). Converted files (mgf format) were searched by MASCOT (Matrix Sciences) against normal and reverse sequences (target decoy strategy) of the UniProt database of *Pseudomonas aeruginosa* UCBPP-PA14

and 3 additional proteins (PiuD, FpvA II, FpvA III) from other *P. aeruginosa*, or *Acinetobacter baumannii* strains ATCC 19606 and ATCC 17978, as well as commonly observed contaminants. The precursor ion tolerance was set to 20 ppm and fragment ion tolerance was set to 0.02 Da. Full tryptic specificity was required (cleavage after lysine or arginine residues unless followed by proline), three missed cleavages were allowed, carbamidomethylation of cysteins (+57 Da) was set as fixed modification and arginine (+10 Da), lysine (+8 Da) and oxidation of methionine (+16 Da) were set as variable modifications.

For quantitative PRM experiments the resolution of the orbitrap was set to 30,000 FWHM (at 200 m/z) and the fill time was set to 50 ms to reach a target value of 1e6 ions . Ion isolation window was set to 0.7 Th and the first mass was fixed to 100 Th. Each condition was analyzed in biological triplicates. All raw-files were imported into Spectrodive (Biognosys AG) for protein and peptide quantification. To control for variation in injected sample amounts, three peptides belonging to the abundant, constitutively expressed protein OprF were also included in the quantification and used for normalization using a value of 26’000 copies per cell as determined from in vitro cultures under diverse culture conditions.

REFERENCES

1 Holmes, A. H. *et al.* Understanding the mechanisms and drivers of antimicrobial resistance. *Lancet* **387**, 176-187, doi:10.1016/S0140-6736(15)00473-0 (2016).

2 Bush, K. & Page, M. G. What we may expect from novel antibacterial agents in the pipeline with respect to resistance and pharmacodynamic principles. *Journal of pharmacokinetics and pharmacodynamics*, doi:10.1007/s10928-017-9506-4 (2017).

3 Page, M. G. Siderophore conjugates. *Annals of the New York Academy of Sciences* **1277**, 115-126, doi:10.1111/nyas.12024 (2013).

4 Mislin, G. L. & Schalk, I. J. Siderophore-dependent iron uptake systems as gates for antibiotic Trojan horse strategies against Pseudomonas aeruginosa. *Metallomics : integrated biometal science* **6**, 408-420, doi:10.1039/c3mt00359k (2014).

5 Tomaras, A. P. *et al.* Adaptation-based resistance to siderophore-conjugated antibacterial agents by Pseudomonas aeruginosa. *Antimicrob Agents Chemother* **57**, 4197-4207, doi:10.1128/AAC.00629-13 (2013).

6 Kim, A. *et al.* Pharmacodynamic Profiling of a Siderophore-Conjugated Monocarbam in Pseudomonas aeruginosa: Assessing the Risk for Resistance and Attenuated Efficacy. *Antimicrob Agents Chemother* **59**, 7743-7752, doi:10.1128/AAC.00831-15 (2015).

7 Tillotson, G. S. Trojan Horse Antibiotics-A Novel Way to Circumvent Gram-Negative Bacterial Resistance? *Infectious diseases* **9**, 45-52, doi:10.4137/IDRT.S31567 (2016).

8 Tacconelli, E. *et al.* Global priority list of antibiotic-resistant bacteria to guide research, discovery, and development of new antibiotics. *http://www.who.int/medicines/publications/WHO-PPL-Short_Summary_25Feb-ET_NM_WHO.pdf?ua=1* (2017).

9 Cornelis, P. & Dingemans, J. Pseudomonas aeruginosa adapts its iron uptake strategies in function of the type of infections. *Frontiers in cellular and infection microbiology* **3**, 75, doi:10.3389/fcimb.2013.00075 (2013).

10 Ferreira, D., Seca, A. M., C, G. A. D. & Silva, A. M. Targeting human pathogenic bacteria by siderophores: A proteomics review. *J Proteomics* **145**, 153-166, doi:10.1016/j.jprot.2016.04.006 (2016).

11 Peterson, A. C., Russell, J. D., Bailey, D. J., Westphall, M. S. & Coon, J. J. Parallel reaction monitoring for high resolution and high mass accuracy quantitative, targeted proteomics. *Mol Cell Proteomics* **11**, 1475-1488, doi:10.1074/mcp.O112.020131 (2012).

12 Bodilis, J. *et al.* Distribution and evolution of ferripyoverdine receptors in Pseudomonas aeruginosa. *Environmental microbiology* **11**, 2123-2135, doi:10.1111/j.1462-2920.2009.01932.x (2009).

13 Coe, F. L., Worcester, E. M. & Evan, A. P. Idiopathic hypercalciuria and formation of calcium renal stones. *Nature reviews. Nephrology* **12**, 519-533, doi:10.1038/nrneph.2016.101 (2016).

14 Schalk, I. J. & Cunrath, O. An overview of the biological metal uptake pathways in Pseudomonas aeruginosa. *Environmental microbiology* **18**, 3227-3246, doi:10.1111/1462-2920.13525 (2016).

15 Subashchandrabose, S. & Mobley, H. L. Back to the metal age: battle for metals at the host-pathogen interface during urinary tract infection. *Metallomics : integrated biometal science* **7**, 935-942, doi:10.1039/c4mt00329b (2015).

16 Lassek, C. *et al.* A metaproteomics approach to elucidate host and pathogen protein expression during catheter-associated urinary tract infections (CAUTIs). *Mol Cell Proteomics* **14**, 989-1008, doi:10.1074/mcp.M114.043463 (2015).

17 Son, M. S., Matthews, W. J., Jr., Kang, Y., Nguyen, D. T. & Hoang, T. T. In vivo evidence of Pseudomonas aeruginosa nutrient acquisition and pathogenesis in the lungs of cystic fibrosis patients. *Infect Immun* **75**, 5313-5324, doi:10.1128/IAI.01807-06 (2007).

18 Bielecki, P. *et al.* Ex vivo transcriptional profiling reveals a common set of genes important for the adaptation of Pseudomonas aeruginosa to chronically infected host sites. *Environmental microbiology* **15**, 570-587, doi:10.1111/1462-2920.12024 (2013).
19 Dotsch, A. *et al.* The Pseudomonas aeruginosa Transcriptional Landscape Is Shaped by Environmental Heterogeneity and Genetic Variation. *MBio* **6**, e00749, doi:10.1128/mBio.00749-15 (2015).
20 Lassek, C., Berger, A., Zuhlke, D., Wittmann, C. & Riedel, K. Proteome and carbon flux analysis of Pseudomonas aeruginosa clinical isolates from different infection sites. *Proteomics* **16**, 1381-1385, doi:10.1002/pmic.201500228 (2016).
21 Taylor, S. L., Wesselingh, S. & Rogers, G. B. Host-microbiome interactions in acute and chronic respiratory infections. *Cell Microbiol* **18**, 652-662, doi:10.1111/cmi.12589 (2016).
22 Gi, M. *et al.* A novel siderophore system is essential for the growth of Pseudomonas aeruginosa in airway mucus. *Sci Rep* **5**, 14644, doi:10.1038/srep14644 (2015).
23 Kehl-Fie, T. E. & Skaar, E. P. Nutritional immunity beyond iron: a role for manganese and zinc. *Curr Opin Chem Biol* **14**, 218-224, doi:10.1016/j.cbpa.2009.11.008 (2010).
24 Marsland, B. J. & Gollwitzer, E. S. Host-microorganism interactions in lung diseases. *Nat Rev Immunol* **14**, 827-835, doi:10.1038/nri3769 (2014).
25 He, J. *et al.* The broad host range pathogen Pseudomonas aeruginosa strain PA14 carries two pathogenicity islands harboring plant and animal virulence genes. *Proc Natl Acad Sci U S A* **101**, 2530-2535 (2004).
26 Hoover, J. L. *et al.* A Robust Pneumonia Model in Immunocompetent Rodents to Evaluate Antibacterial Efficacy against S. pneumoniae, H. influenzae, K. pneumoniae, P. aeruginosa or A. baumannii. *Journal of visualized experiments : JoVE*, doi:10.3791/55068 (2017).
27 Page, M. G. *et al.* In vitro and in vivo properties of BAL30376, a beta-lactam and dual beta-lactamase inhibitor combination with enhanced activity against Gram-negative Bacilli that express multiple beta-lactamases. *Antimicrob Agents Chemother* **55**, 1510-1519, doi:10.1128/AAC.01370-10 (2011).
28 Juhas, M. *et al.* Global regulation of quorum sensing and virulence by VqsR in Pseudomonas aeruginosa. *Microbiology* **150**, 831-841, doi:10.1099/mic.0.26906-0 (2004).
29 Hofer, B. *et al.* Combined effects of the siderophore monosulfactam BAL30072 and carbapenems on multidrug-resistant Gram-negative bacilli. *J Antimicrob Chemother* **68**, 1120-1129, doi:10.1093/jac/dks527 (2013).
30 Rassam, P. *et al.* Supramolecular assemblies underpin turnover of outer membrane proteins in bacteria. *Nature* **523**, 333-336, doi:10.1038/nature14461 (2015).
31 Nikaido, H. & Rosenberg, E. Y. Cir and Fiu proteins in the outer membrane of Escherichia coli catalyze transport of monomeric catechols: study with beta-lactam antibiotics containing catechol and analogous groups. *J Bacteriol* **172**, 1361-1367 (1990).
32 Imperi, F. *et al.* Repurposing the antimycotic drug flucytosine for suppression of Pseudomonas aeruginosa pathogenicity. *Proc Natl Acad Sci U S A* **110**, 7458-7463, doi:10.1073/pnas.1222706110 (2013).
33 Takase, H., Nitanai, H., Hoshino, K. & Otani, T. Impact of siderophore production on Pseudomonas aeruginosa infections in immunosuppressed mice. *Infect Immun* **68**, 1834-1839 (2000).
34 Minandri, F. *et al.* Role of Iron Uptake Systems in Pseudomonas aeruginosa Virulence and Airway Infection. *Infect Immun* **84**, 2324-2335, doi:10.1128/IAI.00098-16 (2016).
35 Pletzer, D., Mansour, S. C., Wuerth, K., Rahanjam, N. & Hancock, R. E. New Mouse Model for Chronic Infections by Gram-Negative Bacteria Enabling the Study of Anti-Infective Efficacy and Host-Microbe Interactions. *MBio* **8**, doi:10.1128/mBio.00140-17 (2017).

36 Damron, F. H., Oglesby-Sherrouse, A. G., Wilks, A. & Barbier, M. Dual-seq transcriptomics reveals the battle for iron during Pseudomonas aeruginosa acute murine pneumonia. *Sci Rep* **6**, 39172, doi:10.1038/srep39172 (2016).
37 Lee, K. *et al.* The ferrichrome receptor A as a new target for Pseudomonas aeruginosa virulence attenuation. *FEMS Microbiol Lett* **363**, doi:10.1093/femsle/fnw104 (2016).
38 Gaddy, J. A. *et al.* Role of acinetobactin-mediated iron acquisition functions in the interaction of Acinetobacter baumannii strain ATCC 19606T with human lung epithelial cells, Galleria mellonella caterpillars, and mice. *Infect Immun* **80**, 1015-1024, doi:10.1128/IAI.06279-11 (2012).
39 Penwell, W. F. *et al.* Discovery and Characterization of New Hydroxamate Siderophores, Baumannoferrin A and B, produced by Acinetobacter baumannii. *Chembiochem : a European journal of chemical biology*, doi:10.1002/cbic.201500147 (2015).
40 Moynie, L. *et al.* Structure and Function of the PiuA and PirA Siderophore-Drug Receptors from Pseudomonas aeruginosa and Acinetobacter baumannii. *Antimicrob Agents Chemother* **61**, doi:10.1128/AAC.02531-16 (2017).
41 Gasser, V. *et al.* Catechol siderophores repress the pyochelin pathway and activate the enterobactin pathway in Pseudomonas aeruginosa: an opportunity for siderophore-antibiotic conjugates development. *Environmental microbiology* **18**, 819-832, doi:10.1111/1462-2920.13199 (2016).
42 van Delden, C., Page, M. G. & Kohler, T. Involvement of Fe uptake systems and AmpC beta-lactamase in susceptibility to the siderophore monosulfactam BAL30072 in Pseudomonas aeruginosa. *Antimicrob Agents Chemother* **57**, 2095-2102, doi:10.1128/AAC.02474-12 (2013).
43 Cassat, J. E. & Skaar, E. P. Iron in infection and immunity. *Cell Host Microbe* **13**, 509-519, doi:10.1016/j.chom.2013.04.010 (2013).
44 Landman, D. *et al.* In vitro activity of the siderophore monosulfactam BAL30072 against contemporary Gram-negative pathogens from New York City, including multidrug-resistant isolates. *Int J Antimicrob Agents* **43**, 527-532, doi:10.1016/j.ijantimicag.2014.02.017 (2014).
45 Konings, A. F. *et al.* Pseudomonas aeruginosa uses multiple pathways to acquire iron during chronic infection in cystic fibrosis lungs. *Infect Immun* **81**, 2697-2704, doi:10.1128/IAI.00418-13 (2013).
46 Marvig, R. L. *et al.* Within-host evolution of Pseudomonas aeruginosa reveals adaptation toward iron acquisition from hemoglobin. *MBio* **5**, e00966-00914, doi:10.1128/mBio.00966-14 (2014).
47 O'Brien, S. *et al.* High virulence sub-populations in Pseudomonas aeruginosa long-term cystic fibrosis airway infections. *BMC Microbiol* **17**, 30, doi:10.1186/s12866-017-0941-6 (2017).
48 Hmelo, L. R. *et al.* Precision-engineering the Pseudomonas aeruginosa genome with two-step allelic exchange. *Nat Protoc* **10**, 1820-1841, doi:10.1038/nprot.2015.115 (2015).
49 Davenport, K. W. *et al.* Draft Genome Assembly of Acinetobacter baumannii ATCC 19606. *Genome announcements* **2**, doi:10.1128/genomeA.00832-14 (2014).
50 Hilker, R. *et al.* Interclonal gradient of virulence in the Pseudomonas aeruginosa pangenome from disease and environment. *Environmental microbiology* **17**, 29-46, doi:10.1111/1462-2920.12606 (2015).
51 Miller, M. A. *et al.* Visualization of murine intranasal dosing efficiency using luminescent Francisella tularensis: effect of instillation volume and form of anesthesia. *PLoS One* **7**, e31359, doi:10.1371/journal.pone.0031359 (2012).
52 Ahrne, E. *et al.* Evaluation and Improvement of Quantification Accuracy in Isobaric Mass Tag-Based Protein Quantification Experiments. *J Proteome Res* **15**, 2537-2547, doi:10.1021/acs.jproteome.6b00066 (2016).

FIGURE LEGENDS

Figure 1: Detection of P. aeruginosa proteins in patient material, animal infection models, and *in vitro* cultures. **A**, Detection of two different peptides using parallel reaction monitoring in tracheal secretions of a human pneumonia patients. Fragmentation products of endogeneous light peptides (upper part) and heavy isotope-labelled internal reference peptide (lower part) are shown in the same colors (e.g., fragment y1 in red, etc.). The amounts are calculated based on the added heavy peptide concentration (fmol, femtomole; amol, attomole). **B**, Copy numbers for *P. aeruginosa* TonB-dependent transporters (TBDTs) in various *in vivo* and *in vitro* conditions. Each column represents an independent sample (MHB, cation-adjusted Müller-Hinton broth; LB, lysogeny broth; BM2, BM2 minimal medium; CAA, casamino acid minimal medium; chCAA, chelex-treated casamino acid medium; M9, m) minimal medium; hSerum, heat-inactivated human serum). Substrate classes are shown on the left (ES, endogeneous siderophores; XS, xenosiderophores; H, heme; oM, metals other than iron; un, unknown). Among xenosiderophores, known substrate classes are shown on the right (Hydroxamat., hydroxamate siderophores). TBDTs that transport advanced Trojan horse conjugates are marked with the dashed line.

Figure 2: Copy numbers for *A. baumannii* TonB-dependent transporters (TBDTs) in various *in vivo* and *in vitro* conditions. Each column represents an independent sample (MHB, cation-adjusted Müller-Hinton broth; ZnMgCA, re-adjusted ions after chelex treatment; apoTF, addition of apo-Transferrin; ISB, iso-sensitest broth). Substrate classes are shown on the left (ES, endogeneous siderophores; XS, xenosiderophores; H, heme; oM, metals other than iron; un, unknown). TBDTs that transport advanced Trojan horse conjugates are marked with the dashed line.

Figure 3: *In vivo* fitness contributions of *P. aeruginosa* TonB-dependent transporters. **A**, Genotype of various *P. aeruginosa* mutants. Black boxes indicate deleted genes. **B**, Competitive indices of various *P. aeruginosa* mutants in a mouse pneumonia model. A $\log_{10}$ value of "0" indicates a wild-type fitness level. Some affected siderophore classes or transporters are labelled (NA, nicotianamine). Statistical significance for divergence from wild-type fitness, or differences between two groups were analyzed using t-test (n.s., $P > 0.05$; *, $P < 0.05$; **, $P < 0.01$; ***, $P < 0.001$).

Figure 4: Predicted suitability of *P. aeruginosa* TonB-dependent transporters for targeting with Trojan horse conjugate antibiotics. Various criteria were analyzed to obtain a final score for treatment with a single drug, or using a combination of antimicrobials (red, suitable; yellow, partially suitable; white, no-suitable).

A

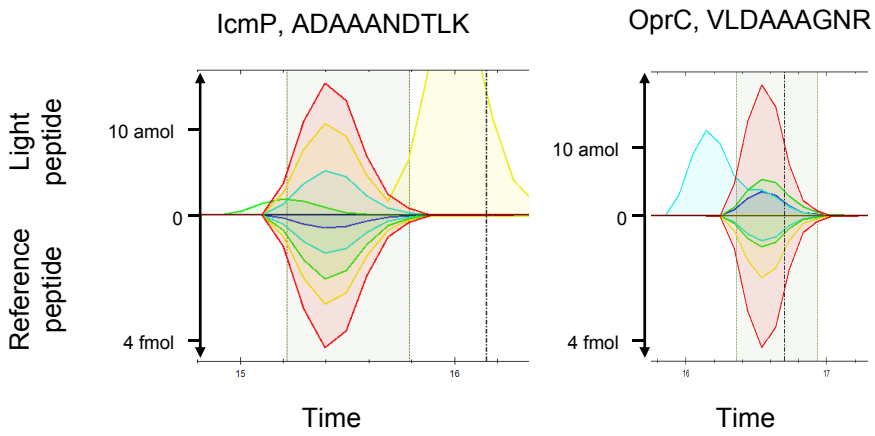
IcmP, ADAAANDTLK
OprC, VLDAAAGNR
Light peptide
Reference peptide
10 amol
0
4 fmol
Time

B

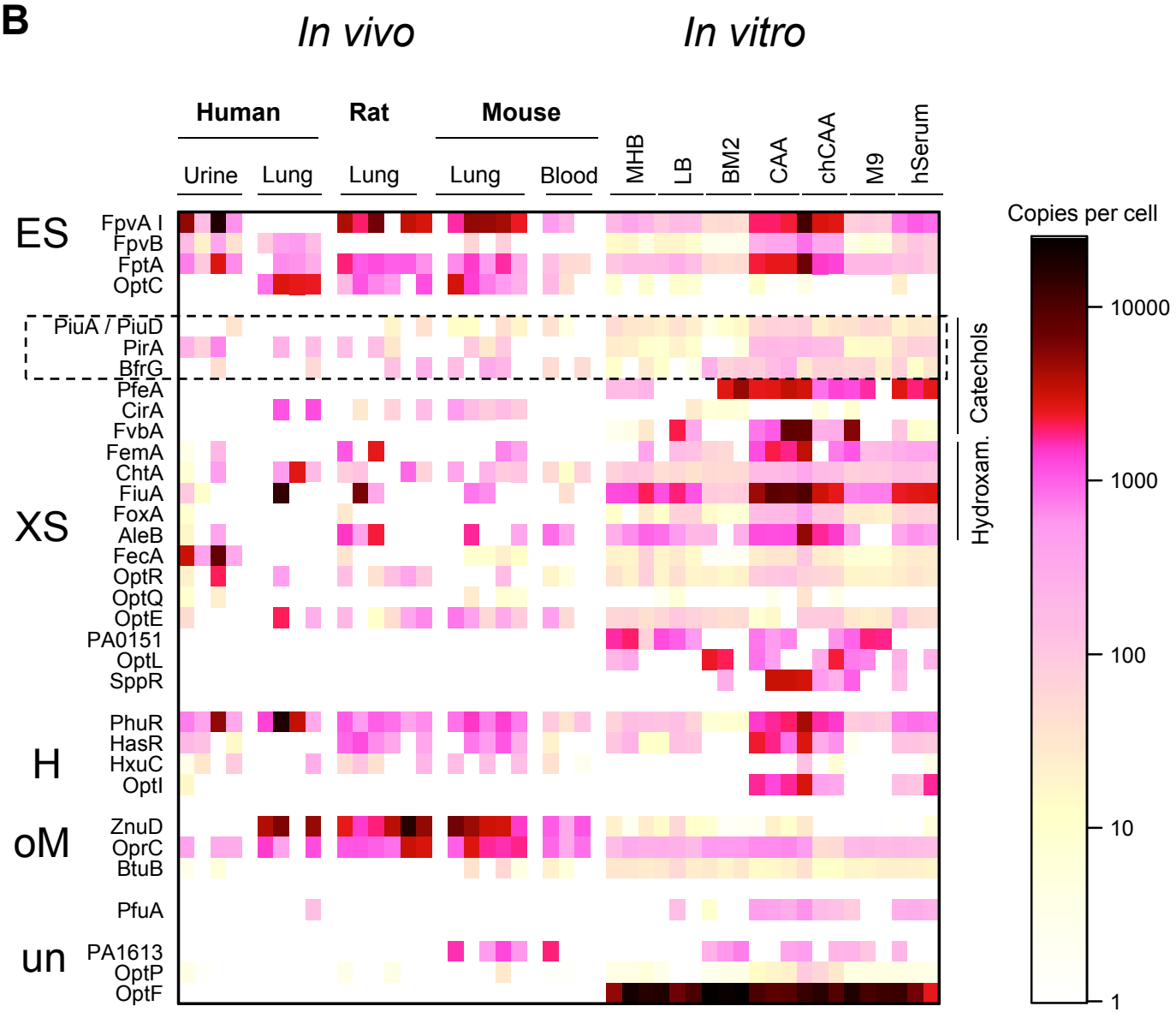
In vivo
In vitro
Human
Rat
Mouse
Urine
Lung
Lung
Lung
Blood
MHB
LB
BM2
CAA
chCAA
M9
hSerum
ES
XS
H
oM
un
FpvA I
FpvB
FptA
OptC
PiuA / PiuD
PirA
BfrG
PfeA
CirA
FvbA
FemA
ChtA
FiuA
FoxA
AleB
FecA
OptR
OptQ
OptE
PA0151
OptL
SppR
PhuR
HasR
HxuC
OptI
ZnuD
OprC
BtuB
PfuA
PA1613
OptP
OptF
Catechols
Hydroxam.
Copies per cell
10000
1000
100
10
1

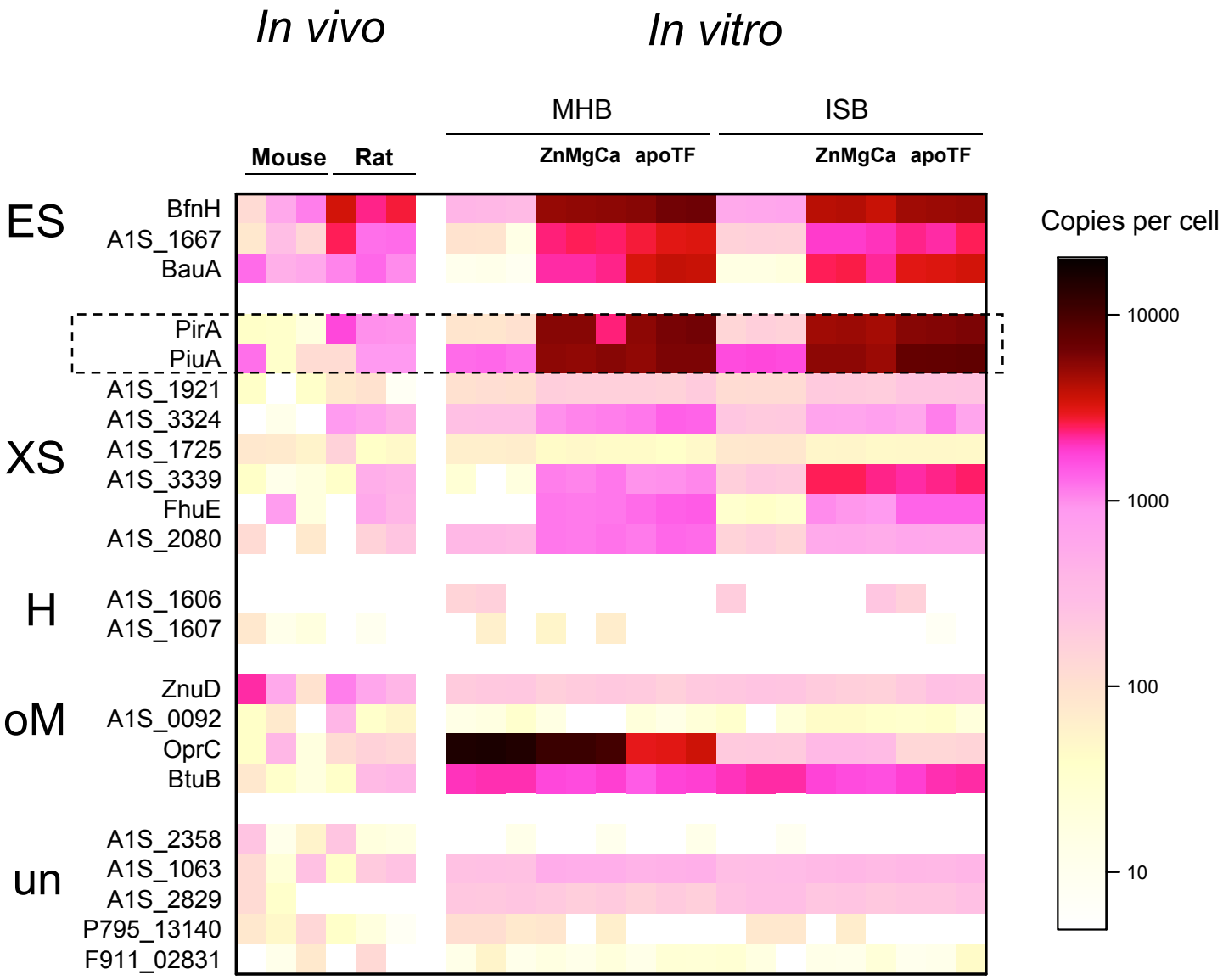
In vivo
In vitro
MHB
ISB
Mouse
Rat
ZnMgCa
apoTF
ZnMgCa
apoTF
ES
BfnH
A1S_1667
BauA
PirA
PiuA
XS
A1S_1921
A1S_3324
A1S_1725
A1S_3339
FhuE
A1S_2080
H
A1S_1606
A1S_1607
oM
ZnuD
A1S_0092
OprC
BtuB
un
A1S_2358
A1S_1063
A1S_2829
P795_13140
F911_02831
Copies per cell
10000
1000
100
10

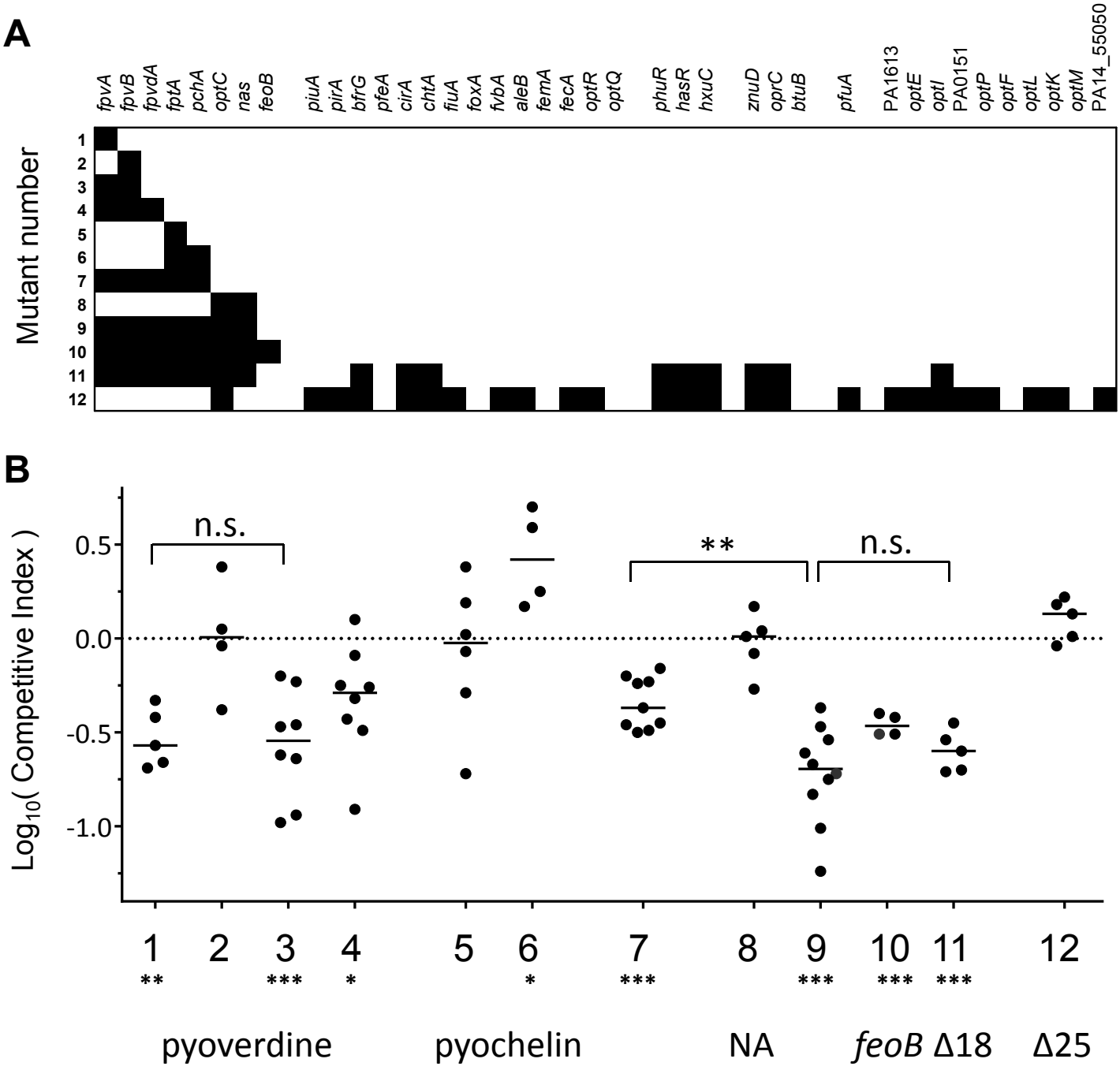
A
fpvA fpvB fpvdA fptA pchA optC nas feoB piuA pirA bfrG pfeA cirA chtA fiuA foxA fvbA aleB femA fecA optR optQ phuR hasR hxuC znuD oprC btuB pfuA PA1613 optE optI PA0151 optP optF optL optK optM PA14_55050
Mutant number
1 2 3 4 5 6 7 8 9 10 11 12
B
Log10(Competitive Index)
0.5
0.0
-0.5
-1.0
n.s.
**
n.s.
1 2 3 4 5 6 7 8 9 10 11 12
** *** * * *** *** *** ***
pyoverdine
pyochelin
NA
feoB Δ18
Δ25

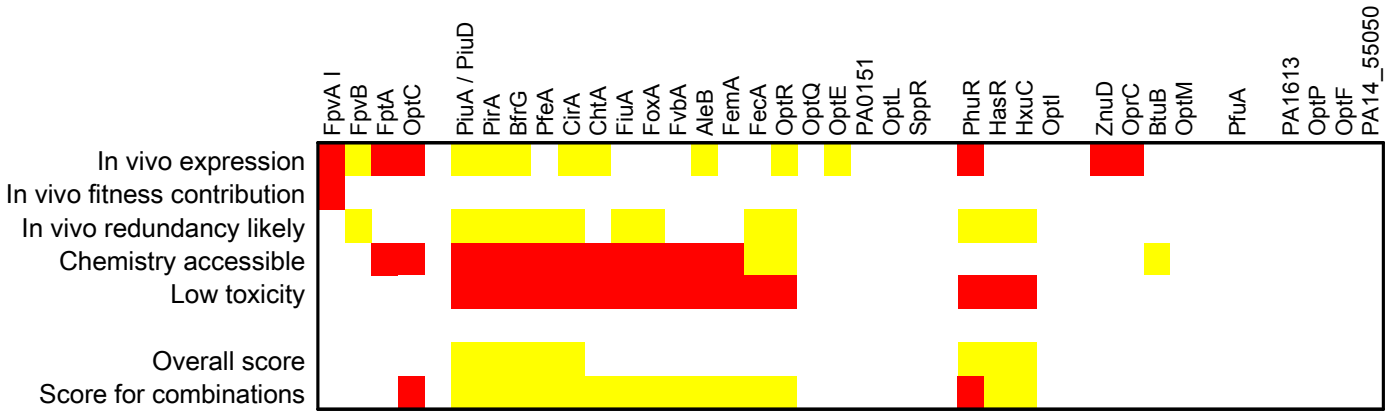
FpvA I
FpvB
FptA
OptC
PiuA / PiuD
PirA
BfrG
PfeA
CirA
ChtA
FiuA
FoxA
FvbA
AleB
FemA
FecA
OptR
OptQ
OptE
PA0151
OptL
SppR
PhuR
HasR
HxuC
OptI
ZnuD
OprC
BtuB
OptM
PfuA
PA1613
OptP
OptF
PA14_55050
In vivo expression
In vivo fitness contribution
In vivo redundancy likely
Chemistry accessible
Low toxicity
Overall score
Score for combinations

Table S1: Comprehensive list of TonB-dependent Transporters in *P. aeruginosa*

PA14 locus	PAO1 locus	Name	Alternative name	Substrates	Confidence level*	PMID	Absence among clinical isolates
PA14_33680	PA2398	FpvA I		Ferri-pyoverdine I	3	1903349	20.51282051
PA14_09970	PA4168	FpvB	OptB	Ferri-pyoverdine I	3	15184553	1.282051282
PA14_09340	PA4221	FptA		Ferri-pyochelin	3	1910015	0.256410256
PA14_63960	PA4837	OptC		nicotianamine-like	2	26446565	0.256410256
PA14_58570	PA4514	PiuA / PiuD		MC-1, BAL30072, SMC-3176, cefiderocol	3	23755848, 23422914, 26438502, this study	0.256410256
PA14_52230	PA0931	PirA		Ferri-enterobactin, MC-1, BAL30072, SMC-3176, cefiderocol	3	5899402, 23755848, 23422914, 26438502, this stuc	0.769230769
PA14_05640	PA0434	BfrG	OptJ	MC-1, BAL30072, SMC-3176, cefiderocol	3	this study	0.256410256
PA14_29350	PA2688	PfeA	FepA	Ferri-enterobactin, Ferri-catechols	3	15899402, 2174865, 26718479	0.512820513
PA14_39650	PA1922	CirA	OptT	Ferri-enterobactin (catechol)	2	12142471	0.769230769
PA14_10200	PA4156	FvbA	OptV	Ferri-vibriobactin (catechol)	3	21546589	1.282051282
PA14_39820	PA1910	FemA	UfrA	Ferri-mycobactin (catechol)	3	18086184	0.769230769
PA14_61850	PA4675	ChtA	IutA/OptH	Ferri-aerobactin (citrate-hydroxamate)	3	16549659	0.769230769
PA14_06160	PA0470	FiuA		Ferrichrome, Ferrioxamine (hydroxamate)	3	16043697, 16484199, 20047910	0.256410256
PA14_32740	PA2466	FoxA	OptS	Ferrioxamine (hydroxamate)	3	16043697	2.051282051
PA14_46640	PA1365	AleB	OptN	Ferri-alcalagin (dihydroxamate)	2	12142471	2.051282051
PA14_13430	PA3901	FecA		Ferri-citrate	3	19118371	1.025641026
PA14_21730	PA3268	OptR		Ferri-citrate	2	12142471	0.256410256
PA14_34990	PA2289	OptQ		Ferri-siderophore	1	18931447	2.820512821
PA14_26420	PA2911	OptE		siderophore (InterPro family IPR010105)	1	26578582	0.256410256
PA14_01870	PA0151	PA0151		siderophore (InterPro family IPR010105)	1	26578582	0.512820513
PA14_37490	PA2089	OptL		siderophore	1	18086184	2.307692308
PA14_37900	PA2057	SppR		siderophore	1	26995781	2.051282051
PA14_62350	PA4710	PhuR		Heme, Protoporphyrin	3	10658665, 28184354	3.58974359
PA14_20010	PA3408	HasR		Heme, Protoporphyrin	3	10658665, 28184354	1.025641026
PA14_47380	PA1302	HxuC		Heme	2	12142471	0.512820513
PA14_64710	PA4897	OptI		Heme	1	26578582	0.256410256
PA14_54180	PA0781	ZnuD	Omr	Zinc	2	26290475	0.256410256
PA14_15070	PA3790	OprC		Copper	1	8760927	N/A
PA14_47800	PA1271	BtuB	OptG	Cobalamin	2	12142471	0.512820513
PA14_37730	PA2070	OptM		metal uptake	1	18086184	2.564102564
PA14_47140	PA1322	PfuA		carbohydrate	1	19241370	0.512820513
PA14_43650	PA1613	PA1613					0.256410256
PA14_02410	PA0192	OptP					2.051282051
PA14_30590	PA2590	OptF		adjacent gene involved in quorum sensing	1	15073293	3.846153846
PA14_55050		PA14_55050					96.92307692

*1: weak indirect evidence; 2: similarity to exp validated TBDT; 3: direct experimental validation in *P. aeruginosa*

Table S2: Comprehensive list of TonB-dependent transporters in *A. Baumannii*

Locus	Name	PMID	Description
A1S_1655	BfnH	26235845	Baumannoferrin receptor
A1S_1667	A1S_1667		Putative ferric hydroxamate siderophore receptor
A1S_2385	BauA	15528653	Ferric acinetobactin receptor BauA
A1S_0980	PirA	28137795	Ferric enterobactin receptor
A1S_0474	PiuA	28137795	Putative ferric siderophore receptor protein
A1S_1921	A1S_1921		Ferrichrome-iron receptor
A1S_3324	A1S_3324		Possible ferrichrome receptor protein
A1S_1725	A1S_1725		Putative ferric siderophore receptor protein
A1S_3339	A1S_3339		Putative ferric siderophore receptor protein
A1S_2076	FhuE		Receptor for Fe(III)-coprogen, Fe(III)-ferrioxamine B and Fe(III)-rhodotrulic acid uptake (FhuE)
A1S_2080	A1S_2080		Putative siderophore receptor
A1S_1606	A1S_1606	19130255	Hemin uptake
A1S_1607	A1S_1607	19130255	Hemin uptake
A1S_2892	ZnuD	23236280	Zinc-regulated TonB-dependent receptor
A1S_0092	A1S_0092		Zinc starvation induced receptor protein
A1S_0170	OprC		Putative copper receptor
A1S_2877	BtuB		Vitamin B12 receptor
A1S_2358	A1S_2358		Putative TonB-dependent receptor
A1S_1063	A1S_1063		TonB-dependent siderophore receptor (Uncharacterized protein)
A1S_2829	A1S_2829		TonB-dependent receptor (Uncharacterized protein)
P795_13140	P795_13140		
F911_02831	F911_02831		TonB-dependent receptor (Uncharacterized protein)

Part III

Additional papers

3

Role of *Pseudomonas aeruginosa* porins in nutrient uptake and antimicrobial killing

Julien Buyck[1], Christian Schleberger[1], **Pamela Saint Auguste**[1], Sandra Söderholm[1], Thomas Bock[2], Scott Sucoloski[3], Jennifer Hoover[3], Josh West[3], Klaus Gebhardt[4], Malcolm Page[4], Michael Hogardt[5], Dominik Vogt[6], Adrian Egli[6], Dirk Bumann[1]

[1] Infection Biology, [2] Proteomics Core Facility, Biozentrum, University Basel, CH-4056 Basel, Switzerland; [3] Antibacterial Discovery Performance Unit, GlaxoSmithKline, Collegeville, PA, USA; [4] Basilea, CH-4056 Basel, Switzerland; [5] University Hospital, Frankfurt, Germany; [6] University Hospital Basel, CH-4056 Basel, Switzerland

State of the paper: In preparation

3.1 Abstract of the paper

Pseudomonas aeruginosa is a major threat to human health because of its increasing multi-drug resistance. A major roadblock for development of novel drugs is the poor permeability of the *P. aeruginosa* outer membrane. Several molecules can actually penetrate this barrier and this could provide hints for improving drug candidates, but physico-chemical constraints and underlying molecular mechanisms remain largely unclear. Here, we determined the expression and function of 40 different *P. aeruginosa* porins that can form water-filled channels in the outer membrane. Our proteome analysis revealed that during infection in human patients and rodent models, *P. aeruginosa* expressed only a subset of some 12 porins, that together contributed to *P. aeruginosa in vivo* fitness. Another key pathogen with low envelope peremabiltiy, *Acinetobacter baumannii*, showed comparable *in vivo* expression patterns. To determine transport substrates for each porin, we deleted all 40 porin genes to obtain a porin-free *P. aeruginosa* Δ40 strain, and then complemented this strain with single-porin expression constructs. Growth and nutrient uptake experiments revealed a crucial role of porins for uptake of many but not all nutrients. Several porins had large, overlapping substrate spectra and seemed to discriminate solutes primarily based on size instead of charge, dipole, or hydrophobicity. Surprisingly, the porin-free Δ40 strains had unaltered susceptibility against diverse classes of antibi-

otics except for the well-known slight OprD-dependency of carbapenems. These data indicated unexpected porin-independent translocation pathways for diverse antimicrobials. On the other hand, forced expression of cryptic porins sensitized *P. aeruginosa* to some otherwise ineffective antimicrobials such as fosfomycin and aztreonam. Together, these data challenge key dogmas about a crucial barrier for novel antimicrobials and suggest new opportunities for overcoming this barrier.

3.2 Statement of my work

- Development of the mutagenesis protocol that allows the generation of markerless deletions in UCBPP-PA14;
- Development of the targeted proteomic methods (SRM mainly done by Dr. Christian Schleberger and the PCF): Contribution in the peptides panel creation;
- Overexpression of selected simple porins as inclusion bodies;
- *In vivo* growth competition assays using septicemia and intranasal models to evaluate the fitness of selected simple porins mutants. Basilea Pharmaceutica performed the speticemia infections.

3.3 Theoretical background on targeted proteomics

In order to determine the abundance of porins in preclinical and clinical samples, we needed a robust technique that overcomes the problem of the background complexity in our *in vivo* samples. Most *in vivo* studies used transcriptomics thanks to the advances in microarray technologies. Microarrays detect gene expression profiles by measuring mRNA. However, this approach is subject to some limitations, since there is a poor correlation between mRNA and protein abundance.

Mass spectrometry has progressively become the method of choice for analysis of complex protein samples (Aebersold and Mann, 2003). In such approach, proteins are solubilized, denatured and digested into peptides by trypsin. The peptide mix is then fractionated and subjected to the mass spectrometric analysis. In the mass spectrometer, the peptides are ionized into precursor ions, the precursors are subsequently fragmented by collisional activation and the resulting product-ion mass spectra are recorded and used to identify the amino acids sequence of the selected peptides by database comparison.

The discovery-based or shotgun mass-spectrometry-based proteomic approach has been the most widely used method and has generated the vast majority of proteomic data available today. It measures the most abundant peptides, giving a relative quantification of proteins depending on the samples. Although shotgun proteomics can achieve high-

throughput screenings, the limitation of the technique lies in the lack of reproducibility and sensitivity for complex samples (Domon and Aebersold, 2010). Recent advances in mass spectrometry instrumentation favoured the use of targeted proteomics over the common shotgun proteomics.

Selective Monitoring Reaction (SRM), the gold standard of targeted proteomics, allows a higher reproducibility and sensitivity than shotgun approach and enables absolute quantification of proteins, by selecting predefined precursors ions and its subsequent predefined product-ions (also called transition). Recently, the Parallel Monitoring Reaction (PRM) has been developed thanks to increased advances in high resolution and accurate mass instruments. PRM is the same as SRM, except that all the product-ions of the selected precursors are measured, enabling a higher resolution and sensitivity in detection of trace proteins and discrimination of host proteins background (Domon and Aebersold, 2010; Aebersold and Mann, 2003).

3.4 Identification of simple porins *in vivo*

GFP-labelled *P. aeruginosa* were used to infect mice in a septicemia model. After an infection time of 24 to 48h, the bacteria were purified from the lungs and the blood by flow cytometry and further analysed by proteomics. To be able to measure quantitative protein abundance with high sensitivity, mass spectrometry-based proteomics is used. *P. aeruginosa* membrane were solubilized with 5% sodium deoxycholate and digested with trypsin to obtain peptides. The mixture was separated by nano Liquid chromatography and then analyzed by mass spectrometer. Ion precursors were selected according to our list of porins of interest for further fragmentation, giving spectra that could then be compared to a genome database. This results in the proteins identification with their relative abundance.

The intensities of the porins varied widely, low abundant porins and their peptides could be easily missed among hundreds of abundant proteins. To target the mass spectrometer to these low abundant peptides, we over-expressed the respective proteins and measured their peptides in simple mixtures. We started with the simple porins. In total, we cloned the 9 porins that we had not been able to see in the MS of complex samples and expressed them in *E. coli* as inclusion bodies (Figure 3.1). They were then added to the membrane preparation and analysed as explained. Based on these data, we could clearly identify the previously undetectable simple porins.

OprF is the most abundant porins of *P. aeruginosa*. We included this protein in our experiment because the shotgun analysis could not detect reliable peptides for OprF identification.

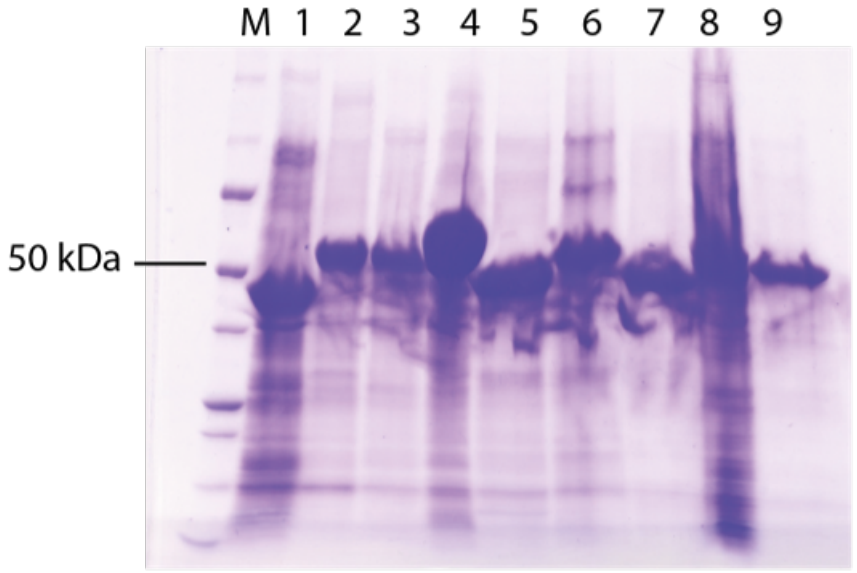

Figure 3.1: SDS-PAGE of simple porins fraction after inclusion bodies washing. SDSPAGE (12 %) analysis of fractions after inclusion bodies washing, solubilization and purification of selected simple porins. M corresponds to the marker. Lane 1: OprB3; Lane 2: OprF; Lane 3: FadL3; Lane 4: AlgE; Lane 5: OccD7; Lane 6: OccD8; Lane 7: OccK4; Lane 8: OprO; Lane 9: OprP

3.5 *In-silico* digestion of proteins for rapid and robust panel generation

Based on empirical evidences, we then developed an algorithm that performed an in-silico enzymatic digestion of proteins and a pre-selection of the "best flying" peptides according to the following criteria: (i) the peptides should be short and the priority is given to those containing proline residues, because they are better targets for SRM; (ii) three peptides should be selected per protein to get a reliable quantification and avoid incorrect detection due to post-translational modifications; (iii) we should avoid targeting peptides with a high propensity for artifactual modifications, i.e. avoid methionine and glutamate at the N-terminus; (iv) neighbouring cleavage site (at R or K) should also be avoided; (v) we selected conserved peptides among different strains to have universal set up but discriminate against the proteomes of diverses hosts (mouse, rat and human).

In order to set up the targeted proteomic assays, we ordered heavy isotope labelled peptides from proteins of interest, according to detected peptides from previous shotgun datasets and *in silico* digestion. The heavy isotope labelled peptides were then measured by the mass spectrometer to refine our panel of proteins with the most reliable peptides for identification. These panels were further used for quantification of our proteins of interest in various samples.

3.6 Quantification of simple porins *in vivo*

The expression level of simple porins was determined in various human patients samples and in different rodents samples (Figure 3.2). Overall, the data revealed a constant expression pattern among the different samples with a dominant subset of simple porins, which included the major porin OprF (Nestorovich et al., 2006; Rawling et al., 1998; Sugawara et al., 2006), OprD family porins (Ochs et al., 1999b; Ochs et al., 1999a; Tamber and Hancock, 2006), the cation-selective channel OprG (McPhee et al., 2009; Touw et al., 2010) and the long-chain fatty acid porin FadL (Hancock and Brinkman, 2002).

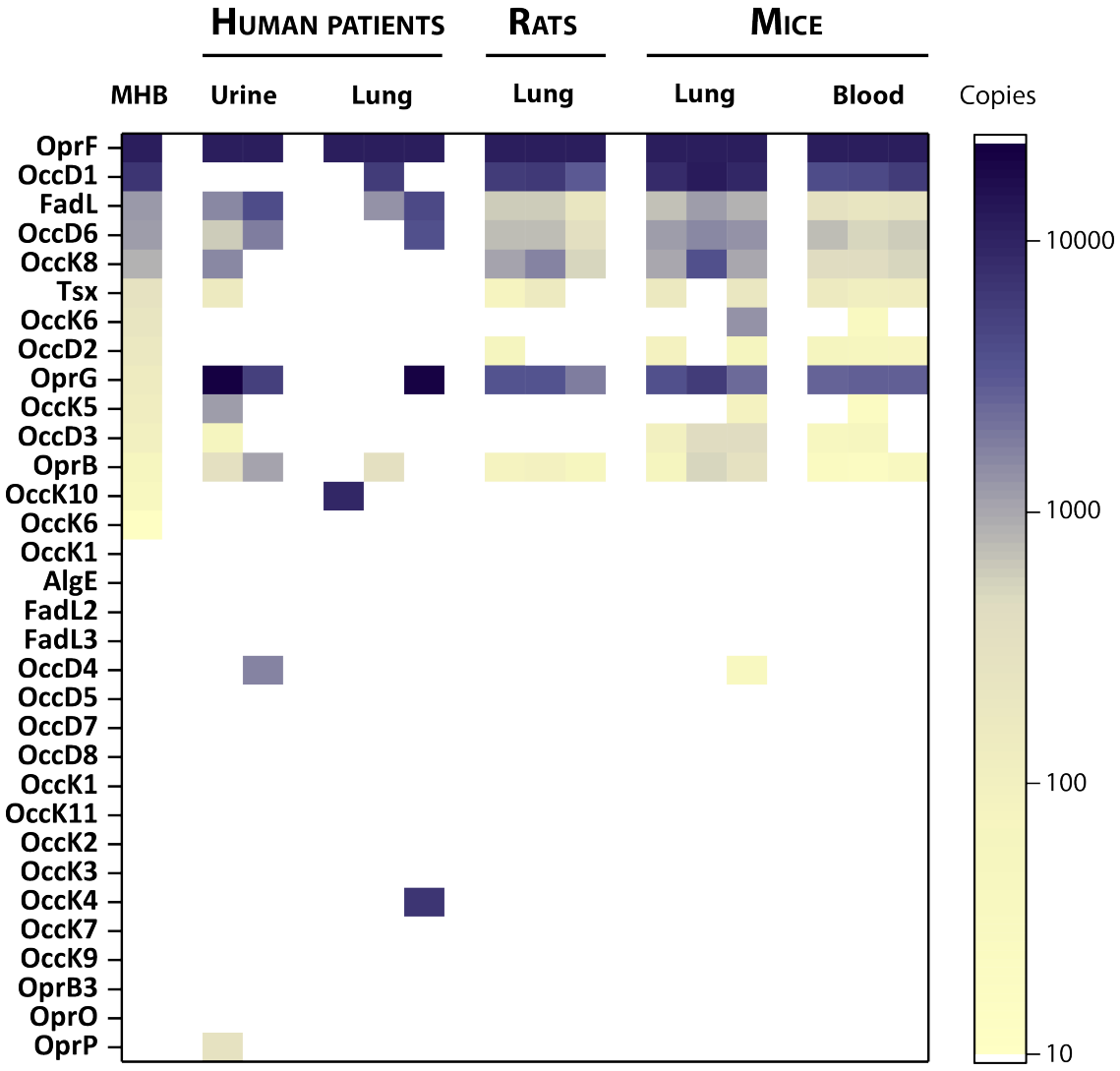

Figure 3.2: Expression level of simple porins in human patients and rodent models. Targeted proteomics (SRM) on urine and lavage samples from human patients that were acutely infected with *P. aeruginosa*; and lung and blood samples from rat and mice in pneumonia and septicemia model. The simple porins are ordered according to their expression *in vitro* in Mueller-Hinton broth.

4 Limited impact of the efflux on clinical multi-drug resistance of *Escherichia coli* and *Pseudomonas aeruginosa*

Olivier Cunrath[1*], Julien Buyck[1*], Dominik Meinel[2], **Pamela Saint Auguste**[1], Vincent Trebosc[4], Jonas Körner[1], Christoph Dehio[1], Christian Kemmer[4], Adrian Egli[2,3], Dirk Bumann[1]

[1] Focal Area Infection Biology, Biozentrum; [2] Clinical Microbiology, University Hospital Basel; [3] Applied Microbiology Research, Department of Biomedicine, University of Basel, Basel, Switzerland. [4] BioVersys AG, Basel, Switzerland.

∗ These authors contributed equally to the work.

State of the paper: Manuscript submitted to Nature Medicine.

4.1 Abstract

Extensive efforts have been devoted to develop efflux inhibitors for combatting multi-drug resistant (MDR) bacterial pathogens. However, we show here using a versatile strategy for genetic inactivation that major efflux systems make only limited contributions to high-level resistance against old and new antimicrobials in MDR clinical isolates of two key pathogens causing major threats to human health worldwide, *Escherichia coli* expressing extended spectrum β-lactamases (ESBL) and *Pseudomonas aeruginosa*. Novel control strategies for MDR pathogens are urgently needed, but efflux inhibition might have limited impact.

4.2 Statement of my work

Design the original markerless deletion method in *Pseudomonas aeruginosa*.

4.3 Draft paper

Limited impact of efflux on clinical multi-drug resistance of *Escherichia coli* and *Pseudomonas aeruginosa*

Olivier Cunrath[1‡], Julien Buyck[1‡], Dominik Meinel[2,3], Pamela Saint Auguste[1], Vincent Trebosc[4], Jonas Körner[1], Christoph Dehio[1], Christian Kemmer[4], Adrian Egli[2,3], Dirk Bumann[1*]

[1]Focal Area Infection Biology, Biozentrum; [2]Clinical Microbiology, University Hospital Basel; [3]Applied Microbiology Research, Department of Biomedicine, University of Basel, Basel, Switzerland. [4]BioVersys AG, Basel, Switzerland.

‡These authors contributed equally to the work.

Correspondence and requests for materials should be addressed to dirk.bumann@unibas.ch.

Dirk Bumann

Biozentrum

Klingelbergstrasse 50/70

CH-4056 Basel

Phone: +41 61 267 2382

ABSTRACT

Extensive efforts have been devoted to develop efflux inhibitors for combatting multi-drug resistant (MDR) bacterial pathogens. However, we show here using a versatile strategy for genetic inactivation that major efflux systems make only limited contributions to high-level resistance against old and new antimicrobials in MDR clinical isolates of two key pathogens causing major threats to human health worldwide, *Escherichia coli* expressing extended spectrum β-lactamases (ESBL) and *Pseudomonas aeruginosa*. Novel control strategies for MDR pathogens are urgently needed, but efflux inhibition might have limited impact.

Multi-drug resistant (MDR) Gram-negative bacterial pathogens represent a major global threat to human health. MDR pathogens drive clinical usage of last-resort antibiotics such as carbapenems and colistin further amplifying resistance development and emergence of pan-resistant pathogens [1]. As a consequence, deaths attributable to antimicrobial resistance may rise sharply, although the global burden of MDR remains difficult to estimate [2]. Resistance is multi-factorial but one promiscuous mechanism covering diverse antibiotic classes is the expression of so-called resistance-nodulation-division (RND) superfamily exporters, which mediate active efflux of small molecules including many antibiotics [3-6]. In laboratory strains of various Gram-negative bacterial pathogens, upregulation of RND efflux systems increases resistance to diverse antibiotics, while genetic inactivation of such systems renders mutants hypersensitive. Over-expression of RND efflux systems is observed in many multi-drug resistant (MDR) clinical isolates suggesting that efflux might be involved in increasing resistance [7]. Based on these observations, academia and industry have devoted major efforts to develop efflux inhibitors, hoping that such inhibitors could broadly restore sensitivity to old antimicrobials, and/or brake the intrinsic resistance of Gram-negative bacteria against drugs that are efficacious against Gram-positive bacteria lacking RND efflux systems.

Surprisingly, however, the foundation for these efforts has been rather weak. Almost all evidence for the impact of efflux comes from non-representative laboratory strains, while the quantitative contribution of efflux to clinical multi-drug resistance remains unclear due to technical difficulties. Methods for genetically inactivating efflux remain ineffective for MDR clinical strains. Efflux inhibitors are widely used to assess efflux contributions in clinical strains, but currently available inhibitors are hampered by pleiotropic effects on cell envelope integrity and overall bacterial physiology, impairing conclusive interpretation [5]. Efflux system gene expression and sequences can be readily determined, but overexpression and sequence polymorphisms poorly correlate with resistance levels in clinical isolates [8,9].

As part of the IMI Translocation project [10], we developed in this study a method that enables generation of genetically defined efflux mutants in diverse MDR clinical isolates. We employed a suicide plasmid (Figure 1a) and selection for two consecutive single cross-overs using a positive selection marker (thiopurine-S-methyltranferase Tpm conferring resistance to tellurite [11]) that works even in MDR isolates, and a negative selection marker (levan sucrase SacB conferring susceptibility to sucrose) for gene deletion events (see ONLINE METHODS). We employed this method to study the role of efflux in two major MDR pathogens that represent particularly serious threats [1], *Escherichia coli* expressing extended-spectrum β-lactamases (ESBL-*E. coli*) [12], and multi-resistant *Pseudomonas aeruginosa* [13]. We selected several highly resistant *P. aeruginosa* isolates from four different Belgian hospitals [14] that had divergent efflux pump expression patterns (Figure 1b) and resistance patterns (Figure 2a). In addition, we obtained ESBL-*E. coli* clinical isolates that were obtained at the University Hospital Basel from patient blood, sputum, surface swabs, urine, or fecal samples. Whole genome sequencing revealed that these isolates are genetically highly diverse with hundreds to over thousand allelic differences covering a large variety of *E. coli* lineages (Figure 1b), and carry various β-lactamases and other highly heterogeneous acquired resistance genes (Figure 1c), resulting in divergent antimicrobial resistance patterns (Figure 2a).

In *P. aeruginosa* we deleted *oprM* encoding the outer membrane channel of major efflux systems MexAB and MexXY (except for rare isolates of the taxonomic outlier PA7 group [15], in which MexXY uses OprA), as well as minor systems MexMN, MexVW, and partially MexJK. In ESBL-*E. coli* we deleted *tolC* encoding the outer membrane channel of all known *E. coli* RND efflux systems. For several strains, we could obtain clean deletions of *oprM* or *tolC*, respectively, within three days. However, for many others we had to screen hundreds of clones to obtain the desired mutants (see ONLINE METHODS). For some extensively multi-drug resistant *P. aeruginosa* isolates, there was a high background growth even at 200 mg l^{-1} tellurite hampering positive selection for ex-conjugants. Altogether, we managed to obtain *oprM* mutants for seven

out of 12 *P. aeruginosa* isolates (all of which were non-susceptible to agents in three or more antipseudomonal antimicrobial categories thus fulfilling the standard definition for MDR status [16]). In addition, we obtained *tolC* mutants for 17 out of 24 ESBL-*E. coli* isolates (all of which had MDR status). We are aware of genetically defined efflux mutants for a single clinical MDR *P. aeruginosa* isolate (from the rare outlier PA7 group [17]) and none for ESBL-*E-coli* clinical isolates in previous literature.

We tested these mutants and their parental strains for susceptibility to therapeutically relevant antimicrobials according to EUCAST breakpoints (v 6.0; available at http://www.eucast.org/clinical_breakpoints/) using a commercial phenotyping system (Vitek 2, bio-Mérieux Suisse SA, Geneva, Switzerland) and E-tests. We represent the data as minimal inhibitory concentrations that prevent growth (MIC) (Figure 2). High MIC values indicate strong resistance. MIC ranges corresponding to probable clinical treatment failures are shown in red, while likely efficacious treatment is represented by the blue regions. If RND efflux would represent a major contribution to clinical antimicrobial resistance, we would expect our efflux mutants to show markedly decreased MIC values, compared to their parental clinical isolates. Deletion of *oprM* in *P. aeruginosa*, or *tolC* in ESBL-*E. coli*, had indeed some impact on MIC values in various isolates, in some cases similar to what has been observed in fully susceptible laboratory strains [3-6]. However, such changes were almost always too small to convert highly resistant strains into susceptible ones (i.e., moving from the red to the blue areas), and sometimes occurred even in the opposite direction (i.e., getting more resistant) as previously reported [18]. The only exceptions were a single *P. aeruginosa* isolate that converted from amikacin resistant to sensitive upon *oprM* deletion (red arrow in Figure 2a), and a single ESBL-*E. coli* isolate that became susceptible to the aminoglycosides tobramycin and amikacin as well as cotrimoxazol upon *tolC* deletion (red arrows in Figure 2a). The residual high resistance of many mutants was the consequence of other potent resistance mechanisms (such as those mediated by identified acquired resistance genes of our ESBL-*E. coli* isolates shown in Figure 1c).

Efflux has been proposed to have an especially important role during initial encounters with new drugs, at a time when other resistance mechanisms might yet not have evolved [3-6]. Indeed, deletion of *oprM* had in some cases remarkable effects on *P. aeruginosa* susceptibility to aztreonam (which is rarely used against this pathogen) and a ceftazidime / avibactam combination that was approved in 2015, after the *P. aeruginosa* strains of this study had been isolated [14] (Figure 2b). However, several mutants still retained resistance suggesting the presence of potent alternative resistance mechanisms.

We also tested two drugs, tigecycline and azithromycin, that cannot be used therapeutically against *P. aeruginosa* because of high intrinsic resistance. In laboratory strains, this intrinsic resistance can largely be overcome by inactivating just one OprM-dependent efflux pump, MexAB [5]. As expected based on these data, *oprM* deletion very strongly increased sensitivity to both drugs also in several of our clinical isolates (Figure 2c, left). Susceptibility breakpoints for these two drugs have not been established for *P. aeruginosa* but using EUCAST breakpoints for other bacterial pathogens as tentative first approximations, several *oprM* mutants might indeed have become susceptible to clinically achievable tigecycline concentrations (hatched blue area). On the other hand, several mutant strains retained high resistance against tigecycline and no mutant became susceptible to azithromycin.

The *orpM* deletion inactivated the clinically most relevant RND efflux systems in *P. aeruginosa*, MexAB and MexXY [19], which represent the primary targets for efflux inhibitor development programs against MDR *P. aeruginosa*. However, *P. aeruginosa* encodes various other RND efflux systems that are independent of OprM [5]. It is possible that such other efflux systems masked the effect of *oprM* deletion in some of our mutants (as has been shown for one single isolate of the rare PA7 group [17]), but the most important alternative pumps, MexCD-OprJ or MexEF-OprN, were not overexpressed in our most refractory strains 142 and 256 (Figure 1b). In general, it might be challenging to develop promiscuous but safe inhibitors/inhibitor

combinations for all relevant *P. aeruginosa* efflux systems given the toxicity of several otherwise promising inhibitors [3-6]. In addition, highly resistant clinical isolates likely carry already alternative efflux-independent resistance mechanisms.

We also tested erythromycin and fusidic acid, two drugs that are ineffective against *E. coli* laboratory strains because of RND efflux-mediated intrinsic resistance [5]. Indeed, *tolC* deletion (which disrupts all *E. coli* RND efflux systems) greatly increased sensitivity to these drugs in several MDR ESBL-*E. coli* clinical isolates (Figure 2c, right). However, no mutant passed estimated breakpoints for sensitivity, and a sizable fraction showed no or only weak sensitization. These data show that even for "new" drugs, several MDR clinical isolates already carry potent alternative resistance mechanisms limiting the contribution of efflux.

Together, our direct experimental data using genetically defined mutants show that major RND efflux systems contribute to the MDR phenotype and intrinsic resistance of many clinical *P. aeruginosa* and ESBL-*E. coli* strains, but the effect size is often limited due to potent alternative resistance mechanisms. A limited contribution of efflux to high-level resistance has been previously postulated based on observations with laboratory strains [5] and three *Salmonella* isolates from pigs [20]. Our data indicate that efflux inhibitors might have limited impact on therapeutic success with old or even new antimicrobials against human MDR pathogens, arguing against the main motivation for the extensive past and current development programs for such inhibitors. Efflux might have a bigger relative role in strains with only low-level resistance (which we did not include in this study), but this would have probably little relevance for solving the urgent MDR crisis. However, further research on RND efflux systems and their substrate selectivity is still essential to obtain a rational basis for developing efficacious novel drugs that escape efflux. Moreover, efflux systems can contribute to pathogen virulence [21] suggesting a potential role of efflux inhibitors in anti-virulence strategies.

We have investigated diverse clinical MDR isolates of two major bacterial pathogens that have been at the focus of RND efflux research. Future studies could determine the role of these and other efflux systems in clinical multi-drug resistance in additional pathogens using the methods developed in this study.

METHODS

Methods, including statements of data availability and any associated accession codes and references, are available in the online version of the paper.

ACKNOWLEDGEMENTS

DB has received support from the Innovative Medicines Initiative Joint Undertaking under Grant Agreement no 115525, resources, which are composed of financial contribution from the European Union's seventh framework program (FP7/2007–2013) and from EFPIA companies in kind contribution, as part of the Project TRANSLOCATION (http://www.imi.europa.eu/content/translocation). DB has also received support by Schweizerischer Nationalfonds (Projekt 310030_156818). VT acknowledges funding as a Marie Skłodowska-Curie fellow within the Initial Training Network "Translocation", project no. 607694. AE is supported by Schweizerischer Nationalfonds Ambizione (PZ00P3_154709). We thank Alexander Harms for help in constructing *E. coli* strain JKE201. We thank Françoise Van Bambeke for kindly providing *P. aeruginosa* clinical isolates and their strain characteristics. We thank Daniel Lang, Dominik Vogt, Christine Kissling, Elisabeth Schultheiss, and Clarisse Straub (all Clinical Microbiology, University Hospital Basel) for excellent technical assistance.

AUTHOR CONTRIBUTIONS

O.C., J.B., and D.B. designed the study with input from A.E. and C.K.; O.C. and J.B. constructed mutants; D.M. and A.E. determined MIC values and genome sequences; P.S.A., J.K., C.D., V.T., and C.K. provided tools and expertise; D.B. wrote the manuscript with early input from O.C. and J.B. and subsequently all authors provided advice and approved the final manuscript.

REFERENCES

1 Spellberg, B. & Shlaes, D. Prioritized current unmet needs for antibacterial therapies. *Clinical pharmacology and therapeutics* **96**, 151-153, doi:10.1038/clpt.2014.106 (2014).

2 de Kraker, M. E., Stewardson, A. J. & Harbarth, S. Will 10 Million People Die a Year due to Antimicrobial Resistance by 2050? *PLoS Med* **13**, e1002184, doi:10.1371/journal.pmed.1002184 (2016).

3 Alibert, S. *et al.* Multidrug efflux pumps and their role in antibiotic and antiseptic resistance: a pharmacodynamic perspective. *Expert opinion on drug metabolism & toxicology*, 1-9, doi:10.1080/17425255.2017.1251581 (2016).

4 Blair, J. M., Richmond, G. E. & Piddock, L. J. Multidrug efflux pumps in Gram-negative bacteria and their role in antibiotic resistance. *Future microbiology* **9**, 1165-1177, doi:10.2217/fmb.14.66 (2014).

5 Li, X. Z., Plesiat, P. & Nikaido, H. The challenge of efflux-mediated antibiotic resistance in Gram-negative bacteria. *Clinical microbiology reviews* **28**, 337-418, doi:10.1128/CMR.00117-14 (2015).

6 Dreier, J. & Ruggerone, P. Interaction of antibacterial compounds with RND e ffl ux pumps in Pseudomonas aeruginosa. *Front Microbiol* **6**, 660, doi:10.3389/fmicb.2015.00660 (2015).

7 Riou, M. *et al.* Increase of efflux-mediated resistance in Pseudomonas aeruginosa during antibiotic treatment in patients suffering from nosocomial pneumonia. *Int J Antimicrob Agents* **47**, 77-83, doi:10.1016/j.ijantimicag.2015.11.004 (2016).

8 Piddock, L. J. Assess drug-resistance phenotypes, not just genotypes. *Nature microbiology* **1**, 16120, doi:10.1038/nmicrobiol.2016.120 (2016).

9 Khaledi, A. *et al.* Transcriptome Profiling of Antimicrobial Resistance in Pseudomonas aeruginosa. *Antimicrob Agents Chemother* **60**, 4722-4733, doi:10.1128/AAC.00075-16 (2016).

10 Stavenger, R. A. & Winterhalter, M. TRANSLOCATION project: how to get good drugs into bad bugs. *Sci Transl Med* **6**, 228ed227, doi:10.1126/scitranslmed.3008605 (2014).

11 Nowak, J., Seifert, H. & Higgins, P. The tellurite-resistance determinant Tpm of the Acinetobacter baylyi strain ADP1 as a useful nonantibiotic selection marker for genetic manipulation in Acinetobacter baumannii. *ESMID Conference* **P1356** (2013).

12 Iredell, J., Brown, J. & Tagg, K. Antibiotic resistance in Enterobacteriaceae: mechanisms and clinical implications. *BMJ* **352**, h6420, doi:10.1136/bmj.h6420 (2016).

13 Logan, L. K. *et al.* Multidrug- and Carbapenem-Resistant Pseudomonas aeruginosa in Children, United States, 1999-2012. *Journal of the Pediatric Infectious Diseases Society*, doi:10.1093/jpids/piw064 (2016).

14 Riou, M. *et al.* In vivo development of antimicrobial resistance in Pseudomonas aeruginosa strains isolated from the lower respiratory tract of Intensive Care Unit patients with nosocomial pneumonia and receiving antipseudomonal therapy. *Int J Antimicrob Agents* **36**, 513-522, doi:10.1016/j.ijantimicag.2010.08.005 (2010).

15 Roy, P. H. *et al.* Complete genome sequence of the multiresistant taxonomic outlier Pseudomonas aeruginosa PA7. *PLoS One* **5**, e8842, doi:10.1371/journal.pone.0008842 (2010).

16 Magiorakos, A. P. *et al.* Multidrug-resistant, extensively drug-resistant and pandrug-resistant bacteria: an international expert proposal for interim standard definitions for acquired resistance. *Clin Microbiol Infect* **18**, 268-281, doi:10.1111/j.1469-0691.2011.03570.x (2012).

17 Morita, Y., Tomida, J. & Kawamura, Y. Efflux-mediated fluoroquinolone resistance in the multidrug-resistant Pseudomonas aeruginosa clinical isolate PA7: identification of a novel

MexS variant involved in upregulation of the mexEF-oprN multidrug efflux operon. *Front Microbiol* **6**, 8, doi:10.3389/fmicb.2015.00008 (2015).
18 Saw, H. T., Webber, M. A., Mushtaq, S., Woodford, N. & Piddock, L. J. Inactivation or inhibition of AcrAB-TolC increases resistance of carbapenemase-producing Enterobacteriaceae to carbapenems. *J Antimicrob Chemother* **71**, 1510-1519, doi:10.1093/jac/dkw028 (2016).
19 Poole, K. Pseudomonas aeruginosa: resistance to the max. *Front Microbiol* **2**, 65, doi:10.3389/fmicb.2011.00065 (2011).
20 Chen, S. *et al.* Contribution of target gene mutations and efflux to decreased susceptibility of Salmonella enterica serovar typhimurium to fluoroquinolones and other antimicrobials. *Antimicrob Agents Chemother* **51**, 535-542, doi:10.1128/AAC.00600-06 (2007).
21 Alcalde-Rico, M., Hernando-Amado, S., Blanco, P. & Martinez, J. L. Multidrug Efflux Pumps at the Crossroad between Antibiotic Resistance and Bacterial Virulence. *Front Microbiol* **7**, 1483, doi:10.3389/fmicb.2016.01483 (2016).
22 Zankari, E. *et al.* Identification of acquired antimicrobial resistance genes. *J Antimicrob Chemother* **67**, 2640-2644, doi:10.1093/jac/dks261 (2012).

FIGURE LEGENDS

Figure 1: Gene deletion plasmid and diversity of clinical *Escherichia coli* strains.

(**a**) Plasmid for deleting genes in MDR bacterial pathogens. The plasmid carries the *R6K γ* origin of replication which depends on the replication protein π (encoded by *pir*) which is absent in almost all clinical strains; *tpm* encoding thiopurine-S-methyltranferase conferring resistance to tellurite (even MDR strains are mostly sensitive to tellurite); the origin of conjugational transfer *oriT*; *traJ* encoding the transcriptional activator for conjugational transfer genes; *sacB* encoding levan sucrase conferring sensitivity to sucrose. The hooked arrows represent promoters.

(**b**) Strain characteristics of highly resistant *Pseudomonas aeruginosa* clinical isolates (n.d., not detected).

(**c**,**d**) Analysis of clinical *Escherichia coli* strains expressing extended-spectrum β-lactamases by whole genome sequencing. (**c**) Minimum-spanning tree illustrating the phylogenetic relationship based on the cgMLST allelic profiles of 17 strains for which we could obtain *tolC* mutants. The scale bar represents 500 allelic differences. (**d**) Occurrence of acquired antimicrobial resistance genes as detected by ResFinder [22] and inspection of *gyrA* alleles.

Figure 2: Impact of genetic inactivation of efflux on antimicrobial sensitivity.

(**a**,**b**,**c**) Minimal inhibitory concentrations that prevent growth (MICs) of clinical isolates of *Pseudomonas aeruginosa* (left) or ESBL-expressing *Escherichia coli* (right). Data are shown for common therapeutically used antimicrobials (**a**), for rarely used or just recently approved drugs (**b**) (Ceft. / Avib., Ceftazidime / Avibactam), and for drugs that are ineffective against wild-type strains (**c**). Crosses represent values for parental isolates. The impact of *oprM* (*P. aeruginosa*) or *tolC* (ESBL-*E. coli*) deletion is represented by arrows. If there is no arrow, mutant MIC remained at the parental level. MIC values corresponding to clinical resistance (red) or susceptibility (blue) according to EUCAST breakpoints are also shown. Breakpoints for Ceftazidime / Avibactam (**b**) were based on values for Ceftazidime. In (**c**) breakpoints have been estimated based on values for other bacterial pathogens. The thick red arrows mark conversion of clinical resistance to susceptibility as a result of genetic inactivation of major efflux systems. MIC values outside the measurement range are shown above the highest labeled tick, or below the lowest labeled tick, respectively.

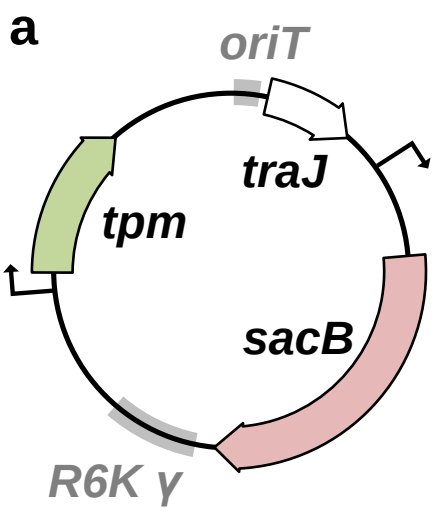

b

Strain	Origin	Serotype	Efflux pump overexpression				β-lactamases
			mexA	*mexC*	*mexE*	*mexX*	
PA116	UZ Brussels	O1					n.d.
PA142	St-Luc	O11					n.d.
PA171	St-Pierre	O4					n.d.
PA182	St-Pierre	O11					n.d.
PA256	Erasme	O6					*bla* VIM-2
PA330	St-Pierre	O11					*bla* OXA-1

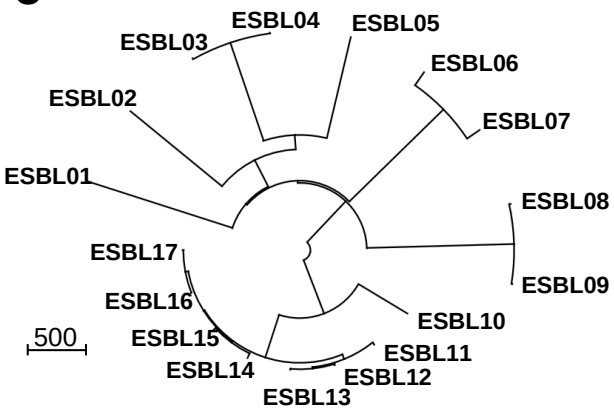

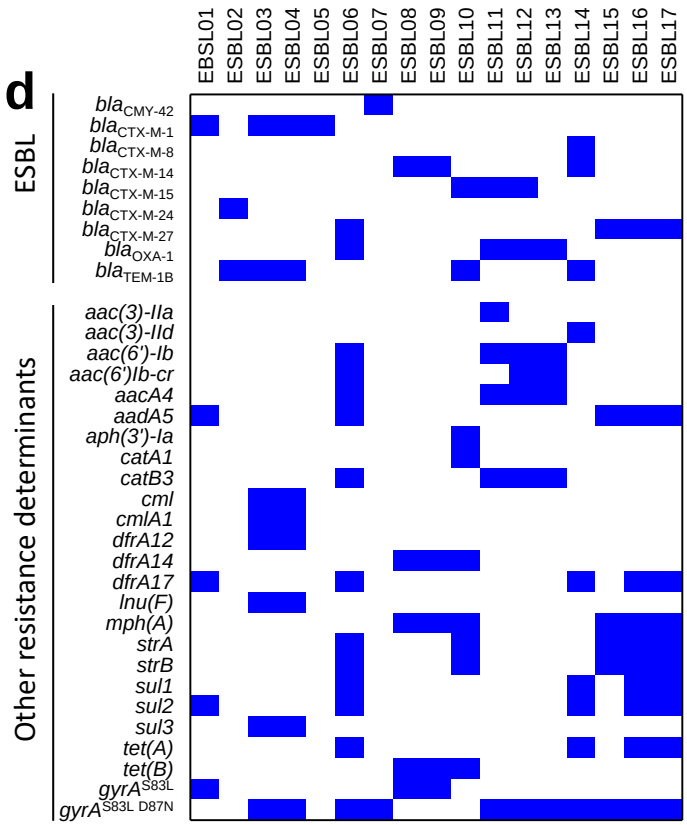

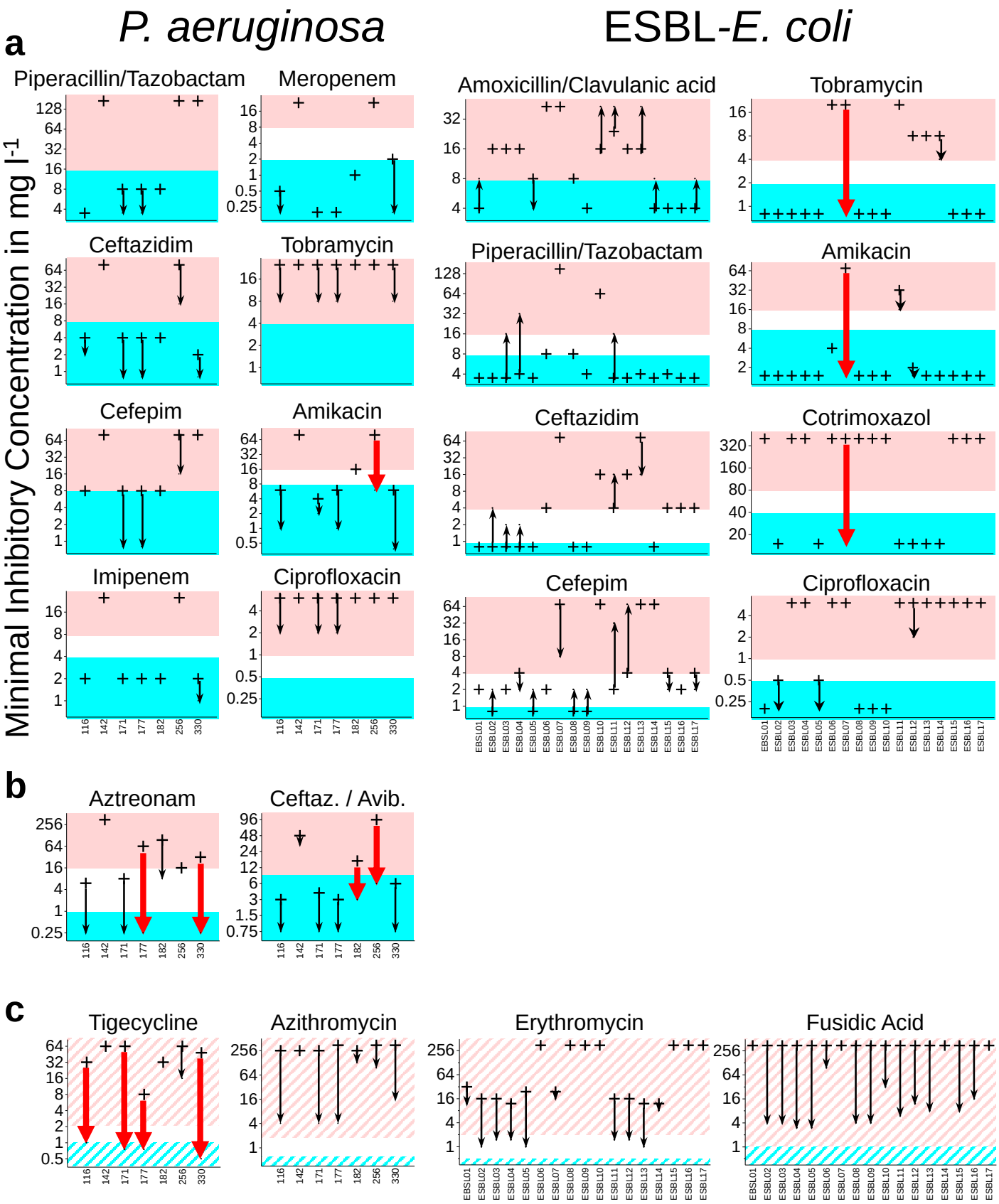
a
P. aeruginosa
ESBL-E. coli
Minimal Inhibitory Concentration in mg l-1
Piperacillin/Tazobactam
Meropenem
Ceftazidim
Tobramycin
Cefepim
Amikacin
Imipenem
Ciprofloxacin
Amoxicillin/Clavulanic acid
Tobramycin
Piperacillin/Tazobactam
Amikacin
Ceftazidim
Cotrimoxazol
Cefepim
Ciprofloxacin
b
Aztreonam
Ceftaz. / Avib.
c
Tigecycline
Azithromycin
Erythromycin
Fusidic Acid

5

Catechol siderophores repress the pyochelin pathway and activate the enterobactin pathway in *Pseudomonas aeruginosa*

Veronique Gasser[1], Etienne Baco[1], Olivier Cunrath[1], **Pamela Saint Auguste**[3], Quentin Perraud[1], Nicolas Zill[1], Christian Schleberger [3], Alexander Schmidt[3], Aurelie Paulen[1], Dirk Bumann[3], Gaetan Mislin[1], Schalk IJ[1].

[1] Université de Strasbourg, ESBS, F-67413, Illkirch, France. [2] UMR 7242, CNRS, F-67413, Illkirch, France. [3] Focal Area Infection Biology, Biozentrum, University of Basel, Basel, Switzerland.

State of the paper: Manuscript published in Environmental Microbiology.

5.1 Abstract of the paper

Previous studies have suggested that antibiotic vectorization by siderophores (iron chelators produced by bacteria) considerably increases the efficacy of such drugs. The siderophore serves as a vector: when the pathogen tries to take up iron via the siderophore, it also takes up the antibiotic. Catecholates are among the most common iron-chelating compounds used in synthetic siderophore-antibiotic conjugates. Using reverse transcription polymerase chain reaction and proteomic approaches, we showed that the presence of catecholate compounds in the medium of *Pseudomonas aeruginosa* led to strong activation of the transcription and expression of the outer membrane transporter PfeA, the ferri-enterobactin importer. Iron-55 uptake assays on bacteria with and without PfeA expression confirmed that catechol compounds imported iron into *P. aeruginosa* cells via PfeA. Uptake rates were between 0.3×10^3 and 2×10^3 Fe atoms/bacterium/min according to the used catechol siderophore in iron-restricted medium, and remained as high as 0.8×10^3 Fe atoms/bacterium/min for enterobactin, even in iron-rich medium. Reverse transcription polymerase chain reaction and proteomic approaches showed that in parallel to this switching on of PfeA expression, a repression of the expression of

pyochelin (PCH) pathway genes (PCH being one of the two siderophores produced by *P. aeruginosa* for iron acquisition) was observed.

5.2 Statement of my work

Shotgun proteomic samples preparation and data analysis of PAO1 exposed to enterobactin, two synthetic catechols bis-catechol vector (BCV) or tris-catechol vector (TCV) in casamino acid medium (CAA).

5.3 Published paper

environmental microbiology

Environmental Microbiology (2016) **18**(3), 819–832 doi:10.1111/1462-2920.13199

Catechol siderophores repress the pyochelin pathway and activate the enterobactin pathway in *Pseudomonas aeruginosa*: an opportunity for siderophore–antibiotic conjugates development

Véronique Gasser,[1,2] **Etienne Baco,[1,2]** **Olivier Cunrath,[1,2†]** **Pamela Saint August,[3]** **Quentin Perraud,[1,2]** **Nicolas Zill,[1,2]** **Christian Schleberger,[3]** **Alexander Schmidt,[3]** **Aurélie Paulen,[1,2]** **Dirk Bumann,[3]** **Gaëtan L. A. Mislin[1,2]** **and Isabelle J. Schalk[1,2*]**

[1] *Université de Strasbourg, ESBS, F-67413, Illkirch, France.*

[2] *UMR 7242, CNRS, F-67413, Illkirch, France.*

[3] *Focal Area Infection Biology, Biozentrum, University of Basel, Basel, Switzerland.*

Summary

Previous studies have suggested that antibiotic vectorization by siderophores (iron chelators produced by bacteria) considerably increases the efficacy of such drugs. The siderophore serves as a vector: when the pathogen tries to take up iron via the siderophore, it also takes up the antibiotic. Catecholates are among the most common iron-chelating compounds used in synthetic siderophore–antibiotic conjugates. Using reverse transcription polymerase chain reaction and proteomic approaches, we showed that the presence of catecholate compounds in the medium of *Pseudomonas aeruginosa* led to strong activation of the transcription and expression of the outer membrane transporter PfeA, the ferri-enterobactin importer. Iron-55 uptake assays on bacteria with and without PfeA expression confirmed that catechol compounds imported iron into *P. aeruginosa* cells via PfeA. Uptake rates were between 0.3×10^3 and 2×10^3 Fe atoms/bacterium/min according to the used catechol siderophore in iron-restricted medium, and remained as high as 0.8×10^3 Fe atoms/bacterium/min for enterobactin, even in iron-rich medium. Reverse transcription polymerase chain reaction and proteomic approaches showed that in parallel to this switching on of PfeA expression, a repression of the expression of pyochelin (PCH) pathway genes (PCH being one of the two siderophores produced by *P. aeruginosa* for iron acquisition) was observed.

Received 13 November, 2015; revised 20 December, 2015; accepted 23 December, 2015. For correspondence. *E-mail isabelle.schalk@unistra.fr; Tel. 33 3 68 85 47 19; Fax 33 3 68 85 48 29. **E-mail veronique.gasser@unistra.fr; Tel. 33 3 68 85 44 46; Fax 33 3 68 85 48 29. †Present address: Biozentrum, University of Basel, Basel, Switzerland.

Introduction

The emergence of resistant and, in some cases pan-resistant (resistant to all the antibiotics currently available) bacteria has led to an urgent need to discover new bactericidal molecules with different targets and innovative strategies for preserving or increasing the efficacy of known antibiotics. In recent years, a number of reviews have highlighted the possible use of bacterial iron uptake pathways as a Trojan horse strategy for promoting the transport of drugs into bacteria, thereby increasing their efficacy (Ji *et al.*, 2012b; Rebuffat, 2012; Page, 2013; Mislin and Schalk, 2014). Iron is a cofactor in many important biological processes, and it is therefore an essential nutrient for bacterial growth and infectious processes (Ratledge and Dover, 2000). One of the most common strategies for obtaining iron used by bacteria involves siderophores, small organic iron chelators [molecular weight between 200 and 2000 Da (Hider and Kong, 2011)]. These molecules are synthesized by bacteria and have a high affinity for iron. They are released into the environment, where they scavenge iron highly efficiently before being taken up again by the bacteria, resulting in the transport of the iron they carry to the bacterial cytoplasm (Schalk *et al.*, 2012; Schalk and Guillon, 2013). Antibiotics can be attached to siderophores in a Trojan horse strategy resulting in the delivery of the conjugates to the bacterial cytoplasm via siderophore-mediated iron uptake pathways.

In Gram-negative bacteria, the ferrisiderophore complexes formed in the environment surrounding the bacterium are transported back across the bacterial outer membrane by specific TonB-dependent transporters (TBDTs). The uptake activity of these transporters is regulated by the inner membrane protein TonB (Schalk *et al.*,

2012). They are further transported across the inner membrane by specific ABC transporters or proton-motive force-dependent permeases (Schalk and Guillon, 2013). The iron is generally then released from the siderophores in the bacterial cytoplasm, through a process involving both iron reduction and an enzymatic degradation or modification of the siderophores (for a review see Schalk and Guillon, 2013). In some siderophore pathways, a different sequence of events occurs: for example, during iron uptake via pyoverdine (PVD) or citrate in Pseudomonas *aeruginosa*, the iron is released from the siderophore in the periplasm, and only the iron is transported further into the cytoplasm, by an ABC transporter (Greenwald *et al*., 2007; Marshall *et al*., 2009; Brillet *et al*., 2012; Schalk and Guillon, 2013).

Most bacteria acquire iron by producing their own siderophores, but they can also use siderophores from other microorganisms (siderophore piracy). *Pseudomonas aeruginosa*, an opportunist pathogen, used as a model organism in this study, produces two major siderophores, PVD and pyochelin (PCH). However, it can also use many xenosiderophore (not produced by the bacterium itself) like PVDs from other pseudomonads, enterobactin (Poole *et al*., 1990), cepabactin (Mislin *et al*., 2006), mycobactin and carboxymycobactin (Llamas *et al*., 2008), desferrichrysin, desferricrocin, coprogen (Meyer, 1992), vibriobactin, aerobactin, fungal siderophores [ferrichrome (Llamas *et al*., 2006) and deferrioxamines (Vasil and Ochsner, 1999; Llamas *et al*., 2006)] and natural chelators, such as citrate (Cox, 1980; Harding and Royt, 1990), (for reviews see Poole and McKay, 2003; Cornelis and Dingemans, 2013).

Many studies have shown that siderophore iron uptake pathways can be used to transport antibiotics into bacteria (Mollmann *et al*., 2009; Ji *et al*., 2012b; Page, 2013; Mislin and Schalk, 2014). Microorganisms have themselves developed siderophore–antibiotic conjugates known as sideromycins (Braun and Braun, 2002; Braun *et al*., 2009; Mislin and Schalk, 2014), in which the antibiotic moiety is connected to the siderophore via a spacer arm. The archetypal conjugates of this type are albomycins (Benz *et al*., 1982; Braun and Braun, 2002; Mislin and Schalk, 2014), ferrimycins (Bickel *et al*., 1965), danomycins (Tsukiura *et al*., 1964), salmycins (Tsukiura *et al*., 1964) and certain microcins (de Lorenzo, 1984; de Lorenzo *et al*., 1984; Thomas *et al*., 2004; Destoumieux-Garzon *et al*., 2006; Nolan and Walsh, 2008). These natural siderophore–antibiotic conjugates can chelate iron(III) and are then transported into the target bacterium via the siderophore-dependent iron uptake pathways. This energy-coupled transport across the bacterial membranes greatly increases the antibiotic efficacy of sideromycins: their minimal inhibitory concentration is often at least two orders of magnitude lower than that of the antibiotic without the siderophore, which enters the cell by diffusion (Braun *et al*., 2009). Trojan horse strategies based on the use of bacterial iron uptake pathways are, therefore, currently considered to be a promising approach for the treatment of infection. Several research teams have developed different synthetic siderophore–antibiotic conjugates (Rivault *et al*., 2007; Page *et al*., 2010; Noel *et al*., 2011; Ji *et al*., 2012a,b; Milner *et al*., 2013; Page, 2013; Wencewicz and Miller, 2013; Wencewicz *et al*., 2013; Fardeau *et al*., 2014; Zheng and Nolan, 2014; Ji and Miller, 2015), some of which have potentially useful antibiotic activities.

However, for such Trojan horse strategies to be effective, the target bacteria must prefer to use xenosiderophores present in their environment rather than producing their own siderophores to obtain iron. In this context, it is vital to have a precise understanding of the ability of bacteria to sense the presence of xenosiderophores (or sideromycins in a Trojan horse strategy) in their environment and to switch from one siderophore pathway to another for iron acquisition. Catecholate siderophores are the iron-chelating compounds most frequently tethered to various antibiotics (Ji *et al*., 2012a; Wencewicz and Miller, 2013; Fardeau *et al*., 2014; Zheng and Nolan, 2014; Chairatana *et al*., 2015). In this study, we therefore evaluated the capacity of *P. aeruginosa* to use several catechol xenosiderophores in conditions of iron limitation: enterobactin (a well known siderophore produced by *Escherichia coli*, used here as a reference), protochelin and azotochelin [siderophores produced by *Azotobacter vinelandii* (Knosp *et al*., 1984; Cornish and Page, 2000)] and two synthetic chelators [the tris-catechol vector, TCV and the bis-catechol vector, BCV (Baco *et al*., 2014)], which could potentially be used for the vectorization of antibiotics for transport into *P. aeruginosa* cells (Fig. 1). We show here that when *P. aeruginosa* cells are grown in the presence of catechol compounds, the expression of the TBDT PfeA (the enterobactin outer membrane transporter) is highly activated, and the expression of the genes encoding for proteins involved in the endogenous PCH iron uptake pathway is repressed. Using ^{55}Fe uptake assays, we show that iron is transported by these catechol compounds via PfeA, into *P. aeruginosa* cells.

Results

Enterobactin, azotochelin, protochelin, BCV and TCV induce the expression of the outer membrane transporter PfeA

Pseudomonas aeruginosa is known to be able to sense xenosiderophores in its extracellular environment, and the detection of these molecules leads to an upregulation of the genes encoding the corresponding ferrisiderophore

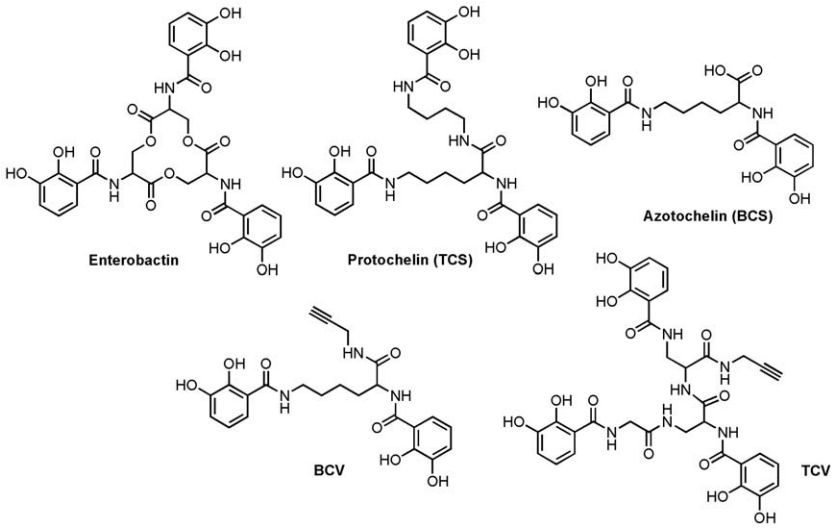

Fig. 1. Structures of enterobactin (ENT), azotochelin (BCS), protochelin (TCS), BCV and TCV.

uptake proteins (Dean and Poole, 1993; Llamas *et al.*, 2008; 2014). We used reverse transcription quantitative polymerase chain reaction (RT-qPCR) and proteomic approaches to investigate whether the presence of catecholate chelators in the growth medium activated the transcription of one or more siderophore TBDTs in *P. aeruginosa*. For both approaches, experiments were carried out with PAO1 ATCC15692 and the corresponding PVD and PCH-deficient Δ*pvdF*Δ*pchA* strain (Table S1) grown in LB or iron-deficient casamino acid medium (CAA) medium, with or without supplementation with 10 μM of enterobactin (the reference compound), azotochelin, protochelin, BCV or TCV.

We studied 10 genes in RT-qPCR experiments: seven genes corresponding to TBDTs (*piuA*, *pirA*, *pfeA*, *cirA*, *fvbA*, *pfuA* and PA0434) potentially involved in iron acquisition via catechol chelators according to the annotation of the *P. aeruginosa* PAO1 genome (Winsor *et al.*, 2011), the *fpvA* and *fptA* genes to assess changes in the transcription of the genes encoding the PVD and PCH TBDTs, and the housekeeping gene *uvrD*, which was used for normalization. Reverse transcription qPCR demonstrated a large increase in transcript levels for *pfeA* (Fig. 2) but not for any of the other TBDT genes tested (fold changes of less than seven for these other genes; Fig. S1) in the presence of enterobactin and the other four catecholate chelators tested. In the iron-deficient CAA medium, all five molecules tested strongly activated the transcription of *pfeA*, even in the wild-type strain PAO1, which produced and secreted large amounts of the endogenous siderophores, PVD and PCH (Cunrath *et al.*, 2015a). Tris-catechol vector and protochelin were the most effective activators of *pfeA* transcription (3000 and 4500-fold changes in PAO1 and Δ*pvdF*Δ*pchA*, respectively), followed by enterobactin (1400-fold change) and azotochelin, with BCV the least effective molecule (520 and 810-fold changes in PAO1 and Δ*pvdF*Δ*pchA* respectively). In Luria–Bertani (LB) medium [containing about 4 μM iron (Cunrath *et al.*, 2015a)], TCV, protochelin and enterobactin were able to promote *pfeA* transcription in both strains tested, with fold changes of between 100 and 700 for TCV (Fig. 2F). In LB medium, TCV was again the most effective compound for the activation of *pfeA* transcription. This activation of *pfeA* transcription in LB medium strongly suggested that *P. aeruginosa* made use of the enterobactin pathway to acquire iron even in iron-rich media, such as LB, if tris-catechol siderophores were present. The proteomic investigation was carried out on the wild-type PAO1 strain grown in CAA medium in the presence of enterobactin, BVC or TCV (Fig. 3). It clearly demonstrated an activation of expression for the PfeA gene but for no other TBDT gene (Fig. 3A).

In conclusion, RT-qPCR and proteomic investigations showed strong induction of the transcription and expression of *pfeA* in the presence of catechol chelators in iron-deficient and iron-rich media.

Enterobactin, azotochelin, protochelin, BCV and TCV can transport iron into P. aeruginosa cells via the TBDT PfeA

The activation of *pfeA* transcription and expression in the presence of the various catechol siderophores strongly suggests that these chelators transport iron into *P. aeruginosa* cells via this TBDT. We therefore assessed the ability of a mutant with a *pfeA* deletion to transport and accumulate ^{55}Fe in the presence of the various catechol siderophores.

In the first experiment (Fig. 4A–E), we prevented iron uptake by the endogenous siderophores by using the PCH and PVD-negative *P. aeruginosa* mutant Δ*pvdF*Δ*pchA* and its *pfeA* deletion mutant derivative

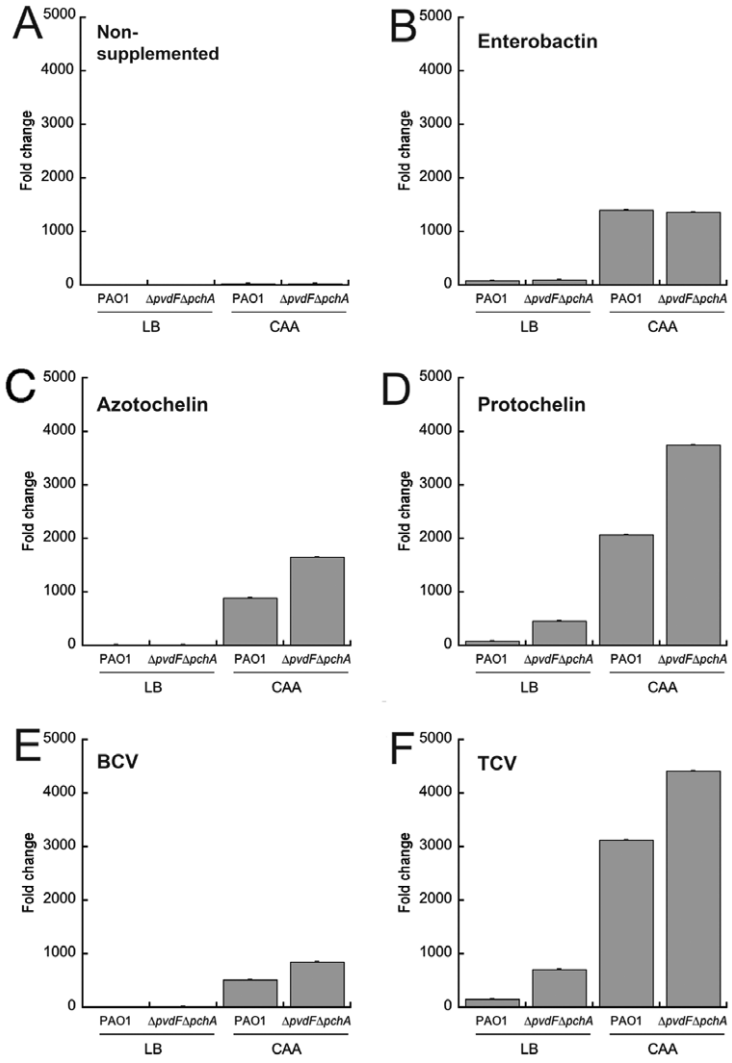

Fig. 2. Analysis of changes in the transcription of the *pfeA* gene. Reverse transcription quantitative PCR was performed on RNA from *P. aeruginosa* PAO1 and the corresponding PVD and PCH-deficient Δ*pvdF*Δ*pchA* cells grown in CAA or LB medium, with and without supplementation with 10 μM enterobactin, azotochelin, protochelin, BCV or TCV. The data are normalized relative to the reference gene *uvrD* and are representative of three independent experiments performed in triplicate ($n = 3$).

Δ*pvdF*Δ*pchA*Δ*pfeA*, grown in the presence of 10 μM enterobactin to induce PfeA expression. We also repeated all the ^{55}Fe uptake experiments with cells subjected to pretreatment with the protonophore carbonyl cyanide *m*-chlorophenylhydrazone (CCCP; Fig. 4A–E), which inhibits the proton-motive force of the bacteria, thereby preventing any TonB-dependent uptake (Clément *et al.*, 2004). Iron-55 uptake was observed in Δ*pvdF*Δ*pchA* cells (shown in black in Fig. 4A–E) in the presence of the five molecules tested, but not in cells that had been treated with CCCP (shown in green in Fig. 4A–E). Thus, none of the five catechol–^{55}Fe complexes tested were able to diffuse across the outer membrane: the iron uptake observed was mediated exclusively by TBDTs. A complete inhibition of iron uptake was also observed for the *pfeA* mutant in the presence of enterobactin-^{55}Fe, protochelin-^{55}Fe and TCV-^{55}Fe (shown in red in Fig. 4A, C and E), as shown by comparison with the Δ*pvdF*Δ*pchA* strain expressing PfeA, indicating that these three compounds transport iron into *P. aeruginosa* cells *via* PfeA only, with no other TBDT able to perform this function. In the presence of BCV and, to a lesser extent, azotochelin (Fig. 4D and B), the inhibition of ^{55}Fe uptake in Δ*pvdF*Δ*pchA*Δ*pfeA* cells was incomplete, suggesting the involvement of another TBDT, in addition to PfeA, in iron acquisition by these two bis-catechol compounds. Iron uptake was restored by the complementation of Δ*pvdF*Δ*pchA*Δ*pfeA* with pMMB190*pfeA*, a pMMB derivative carrying the *pfeA* gene for all five catecholate compounds tested (shown in blue in Fig. 4A–E).

As all the ^{55}Fe uptake assays with the different catechol siderophores were carried out with enterobactin as the inducer of *pfeA* expression, the expression levels of this protein are equivalent in all the uptake assays using PAO1 in Fig. 4A–E. Therefore, the ^{55}Fe transport efficiency of the different catecholate compounds can be compared: uptake rates of 2×10^3 Fe atoms/bacterium/min were recorded in the presence of enterobactin as siderophore,

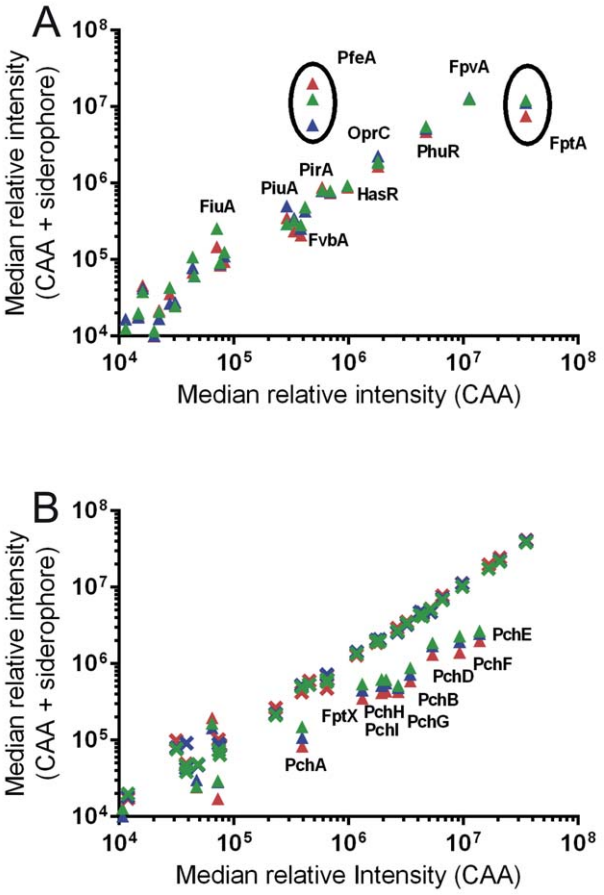

Fig. 3. Analysis of expression changes for TBDTs (A) and proteins of the PVD (B; green, blue and red crosses) and PCH (B; green, blue and red triangles) pathways. Proteomic analyses were performed on *P. aeruginosa* PAO1 cells grown in CAA supplemented or not with 10 μM enterobactin, BCV or TCV. Median values measured in CAA in the absence of any supplementation with catechol compounds were plotted against median values measured in CAA supplemented with either enterobactin (green symbols in panel A and B), BCV (blue symbols in panel A and B) and TCV (red symbols in panel A and B). Median values represent the median of the relative intensity of each protein, normalized against all detected proteins during shotgun analyses ($n = 3$).

1.3×10^3 Fe atoms/bacterium/min in the presence of azotochelin, 0.6×10^3 in the presence of protochelin or BCV and 0.3 10^3 Fe atoms/bacterium/min for TCV. In these experimental conditions, TCV appears about seven times less efficient than enterobactin for ^{55}Fe uptake in *P. aeruginosa*.

We then compared these uptake rates obtained with PVD and PCH-deficient Δ*pvdF*Δ*pchA* cells grown in conditions of iron limitation with those obtained when siderophore-producing PAO1 cells were grown in iron-rich media (Fig. 5 and Table 1). The idea here was to compare ^{55}Fe uptake by catecholate compounds in more favourable (iron-restricted growth conditions with a strain unable to produce any endogenous siderophore) and less favourable conditions (iron-rich growth conditions with a strain able to produce two endogenous siderophores). In addition, we also investigated the effect of (i) a lack of induction of PfeA expression (black bares in Fig. 5), (ii) induction with the siderophore enterobactin (gray bares in Fig. 5) and (iii) induction with the catechol chelator used in the ^{55}Fe uptake assays (white bares in Fig. 5), which lead to the induction of the transporter with different efficiencies according to Fig. 2.

A significant ^{55}Fe uptake via PfeA was observed only when the bacteria were grown in the presence of a catechol chelator inducing PfeA expression (Fig. 5), confirming again that this TBDT must be expressed to observe any ^{55}Fe uptake in the presence of such compounds. However, this rule was not respected in the case PAO1 cells grown in LB with protochelin and TCV used as siderophores. The second interesting point is an efficient iron transport via enterobactin, azotochelin and BCV even in PVD and PCH-producing *P. aeruginosa* cells grown in iron-rich medium. At last, iron uptake rates did not differ significantly between cells in which PfeA expression was induced with enterobactin and cells in which PfeA expression was induced with the siderophores used for ^{55}Fe uptake assays, despite the high capacity of compounds such as TCV to induce PfeA expression (Fig. 2F). This apparent absence of connection between the level of PfeA expression and iron uptake rates may be due to differences in siderophores recognition efficiencies with the different proteins of the enterobactin iron uptake pathway in *P. aeruginosa*.

Thus, all the five catechol compounds transported iron into *P. aeruginosa* cells via PfeA, with enterobactin being the more efficient. The uptake rates could reach with enterobactin 1306 ± 220 Fe atoms/bacterium/min in *P. aeruginosa* cells unable to produce siderophores grown in iron-deficient medium, and it remained as high as 827 ± 64 Fe atoms/bacterium/min, even in a PVD and PCH-producing strain grown in iron-rich medium (Fig. 5 and Table 1).

Enterobactin, azotochelin, protochelin, BCV and TCV repress the expression of the PCH pathway, but not that of the PVD pathway

In parallel with the induction of PfeA expression, proteomic analyses on *P. aeruginosa* cells grown in iron-deficient medium in the presence of 10 μM enterobactin, BCV or TCV showed a repression of the expression of the genes involved in PCH biosynthesis (*pchA*, *pchB*, *pchC*, *pchD*, *pchE*, *pchF* and *pchG*), the genes encoding the outer and inner membrane importers of PCH-Fe (*fptA* and *fptX*, respectively) and the *pchH* and *pchI* genes of the PCH locus, the functions of which are unknown (Fig. 3B).

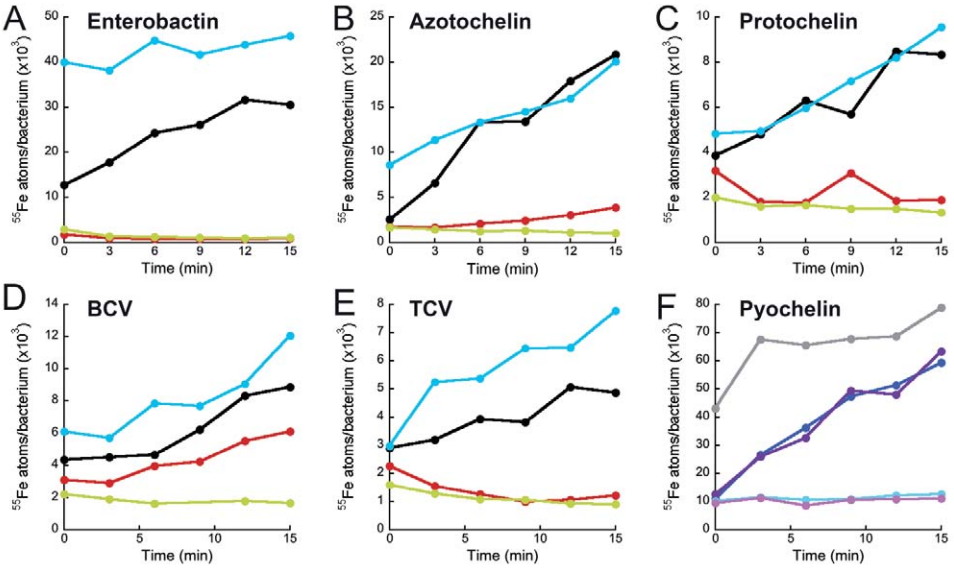

Fig. 4. A–E. Time-dependent ^{55}Fe assimilation in *P. aeruginosa* cells in the presence of ^{55}Fe-loaded enterobactin, azotochelin, protochelin, BCV and TCV. The PVD and PCH-deficient Δ*pvdF*Δ*pchA* strain, its corresponding *pfeA* mutant (Δ*pvdF*Δ*pchA*Δ*pfeA*) and the complemented Δ*pvdF*Δ*pchA* (pME3088Δ*pvdF*) strain were grown in CAA medium in the presence of 10 μM enterobactin to induce PfeA expression. The bacteria were then washed with 50 mM Tris-HCl (pH 8.0), and transport assays were initiated by adding 200 nM enterobactin-^{55}Fe (A), azotochelin-^{55}Fe (B), protochelin-^{55}Fe (C), BCV-^{55}Fe (D) or TCV-^{55}Fe (E). Samples (100 μl) of the suspension were taken at various time points and filtered; the radioactivity retained was measured. The results are expressed as atoms of ^{55}Fe transported per bacterium. For A–E, the black and red lines correspond to ^{55}Fe uptake assays with Δ*pvdF*Δ*pchA* and Δ*pvdF*Δ*pchA*Δ*pfeA* cells, respectively, both grown in the presence of enterobactin; in green: ^{55}Fe uptake assay with Δ*pvdF*Δ*pchA* cells grown in the presence of enterobactin and then treated with 200 μM CCCP (a protonophore), preventing TBDT-dependent transport; in blue: ^{55}Fe uptake assay with Δ*pvdF*Δ*pchA*(pME3088Δ*pvdF*) cells grown in the presence of enterobactin. F. Time-dependent ^{55}Fe assimilation in *P. aeruginosa* cells in the presence of PCH. Δ*pvdF*Δ*pchA* cells were grown in CAA medium in the absence of chelator (grey) or in the presence of 10 μM BCV (dark blue) or TCV (purple), to induce PfeA expression. As above, the bacteria were then washed with 50 mM Tris-HCl (pH 8.0) and transport assays were initiated by adding 200 nM PCH-^{55}Fe. The experiments were repeated with the protonophore CCCP at a concentration of 200 μM (light blue and pink: Δ*pvdF*Δ*pchA* cells treated with CCCP after culture in the presence of 10 μM BCV and TCV respectively). All the experiments in A–F were carried out three times, with similar results obtained in each case.

No effect on the expression of the genes of the PVD locus was observed. Since *P. aeruginosa* cells produce no PVD and PCH in LB [an iron-rich medium; (Cunrath *et al.*, 2015a)], the repression of PCH pathway genes in the presence of catecholate compounds was observed only in conditions of iron limitation (CAA medium). Reverse transcription qPCR experiments confirmed that, in conditions of iron limitation, the presence of catechol compounds in the growth medium of *P. aeruginosa* clearly repressed the transcription of *pchE* (a non-ribosomal peptide synthetase involved in PCH biosynthesis), *fptA* and *fptX* (Fig. 6A), with an 80% decrease in the fold changes recorded. Again, no repression of transcription was observed for the genes of the PVD pathway (*fpvA*, encoding the TBDT; *fpvF*, encoding a periplasmic binding protein involved in ferri-PVD import and *pvdJ*, encoding an enzyme involved in PVD biosynthesis; Fig. 6B).

We investigated the timing of this repression using *P. aeruginosa* cells expressing mCherry-tagged PchE or FptX (*pchEmcherry* and *fptXmcherry*, Table S1). The constructions of these strains have been described previously (Cunrath *et al.*, 2015b; Gasser *et al.*, 2015). Chromosomal insertion of *mcherry* was chosen to obtain physiological protein expression levels. The insertion of *mcherry*, by allelic exchange, into wild-type PAO1 produced strains expressing mCherry fused to the C-terminus of either FptX (*fptXmcherry* strain) or PchE (*pchEmcherry* strain). We monitored the growth of these two strains in iron-depleted CAA medium after addition of 200 μM enterobactin, BCV or TCV, by measuring optical density at 600 nm upon time (Fig. 7). These two strains carrying the fusion proteins grew as well as the parental strains PAO1 and the addition of the catechol compounds stimulated bacterial growth, a feature commonly observed with siderophores (Youard *et al.*, 2007). After 8 h culture, PchE-mCherry and FptX-mCherry were already expressed in *P. aeruginosa* cells, and a clear repression of PchE-mCherry and FptX-mCherry expression was observed, beginning about 1 h after the addition of catechol chelators to the growth medium. This repression was most effective with TCV and least effective with BCV, and persisted over about 20 h of culture.

This switching off of the PCH pathway was confirmed by carrying out PCH–^{55}Fe uptake assays (Fig. 4F) on *P.*

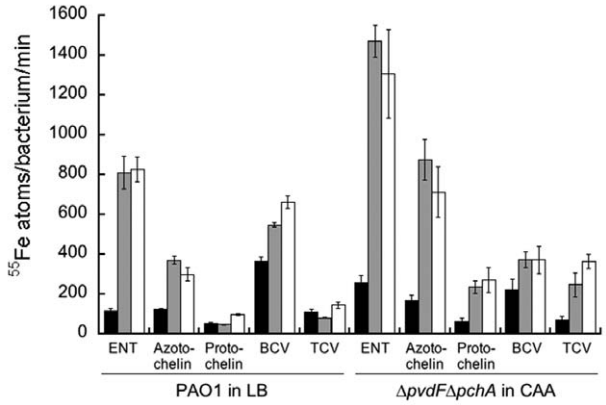

Fig. 5. ^{55}Fe assimilation in *P. aeruginosa* PAO1 and Δ*pvdF*Δ*pchA* cells in the presence of ^{55}Fe-loaded enterobactin, azotochelin, protochelin, BCV and TCV. PAO1 was grown in LB and the corresponding PVD and PCH-deficient Δ*pvdF*Δ*pchA* strain in CAA medium. Cells were grown without enterobactin supplementation to ensure an absence of PfeA expression (black bars) or with 10 μM enterobactin (gray bars) or 10 μM of the catechol compound used for ^{55}Fe uptake (white bars) to induce PfeA expression. The bacteria were then washed with 50 mM Tris-HCl (pH 8.0) and transport assays were initiated by adding the various catechol compounds loaded with ^{55}Fe to a concentration of 200 nM. Samples (100 μl) were taken from the suspensions at various time points and filtered; the radioactivity retained was measured. The results are expressed as atoms of ^{55}Fe transported per bacterium per min. Data of Fig. 5 are presented as well in Table 1.

aeruginosa cells grown in the presence or absence of BCV or TCV. Iron-55 uptake via PCH was observed for bacteria grown in the presence of BCV or TCV, indicating that the repression of the PCH pathway documented by proteomic and RT-qPCR studies was not total, with the bacteria still able to acquire iron via PCH. However, ^{55}Fe uptake was clearly slower in cells grown in the presence of BCV or TCV (no plateau reached after more than 15 min, Fig. 4F curve in blue and red) than in cells grown in the absence of these compounds (plateau reached in about 3 min, Fig. 4F curve in black).

These data show that the presence of catechol chelators in the growth medium of *P. aeruginosa* cells strongly represses the proteins of the PCH pathway. This repression occurred after about 1 h of growth in planktonic conditions in CAA medium and was maintained throughout the rest of the culture period (20 h). This repression was not total, with the bacterium still able to acquire iron via the PCH siderophore.

Discussion

In addition to its own siderophores, PVD and PCH, *P. aeruginosa* can use many siderophores produced by other microorganisms (Poole and McKay, 2003; Cornelis and Dingemans, 2013), consistent with the presence in the genome of this pathogen of more than 30 genes encoding TBDTs (Cornelis and Bodilis, 2009), which act as gates allowing the various ferrisiderophore complexes to enter bacteria. All these siderophore-dependent iron uptake pathways, indicating a high potential of this bacterium to adapt to different conditions of iron limitation, may be also considered as possible gates for the entry of siderophore-antibiotic conjugates in Trojan horse strategies.

We show here that the presence in the growth medium of catechol xenosiderophores (azotochelin and protochelin) or two synthetic chelators (BCV and TCV) that can be linked to antibiotics by click chemistry induced the expression of PfeA in *P. aeruginosa*, as previously reported for enterobactin (Dean and Poole, 1993). By contrast, no other TBDT was induced (Figs 2 and 3A). The efficiency of PfeA induction was highest for TCV, followed by protochelin, enterobactin, azotochelin and, finally BCV. Dean and Poole have shown that two genes, *pfeS* and *pfeR* (located immediately upstream from *pfeA*), encode the sensor kinase and response regulator, respectively, of a two-component system involved in regulating *pfeA* expression in response to enterobactin (Dean and Poole, 1993; Rodrigue *et al.*, 2000). It is tempting to hypothesize that this two-component system is also involved in the regulation of *pfeA* expression in response to other catechol compounds. The sequence of PfeS suggests that it is an inner membrane protein (Dean and Poole, 1993), and further studies are required to gain insight into the mechanism of stimulus perception by this protein: do the catechol compounds interact with this

Table 1. ^{55}Fe assimilation in *P. aeruginosa* PAO1 and Δ*pvdF*Δ*pchA* cells in the presence of ^{55}Fe-loaded enterobactin, azotochelin, protochelin, BCV and TCV.

	^{55}Fe atoms/bacterium/min				
	Enterobactin	Azotochelin	Protochelin	BCV	TCV
PAO1 in LB	827 ± 64	299 ± 33	98 ± 4	661 ± 32	145 ± 14
Δ*pvdF*Δ*pchA* in CAA	1306 ± 220	712 ± 126	273 ± 62	372 ± 68	363 ± 36

PAO1 was grown in LB and the corresponding PVD and PCH-deficient Δ*pvdF*Δ*pchA* strain in CAA medium. Cells were grown with 10 μM of the catechol compound used for ^{55}Fe uptake to induce PfeA expression. The bacteria were then washed with 50 mM Tris-HCl (pH 8.0), and transport assays were initiated by adding the various catechol compounds loaded with ^{55}Fe to a concentration of 200 nM. Samples (100 μl) were taken from the suspensions at various time points and filtered; the radioactivity retained was measured. The results are expressed as atoms of ^{55}Fe transported per bacterium per min ($n = 3$).

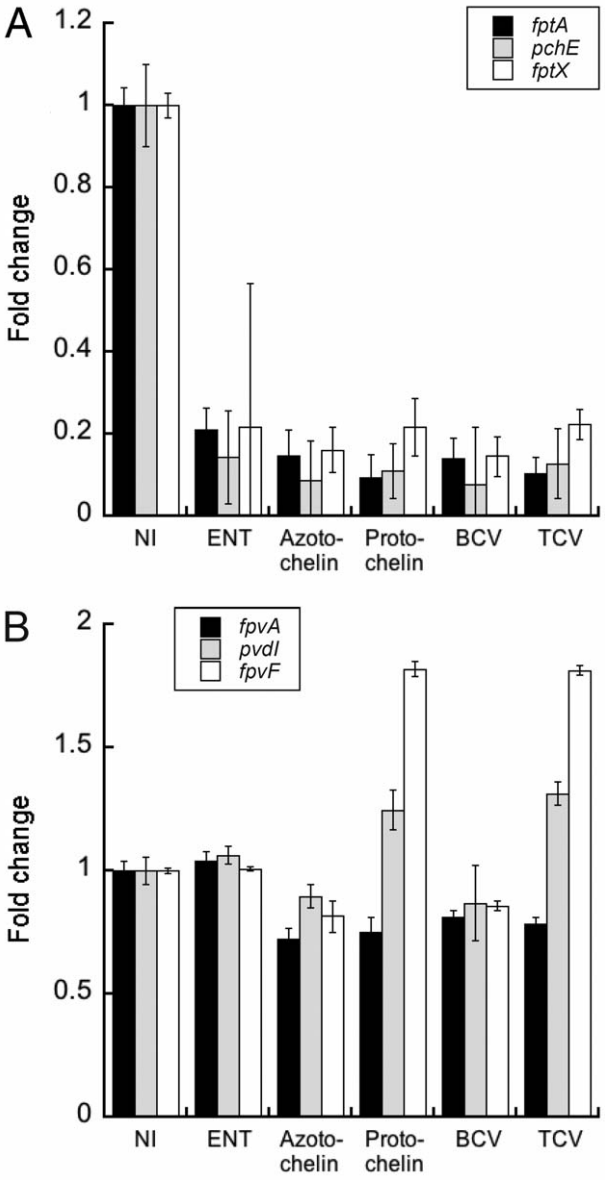

Fig. 6. A. Analysis of changes in transcription for the genes of the PCH pathway. *fptA* and *fptX* encode the outer and inner membrane transporters of PCH-Fe, respectively, and *pchE* encodes an nonribosomal peptide synthetase involved in PCH biosynthesis. Reverse transcription qPCR was performed on *P. aeruginosa* PAO1 grown in CAA medium with or without 10 μM enterobactin, azotochelin, protochelin, BCV or TCV (NI for not induced). B. Analysis of changes in the transcription of genes of the PVD pathway. *fpvA* encodes the TBDT of PVD-Fe, *fpvF* encodes a periplasmic binding protein involved in PVD-Fe uptake, *pvdI* encodes an non-ribosomal peptide synthetases involved in PVD biosynthesis. As for panel B, RT-qPCR was performed on *P. aeruginosa* PAO1 cells grown in CAA medium with or without 10 μM enterobactin, azotochelin, protochelin, BCV or TCV (NI for not induced). For both panels, the data were normalized relative to the reference gene *uvrD* and are representative of three independent experiments performed in triplicate ($n = 3$).

protein only after their transport into the bacterial periplasm or is another mechanism involved?

Despite the current lack of information concerning the molecular mechanisms underlying this stimulation of PfeA expression, the findings presented here already have interesting implications for the development of siderophore conjugates for Trojan horse strategies. First, the induction of PfeA expression (or switching on of the enterobactin pathway) was even significant in a wild-type PAO1 strain, indicating that, in the presence of catechol compounds, *P. aeruginosa* makes use of these molecules to obtain iron, despite its ability to produce the highly

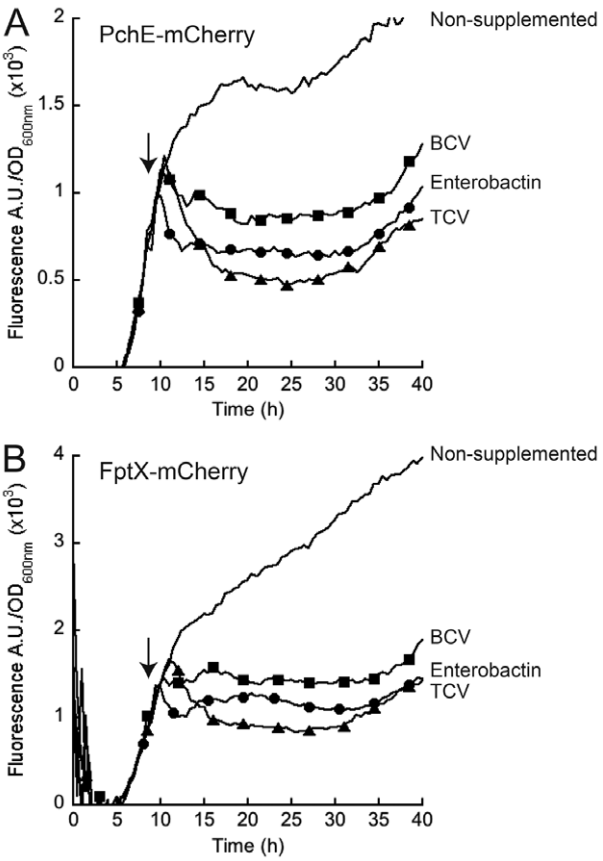

Fig. 7. Monitoring of PchE-mCherry (A) and FptX-mCherry (B) fluorescence during bacterial growth in the presence and absence of enterobactin, BCV or TCV. Fresh CAA medium was inoculated with *pchEmcherry* and *fptXmcherry* cells grown in the same medium, and the resulting suspension was dispensed into the wells of a 96-well plate. For both panels, after 8 h of growth, 200 μM enterobactin (●), BCV (■) or TCV (▲) was added; the control experiment with no siderophore addition is shown in black (black line with no symbols). OD_{600nm} measurements were used to assess growth over time. The fluorescence of mCherry was measured by excitation at 570 nm, with monitoring of the emission of fluorescence at 610 nm. These measurements were performed at 30 min intervals, in a Tecan microplate reader incubated at 30°C, with shaking. Each curve corresponds to the mean of three replicates.

efficient siderophores PVD and PCH. In addition, the enterobactin pathway was switched on even in iron-rich medium (LB), leading to efficient iron uptake via this siderophore: 827 ± 64 Fe atoms/bacterium/min (Fig. 5 and Table 1). The total iron content of bacteria in this medium is in the range of 810 000 Fe atoms/bacterium (Cunrath *et al*., 2015a).

This switching on of the enterobactin pathway was accompanied by a clear repression of the expression of the PCH pathway. However, the PCH pathway was not totally switched off (Fig. 3F), the bacteria were still able to gain access to iron via PCH at any moment. This repression occurred as long as the bacteria were in contact with catechol chelators (Fig. 7). No repression of the PVD pathway was observed. Interestingly, this hierarchy of iron uptake pathway expression reflects the affinity of the siderophores for ferric iron (10^{52} M^{-1}, $10^{30.8}$ M^{-1} and $10^{28.8}$ M^{-2} for enterobactin, PVD and PCH respectively (Carrano and Raymond, 1979; Albrecht-Gary *et al*., 1994; Brandel *et al*., 2012). Moreover iron chelation needs only one molecule of enterobactin or PVD per iron ion, but two molecules of PCH (2:1 -PCH : Fe- stoichiometry) to get an octahedral coordination. This suggests that, when several siderophores are present in the bacterial environment, the siderophore most successful at chelating the available iron will scavenge it and deliver it to the microorganism. Consequently, the bacterium will specifically upregulate the expression of all the proteins required to obtain iron via this specific siderophore. In the presence of tris-catechol chelators, PCH, which has a lower affinity for iron and chelates, this metal with a 2:1 (PCH : Fe) stoichiometry, is probably not competitive for the chelation of this metal. Consequently, fewer PCH–Fe complexes are formed and transported into *P. aeruginosa* cells for activation of the PCH pathway via the cytoplasmic regulator PchR. By contrast, the presence of catechol–Fe complexes in the bacterial environment leads to the enterobactin pathway being switched on. Accordingly, in the development of siderophore-antibiotic conjugates, it may be important to design a siderophore moiety with a high enough affinity for iron to compete with the natural siderophores produced by the pathogen. Consequently, it is not surprising that compounds like siderophore conjugate monocarbams are poorly efficient in a Trojan horse strategy in *P. aeruginosa* infections (Tomaras *et al*., 2013; Kim *et al*., 2015). Such compounds have certainly affinities for iron lower than that of PCH and will not be competitive with the endogenous siderophores to provide iron to *P. aeruginosa* cells. Moreover, the iron chelation stoichiometry of such compounds is not 1:1 (siderophore : Fe) as for many natural siderophores; therefore iron loaded monocarbam conjugates may have complex tridimensional structures, which may be poorly recognized by TBDT for uptake.

Iron-55 uptake assays demonstrated that *P. aeruginosa* cells used the TBDT PfeA to assimilate iron complexed with catechol compounds (Fig. 4). Deletion of the *PfeA* gene abolished completely iron uptake by these compounds, with the exception of BCV, for which another, as yet unidentified TBDT must be involved in BCV–Fe assimilation. Previous studies have suggested that TBDTs are highly specific for iron transport via one specific siderophore or structurally related siderophores, but never siderophores with very different chemical structures (for a review see (Schalk *et al*., 2012). In *P. aeruginosa*, PfeA recognizes the ferric forms of the tris-catechol compounds enterobactin, protochelin and TCV, but also the bis-catechol compounds azotochelin and BCV at the bacterial cell surface and transports them across the outer membrane. Consequently, PfeA should be able to take up BCV–antibiotic and TCV–antibiotic conjugates.

In all conditions tested, enterobactin was the most efficient siderophore for iron uptake into *P. aeruginosa*, whereas protochelin with TCV were the least efficient (Figs 4 and 5 and Table 1): 1306 ± 220 Fe atoms/bacterium/min for enterobactin and 273 ± 62 Fe atoms/bacterium/min for protochelin, for cells grown in iron-deficient conditions. Surprisingly, the uptake rates of the different catechol chelators did not reflect the ability of these compounds to induce PfeA expression. This apparent absence of connection between the level of PfeA expression and the rates of iron uptake mediated by catechol siderophores may be due to differences in the recognition and interaction efficiencies between these catecholate compounds and the different protein partners involved in iron acquisition via enterobactin in *P. aeruginosa*.

The iron uptake rates of enterobactin (1306 ± 220 Fe atoms/bacterium/min in iron-deficient medium and 827 ± 64 Fe atoms/bacterium/min in LB – Fig. 5 and Table 1) indicate that this siderophore should be able to transport large amounts of antibiotics in a Trojan horse strategy. The lower uptake rate of protochelin and TCV probably reflects difficulties interacting with one of the proteins involved in enterobactin uptake pathway: PfeA or another, unidentified partner. Iron uptake via enterobactin has been studied in detail in *E. coli* and involves transport across the outer membrane by the TBDT FepA, across the inner membrane by the ABC transporter FepBCD and the release of the metal from the siderophore in the cytoplasm, via a mechanism involving iron reduction and siderophore hydrolysis (Raymond *et al*., 2003; Schalk and Guillon, 2013). This scenario does not seem to apply to *P. aeruginosa*, particularly as the operon containing *pfeA* in this bacterium contains only the PA2689 gene (downstream from *pfeA*) encoding a putative esterase (Winsor *et al*., 2011) with a typical signalling sequence, suggesting a periplasmic distribution. No gene coding for an inner

membrane transporter is present on the genome in the vicinity of *pfeA*, strongly suggesting that, as for iron acquisition via PVD, iron may be released from enterobactin and other catechol chelators in the periplasm of *P. aeruginosa* rather than in the cytoplasm as in *E. coli*. However, further studies are required to obtain insight into the enterobactin pathway in *P. aeruginosa*, to identify the various protein partners and molecular mechanisms involved and to improve our understanding to facilitate the design of optimal catechol–antibiotic conjugates transported into *P. aeruginosa* cells with the same efficiency as for the natural siderophore enterobactin.

In conclusion, the development of Trojan horse strategies involves considering different parameters to ensure the design of siderophore–antibiotic compounds with a high probability of ensuring effective drug delivery. It involves the synthesis of siderophore–antibiotic conjugates having a very high affinity for iron, able to compete for this nutrient with the endogenous siderophores produced by the target bacterium. Moreover, it is crucial that the siderophore–antibiotic conjugates once loaded with iron can still be recognized by TBDTs with good affinities. Consequently, vectors having structural homologies with natural siderophores will be vectors with the highest probability to transport efficiently antibiotics into bacteria. At last, the development of such Trojan horse strategies also requires an excellent knowledge of the molecular mechanisms involved in ferrisiderophore uptake.

The data presented here indicate that enterobactin–antibiotic conjugates should have a high potential for activating PfeA transcription, facilitating the transport of large amounts of antibiotic into the bacteria (the transport of 800 to 2000 molecules of antibiotic might be predicted). The high potential of TCV to activate the transcription of PfeA is also of potential interest in such a study, to ensure that the catechol–antibiotic conjugates remain close to the bacterial cell surface, ready to be transported. An ideal catechol vector for the transport of antibiotics into bacteria would be a compound able to activate the transcription of PfeA, like TCV, but able to ensure transport with the uptake rate of enterobactin.

Materials and methods

Chemicals

The pyochelin (PCH) used for ^{55}Fe uptake assays was synthesized and purified as previously described (Zamri and Abdallah, 2000; Youard *et al*., 2007). Enterobactin was purchased from Sigma-Aldrich. Azotochelin (BCS), BCV and TCV were synthesized as previously described (Baco *et al*., 2014). The syntheses of protochelin (TCS) is described in the Supplementary Material.

Bacterial strains, plasmids and growth conditions

The *P. aeruginosa* and *Escherichia coli* strains and plasmids used in this study are listed in Table S1. *Escherichia coli* strains were routinely grown in LB (Difco) at 37°C. *Pseudomonas aeruginosa* strains were first grown overnight at 30°C in LB broth and were then washed, re-suspended and cultured overnight at 30°C in iron-deficient CAA medium (composition: 5 g l^{-1} low-iron CAA (Difco), 1.46 g l^{-1} K_2HPO_4 $3H_2O$, 0.25 g l^{-1} $MgSO_4$ $7H_2O$. Carbenicillin was added at a concentration of 150 μg ml^{-1} when required.

Mutant construction

All enzymes for deoxyribonucleic acid (DNA) manipulation were purchased from Fermentas and were used in accordance with the manufacturer's instructions. *Escherichia coli* strain TOP10 (Invitrogen) was used as the host strain for all plasmids. The DNA fragments from *P. aeruginosa* used for cloning were amplified from the genomic DNA of the PAO1 strain with Phusion High-Fidelity DNA polymerase (ThermoFisher Scientific). The primers used are listed in Table S2. As previously described (Guillon *et al*., 2012), the general procedure involved the insertion of the 700 bp flanking sequences on either side of the gene to be deleted into the pME3088 suicide vector (Voisard *et al*., 1994). Mutations in the chromosomal genome of *P. aeruginosa* were generated by transferring the suicide vector from *E. coli* TOP10 strains into the PAO1 strain and allowing the plasmid to integrate into the chromosome, with selection for tetracycline resistance. A second crossing-over event excising the vector was achieved by enrichment for tetracycline-sensitive cells to generate the corresponding mutants (Ye *et al*., 1995). All gene-deletion mutants were verified by PCR and sequencing.

For construction of the complementation plasmid encoding *pfeA* under the control of its own promoter, the gene was amplified from the chromosomal DNA of *P. aeruginosa* PAO1 by PCR with the pfeAatg-104F and pfeAstop+31R primers (Table S2). The PCR fragment was trimmed by digestion with *Eco*RI and *Hin*dIII and inserted between the sites for these enzymes in pMMB190 (Morales *et al*., 1991) and bacteria transformed with this vector.

Growth and quantification of fluorescence intensity

The cells were cultured overnight in CAA medium, pelleted by centrifugation and re-suspended in fresh CAA medium, and the resulting suspension was diluted so as to obtain an optical density at 600 nm of 0.01 units. We dispensed 200 μl of the suspension per well into a 96-well plate (Greiner, U-bottomed microplate). The plate was

incubated at 30°C, with shaking, in a Tecan microplate reader (Infinite M200, Tecan) for measurements of OD_{600nm} and mCherry (excitation/emission wavelengths: 570 nm/610 nm) fluorescence at 30 min intervals, for 40 h. After 8 h of culture, we added 200 μM enterobactin, BCV or TCV and continued measurements of OD_{600nm} and mCherry fluorescence. We calculated the mean of three replicates for each measurement.

Quantitative real-time PCR

Specific gene expression was measured by RT-qPCR, as previously described (Gross and Loper, 2009). Briefly, overnight cultures of strains grown in LB or CAA medium were pelleted, re-suspended and diluted in fresh medium to obtain an OD_{600nm} of 0.1 units. The cells were then incubated in the presence or absence of 10 μM enterobactin, azotochelin, protochelin, BCV and TCV, with vigorous shaking, at 30°C for 3 h (LB medium) or 8 h (CAA medium). An aliquot of 2.5×10^8 cells from this culture was added to two volumes of RNAprotect Bacteria Reagent (Qiagen). Total RNA was extracted with an RNeasy Mini kit (Qiagen), treated with DNase (RNase-Free DNase Set, Qiagen) and purified with an RNeasy Mini Elute cleanup kit (Qiagen). We then reverse-transcribed 1 μg of total RNA with a High-Capacity RNA-to-cDNA Kit, in accordance with the manufacturer's instructions (Applied Biosystems). The amounts of specific complementary DNAs were assessed in a StepOne Plus instrument (Applied Biosystems) with Power Sybr Green PCR Master Mix (Applied Biosystems) and the appropriate primers (Table S1), with the *uvrD* messenger RNA used as an internal control. The transcript levels for a given gene in a given strain were normalized with respect to those for *uvrD* and are expressed as a ratio (fold change) relative to the reference conditions.

Proteomics analysis

For the digestion and cleanup steps, 10^9 *P. aeroginosa* cells were lysed in 50 μl lysis buffer (2% sodium deoxycholate, 0.1M ammoniumbicarbonate) and disrupted by two cycles of sonication for 20 s (Hielscher Ultrasonicator). Protein concentration was determined by BCA assay (Thermo Fisher Scientific) using a small sample aliquot.

Proteins were reduced with 5 mM TCEP [Tris (2-Carboxyethyl) phosphine hydrochloride] for 10 min at 95°C, alkylated with 10 mM iodoacetamide for 30 min in the dark at room temperature. Samples were diluted with 0.1M ammonium bicarbonate solution to a final concentration of 1% sodium deoxycholate before digestion with trypsin (Promega) at 37°C overnight (protein to trypsin ratio: 50:1). After digestion, the samples were supplemented with TFA to a final concentration of 0.5% and HCl to a final concentration of 50 mM. Precipitated sodium deoxycholate was removed by centrifugation (15 min at 4°C at 14,000 rpm). Then, peptides were desalted on C18 reversed phase spin columns according to the manufacturer's instructions (Macrospin, Harvard Apparatus), dried under vacuum and stored at –80°C until further processing.

For the shotgun proteomics assays, 1 μg of peptides of each sample were subjected to liquid chromatography-mass spectrometry (LC-MS) analysis using a dual pressure LTQ-Orbitrap Elite mass spectrometer connected to an electrospray ion source (both Thermo Fisher Scientific) as described recently (Glatter *et al*., 2012) with a few modifications. In brief, peptide separation was carried out using an EASY nLC-1000 system (Thermo Fisher Scientific) equipped with a reversed-phase high-performance liquid chromatography column (75 μm × 45 cm) packed in-house with C18 resin (ReproSil-Pur C18–AQ, 1.9 μm resin; Dr. Maisch GmbH, Ammerbuch-Entringen, Germany) using a linear gradient from 95% solvent A (0.15% formic acid, 2% acetonitrile) and 5% solvent B (98% acetonitrile, 0.15% formic acid) to 28% solvent B over 120 min at a flow rate of 0.2 μl min^{-1}. The data acquisition mode was set to obtain one high-resolution MS scan in the Fourier Transform part of the mass spectrometer at a resolution of 240 000 full width at half-maximum (at m/z 400) followed by tandem mass spectrometry (MS/MS) scans in the linear ion trap of the 20 most intense ions using rapid scan speed. The charged state screening modus was enabled to exclude unassigned and singly charged ions and the dynamic exclusion duration was set to 30s. The ion accumulation time was set to 300 ms (MS) and 25 ms (MS/MS).

For label-free quantification, the generated raw files were imported into the PROGENESIS LC-MS software (Nonlinear Dynamics, Version 4.0) and analysed using the default parameter settings. Tandem mass spectrometry data were exported directly from PROGENESIS LC-MS in mgf format and searched against a decoy database the forward and reverse sequences of the predicted proteome from *P. aeruginosa* (NCBI, http://www.ncbi.nlm.nih.gov/, 11985 protein sequences, downloaded 2014/01/10) using MASCOT (version 2.4.0). The search criteria were set as follows: full trypsic specificity was required (cleavage after lysine or arginine residues); three missed cleavages were allowed; carbamidomethylation (C) was set as fixed modification; oxidation (M) as variable modification. The mass tolerance was set to 10 ppm for precursor ions and 0.6 Da for fragment ions. Results from the database search were imported into PROGENESIS, and the final peptide feature list and the protein list containing the summed peak areas of all identified peptides for each protein, respectively, were exported from PROGENESIS LC-MS. Both lists were further statically analysed using an in-house developed R

script (SafeQuant) and the peptide and protein false discovery rate was set to 1% using the number of reverse hits in the dataset (Glatter *et al*., 2012).

Iron uptake

The protonophore CCCP was purchased from Sigma. Obtained was $^{55}FeCl_3$ from Perkin Elmer Life and Analytical Sciences (Billerica, MA, USA), in solution, at a concentration of 71.1 mM, with a specific activity of 10.18 Ci/g. Siderophore–^{55}Fe complexes were prepared at ^{55}Fe concentrations of 20 μM, with a siderophore : iron (mol : mol) ratio of 20:1. Iron uptake assays were carried out as previously described for PVD–Fe transport (Schalk *et al*., 2001; Hoegy and Schalk, 2014), except that bacteria were grown in CAA medium in the presence or absence of 10 μM enterobactin or catechol chelator, to induce PfeA expression. The bacteria were then washed with 50 mM Tris-HCl pH 8.0, to eliminate the siderophores used to induce PfeA expression, and diluted to an OD_{600nm} of 1. Bacteria were then incubated in the presence of 200 nM chelator-^{55}Fe, and the incorporation of radioactivity into the bacteria over time was monitored by filtration (Schalk *et al*., 2001; Hoegy and Schalk, 2014). The experiments were repeated with cells pretreated with 200 μM CCCP. This compound inhibits the proton-motive force across the bacterial cell membrane, thereby inhibiting TonB-dependent iron uptake (Clément *et al*., 2004). For the data presented in Table 1, the radioactivity incorporated into the bacteria was monitored after 15 min of incubation with the chelator–^{55}Fe complexes. Iron-55 uptake assays in the presence of PCH-^{55}Fe (200 nM) were carried out as for enterobactin except that the bacteria were harvest by centrifugation, as previously described (Hoegy *et al*., 2009; Hoegy and Schalk, 2014), and not by filtration to avoid an adsorption of PCH-^{55}Fe on the GFB filters (Whatman).

Acknowledgements

This work was partly funded by the Centre National de la Recherche Scientifique and grants from the ANR (*Agence Nationale de Recherche*, *IronPath* ANR-12-BSV8-0007-01). In addition, these results were generated as part of the work of the Translocation Consortium (http://www.imi.europa.eu/content/translocation) supported by the Innovative Medicines Joint Undertaking under Grant Agreement no. 115525, through financial contributions from the European Union's Seventh Framework Programme (FP7/2007-2013) and contributions in kind from EFPIA companies. O. Cunrath held fellowships, initially from the French Ministère de la Recherche et de la Technologie, and then from the Fondation pour la Recherche Médicale.

References

Albrecht-Gary, A.M., Blanc, S., Rochel, N., Ocacktan, A.Z., and Abdallah, M.A. (1994) Bacterial iron transport: coordination properties of pyoverdin PaA, a peptidic siderophore of *Pseudomonas aeruginosa*. *Inorg Chem* **33:** 6391–6402.

Baco, E., Hoegy, F., Schalk, I.J., and Mislin, G.L. (2014) Diphenyl-benzo[1,3]dioxole-4-carboxylic acid pentafluorophenyl ester: a convenient catechol precursor in the synthesis of siderophore vectors suitable for antibiotic Trojan horse strategies. *Org Biomol Chem* **12:** 749–757.

Benz, G., Schroeder, T., Kurz, J., Wuensche, C., Karl, W., Steffens, G., Pfitzner, J., *et al*. (1982) Konstitution der Desferriform der Albomycine δ1, δ2, ε. *Angew Chem* **21:** 1322–1335.

Bickel, H., Mertens, P., Prelog, V., Seibl, J., and Walser, A. (1965) Constitution of ferrimycin A1. *Antimicrob Agents Chemother (Bethesda)* **5:** 951–957.

Brandel, J., Humbert, N., Elhabiri, M., Schalk, I.J., Mislin, G.L.A., and Albrecht-Garry, A.-M. (2012) Pyochelin, a siderophore of *Pseudomonas aeruginosa*: physicochemical characterization of the iron(III), copper(II) and zinc(II) complexes. *Dalton Trans* **41:** 2820–2834.

Braun, V., and Braun, M. (2002) Active transport of iron and siderophore antibiotics. *Curr Opin Microbiol* **5:** 194–201.

Braun, V., Pramanik, A., Gwinner, T., Koberle, M., and Bohn, E. (2009) Sideromycins: tools and antibiotics. *Biometals* **22:** 3–13.

Brillet, K., Ruffenach, F., Adams, H., Journet, L., Gasser, V., Hoegy, F., *et al*. (2012) An ABC transporter with two periplasmic binding proteins involved in iron acquisition in *Pseudomonas aeruginosa*. *ACS Chem Biol* **7:** 2036–2045.

Carrano, C.J., and Raymond, K.N. (1979) Ferric ion sequestering agents. 2. Kinetics and mechanism of iron removal from transferrin by enterobactin and synthetic tricatechols. *J Am Chem Soc* **101:** 5401–5404.

Chairatana, P., Zheng, T., and Nolan, E.M. (2015) Targeting virulence: salmochelin modification tunes the antibacterial activity spectrum of beta-lactams for pathogen-selective killing of *Escherichia coli*. *Chem Sci* **6:** 4458–4471.

Clément, E., Mesini, P.J., Pattus, F., Abdallah, M.A., and Schalk, I.J. (2004) The binding mechanism of pyoverdin with the outer membrane receptor FpvA in *Pseudomonas aeruginosa* is dependent on its iron-loaded status. *Biochemistry* **43:** 7954–7965.

Cornelis, P., and Bodilis, J. (2009) A survey of TonB-dependent receptors in fluorescent pseudomonads. *Environ Microbiol Rep* **1:** 256–262.

Cornelis, P., and Dingemans, J. (2013) *Pseudomonas aeruginosa* adapts its iron uptake strategies in function of the type of infections. *Front Cell Infect Microbiol* **3:** 75.

Cornish, A.S., and Page, W.J. (2000) Role of molybdate and other transition metals in the accumulation of protochelin by *Azotobacter vinelandii*. *Appl Environ Microbiol* **66:** 1580–1586.

Cox, C.D. (1980) Iron uptake with ferripyochelin and ferriccitrate by *Pseudomonas aeruginosa*. *J Bacteriol* **142:** 581–587.

Cunrath, O., Geoffroy, V.A., and Schalk, I.J. (2015a) Metallome of *Pseudomonas aeruginosa*: a role for siderophores. *Environ Microbiol* doi: 10.1111/1462-2920.12971.

Cunrath, O., Gasser, V., Hoegy, F., Reimmann, C., Guillon, L., and Schalk, I.J. (2015b) A cell biological view of

the siderophore pyochelin iron uptake pathway in *Pseudomonas aeruginosa*. *Environ Microbiol* **17:** 171–185.

Dean, C.R., and Poole, K. (1993) Expression of the ferric enterobactin receptor (PfeA) of *Pseudomonas aeruginosa*: involvement of a two-component regulatory system. *Mol Microbiol* **8:** 1095–1103.

Destoumieux-Garzon, D., Peduzzi, J., Thomas, X., Djediat, C., and Rebuffat, S. (2006) Parasitism of iron-siderophore receptors of *Escherichia coli* by the siderophore-peptide microcin E492m and its unmodified counterpart. *Biometals* **19:** 181–191.

Fardeau, S., Dassonville-Klimpt, A., Audic, N., Sasaki, A., Pillon, M., Baudrin, E., *et al*. (2014) Synthesis and antibacterial activity of catecholate-ciprofloxacin conjugates. *Bioorg Med Chem* **22:** 4049–4060.

Gasser, V., Guillon, L., Cunrath, O., and Schalk, I.J. (2015) Cellular organization of siderophore biosynthesis in *Pseudomonas aeruginosa*: evidence for siderosomes. *J Inorg Biochem* **148:** 27–34.

Glatter, T., Ludwig, C., Ahrne, E., Aebersold, R., Heck, A.J., and Schmidt, A. (2012) Large-scale quantitative assessment of different in-solution protein digestion protocols reveals superior cleavage efficiency of tandem Lys-C/trypsin proteolysis over trypsin digestion. *J Proteome Res* **11:** 5145–5156.

Greenwald, J., Hoegy, F., Nader, M., Journet, L., Mislin, G.L.A., Graumann, P.L., and Schalk, I.J. (2007) Real-time FRET visualization of ferric-pyoverdine uptake in *Pseudomonas aeruginosa*: a role for ferrous iron. *J Biol Chem* **282:** 2987–2995.

Gross, H., and Loper, J.E. (2009) Genomics of secondary metabolite production by *Pseudomonas* spp. *Nat Prod Rep* **26:** 1408–1446.

Guillon, L., El Mecherki, M., Altenburger, S., Graumann, P.L., and Schalk, I.J. (2012) High cellular organisation of pyoverdine biosynthesis in *Pseudomonas aeruginosa*: localization of PvdA at the old cell pole. *Environ Microbiol* **14:** 1982–1994.

Harding, R.A., and Royt, P.W. (1990) Acquisition of iron from citrate by *Pseudomonas aeruginosa*. *J Gen Microbiol* **136:** 1859–1867.

Hider, R.C., and Kong, X. (2011) Chemistry and biology of siderophores. *Nat Prod Rep* **27:** 637–657.

Hoegy, F., and Schalk, I.J. (2014) Monitoring iron uptake by siderophores. *Methods Mol Biol* **1149:** 337–346.

Hoegy, F., Lee, X., Noël, S., Mislin, G.L.A., Rognan, D., Reimmann, C., and Schalk, I.J. (2009) Stereospecificity of the siderophore pyochelin outer membrane transporters in fluorescent Pseudomonads. *J Biol Chem* **284:** 14949–14957.

Ji, C., and Miller, M.J. (2015) Siderophore-fluoroquinolone conjugates containing potential reduction-triggered linkers for drug release: synthesis and antibacterial activity. *Biometals* **28:** 541–551.

Ji, C., Miller, P.A., and Miller, M.J. (2012a) Iron transport-mediated drug delivery: practical syntheses and in vitro antibacterial studies of tris-catecholate siderophore-aminopenicillin conjugates reveals selectively potent antipseudomonal activity. *J Am Chem Soc* **134:** 9898–9901.

Ji, C., Juarez-Hernandez, R.E., and Miller, M.J. (2012b) Exploiting bacterial iron acquisition: siderophore conjugates. *Future Med Chem* **4:** 297–313.

Kim, A., Kutschke, A., Ehmann, D.E., Patey, S.A., Crandon, J.L., Gorseth, E., *et al*. (2015) Pharmacodynamic profiling of a siderophore-conjugated monocarbam in *Pseudomonas aeruginosa*: assessing the risk for resistance and attenuated efficacy. *Antimicrob Agents Chemother* **59:** 7743–7752.

Knosp, O., von Tigerstrom, M., and Page, W.J. (1984) Siderophore-mediated uptake of iron in *Azotobacter vinelandii*. *J Bacteriol* **159:** 341–347.

Llamas, M.A., Sparrius, M., Kloet, R., Jimenez, C.R., Vandenbroucke-Grauls, C., and Bitter, W. (2006) The heterologous siderophores ferrioxamine B and ferrichrome activate signaling pathways in *Pseudomonas aeruginosa*. *J Bacteriol* **188:** 1882–1891.

Llamas, M.A., Mooij, M.J., Sparrius, M., Vandenbroucke-Grauls, C.M., Ratledge, C., and Bitter, W. (2008) Characterization of five novel *Pseudomonas aeruginosa* cell-surface signalling systems. *Mol Microbiol* **67:** 458–472.

Llamas, M.A., Imperi, F., Visca, P., and Lamont, I.L. (2014) Cell-surface signaling in *Pseudomonas*: stress responses, iron transport, and pathogenicity. *FEMS Microbiol Rev* **38:** 569–597.

de Lorenzo, V. (1984) Isolation and characterization of microcin E492 from *Klebsiella pneumoniae*. *Arch Microbiol* **139:** 72–75.

de Lorenzo, V., Martinez, J.L., and Asensio, C. (1984) Microcin-mediated interactions between *Klebsiella pneumoniae* and *Escherichia coli* strains. *J Gen Microbiol* **130:** 391–400.

Marshall, B., Stintzi, A., Gilmour, C., Meyer, J.M., and Poole, K. (2009) Citrate-mediated iron uptake in *Pseudomonas aeruginosa*: involvement of the citrate-inducible FecA receptor and the FeoB ferrous iron transporter. *Microbiology* **155:** 305–315.

Meyer, J.M. (1992) Exogenous siderophore-mediated iron uptake in *Pseudomonas aeruginosa*: possible involvement of porin OprF in iron translocation. *J Gen Microbiol* **138:** 951–958.

Milner, S.J., Seve, A., Snelling, A.M., Thomas, G.H., Kerr, K.G., Routledge, A., and Duhme-Klair, A.K. (2013) Staphyloferrin A as siderophore-component in fluoroquinolone-based Trojan horse antibiotics. *Org Biomol Chem* **11:** 3461–3468.

Mislin, G.L.A., and Schalk, I.J. (2014) Siderophore-dependent iron uptake systems as gates for antibiotic Trojan horse strategies against *Pseudomonas aeruginosa*. *Metallomics* **6:** 408–420.

Mislin, G.L.A., Hoegy, F., Cobessi, D., Poole, K., Rognan, D., and Schalk, I.J. (2006) Binding properties of pyochelin and structurally related molecules to FptA of *Pseudomonas aeruginosa*. *J Mol Biol* **357:** 1437–1448.

Mollmann, U., Heinisch, L., Bauernfeind, A., Kohler, T., and Ankel-Fuchs, D. (2009) Siderophores as drug delivery agents: application of the 'Trojan Horse' strategy. *Biometals* **22:** 615–624.

Morales, V.M., Backman, A., and Bagdasarian, M. (1991) A series of wide-host-range low-copy-number vectors

that allow direct screening for recombinants. *Gene* **97:** 39–47.
Noel, S., Gasser, V., Pesset, B., Hoegy, F., Rognan, D., Schalk, I.J., and Mislin, G.L.A. (2011) Synthesis and biological properties of conjugates between fluoroquinolones and a N3''-functionalized pyochelin. *Org Biomol Chem* **9:** 8288–8300.
Nolan, E.M., and Walsh, C.T. (2008) Investigations of the MceIJ-catalyzed posttranslational modification of the microcin E492 C-terminus: linkage of ribosomal and nonribosomal peptides to form 'trojan horse' antibiotics. *Biochemistry* **47:** 9289–9299.
Page, M.G. (2013) Siderophore conjugates. *Ann N Y Acad Sci* **1277:** 115–126.
Page, M.G., Dantier, C., and Desarbre, E. (2010) In vitro properties of BAL30072, a novel siderophore sulfactam with activity against multiresistant gram-negative bacilli. *Antimicrob Agents Chemother* **54:** 2291–2302.
Poole, K., and McKay, G.A. (2003) Iron acquisition and its control in *Pseudomonas aeruginosa*: many roads lead to Rome. *Front Biosci* **8:** d661–d686.
Poole, K., Young, L., and Neshat, S. (1990) Enterobactin-mediated iron transport in *Pseudomonas aeruginosa*. *J Bacteriol* **172:** 6991–6996.
Ratledge, C., and Dover, L.G. (2000) Iron metabolism in pathogenic bacteria. *Annu Rev Microbiol* **54:** 881–941.
Raymond, K.N., Dertz, E.A., and Kim, S.S. (2003) Enterobactin: an archetype for microbial iron transport. *Proc Natl Acad Sci USA* **100:** 3584–3588.
Rebuffat, S. (2012) Microcins in action: amazing defence strategies of *Enterobacteria*. *Biochem Soc Trans* **40:** 1456–1462.
Rivault, F., Liébert, C., Burger, A., Abdallah, M.A., Schalk, I.J., and Mislin, G.L. (2007) Synthesis of pyochelin-norfloxacin conjuguates. *Bioorg Med Chem Lett* **17:** 640–644.
Rodrigue, A., Quentin, Y., Lazdunski, A., Mejean, V., and Foglino, M. (2000) Two-component systems in *Pseudomonas aeruginosa*: why so many? *Trends Microbiol* **8:** 498–504.
Schalk, I.J., and Guillon, L. (2013) Fate of ferrisiderophores after import across bacterial outer membranes: different iron release strategies are observed in the cytoplasm or periplasm depending on the siderophore pathways. *Amino Acids* **44:** 1267–1277.
Schalk, I.J., Hennard, C., Dugave, C., Poole, K., Abdallah, M.A., and Pattus, F. (2001) Iron-free pyoverdin binds to its outer membrane receptor FpvA in *Pseudomonas aeruginosa*: a new mechanism for membrane iron transport. *Mol Microbiol* **39:** 351–360.
Schalk, I.J., Mislin, G.L.A., and Brillet, K. (2012) Structure, function and binding selectivity and stereoselectivity of siderophore-iron outer membrane transporters. *Curr Top Membr* **69:** 37–66.
Thomas, X., Destoumieux-Garzon, D., Peduzzi, J., Afonso, C., Blond, A., Birlirakis, N., *et al*. (2004) Siderophore peptide, a new type of post-translationally modified antibacterial peptide with potent activity. *J Biol Chem* **279:** 28233–28242.
Tomaras, A.P., Crandon, J.L., McPherson, C.J., Banevicius, M.A., Finegan, S.M., Irvine, R.L., *et al*. (2013) Adaptation-based resistance to siderophore-conjugated antibacterial agents by *Pseudomonas aeruginosa*. *Antimicrob Agents Chemother* **57:** 4197–4207.
Tsukiura, H., Okanishi, M., Ohmori, T., Koshiyama, H., Miyaki, T., Kitazima, H., and Kawaguchi, H. (1964) Danomycin, a new antibiotic. *J Antibiot (Tokyo)* **17:** 39–47.
Vasil, M.L., and Ochsner, U.A. (1999) The response of *Pseudomonas aeruginosa* to iron: genetics, biochemistry and virulence. *Mol Microbiol* **34:** 399–413.
Voisard, C., Bull, C., Keel, C., Laville, J., Maurhofer, M., Schnider, U., *et al*. (1994) Biocontrol of root diseases by *Pseudomonas fluorescens* CHAO: current concepts and experimental approaches. In *Molecular Ecology of Rhizosphere Microorganisms*. O'Gara, F., Dowling, D.N., and Boesten, B. (eds). Weinheim, Germany: VCH, pp. 67–89.
Wencewicz, T.A., and Miller, M.J. (2013) Biscatecholate-monohydroxamate mixed ligand siderophore-carbacephalosporin conjugates are selective sideromycin antibiotics that target *Acinetobacter baumannii*. *J Med Chem* **56:** 4044–4052.
Wencewicz, T.A., Long, T.E., Mollmann, U., and Miller, M.J. (2013) Trihydroxamate siderophore-fluoroquinolone conjugates are selective sideromycin antibiotics that target *Staphylococcus aureus*. *Bioconjug Chem* **24:** 473–486.
Winsor, G.L., Lam, D.K., Fleming, L., Lo, R., Whiteside, M.D., Yu, N.Y., *et al*. (2011) *Pseudomonas* Genome Database: improved comparative analysis and population genomics capability for *Pseudomonas* genomes. *Nucleic Acids Res* **39:** D596–D600.
Ye, R.W., Haas, D., Ka, J.O., Krishnapillai, V., Zimmermann, A., Baird, C., and Tiedje, J.M. (1995) Anaerobic activation of the entire denitrification pathway in *Pseudomonas aeruginosa* requires Anr, an analog of Fnr. *J Bacteriol* **177:** 3606–3609.
Youard, Z.A., Mislin, G.L., Majcherczyk, P.A., Schalk, I.J., and Reimmann, C. (2007) *Pseudomonas fluorescens* CHA0 produces enantio-pyochelin, the optical antipode of the *Pseudomonas aeruginosa* siderophore pyochelin. *J Biol Chem* **282:** 35546–35553.
Zamri, A., and Abdallah, M.A. (2000) An improved stereocontrolled synthesis of pyochelin, a siderophore of *Pseudomonas aeruginosa* and *Burkholderia cepacia*. *Tetrahedron* **56:** 249–256.
Zheng, T., and Nolan, E.M. (2014) Enterobactin-mediated delivery of beta-lactam antibiotics enhances antibacterial activity against pathogenic *Escherichia coli*. *J Am Chem Soc* **136:** 9677–9691.

Supporting information

Additional Supporting Information may be found in the online version of this article at the publisher's website:

Fig. S1. Analysis of transcriptional changes in TDBT genes.
Scheme S1. Synthesis of protochelin. (i) 1,4-diaminobutane, CH2Cl2, 20°C; (ii) **2**, HATU, DIPEA, THF; 20°C; (iii) TFA, TIPS, CH2Cl2, 20°C.
Table S1. Strains and plasmids used in this study.
Table S2. Oligonucleotides used in this study.

6

TonB-Dependent Receptor Repertoire of *Pseudomonas aeruginosa* for Uptake of Siderophore-Drug Conjugates

Alexandre Luscher[1,2], Lucile Moynie[3], **Pamela Saint Auguste**[4], Dirk Bumann[4], Lena Mazza[1,2], Daniel Pletzer[5], James H. Naismith [3], Thilo Kohler[1,2].

[1] Service of Infectious Diseases, University Hospital Geneva, Geneva, Switzerland [2] Department of Microbiology and Molecular Medicine, University of Geneva, Geneva, Switzerland [3] School of Chemistry and Biomedical Sciences Research Complex, University of St Andrews, Fife, Scotland, United Kingdom [4] Focal Area Infection Biology, Biozentrum, University of Basel, Basel, Switzerland [5] Jacobs University, Bremen, Germany

State of the paper: Manuscript published in Antimicrobial Agents and Chemotherapy.

6.1 Abstract of the paper

The conjugation of siderophores to antimicrobial molecules is an attractive strategy to overcome the low outer membrane permeability of Gram-negative bacteria. In this Trojan horse approach, the transport of drug conjugates is redirected via TonB-dependent receptors (TBDR), which are involved in the uptake of essential nutrients, including iron. Previous reports have demonstrated the involvement of the TBDRs PiuA and PirA from *Pseudomonas aeruginosa* and their orthologues in Acinetobacter baumannii in the uptake of siderophore-beta-lactam drug conjugates. By in silico screening, we further identified a PiuA orthologue, termed PiuD, present in clinical isolates, including strain LESB58. The piuD gene in LESB58 is located at the same genetic locus as piuA in strain PAO1. PiuD has a similar crystal structure as PiuA and is involved in the transport of the siderophore-drug conjugates BAL30072, MC-1, and cefiderocol in strain LESB58. To screen for additional siderophore-drug uptake systems, we overexpressed 28 of the

34 TBDRs of strain PAO1 and identified PfuA, OptE, OptJ, and the pyochelin receptor FptA as novel TBDRs conferring increased susceptibility to siderophore-drug conjugates. The existence of a TBDR repertoire in *P. aeruginosa* able to transport siderophore drug molecules potentially decreases the likelihood of resistance emergence during therapy.

6.2 Statement of my work

Shotgun proteomic samples preparation and data analysis of PAO1 cells grown in Mueller-Hinton broth (MHB) and in MHB treated with Chelex. Different TonB-defficient mutants constructions and related proteomic analysis.

6.3 Published paper

AMERICAN SOCIETY FOR MICROBIOLOGY | Antimicrobial Agents and Chemotherapy®

TonB-Dependent Receptor Repertoire of *Pseudomonas aeruginosa* for Uptake of Siderophore-Drug Conjugates

Alexandre Luscher,[a,b] Lucile Moynié,[c*] Pamela Saint Auguste,[d] Dirk Bumann,[d] Lena Mazza,[a,b] Daniel Pletzer,[e*] James H. Naismith,[c*] Thilo Köhler[a,b]

[a]Service of Infectious Diseases, University Hospital Geneva, Geneva, Switzerland
[b]Department of Microbiology and Molecular Medicine, University of Geneva, Geneva, Switzerland
[c]School of Chemistry and Biomedical Sciences Research Complex, University of St Andrews, Fife, Scotland, United Kingdom
[d]Biozentrum, University of Basel, Basel, Switzerland
[e]Jacobs University, Bremen, Germany

ABSTRACT The conjugation of siderophores to antimicrobial molecules is an attractive strategy to overcome the low outer membrane permeability of Gram-negative bacteria. In this Trojan horse approach, the transport of drug conjugates is redirected via TonB-dependent receptors (TBDR), which are involved in the uptake of essential nutrients, including iron. Previous reports have demonstrated the involvement of the TBDRs PiuA and PirA from *Pseudomonas aeruginosa* and their orthologues in *Acinetobacter baumannii* in the uptake of siderophore-beta-lactam drug conjugates. By *in silico* screening, we further identified a PiuA orthologue, termed PiuD, present in clinical isolates, including strain LESB58. The *piuD* gene in LESB58 is located at the same genetic locus as *piuA* in strain PAO1. PiuD has a similar crystal structure as PiuA and is involved in the transport of the siderophore-drug conjugates BAL30072, MC-1, and cefiderocol in strain LESB58. To screen for additional siderophore-drug uptake systems, we overexpressed 28 of the 34 TBDRs of strain PAO1 and identified PfuA, OptE, OptJ, and the pyochelin receptor FptA as novel TBDRs conferring increased susceptibility to siderophore-drug conjugates. The existence of a TBDR repertoire in *P. aeruginosa* able to transport siderophore-drug molecules potentially decreases the likelihood of resistance emergence during therapy.

KEYWORDS *Pseudomonas aeruginosa*, TonB-dependent receptor, siderophore-drug conjugate

With the shortage of novel classes of antimicrobials, alternative approaches aiming to increase antimicrobial penetration into Gram-negative bacteria have gained widespread interest. Such approaches include the inhibition of broad-spectrum efflux pumps (1), adjuvants that increase cell permeability (2), and the redirection of drug uptake through specific nutrient transport systems (3). The most prominent example of the latter approach is the hijacking of essential bacterial iron transport systems by linking antimicrobial molecules to siderophores in a Trojan horse strategy. The recent development of such compounds by all major pharmaceutical companies historically involved in antimicrobial drug development highlights the increasing interest in this appealing concept (4–7). So far, most of the efforts have focused on the design and study of beta-lactam-siderophore conjugates. Since their targets are located in the periplasmic space, the conjugates do not require further translocation across the inner membrane. Moreover, the conjugates are designed such that the siderophore moiety does not interfere with the drug target interaction and does not require prior cleavage (8). The beta-lactam scaffolds used for the design of such conjugates include penicillins

Received 1 February 2018 **Returned for modification** 9 February 2018 **Accepted** 12 March 2018

Accepted manuscript posted online 19 March 2018

Citation Luscher A, Moynié L, Auguste PS, Bumann D, Mazza L, Pletzer D, Naismith JH, Köhler T. 2018. TonB-dependent receptor repertoire of *Pseudomonas aeruginosa* for uptake of siderophore-drug conjugates. Antimicrob Agents Chemother 62:e00097-18. https://doi.org/10.1128/AAC.00097-18.

Address correspondence to Thilo Köhler, thilo.kohler@unige.ch.

* Present address: Daniel Pletzer, University of British Columbia, Vancouver, Canada; Lucile Moynié, Rutherford Appleton Laboratory, Didcot, Oxford, United Kingdom; James H. Naismith, Division of Structural Biology, Oxford, United Kingdom.

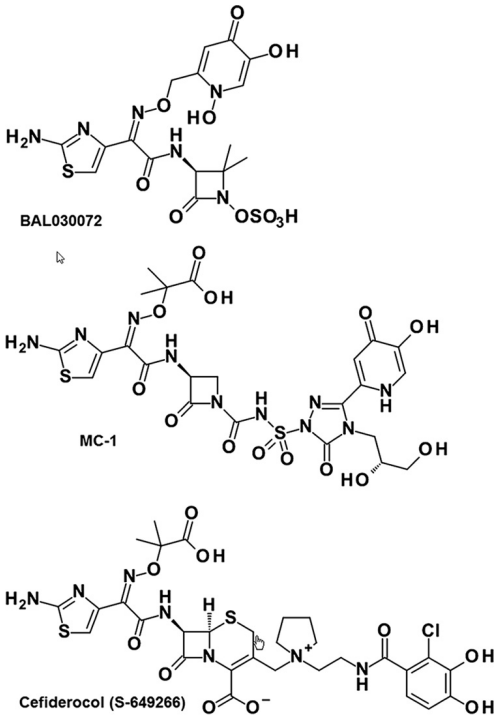

FIG 1 Siderophore-drug conjugates used in this study. BAL30072 and MC-1 contain a dihydroxypyridone as a siderophore, while cefiderocol contains a chlorinated catechol group.

(9), cephalosporins (KP736 and cefiderocol) (7, 10), and monobactams (BAL30072 and MC-1) (4, 5). The iron-binding moiety of these beta-lactam conjugates is either a catechol-type siderophore such as dihydroxypyridone or a mixed catechol/hydroxamate (11). Both the monobactam (5, 12–14) and the cephalosporin conjugates (15) showed potent activity against the Gram-negative nonfermenters *Pseudomonas aeruginosa* and *Acinetobacter baumannii*.

Two TonB-dependent receptors (TBDRs), PiuA and PirA, have been shown to be responsible for the uptake of BAL30072, MC-1, and cefiderocol in *P. aeruginosa* (5, 16, 17). We previously observed that some *P. aeruginosa* isolates did not carry the *piuA* gene, although they were susceptible to BAL30072 (16). Therefore, we suspected that other TonB-dependent receptors (TBDRs) might be present in these strains or that their expression differs with respect to the PAO1 reference strain. Furthermore, the expression of TBDRs is often regulated by sigma/anti-sigma factors or two-component systems (18) and is induced by the presence of the corresponding siderophore (19, 20). These receptors could potentially participate in siderophore-drug uptake, but their contribution is masked under standard noninducing conditions. Therefore, we performed an *in silico* screen for PiuA orthologues in the *P. aeruginosa* genome database, and we additionally expressed from plasmids 28 of the 34 TBDRs of PAO1. This enabled us to identify a novel TBDR, termed PiuD, sharing 60% amino acid identity with PiuA, as well as five additional TBDRs of PAO1, potentially involved in the uptake of three different siderophore-drug conjugates, including the most recent catechol-based compound, cefiderocol (21).

RESULTS

***piuD* and *piuA* encode homologous proteins and are mutually exclusive in *P. aeruginosa* genomes.** We and others (5) previously identified the TonB-dependent receptors (TBDR) PiuA and PirA as transporters for the uptake of siderophore-drug conjugates BAL30072 and MC-1 (Fig. 1) both in *P. aeruginosa* (16) and in *A. baumannii* (22). When performing PCR amplifications of *piuA* from *P. aeruginosa* clinical isolates, we noticed the absence of a *piuA* signal in 54% of genotypically nonredundant isolates

TABLE 1 Susceptibility of *piuD* and *pirA* deletion mutants of *P. aeruginosa* PAO1 and LESB58

Strain	MIC (mg/liter)[a]				
	BAL	MC-1	ATM	CFD	CAZ
PAO1	1	0.5	4	0.5	2
PAO1Δ*piuA*	8	8	4	8	2
PAO1Δ*pirA*	1	0.5	4	0.5	2
PAO1Δ*piuA*Δ*pirA*	16	16	4	16	2
LESB58	1	1	16	0.06	4
LESB58Δ*piuD*	4	2	16	2	4
LESB58Δ*pirA*	16	8	16	0.125	4
LESB58Δ*piuD*Δ*pirA*	32	32	16	4	4

[a]MICs were determined in MHB-Chelex. BAL, BAL30072; ATM, aztreonam; CFD, cefiderocol; CAZ, ceftazidime.

collected from intensive care unit patients (data not shown). We performed a homology search for potential orthologues of PiuA in the genome of LESB58, a strain that we previously showed lacks the *piuA* gene (16). The BLAST algorithm identified an open reading frame (ORF) of 766 amino acids in strains LESB58 (PALES_48941) and 39016 (PA39016_000870080), showing 60% amino acid identity with PiuA of PAO1 (753 amino acids). The highest sequence identity was observed in the N terminus (99% amino acid identity in the first 84 residues, including the signal sequence) and the putative substrate binding loops (NL1 to NL3) (see Fig. S1 in the supplemental material). We termed this PiuA orthologue PiuD. The *piuD* gene has a GC content of 59%, which is below the average of 66% for *P. aeruginosa*. To determine whether *piuD* would be present in strains from which *piuA* could not be amplified, we performed a multiplex PCR with *piuA* and *piuD* primer sets on the same set of genetically distinct clinical isolates tested above for *piuA*. The multiplex PCR confirmed our hypothesis, showing a PCR band either for *piuA* or for *piuD*, suggesting that both genes are mutually exclusive in *P. aeruginosa* genomes (see Fig. S2A). The *piuD* gene was found to be embedded in the same genomic context as *piuA* (16), since the gene products of *piuB* (PA4513) located downstream of *piuA* and those of the two genes *piuC* (PA4515) and *piuE* (PA4516), transcribed in an opposite direction, shared ≥98% amino acid identities with their homologues in LESB58 (Fig. S2B).

Contribution of PiuD and PirA to the activity of siderophore-beta-lactam conjugates. We compared the contributions of PiuA and PiuD with that of PirA, conserved in PAO1 and LESB58, to the activity of various siderophore-drug conjugates. To this end, we constructed deletion mutants in the *piuD* (PALES_48941) and *pirA* (PALES_43851) genes of LESB58. We tested the monobactam drugs BAL30072 (4) and MC-1 (5), conjugated to a hydroxypyridone siderophore, as well as the cephalosporin derivative cefiderocol, linked to a catechol siderophore (7) (Fig. 1). In the PAO1 background, both types of conjugates were strongly affected by the deletion of *piuA* (8- to 32-fold increase in MICs) but not by a *pirA* deletion. Surprisingly, the deletion of the *pirA* gene in the LESB58 background showed a stronger effect on the activities of the hydroxypyridone conjugates (8- to 16-fold increase in MICs) than on the catechol conjugate cefiderocol (2-fold increase in MICs). Conversely, the deletion of *piuD* increased cefiderocol MICs 32-fold, while MICs for MC-1 and BAL30072 increased by only 2- and 4-fold, respectively (Table 1). This could reflect the different expression levels of these receptors and/or the different affinities for the two types of siderophore-drug conjugates.

To address this question, we extracted RNA from PAO1 and LESB58 from late exponential-phase cells grown under the same conditions as for the MIC assays and measured by reverse transcription-quantitative PCR (qRT-PCR) the expression of *piuA* and *piuD* in comparison to that of *pirA*. As shown in Fig. 2, *pirA* was expressed 3-fold less than *piuA* in PAO1, while the relative expression levels between *pirA* and *piuD* were comparable in strain LESB58. The low basal expression level of *pirA* might therefore not be sufficient to contribute to siderophore-drug uptake in PAO1, as highlighted by the

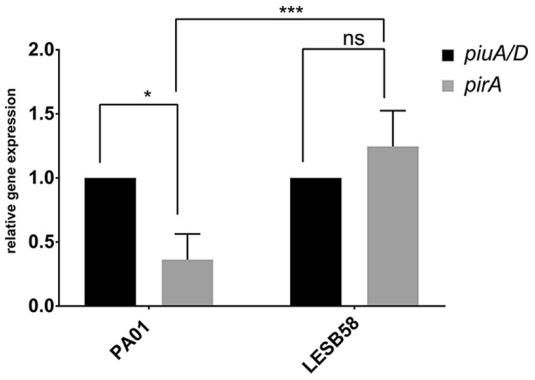

FIG 2 Expression analysis of *pirA* and *piuA* in PAO1 and *pirA* and *piuD* in LESB58. RNA was extracted from cells grown to late exponential phase in MHB. qPCR was performed using target-gene-specific primers. Expression of *pirA* is 3-fold lower than *piuA* in a PAO1 background, while *piuD* and *pirA* expression levels are comparable in strain LESB58. Values are the expression ratios of the target gene divided by the *rpsL* housekeeping gene. The expression of *piuA* and *piuD* was set to 1 (100%) in the respective strain. Values show the means from three independent experiments performed in duplicates. Error bars indicate standard deviations. *, $P < 0.05$ by Student *t* test; ***, $P < 0.001$ by analysis of variance (ANOVA); ns, not significant.

identical MIC values of the *pirA* mutant and the wild-type strain PAO1 (Table 1). In contrast, in LESB58, PirA seemed to transport preferentially the hydroxypyridones BAL30072 and MC-1, while cefiderocol uptake occurred mainly via PiuD. Since PirA amino acid sequences from PAO1 and LESB58 (PALES_43851) are 99% identical, this difference was not due to altered substrate affinities.

Crystal structure of PiuD from *P. aeruginosa*. We previously determined the crystal structure of PiuA from *P. aeruginosa* and its orthologue from *A. baumannii* (22). Here, we determined the structure of PiuD from strain 39016, which shows 99.6% amino acid identity with PiuD (PALES_48941) from LESB58. The obtained PiuD structure was similar to that of PiuA from PAO1. The crystallographic asymmetric unit has two monomers (denoted A and B). PiuD comprised two domains, a 22-stranded transmembrane β-barrel and an N-terminal plug domain (residues 27 to 156) folded inside the barrel (Fig. 3). The plug domain has two β-sheets and two α-helices, which together, occluded the central pore. As often occurs in the TBDR structures, some of the extracellular loops were not experimentally located in the PiuD structure. In the B monomer, these regions, namely, NL1 (83 and 84), NL3 (113 and 114), the loop 138 to 141 of the plug domain, L7 (504 to 530), L8 (564 to 572), and L9 (609 to 624), were presumed to be disordered. The closest structural relatives were PiuA of *A. baumannii* (root mean square deviation [RMSD] of 1.1 Å over 701 residues) and *P.*

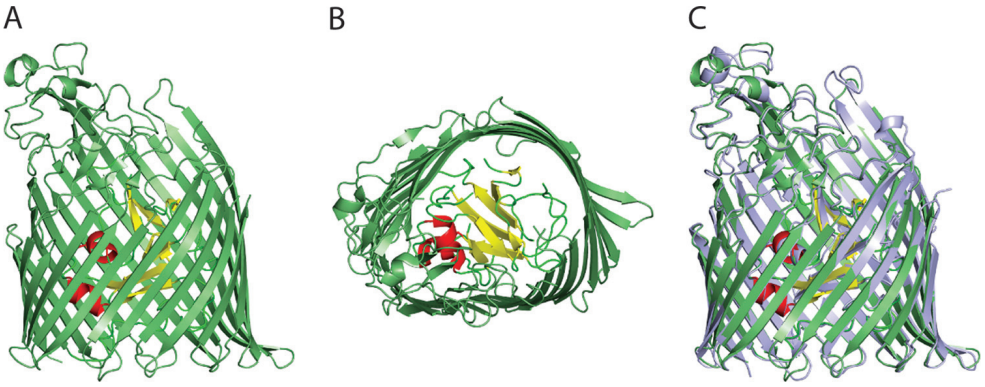

FIG 3 Crystal structure of PiuD from *P. aeruginosa*. Side (A) and extracellular (B) views of PiuD. The 22-stranded transmembrane β-barrel is colored in green. β-Sheets of the plug domain are colored in yellow, loops in green, and helices in red. (C) Structural comparison between PiuA (light blue) and PiuD (green).

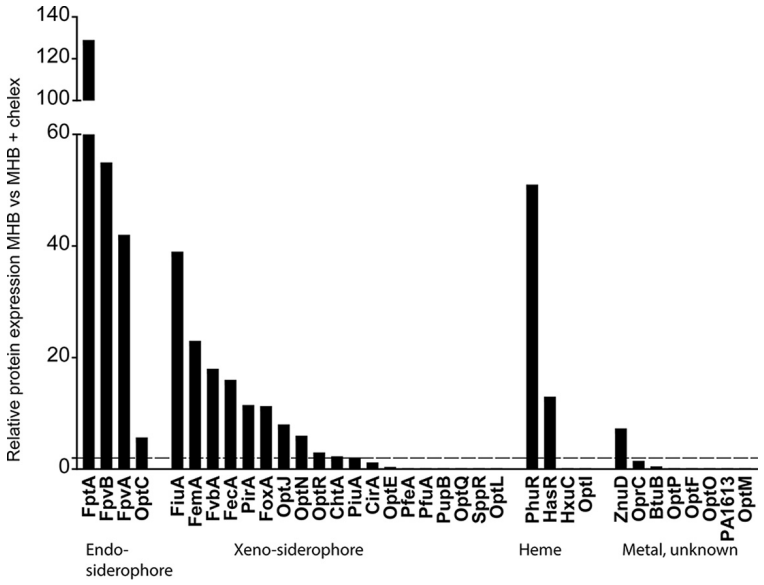

FIG 4 Proteomic analysis of TBDRs from *P. aeruginosa* PAO1. Protein expression levels were compared between cells grown for 20 h in MHB or Chelex-treated MHB. The dashed line indicates the 2-fold induction threshold level.

aeruginosa (1.1 Å over 656 residues) and the pyochelin receptor FptA from *P. aeruginosa* (1.8 Å over 655 residues) (23). As a consequence of the disorder, one side of the extracellular β-barrel was absent. A "belt" of outward facing hydrophobic residues (Trp 445, 486, 541, and 594, Phe 157, 180, 217, 350, 648, and 731, and Tyr 645 and 685), sits at the periplasmic end of the barrel, a characteristic of outer membrane proteins.

Proteomic analysis under Fe chelation. To identify further siderophore-drug transporters, we reasoned that under iron-limiting conditions, the expression of Fe-repressed TBDRs would be upregulated and could potentially contribute to the transport of siderophore-drug conjugates. Therefore, we performed a proteome analysis using PAO1 cells grown in Mueller-Hinton broth (MHB) and in MHB treated with Chelex, which complexes ferric iron but also divalent metal cations. The TBDRs for the endogenous siderophores pyochelin (FptA) and pyoverdin (FpvA and FpvB) showed the strongest induction in the Chelex-treated medium (40- to 130-fold increases) (Fig. 4). We also observed an induction of the heme receptors PhuR and HasR, as well as of the Zn transporter ZnuD. The expression of the known siderophore-drug transporters PiuA and PirA increased 2- and 10-fold, respectively, upon iron chelation. Among the TBDRs expected or reported to transport xenosiderophores, 11 showed a $>$2-fold increase in expression. CirA was below the 2-fold induction threshold, and six xenosiderophore receptors were not expressed or were expressed below the detection limit.

Constitutive expression of TonB-dependent receptors in PAO1. To assess the possible involvement of these receptors in siderophore-drug uptake, we cloned 26 of the 34 TBDR genes from PAO1 (see Table S1), including the Chelex-induced TBDRs (FiuA, FemA, FoxA, OptJ, OptN, ChtA, and CirA) and those that were undetectable. We cloned the corresponding genes into a vector harboring a constitutively expressed promoter in *P. aeruginosa* and transferred the resulting plasmids into strain PAO1. We excluded the heme/hemophore transporters (PhuR, HasR, HxuC, and OptI), the cobalamin transporter BtuB (PA1271), and the citrate receptor FecA. For comparison, we included the previously identified receptor genes *piuA* and *pirA*, as well as the newly identified *piuA* orthologue *piuD*. The susceptibility data clearly showed that six TBDRs, namely, PiuD, OptJ, FemA, OptE, PfuA, and FptA, increased by at least 4-fold the susceptibility of PAO1 to the three siderophore-drug conjugates tested (shown in bold in Table 2). The strain harboring pPA0151 showed a 4-fold increase in susceptibility only

TABLE 2 Effect of overexpression of TonB-dependent receptors on *P. aeruginosa* susceptibilities to three siderophore-drug conjugates

Strain or plasmid[a]	MIC (mg/liter)[b]				
	BAL	MC-1	ATM	CFD	CAZ
PAO1	1	0.25	4	0.5	1
pIApX2 (vector)	1	0.25	4	0.5	1
ppiuA1.1	0.06–0.125	0.06	4	0.03–0.06	1
ppirA1.1	0.06–0.125	0.06	4	0.03–0.06	1
ppiuD	**0.06–0.125**	**0.03**	4	**0.03**	1
poptJ (PA0434)	**0.06–0.125**	**0.03**	4	**0.03–0.06**	1
pfemA (PA1910)	**0.125**	**0.06**	2	**0.06**	1
poptE (PA2911)	**0.25**	**0.06**	2	**0.125**	1
ppfuA (PA1322)	**0.03**	**0.03**	2	**0.03**	1
pfptA	**0.125**	**0.06**	2	**0.125**	0.5
pPA0151	**0.25**	**0.06**	2	0.25	**0.25**
pchtA (PA4675)	0.5	0.125	2	**0.125**	ND[c]
pfiuA (PA0470)	0.5	ND	4	0.25	1
pfoxA (PA2466)	1	0.125	2	0.25	1
ppfeA (PA2688)	1	0.25	4	0.5	ND
pcirA (PA1922)	1	0.25	4	0.25–0.5	1
poptN (PA1365)	1	0.25	4	0.5	ND
poptF (PA2590)	1	ND	4	0.5	0.5
poptQ (PA2289)	1	ND	2	0.25	0.5
poptR (PA3268)	1	0.25	2	0.5	1
pznuD (PA0781)	1	ND	2	ND	ND
optO (PA2335)	0.5	0.25	2	0.5	1
poptP (PA0192)	1	0.25	2	0.5	1
poptL (PA2089)	1	0.25	4	0.5	1
poptC (PA4837)	1	0.125	2	0.5	1
pPA1613	1	0.125	4	0.5	1
poptM (PA2070)	1	0.25	4	0.5	1
psppR (PA2057)	0.5	0.25	4	0.5	2
pfvbA (PA4156)	0.5	0.125	4	0.5	0.5
pfpvA	2	0.5	8	0.5	1
pfpvB	1	0.25	4	1	1

[a]Plasmids in boldface font conferred a ≥4-fold increase in susceptibility to all siderophore-drug conjugates compared to the vector control.
[b]BAL, BAL30072; ATM, aztreonam; CFD, cefiderocol; CAZ, ceftazidime.
[c]ND, not done.

for the dihydroxypyridone-containing drugs BAL30072 and MC-1, and the strain harboring ChtA only showed increased susceptibility for the catechol-based cefiderocol. Surprisingly, the overexpression of PfuA, which was undetectable by proteome analysis, produced the largest increase in susceptibility (>32-fold for BAL30072). With the exception of a 4-fold-decreased MIC for ceftazidime (pPA0151), we observed no significant changes in MICs for the nonsiderophore drugs aztreonam and ceftazidime. Since OptJ was induced to a similar level as PirA under Chelex treatment (Fig. 4), we constructed deletions in *optJ* in PAO1 and its *piuA* and *pirA* deletion mutants. As for a *pirA* deletion in PAO1, *optJ* deletion had no effect on siderophore-drug conjugate MICs (see Table S4). However, a consistent 2-fold increase in BAL30072 MICs in a *piuA* deletion background suggests a minor contribution of OptJ under uninduced conditions in a PAO1 background.

To assess whether the observed changes in susceptibility could result from indirect effects on the expression level of the main siderophore-drug transporter PiuA, we introduced the relevant constructs in a PAO1Δ*piuA* deletion mutant and tested the drug susceptibilities. PiuA, PirA, and PiuD expression decreased the MICs of all three siderophore-drug conjugates by 8- to ≥32-fold (Table 3). Interestingly, PirA overexpression produced only a 4- to 8-fold MIC decrease for cefiderocol compared to that of the vector control, while PiuD expression resulted in a ≥32-fold MIC decrease (Table 3). This finding is in agreement with the susceptibilities of *pirA* and *piuD* mutants in strain LESB58 (Table 1), which suggested preferential transport of cefiderocol via PiuD. The overexpression of PfuA showed MIC changes exceeding those conferred by PiuA and

TABLE 3 Effect of overexpression of TonB-dependent receptors on siderophore-drug conjugates activities in a *piuA* deletion mutant of *P. aeruginosa*

Strain or plasmid	MIC (mg/liter)[a]				
	BAL	MC-1	ATM	CFD	CAZ
PAO1Δ*piuA*	8	2	8	8	2
pIApX2 (vector)	8	4	4	8	2
ppiuA	**0.25**	**0.03**	4	**0.06**	2
ppirA	**0.25**	**0.06**	4	**1–2**	2
ppiuD	**0.125**	**0.03**	8	**0.03–0.125**	2
ppfuA	**0.03**	**0.03**	4	**0.03**	2
pfptA	4	**0.5**	2	**0.25**	2
poptE	4	**0.5**	4	**2**	2
poptJ	4	**1**	4	4–8	2
pfemA	8	2	4	8	2
pPA0151	8	4	2	8	1

[a]MIC changes of ≥4-fold compared to the vector control are shown in boldface font. BAL, BAL30072; ATM, aztreonam; CFD, cefiderocol; CAZ, ceftazidime.

PirA, suggesting efficient siderophore-drug transport independent of PiuA. Similar results were obtained in a *piuA-pirA* double mutant (data not shown). On the other hand, FptA and OptE expression produced 2- to 8-fold decreases for MC-1 and cefiderocol, and OptJ produced a decrease only for MC-1. Finally, FemA and PA0151 expression showed no significant MIC changes in a *piuA* deletion mutant, suggesting an indirect effect on PiuA expression, when overexpressed in a PAO1 wild-type strain.

To further evaluate if additional TBDRs would be involved in the uptake of siderophore-drug conjugates, we determined the susceptibilities under iron-limited growth conditions in MHB Chelex and in a minimal Casamino Acids medium. We observed 2-fold decreases in MICs of BAL30072 and MC-1 in PAO1 and the *pirA* mutant, and a 4- to 8-fold drop in the *piuA* mutant backgrounds. The increase in susceptibility was even more pronounced for cefiderocol (8- to 64-fold decreases) for the strains tested. MICs for the nonsiderophore drugs aztreonam and ceftazidime were not affected (see Table S5). The MICs were comparable or even lower than those obtained by the overexpression of the individual receptors from the plasmids in the *piuA* mutant background (Table 3), suggesting a simultaneous expression of several TBDRs besides PiuA and PirA for the uptake of siderophore-drug conjugates in *P. aeruginosa* under iron-limited conditions.

DISCUSSION

The Trojan horse strategy has recently gained renewed interest, as illustrated by the development of novel siderophore-beta-lactam conjugates by pharmaceutical companies (4, 12) and academic research groups (9, 24). These differ in the beta-lactam scaffolds (penicillins, monobactams, and cephems) as well as the attached siderophore moieties (mono-, tris-catechols and mixed catechol-hydroxamates). Initial investigations have identified two TBDR proteins, PiuA and PirA, in *P. aeruginosa* (5, 16) and their orthologues in *A. baumannii* (22). These are the main transporters for BAL30072 and MC-1. While the deletion of these TBDRs affected the activity of these compounds under standard MIC determination conditions, it remained unclear whether additional TBDRs expressed under iron deficiency or upon substrate-induced expression can contribute to drug susceptibility.

We have addressed these questions by screening for orthologues of PiuA in clinical strains and by overexpressing 28 of the 34 TBDRs from *P. aeruginosa* PAO1, thereby mimicking induction under specific physiological conditions or by natural substrates. An *in silico* screen identified PiuD in LESB58 and other clinical isolates as a homologue of PiuA, sharing 60% amino acid identity. The *piuD* gene was located in the same genetic environment as *piuA*, including the conserved intergenic promoter region (see Fig. S2 in the supplemental material). The lower GC content of the *piuD* gene (59% compared to 66% for PAO1) suggests an acquisition by horizontal gene transfer. The

natural substrates of PiuA and PiuD are unknown, but the presence of conserved genes within the *piu* locus, including the oxidoreductase genes *piuC* and *piuB* and the ORF PA4516 (*piuE*), suggests that the metabolic fates of the natural substrates of these receptors are similar.

The amino acid similarity between PiuA and PiuD (Fig. S1) results in very similar crystal structures (Fig. 3). Like PiuA, PiuD also has a distinctive cluster of aromatic and positively charged residues located inside the pore at the extracellular face (see Fig. S3). This cluster is formed by Trp residues 311 and 327, Tyr 309, 710, and 714, Phe 94 (from the plug domain), His 713, and Arg 329 and 333 (Fig. S3). In PiuA, Trp 239, Tyr 307, 325, and 697, Phe 94, His 700, Lys 329, and Arg 331 form a cluster in the same position (Fig. S3). In the pyoverdin (FpvA) and pyochelin (FptA) receptors, this cluster is directly involved in the recognition of siderophores (23, 25). So far, there is no cocrystal structure available for a TBDR with its siderophore-drug conjugate, and only two cocomplexes between natural siderophores and their corresponding receptors have been solved (26–28). However, several binding and mutation studies regarding siderophore receptors and their cognate substrates have been reported (29–31), and their results are compatible with biphasic binding kinetics involving an initial binding in the loop extremities and a secondary binding at a site deeper inside the barrel, leading eventually to substrate translocation.

Our proteomic analysis revealed that divalent metal cation chelation induced the expression of 18 of the 34 TBDRs in PAO1. These include receptors for the endogenous siderophores pyoverdin (FpvA and FpvB), pyochelin (FptA), and nicotianamine (OptC) (32), as well as the heme (PhuR and HasR) and zinc (ZnuD) transporters. The other induced receptors could transport xenosiderophores that *P. aeruginosa* may encounter in the environment or during polymicrobial infections. A subset of these likely requires the cognate siderophore as an inducer. One example is PfeA from PAO1, sensing the presence of the exogenous siderophore enterobactin from *Escherichia coli* via the two-component system PfeR-PfeS (33). Similarly, the siderophore mycobactin from *Mycobacterium smegmatis* induces by 30-fold the expression of FemA in *P. aeruginosa* (19). Strikingly, the overexpression of PfuA resulted in the largest increase in susceptibility to all three siderophore-drug conjugates tested. The closest homologues of PfuA turned out to be PiuA in PAO1 and PiuD in LESB58, both sharing a 39% amino acid identity (57% similarity). The natural substrate of PfuA is unknown. A Fur binding site precedes the *pfuA* gene (34), suggesting iron repression; however, additional regulators and the presence of the substrate are likely required for induction of this TBDR in PAO1. Its closest orthologue in *E. coli* is Fiu, a TBDR also involved in the transport of BAL30072 (our unpublished data). Other receptors, undetectable by mass spectrometry (MS) analysis, may respond to other organic compounds or metal ions. Importantly, we identified the pyochelin receptor FptA as a candidate for the uptake of siderophore-drug conjugates. This receptor is the most highly induced receptor under iron limitation, as highlighted by our proteome analysis. FptA is also strongly expressed in lung and blood samples from mice and rats infected with *P. aeruginosa* and in human urine and respiratory samples (D. Bumann, unpublished results). The identification of the natural substrates of xenosiderophore receptors, as for instance PfuA, should provide an elegant way to induce specifically the expression of a receptor for the uptake of siderophore-drug conjugates. It also remains to be determined if siderophore-drug conjugates can act as inducers of their own transport, although this would require conjugate analogues deprived of antibiotic activity. The increased susceptibility to all three siderophore-drug conjugates under iron-limited conditions supports our findings on the plasmid-mediated expression of the individual TBDRs.

In summary, we have provided evidence for an overlapping subset of TBDRs in *P. aeruginosa* able to transport three different siderophore-drug conjugates, presenting two different types of iron-complexing substituents and on the basis of two classes of beta-lactams. The redundancy of TBDR recognition profiles should be an advantage during therapeutic treatments, since it should limit the risk of resistance emergence to these novel drug conjugates.

MATERIALS AND METHODS

Bacterial strains and growth conditions. The strains and plasmids used in this study are listed in Table S1 in the supplemental material. *E. coli* and *P. aeruginosa* were grown in lysogeny broth (LB) at 37°C with shaking (250 rpm). *E. coli* DH10B was used as the cloning host and *E. coli* SM10 as the donor for biparental matings. Gentamicin (15 μg/ml for *E. coli* and 50 μg/ml for *P. aeruginosa*) or carbenicillin (200 μg/ml) was added for plasmid -carrying strains. MICs were determined in Mueller-Hinton broth (MHB) according to CLSI guidelines (35) and were repeated at least on three different occasions. Cation-depleted MHB was prepared by dissolving 11 g of Chelex (C7901; Sigma-Aldrich) in 100 ml MHB. After stirring for 6 h, the suspension was filtered and the filtrate autoclaved at 115°C for 15 min. The Chelex-treated MHB was supplemented with 2 mM $MgSO_4$ and 0.2 mM $CaCl_2$ (final concentrations). The M9 Casamino Acids medium contained 1× M9 salts, supplemented with 0.5% Casamino Acids (filter sterilized), and 2 mM $MgSO_4$.

PCR amplifications and DNA modifications. PCR primers are listed in Table S2. All primer sequences were based on the sequences from the pseudomonas.com website (36). For screening PCRs, bacterial cells were boiled at 95°C for 5 min and subsequently pelleted at 13,000 rpm for 1 min. Phusion DNA polymerase (Thermo Scientific) was used for high-fidelity PCRs (supplemented with 5% dimethyl sulfoxide [DMSO]). Restriction digestions were performed according to the manufacturer's instructions at the appropriate temperature. All ligation reactions were carried out at room temperature using T4 DNA ligase (Promega). DNA preparations were performed using the GeneJET PCR purification or the GeneJET gel extraction kit (Thermo Scientific).

Construction of knockout mutants. The generation of unmarked knockout mutants was based on the protocol described by Hoang et al. (37). Briefly, DNA fragments of 500 to 700 bp were PCR-amplified using primer pairs A1/A2 and B1/B2, respectively. For the deletion of *pirA* in strain LESB58, the up- and downstream regions flanking the gene were PCR amplified. For the knockout of *piuD* in strain LESB58, the amplified fragments were located in the 5′ and 3′ regions of the genes. After amplification, the obtained A and B fragments were gel purified, and approximately 40 ng of each fragment was used in a PCR fusion amplification with primers A1 and B2, which share an 18-bp homologous region. The resulting fusion products were gel purified and further cloned into the suicide vectors pEX18Gm via HindIII/EcoRI restriction sites (*pirA*) and pEX18Gm via SalI/EcoRI (*piuD*). The cloned knockout fragments were verified by sequencing. The replacement vectors were mobilized into *P. aeruginosa* via biparental conjugation, and the generation of the unmarked mutants was carried out as previously described (38). The defined gene knockouts were verified by PCR amplification using the external primers and subsequent Sanger sequencing.

Construction of expression plasmids. The coding regions, including at least 50 nucleotides (nt) upstream of the ATG initiation codon and 20 nt downstream of the STOP codon, were amplified by PCR from genomic DNA of *P. aeruginosa* 39016 (*piuD*) or PAO1. The *piuD* coding region was amplified with primers piuD-Xba and piuD-Hind and cloned as a 2,526-bp XbaI-HindIII DNA fragment into the expression vector plApX2, yielding plasmid ppiuD. All other constructs were prepared in a similar way using the primers shown in Table S2. The Q5 high-fidelity DNA polymerase (NEB) was used for all amplifications. PCR conditions were as follows: denaturation at 98°C for 2 min, followed by 27 cycles of 98°C for 20 s, 57°C for 30 s, and 72°C for 2 min, and a final extension at 72°C for 4 min. The plasmids were transferred into *P. aeruginosa* by electroporation, and cells were spread on LB agar supplemented with carbenicillin at 200 mg/liter. All constructs were verified by Sanger sequencing.

Quantitative real-time PCR. Overnight cultures of strains grown in LB were diluted and inoculated into fresh MHB and grown in microtiter plates (200 μl/well) until reaching late exponential phase. Three wells were combined to form one sample. RNA was extracted using the RNeasy kit (Qiagen, Germany), according to the manufacturer's protocol. Residual genomic DNA was removed by treatment with RNase-free DNase (Promega). One microgram of RNA was reverse transcribed using ImProm-II reverse transcriptase (Promega). Gene-specific primers were used for PCRs using the Rotor-Gene SYBR green PCR kit (Qiagen). qPCRs were performed in a Rotor-Gene 3000 (Corbett Research, Australia) using the following conditions: 2 min at 95°C, followed by 35 cycles of 20 s at 95°C, 30 s at 60°C, and 30 s at 72°C, followed by a final extension at 72°C for 3 min. The ribosomal *rpsL* gene was used as a housekeeping reference gene (39).

Cloning, overexpression, and purification of PiuD from *P. aeruginosa*. The signal peptide of the proteins was predicted with Signal P4.0 (40) and excluded from cloning. The coding sequence of the mature protein was amplified from the genomic *P. aeruginosa* strain 39016 using KOD DNA polymerase (Novagen) and the primers piuD-39016-F and piuD-39016-R. The PCR product was digested by BspHI and XhoI restriction enzymes and cloned into the pTAMACHis6 vector using restriction sites NcoI and XhoI. The construct results in an expressed protein with an N-terminal TamA signal sequence for the outer membrane localization and a noncleavable C-terminal His_6 tag. The pTAMACHis6 expression vector was obtained by replacing the PelB signal peptide of pEPELBCHIS (courtesy of Huanting Liu, University St Andrews) with the TamA signal peptide (41). PiuD was overexpressed in *E. coli* C43(DE3) cells. The expression and purification steps were as described for PiuA (22). The fractions were pooled and loaded on a Superdex S200 gel filtration column (GE Healthcare) equilibrated with 10 mM Tris (pH 8), 150 mM NaCl, and 0.45% (vol/vol) tetraethylene glycol monooctyl ether (C8E4). Protein fractions were pooled and concentrated to 10 mg/ml.

Crystallization and structure determination. Crystals of PiuD appeared at 20°C after a few days by mixing 2 μl of protein solution (10 mg/ml) with 1 μl of reservoir solution containing 14% poly(ethylene glycol) methyl ether (PEG MME 5000) and 0.1 M bicine (pH 9). Crystals were frozen with the same solution containing 35% PEG MME 5000. The data were collected at ID23-1 at the ESRF. The data were processed

with GrenADES (42–46). The structure of PiuD was solved by molecular replacement using *P. aeruginosa* PiuA coordinates (PDB code 5FOK) as a model, with the program PHASER (47). The models were adjusted with Coot (48), and the refinement was carried out using REFMAC in the CCP4 program suite with TLS parameters (49). The quality of all structures was checked with MolProbity (50). The figures were drawn using PyMOL (version 1.8; Schrödinger, LLC). The final refinement statistics are given in Table S3.

Proteomics analysis. Sample preparation and MS analysis were performed as described previously (33). Briefly, *P. aeruginosa* was grown in MHB or MHB treated with Chelex (Sigma-Aldrich, Switzerland) under standard MIC determination conditions in microtiter plates without shaking at 37°C for 18 h. The cells from three wells were combined to yield sufficient material for proteome analysis. Three replicate samples were lysed, and the proteins were reduced with 5 mM Tris (2-carboxyethyl) phosphine hydrochloride and alkylated with iodoacetamide. The samples were diluted before digestion with trypsin at 37°C overnight. The peptides were desalted on a C_{18} reversed-phase column and dried under vacuum. One microgram of peptide was injected into a liquid chromatography-mass spectrometer (LTQ-Orbitrap Elite). The peptides were separated using an EASY nLC-1000 system (Thermo Fisher scientific) using a C_{18} high-performance liquid chromatography (LC) column. Tandem mass spectrometry data were exported from Progenesis LC-MS and searched against a protein decoy database of *P. aeruginosa*.

Statistics. Data were analyzed and plotted using GraphPad Prism (ver 7.02).

Accession number(s). Atomic coordinates and structure factors for PiuD have been deposited in the Protein Data Bank (accession no. 5NEC).

SUPPLEMENTAL MATERIAL

Supplemental material for this article may be found at https://doi.org/10.1128/AAC.00097-18.

SUPPLEMENTAL FILE 1, PDF file, 1.4 MB.

ACKNOWLEDGMENTS

The research leading to these results was conducted as part of the Translocation consortium (www.translocation.eu) and has received support from the Innovative Medicines Joint Undertaking under grant agreement no. 115525, resources which are composed of financial contribution from the European Union's seventh framework program (FP7/2007-2013) and EFPIA companies in kind contribution.

We thank Y. Braun and H. Weingart (Jacobs University Bremen) for help with the construction of the LESB58 mutants. We also thank E. Desarbre (Basilea Pharmaceutical Ltd.) for helpful discussions.

REFERENCES

1. Mahmood HY, Jamshidi S, Sutton JM, Rahman KM. 2016. Current advances in developing inhibitors of bacterial multidrug efflux pumps. Curr Med Chem 23:1062–1081. https://doi.org/10.2174/0929867323666160304150522.
2. Gill EE, Franco OL, Hancock RE. 2015. Antibiotic adjuvants: diverse strategies for controlling drug-resistant pathogens. Chem Biol Drug Des 85:56–78. https://doi.org/10.1111/cbdd.12478.
3. Möllmann U, Heinisch L, Bauernfeind A, Köhler T, Ankel-Fuchs D. 2009. Siderophores as drug delivery agents: application of the "Trojan horse" strategy. Biometals 22:615–624. https://doi.org/10.1007/s10534-009-9219-2.
4. Page MG, Dantier C, Desarbre E. 2010. *In vitro* properties of BAL30072, a novel siderophore sulfactam with activity against multiresistant Gram-negative bacilli. Antimicrob Agents Chemother 54:2291–2302. https://doi.org/10.1128/AAC.01525-09.
5. McPherson CJ, Aschenbrenner LM, Lacey BM, Fahnoe KC, Lemmon MM, Finegan SM, Tadakamalla B, O'Donnell JP, Mueller JP, Tomaras AP. 2012. Clinically relevant Gram-negative resistance mechanisms have no effect on the efficacy of MC-1, a novel siderophore-conjugated monocarbam. Antimicrob Agents Chemother 56:6334–6342. https://doi.org/10.1128/AAC.01345-12.
6. Kim A, Kutschke A, Ehmann DE, Patey SA, Crandon JL, Gorseth E, Miller AA, McLaughlin RE, Blinn CM, Chen A, Nayar AS, Dangel B, Tsai AS, Rooney MT, Murphy-Benenato KE, Eakin AE, Nicolau DP. 2015. Pharmacodynamic profiling of a siderophore-conjugated monocarbam in *Pseudomonas aeruginosa*: assessing the risk for resistance and attenuated efficacy. Antimicrob Agents Chemother 59:7743–7752. https://doi.org/10.1128/AAC.00831-15.
7. Kohira N, West J, Ito A, Ito-Horiyama T, Nakamura R, Sato T, Rittenhouse S, Tsuji M, Yamano Y. 2016. *In vitro* antimicrobial activity of siderophore cephalosporin S-649266 against *Enterobacteriaceae* clinical isolates including carbapenem-resistant strains. Antimicrob Agents Chemother 60:729–734. https://doi.org/10.1128/AAC.01695-15.
8. Wencewicz TA, Mollmann U, Long TE, Miller MJ. 2009. Is drug release necessary for antimicrobial activity of siderophore-drug conjugates? Syntheses and biological studies of the naturally occurring salmycin "Trojan horse" antibiotics and synthetic desferridanoxamine-antibiotic conjugates. Biometals 22:633–648. https://doi.org/10.1007/s10534-009-9218-3.
9. Ji C, Miller PA, Miller MJ. 2012. Iron transport-mediated drug delivery: practical syntheses and *in vitro* antibacterial studies of tris-catecholate siderophore-aminopenicillin conjugates reveals selectively potent anti-pseudomonal activity. J Am Chem Soc 134:9898–9901. https://doi.org/10.1021/ja303446w.
10. Maejima T, Inoue M, Mitsuhashi S. 1991. *In vitro* antibacterial activity of KP-736, a new cephem antibiotic. Antimicrob Agents Chemother 35:104–110. https://doi.org/10.1128/AAC.35.1.104.
11. Wencewicz TA, Miller MJ. 2013. Biscatecholate-monohydroxamate mixed ligand siderophore-carbacephalosporin conjugates are selective sideromycin antibiotics that target *Acinetobacter baumannii*. J Med Chem 56:4044–4052. https://doi.org/10.1021/jm400265k.
12. Han S, Caspers N, Zaniewski RP, Lacey BM, Tomaras AP, Feng X, Geoghegan KF, Shanmugasundaram V. 2011. Distinctive attributes of beta-lactam target proteins in *Acinetobacter baumannii* relevant to development of new antibiotics. J Am Chem Soc 133:20536–20545. https://doi.org/10.1021/ja208835z.
13. Mima T, Kvitko BH, Rholl DA, Page MG, Desarbre E, Schweizer HP. 2011. *In vitro* activity of BAL30072 against *Burkholderia pseudomallei*. Int J Antimicrob Agents 38:157–159. https://doi.org/10.1016/j.ijantimicag.2011.03.019.

14. Russo TA, Page MG, Beanan JM, Olson R, Hujer AM, Hujer KM, Jacobs M, Bajaksouzian S, Endimiani A, Bonomo RA. 2011. *In vivo* and *in vitro* activity of the siderophore monosulfactam BAL30072 against *Acinetobacter baumannii*. J Antimicrob Chemother 66:867–873. https://doi.org/10.1093/jac/dkr013.
15. Ito A, Kohira N, Bouchillon SK, West J, Rittenhouse S, Sader HS, Rhomberg PR, Jones RN, Yoshizawa H, Nakamura R, Tsuji M, Yamano Y. 2016. *In vitro* antimicrobial activity of S-649266, a catechol-substituted siderophore cephalosporin, when tested against non-fermenting Gram-negative bacteria. J Antimicrob Chemother 71:670–677. https://doi.org/10.1093/jac/dkv402.
16. van Delden C, Page MG, Köhler T. 2013. Involvement of Fe uptake systems and AmpC beta-lactamase in susceptibility to the siderophore monosulfactam BAL30072 in *Pseudomonas aeruginosa*. Antimicrob Agents Chemother 57:2095–2102. https://doi.org/10.1128/AAC.02474-12.
17. Ito A, Nishikawa T, Matsumoto S, Yoshizawa H, Sato T, Nakamura R, Tsuji M, Yamano Y. 2016. Siderophore cephalosporin cefiderocol utilizes ferric iron transporter systems for antibacterial activity against *Pseudomonas aeruginosa*. Antimicrob Agents Chemother 60:7396–7401. https://doi.org/10.1128/AAC.01405-16.
18. Cornelis P, Matthijs S, Van Oeffelen L. 2009. Iron uptake regulation in *Pseudomonas aeruginosa*. Biometals 22:15–22. https://doi.org/10.1007/s10534-008-9193-0.
19. Llamas MA, van der Sar A, Chu BC, Sparrius M, Vogel HJ, Bitter W. 2009. A novel extracytoplasmic function (ECF) sigma factor regulates virulence in *Pseudomonas aeruginosa*. PLoS Pathog 5:e1000572. https://doi.org/10.1371/journal.ppat.1000572.
20. Llamas MA, Sparrius M, Kloet R, Jimenez CR, Vandenbroucke-Grauls C, Bitter W. 2006. The heterologous siderophores ferrioxamine B and ferrichrome activate signaling pathways in *Pseudomonas aeruginosa*. J Bacteriol 188:1882–1891. https://doi.org/10.1128/JB.188.5.1882-1891.2006.
21. Ito A, Sato T, Ota M, Takemura M, Nishikawa T, Toba S, Kohira N, Miyagawa S, Ishibashi N, Matsumoto S, Nakamura R, Tsuji M, Yamano Y. 2018. *In vitro* antibacterial properties of cefiderocol, a novel siderophore cephalosporin, against Gram-negative bacteria. Antimicrob Agents Chemother 62:e01454-17. https://doi.org/10.1128/AAC.01454-17.
22. Moynié L, Luscher A, Rolo D, Pletzer D, Tortajada A, Weingart H, Braun Y, Page MG, Naismith JH, Köhler T. 2017. Structure and Function of the PiuA and PirA Siderophore-Drug Receptors from *Pseudomonas aeruginosa* and *Acinetobacter baumannii*. Antimicrob Agents Chemother 61:e02531-16. https://doi.org/10.1128/AAC.02531-16.
23. Cobessi D, Celia H, Pattus F. 2005. Crystal structure at high resolution of ferric-pyochelin and its membrane receptor FptA from *Pseudomonas aeruginosa*. J Mol Biol 352:893–904. https://doi.org/10.1016/j.jmb.2005.08.004.
24. Zheng T, Nolan EM. 2014. Enterobactin-mediated delivery of beta-lactam antibiotics enhances antibacterial activity against pathogenic *Escherichia coli*. J Am Chem Soc 136:9677–9691. https://doi.org/10.1021/ja503911p.
25. Cobessi D, Celia H, Folschweiller N, Schalk IJ, Abdallah MA, Pattus F. 2005. The crystal structure of the pyoverdine outer membrane receptor FpvA from *Pseudomonas aeruginosa* at 3.6 angstroms resolution. J Mol Biol 347:121–134. https://doi.org/10.1016/j.jmb.2005.01.021.
26. Ferguson AD, Hofmann E, Coulton JW, Diederichs K, Welte W. 1998. Siderophore-mediated iron transport: crystal structure of FhuA with bound lipopolysaccharide. Science 282:2215–2220. https://doi.org/10.1126/science.282.5397.2215.
27. Locher KP, Rees B, Koebnik R, Mitschler A, Moulinier L, Rosenbusch JP, Moras D. 1998. Transmembrane signaling across the ligand-gated FhuA receptor: crystal structures of free and ferrichrome-bound states reveal allosteric changes. Cell 95:771–778. https://doi.org/10.1016/S0092-8674(00)81700-6.
28. Yue WW, Grizot S, Buchanan SK. 2003. Structural evidence for iron-free citrate and ferric citrate binding to the TonB-dependent outer membrane transporter FecA. J Mol Biol 332:353–368. https://doi.org/10.1016/S0022-2836(03)00855-6.
29. Payne MA, Igo JD, Cao Z, Foster SB, Newton SM, Klebba PE. 1997. Biphasic binding kinetics between FepA and its ligands. J Biol Chem 272:21950–21955. https://doi.org/10.1074/jbc.272.35.21950.
30. Cao Z, Qi Z, Sprencel C, Newton SM, Klebba PE. 2000. Aromatic components of two ferric enterobactin binding sites in *Escherichia coli* FepA. Mol Microbiol 37:1306–1317. https://doi.org/10.1046/j.1365-2958.2000.02093.x.
31. Annamalai R, Jin B, Cao Z, Newton SM, Klebba PE. 2004. Recognition of ferric catecholates by FepA. J Bacteriol 186:3578–3589. https://doi.org/10.1128/JB.186.11.3578-3589.2004.
32. Gi M, Lee KM, Kim SC, Yoon JH, Yoon SS, Choi JY. 2015. A novel siderophore system is essential for the growth of *Pseudomonas aeruginosa* in airway mucus. Sci Rep 5:14644. https://doi.org/10.1038/srep14644.
33. Gasser V, Baco E, Cunrath O, August PS, Perraud Q, Zill N, Schleberger C, Schmidt A, Paulen A, Bumann D, Mislin GL, Schalk IJ. 2016. Catechol siderophores repress the pyochelin pathway and activate the enterobactin pathway in *Pseudomonas aeruginosa*: an opportunity for siderophore-antibiotic conjugates development. Environ Microbiol 18:819–832. https://doi.org/10.1111/1462-2920.13199.
34. Ochsner UA, Vasil ML. 1996. Gene repression by the ferric uptake regulator in *Pseudomonas aeruginosa*: cycle selection of iron-regulated genes. Proc Natl Acad Sci U S A 93:4409–4414.
35. Clinical and Laboratory Standards Institute. 2009. Methods for dilution antimicrobial susceptibility tests for bacteria that grow aerobically, 8th ed. Approved standard M7-A8. Clinical and Laboratory Standards Institute, Wayne, PA.
36. Winsor GL, Griffiths EJ, Lo R, Dhillon BK, Shay JA, Brinkman FS. 2016. Enhanced annotations and features for comparing thousands of *Pseudomonas* genomes in the *Pseudomonas* genome database. Nucleic Acids Res 44:D646–D653. https://doi.org/10.1093/nar/gkv1227.
37. Hoang TT, Karkhoff-Schweizer RR, Kutchma AJ, Schweizer HP. 1998. A broad-host-range Flp-FRT recombination system for site-specific excision of chromosomally-located DNA sequences: application for isolation of unmarked *Pseudomonas aeruginosa* mutants. Gene 212:77–86. https://doi.org/10.1016/S0378-1119(98)00130-9.
38. Pletzer D, Lafon C, Braun Y, Köhler T, Page MG, Mourez M, Weingart H. 2014. High-throughput screening of dipeptide utilization mediated by the ABC transporter DppBCDF and its substrate-binding proteins DppA1-A5 in *Pseudomonas aeruginosa*. PLoS One 9:e111311. https://doi.org/10.1371/journal.pone.0111311.
39. Dumas JL, van Delden C, Perron K, Köhler T. 2006. Analysis of antibiotic resistance gene expression in *Pseudomonas aeruginosa* by quantitative real-time-PCR. FEMS Microbiol Lett 254:217–225. https://doi.org/10.1111/j.1574-6968.2005.00008.x.
40. Petersen TN, Brunak S, von Heijne G, Nielsen H. 2011. SignalP 4.0: discriminating signal peptides from transmembrane regions. Nat Methods 8:785–786. https://doi.org/10.1038/nmeth.1701.
41. Liu J, Wolfe AJ, Eren E, Vijayaraghavan J, Indic M, van den Berg B, Movileanu L. 2012. Cation selectivity is a conserved feature in the OccD subfamily of *Pseudomonas aeruginosa*. Biochim Biophys Acta 1818:2908–2916. https://doi.org/10.1016/j.bbamem.2012.07.009.
42. Sauter NK, Grosse-Kunstleve RW, Adams PD. 2004. Robust indexing for automatic data collection. J Appl Crystallogr 37:399–409. https://doi.org/10.1107/S0021889804005874.
43. Zhang Z, Sauter NK, van den Bedem H, Snell G, Deacon AM. 2006. Automated diffraction image analysis and spot searching for high-throughput crystal screening. J Appl Crystallogr 39:112–119. https://doi.org/10.1107/S0021889805040677.
44. Kabsch W. 1993. Automatic processing of rotation diffraction data from crystals of initially unknown symmetry and cell constants. J Appl Crystallogr 26:795–800. https://doi.org/10.1107/S0021889893005588.
45. Evans P. 2006. Scaling and assessment of data quality. Acta Crystallogr D Biol Crystallogr 62:72–82. https://doi.org/10.1107/S0907444905036693.
46. Monaco S, Gordon E, Bowler MW, Delageniere S, Guijarro M, Spruce D, Svensson O, McSweeney SM, McCarthy AA, Leonard G, Nanao MH. 2013. Automatic processing of macromolecular crystallography X-ray diffraction data at the ESRF. J Appl Crystallogr 46:804–810. https://doi.org/10.1107/S0021889813006195.
47. McCoy AJ, Grosse-Kunstleve RW, Adams PD, Winn MD, Storoni LC, Read RJ. 2007. Phaser crystallographic software. J Appl Crystallogr 40:658–674. https://doi.org/10.1107/S0021889807021206.
48. Emsley P, Cowtan K. 2004. Coot: model-building tools for molecular graphics. Acta Crystallogr D Biol Crystallogr 60:2126–2132. https://doi.org/10.1107/S0907444904019158.
49. Murshudov GN, Vagin AA, Dodson EJ. 1997. Refinement of macromolecular structures by the maximum-likelihood method. Acta Crystallogr D Biol Crystallogr 53:240–255. https://doi.org/10.1107/S0907444996012255.
50. Chen VB, Arendall WB, III, Headd JJ, Keedy DA, Immormino RM, Kapral GJ, Murray LW, Richardson JS, Richardson DC. 2010. MolProbity: all-atom structure validation for macromolecular crystallography. Acta Crystallogr D Biol Crystallogr 66:12–21. https://doi.org/10.1107/S0907444909042073.

Part IV

General discussion and perspectives

7 General Discussion

Antimicrobial resistance is a serious public health threat worldwide. Last resort antibiotics are failing, threatening patients and the healthcare systems (ECDC., 2017). Developing new antibiotics is a considerable challenge because of the rapid emergence of resistance in bacteria through the genetic changes upon antibiotics exposure and the misuses of antibiotic treatment by hospitals (ECDC., 2017). Gram-negative bacteria possess a bacterial envelope composed of an outer membrane, a peptidoglycan layer and an inner membranes that delimit a periplasmic space. The outer membrane plays a crucial role due to its dual function as a protective layer against toxic compounds and as an interface for nutrient exchange with the environment (Hancock and Brinkman, 2002). The outer membrane is therefore the first line of bacterial defence against antibiotics. *Pseudomonas aeruginosa* (*P. aeruginosa*) is intrinsically resistant to many antibiotics partly due to its large number of porins and efflux pumps (Hancock and Brinkman, 2002). By this means, it has a tight control over influx and efflux of molecules across the outer membrane, making the development of novel therapeutic options even more challenging. The transport of antibiotics across the outer membrane is thus a major issue.

An approach to circumvent the intrinsic resistance of pathogens, such as *P. aeruignosa*, is the Trojan horse approach through the use of the bacterial transport machinery (Möllmann et al., 2009; Mislin and Schalk, 2014). In a Trojan horse approach, a toxic compound is efficiently transported across the outer membrane via endogenous bacterial active transporters, i.e. the TonB-dependent transporters (TBDTs) in *P. aeruginosa* (Möllmann et al., 2009; Mislin and Schalk, 2014). This includes non-iron metalloporphyrins, hybrid siderophores and siderophore-antibiotic conjugates. The Trojan horse approach is by far the most advanced strategy to solve the antibiotic translocation issue. However, several studies reported a lack of correlation between *in vitro* efficacy and *in vivo* antibacterial activity of such conjugates (McPherson et al., 2012a; Tomaras et al., 2013; Kim et al., 2015a; Tillotson, 2016). Indeed, *P. aeruginosa* developed resistance to these conjugates through facile inactivation of the TBDT transporting the conjugates (McPherson et al., 2012a; Tomaras et al., 2013; Kim et al., 2015a; Tillotson, 2016). In order to prevent the rapid development of resistance, the Trojan horse compound should target a subtrate mimetics that is essential for the growth of *P. aeruginosa in vivo*. The substrate mimetic would then be actively transported via one or several endogenous TBDTs, getting around the vigilance of *P. aeruginosa*. Inactivation of the involved TBDT(s) would contribute to the fitness reduction of the pathogen *in vivo* and would prevent the development of antibacterial resistance.

P. aeruginosa UCBPP-PA14 encodes a large number of TBDTs (Winsor et al., 2016). Expression levels of the TBDTs are highly modulated by the environmental conditions surrounding the pathogen: *in vitro*, preclinical and clinical environments might exhibit different expression patterns of UCBPP-PA14 TBDTs. There have been several transcriptomics studies on *Pseudomonas* to unravel its physiology *in vivo* (Son et al., 2007; Bielecki et al., 2011; Bielecki et al., 2013), such as studies on biofilm formation, metabolic networks (Turner et al., 2014), iron involvement during infection (Ochsner et al., 2002; Damron et al., 2016) and secretion of virulence factors (Barbier et al., 2014; Wurtzel et al., 2012). However the coverage of TBDTs remains poor, presumably due to their low level of expression compared to the dominance of host materials in animal and human samples. In order to develop successful Trojan horse compounds, we desperately need to get more insights on bacterial transport capabilities *in vivo*. We thus developed an ultra-sensitive targeted proteomic approach to determine absolutely the abundance of TBDTs *in vitro* and in various hosts. Based on the expression data, we generated mutants lacking highly expressed TBDTs and evaluated them in a competitive fitness assay *in vivo*.

7.1 Development of an ultra-sensitive targeted proteomic approach

Advances made in discovery based proteomics approaches are largely due to technological improvements made in high performance mass spectrometers (Charretier and Schrenzel, 2016). The development of increasing number of sophiticated techniques allows for label-free quantification of *P. aeruginosa* bacterial proteins in different environments (Charretier and Schrenzel, 2016). There have been several studies on the identification and quantification of (i) enzymes responsible for antibiotic inhibition such as cephasloporin AmpC (Glatter et al., 2015; Charretier and Schrenzel, 2016) and of (ii) OprD porin loss (Choi et al., 2011; Toyofuku et al., 2012; Casabona et al., 2013) *in vitro*. Two recent studies also measured the differential expression level of *P. aeruginosa* in absence or presence of the antibiotics azithromycin and ciprofloxacin using the same proteomic approach (Leal et al., 2016; Peng et al., 2017). To date, there are many studies of quantitative proteomics of *P. aeruginosa in vitro*, however, only few studies on *P. aeruginosa* proteome have been reported *in vivo* (Lassek et al., 2015; Charretier et al., 2015; King et al., 2017). Indeed, proteomic analyses of *P. aeruginosa in vivo* are challenging since the samples usually contain low loads of *P. aeruginosa* but a high excess of host proteins.

We thus optimized with the proteomic core facility (PCF) of the Biozentrum, two targeted proteomic assays to identify and absolutely quantify *P. aeruginosa* outer membrane proteins: the selective monitoring reaction (SRM) and the parallel monitoring reaction (PRM). SRM allows for reliable quantification of 10 – 100 target proteins in semi-complex biological samples (Shi et al., 2012). This technique is widely used to identify and quantify

protein biomarkers in different types of diseases (Shi et al., 2016). In contrast to SRM, PRM enables higher resolution and higher sensitivity for absolute peptide quantification in complex *in vivo* samples (Peterson et al., 2012). Indeed, this technique employs an Orbitrap mass analyzer that reduces considerably the complex biological background interferences with *P. aeruginosa* peptides. PRM methogology has been well documented in several reviews (Shi et al., 2016) but in contrast to SRM, its reported applications remain limited to analyses of plasma samples (Kim et al., 2015c; Lesur et al., 2015; Thomas et al., 2015) and quantification of kinases in human cancer cell lines (Kim et al., 2015b).

We collected and analyzed by PRM several preclinical and clinical samples containing *P. aeruginosa* from different collaborators. PRM enables us to reach attomole sensitivity and be able to detect as little as 10 copies per cell for certain peptides, despite the excess of host proteins. This high sensitivity allowed for direct protein identification and quantification in clinical samples from acute pneumonia patients that contain at least around 100'000 CFUs per ml sputum/lavage. As a comparison, previous transcriptomic studies were carried out with sputum from CF patients that contain up to 1000-fold higher *P. aeruginosa* loads than in our samples (Palmer et al., 2005). The high level of resolution and sensitivity of PRM enable us to quantify absolutely the TBDT abundance in several *in vivo* samples. To our knowledge, we were the first to use PRM for bacterial protein quantification in animal and human patients samples.

7.2 TBDTs expression levels correlate in human and animal samples

P. aeruginosa physiology *in vivo* is poorly understood. In order to study the transport capabilities of the pathogen, we would need a comprehensive list of the TBDTs expressed in *P. aeruginosa in vivo*. *P. aeruginosa* gene expression has been extensively studied *in vitro*, in animal models, and human patients (burn wounds (Bielecki et al., 2008; Turner et al., 2014), bladder catheters (Sabharwal et al., 2014; Cole et al., 2014), CF sputum with very high *P. aeruginosa* loads (Harmer et al., 2013)), but the expression of TBDTs was overlooked, potentially because TBDTs are often poorly detected *in vivo* because of the predominance of host material in the samples.

We analyzed the expression patterns of *P. aeruginosa* TBDTs in various samples: blood from septicemia mouse model, mice and rat lung from intrabronchial model, and lung and urine from acute pneumonia patients. Overall, proteomic analyses of *P. aeruginosa* TBDTs revealed similar expression patterns in the animal models tested and in the human patients samples, suggesting that *P. aeruginosa* presents similar transport capabilities in these different conditions, despite of the potential differences in airway microbial community and host innate immunity (Haley, 2003; Mestas and Hughes, 2004; Bryant

and Monie, 2012). The expression data highlighted the presence of a subset of highly abundant TBDTs among the different *in vivo* conditions. This subset included (i) the engodenous siderophore TBDTs, especially the type I pyoverdine transporter FpvAI, (ii) the non-iron heavy metal TBDTs (zinc-related ZnuD, cupper-related OprC) and, (iii) to a lesser extent the heme TBDTs. The presence of these TBDTs indicated similar heavy metal bioavailability in the different *in vivo* settings.

The highest abundance of pyoverdine transporter FpvAI was not unexpected in such conditions since *in vivo* environment is characterized by iron scarcity (Parrow et al., 2013). Therefore, *P. aeruginosa* might use its highest-affinity siderophore pyoverdine (10^{32} M^{-1}) to scavenge iron and to secrete PvdS-related proteases PrpL, AprA, exotoxin A and other virulence factors (Balasubramanian et al., 2012). By this means, *P. aeruginosa* can thus efficiently compete for iron against transferrin and lactoferrin (with binding constants of 10^{20}-10^{21} M^{-1} and 10^{22}-10^{24} M^{-1} respectively) (Xiao and Kisaalita, 1997; Majka et al., 2013). In the lungs, the high-affinity pyochelin transporter FptA and the nicotianamine transporter OptC, described to promote the growth of *P. aeruginosa* in an artificial lung condition (Gi et al., 2014), were relatively highly expressed, suggesting that they might partially contribute to iron scavenging in low oxygen conditions. Interestingly, OptC was not detected in any of the human urine samples, which correlates with the potential presence of ferrous iron, in the lung but not in urine, that nicotianamine binds with high affinity in low-oxygen lung environment (Wirén et al., 1999; Callahan et al., 2007).

The high expression of ZnuD might reveal a poor bioavailability of zinc in these different *in vivo* conditions. In the airway lumen, the high-affinity zinc transporter ZnuD abundance could be explained by the presence of polymorphonuclear neutrophils that release calprotectin, which sequesters zinc and manganese (D'Orazio et al., 2015). The copper-related transporter OprC was also highly expressed, but so far we have no clear evidence on OprC function in *P. aeruginosa* (Cunrath et al., 2015). Indeed, its role in the copper acquisition is controversial (Cunrath et al., 2015), since OprC was shown to be repressed by high concentration of copper (Yoneyama and Nakae, 1996) but it was not induce under copper starvation *in vitro*, despite his high affinity for copper (K_d = 2.6 µM) (Frangipani et al., 2008).

Heme transporters PhuR and HasR were relatively abundant in the animal lung samples, whereas in human samples, we mainly found a constant expression of PhuR. The dominance of PhuR over HasR was already described by Smith and coworkers (Smith and Wilks, 2015). They showed that PhuR enables a heme transport that is more efficient than HasR (Smith and Wilks, 2015). It was also shown in the *Pseudomonas* lineage DK2 clinical strain, that the loss of pyoverdine utilization was associated with mutations in the promoter regions of the *phu* system, leading to an increased expression of PhuR (Marvig et al., 2014). The absence of pyoverdine transporter FpvAI and the high abundance of

PhuR in human lung samples seemed to correlate with an adaptation of *P. aeruginosa* towards heme utilization as reporter by Marvig and coworkers (Marvig et al., 2014).

The expression levels of xenosiderophore TBDTs were quite variable among the different samples as expected due to the rich microbiome of the urinary tract (Whiteside et al., 2015) and the lung environment (Dickson and Huffnagle, 2015). This information might be valuable to identify the presence of other microorganisms at the site of infection, because the xenosiderophore TBDTs are induced in presence of their cognitive siderophores. The ferri-alcalagin E transporter AleB, the ferrichrome transporter FiuA and the ferri-mycobactin transporter FemA were relatively highly expressed compared to others xenosiderophore TBDTs, their involvement in cell-surface signalling might contribute to their higher expression (Llamas et al., 2014).

To summarize, PRM data revealed general insight into nutrient access in different hosts during infection: heavy metal and heme were scarcely available during infection, therefore *P. aeruginosa* harboured high affinity systems to scavenge these nutrients from the host. TBDTs are considered as last resort transport systems employed upon starvation of specific nutrients (Noinaj et al., 2010). It is thus surprising that *P. aeruginosa* employed several TBDTs with similar transport capabilities. One possible explanation would be that *P. aeruginosa* growth and/or pathogenesis might rely on few TBDTs that transport essential nutrients while the other TBDTs are moderately expressed as part of a nutrient surveillance program. We would still need to understand the reasons why *P. aeruginosa* expressed so many TBDTs *in vivo*. Moreover, Turner and coworkers showed that gene expression *in vivo* was not necessarily correlated with its importance for fitness *in vivo* (Turner et al., 2014). Therefore, there is a crucial need to discriminate the relevant TBDTs *in vivo*.

7.3 Unsuitable *in vitro* conditions might lead to misconceptions

According to the Committee for Laboratory Standards Institute (CLSI) or European Committee for Antimicrobial Susceptibility Testing (EUCAST), susceptibility testing should be performed on specific standardized media, such as Mueller-Hinton broth (MHB) supplemented with certain ions such as calcium and magnesium (Kahlmeter et al., 2006). However, such rich media contain high levels of iron, e.g. 4 µM in LB (Cunrath et al., 2015), which does not reflect the physiological concentration of iron in the host (10^{-24} M) (Raymond et al., 2003). Therefore, MIC determination of the Trojan horse conjugates have been performed in iron-deficient conditions to evaluate their antibacterial acitivity (Möllmann et al., 2009; Page et al., 2010; McPherson et al., 2012a; Kim et al., 2015a). Despite these improvements, several studies reported a lack of correlation between *in vitro* testing and *in vivo* efficacy of the conjugates (McPherson et al., 2012a; Tomaras et al., 2013; Kim et al., 2015a; Tillotson, 2016), suggesting suboptimal *in vitro* assays. In

order to prevent false positives and resistance emergence, the development of suitable *in vitro* assays are critical to study the antibacterial activity of the conjugates and should be representative of the *in vivo* restrictive conditions.

To assess this problem, we measured TBDTs expression level in commonly used laboratory rich media (Mueller-Hinton broth (MHB) and Luria-Bertani medium (LB)), iron restricted media (casamino acids medium (CAA)), iron-deficient media (M9 supplemented with 30 mM succinate, BM2 with 20 mM acetonamine and chelexed CAA (chCAA) with addition of essential metals). Expression levels of TBDTs *in vitro* exhibited a completely different pattern than *in vivo*. Overall, all classes of TBDTs were constantly expressed in rich and iron restricted/deficient media compared to the scattered *in vivo* expression. Broad expression of TBDTs in rich media was not surprising as it was reported in a recent study that even in a rich media like LB, growth of the bacteria depends on high affinity transport capabilities (Cunrath et al., 2015). Even if the the absolute concentration of iron is high in these conditions, iron is not necessarily bioavailable in its free form, it could be either complexed to iron chelators present in the media or partially insoluble due to the presence of oxygen.

P. aeruginosa showed 10 times higher TBDTs expression in CAA and chCAA than in rich media, which was expected since CAA presents 200 times lower iron concentration than LB (Cunrath et al., 2015). In contrast to CAA, expression level in minimal media such as BM2 and M9 did not seem to rely on TBDTs, because iron concentration in these media was higher than in CAA (Cunrath et al., 2015). *P. aeruginosa* growth in 100 % human serum showed a different expression pattern than in human samples. Human serum contains a variety of nutrients including proteins and peptides (such as albumins, globulins, lipoproteins, enzymes and hormones), nutrients (such as carbohydrates, lipids and amino acids), electrolytes, organic wastes and variety of other small organic molecules suspended or dissolved in them (Psychogios et al., 2011). Iron concentration was estimated as 9 mM in the human serum (Psychogios et al., 2011), which explains the low contribution of the TBDTs to the growth of *P. aeruginosa* in this condition.

Together, our expression data suggested that CAA was the most suitable *in vitro* medium among our media collection. In CAA, pyoverdine, pyochelin and heme TBDTs were highly expressed, indicating severe restriction of iron in the medium, more than *in vivo*. Moreover, levels of zinc did not correspond to *in vivo*, since the zinc-related transporter ZnuD was expressed at basal level in CAA. In order to better reflect *in vivo* settings, CAA should be depleted in zinc. Zinc deficiency could be achieve by using strong zinc chelators: diethylenetriaminepentaacetic acid (DTPA) for mild zinc deficiency and N,N,N',N'-tetrakis(2-pyridylmethyl) ethylenediamine (TPEN) for severe zinc deficiency (Cho et al., 2007). A number of xenosiderophore TBDTs were also highly expressed due to the presence of siderophores such as enterobactin and ferrichrome, potentially derived

from the bovine casein used to prepare the casamino acids mix (BD, 2017). Therefore, CAA is also a good candidate to study xenosiderophore TBDTs. In order to mimic better the lung environment, we might also consider to supplement CAA with mucin proteins such as the principal component of mucin Muc5AC (WICKSTRÖM et al., 1998), in order to induce the expression of the nicotianamine transporter OptC for example (Gi et al., 2014). Other mucin-based media such as artificial lung media derived from human cell lines or artificial sputum from porcine mucin might be a solution to mimic better the lung environment.

Severe iron depletion, such as the one observed in CAA, would support the very high expression level of TBDTs. Because the siderophore-drug conjugates are mainly transported by TBDTs, such severe iron restriction could lead to overly optimistic siderophore-drug conjugate antibacterial activity *in vitro*. In MHB and LB, we showed that the expression of PiuA and PirA, which transport most of the recent conjugates (Tomaras et al., 2013; Kim et al., 2015a), were 5-10 times lower than in CAA, which might explain the increased susceptibility of *P. aeruginosa* to BAL30072 in CAA (Van Delden et al., 2013; Moynié et al., 2017). The difference in PiuA and PirA abundance between standard *in vitro* assay and multiple *in vivo* conditions might also contribute to the inconsistent *in vivo* efficacy of the recent siderophore-drug conjugates (Tomaras et al., 2013; Kim et al., 2015a).

Understanding the host microenvironment is thus essential for the development of *in vitro* assays that better mimic *in vivo* phenotypes of *P. aeruginosa*. Deeper knowledge of *P. aeruginosa* phenotypes *in vivo* is key to understand whether a specific *in vitro* assay is suitable for the evaluation of the antibacterial activity of the Trojan horse mimetics.

7.4 Intranasal mouse infection model to evaluate bacterial fitness *in vivo*

Animal models are a valuable tool to study lung physiology and pathology, they provide insights in the initiation and the maintenance of *P. aeruginosa* infections. They are also important resource for the development and the testing of new therapeutic options *in vivo*. Rodents have been the most studied model organisms (Hudson-Shore, 2016). Numerous *in vivo* infection models have been used to study *P. aeruginosa* virulence (Kukavica-Ibrulj and Levesque, 2008). Acute pneumonia models are useful to study non-CF-related pneumonia but might also be interesting to study the initial phase of lung infection during *P. aeruginosa* colonization of CF airways. Acute pneumonia models are mainly characterized by the introduction of free-living and mobile *P. aeruginosa* cells into the lung (Kukavica-Ibrulj and Levesque, 2008).

Intranasal instillation is the most commonly used pneumonia mouse model for lung infections (Miller et al., 2012). It has several advantages over its alternative methods

(intubation and aerosol administration): (i) intranasal instillation is technically simple and fast, since drops of inoculum are administrated at the nostril of the mouse; (ii) in contrast to intubation, there are very little risk to injure the animals during the instillation. Most of *P. aeruginosa* studies using the intranasal method employed the less virulent strain PAO1 (Minandri et al., 2016; Damron et al., 2016). Intranasal instillation with UCBPP-PA14 was reported to be unsuccessful in establishing reproducible lung infection (Hilker et al., 2015). Therefore, we developed an intranasal model, where the instillation was optimized using inhaled anesthesia prior to mice instillation, as suggested by Miller and coworkers (Miller et al., 2012).

Short inhalation of the general anesthetic isoflurane, prior to mice instillation, had a significant impact on the success of the infection. Miller and coworkers speculated that after the removal of the mice from the anesthesia chamber, the mice were in a transient hypoxia, which resulted in deeper breathing and deeper inhalation of larger volumes of inoculum per breath (Miller et al., 2012). This procedure may therefore facilitate the efficient delivery of *P. aeruginosa* in the lower respiratory tract. By applying this technique, we successfully managed to obtain reproducible results with UCBPP-PA14 using a intranasal method, in contrast to previous findings (Hilker et al., 2015).

The developed intranasal model was valuable for our *in vivo* analyses but it was not an ideal model reflecting human pneumonia, because we used high loads of *P. aeruginosa* cells (10^7 - 10^7 CFUs) and short period of infections (10 h), leading to few generations of *P. aeruginosa*. However, it is common to use very high inocula in rodent models (Minandri et al., 2016; Damron et al., 2016), unless we employ neutropenic mice. In addition, our expression data showed patterns that were actually surprisingly similar from very artificial rodent conditions to human pneumonia patients.

7.5 Endogenous siderophore TBDTs loss contributes to bacterial fitness loss

Several studies highlighted the importance of TBDTs *in vivo* (Takase et al., 2000b; Noinaj et al., 2010; Minandri et al., 2016; Damron et al., 2016). Inactivation of TonB1, which is responsible for TBDTs substrates transport, was shown to render *P. aeruginosa* PAO1 completely avirulent in two mouse models of infection (Takase et al., 2000b; Minandri et al., 2016), indicating that some TonB1-related TBDTs are crucial *in vivo*. In literature, we found several reports on the relevance of pyoverdine, pyochelin and heme TBDTs *in vivo* (Takase et al., 2000b; Marvig et al., 2014; Minandri et al., 2016; Damron et al., 2016). On the other hand, the role of xenosiderophore TBDTs and their associated siderophores have been poorly studied *in vivo* (Skurnik et al., 2013; Lee et al., 2016). In order to induce the expression of xenosiderophore TBDTs (Gensberg et al., 1992; Llamas et al., 2006), xenosiderophores from airway microbiota should be present in large quantities at the

infection site and should successfully compete with endogenous siderophores (Hibbing et al., 2010). Recently, inactivation of the ferrichrome transporter FiuA was shown to reduce fitness and virulence of *P. aeruginosa in vivo* (Lee et al., 2016). Using a tranposon library, the xenosiderophore TBDTS CirA, FoxA and OptL have also been associated with virulence (Skurnik et al., 2013). Apart from FiuA, the other xenosiderophore TBDTs have not yet been investigated *in vivo*, but seemed to have no impact on *in vivo* fitness in two different mouse models (Skurnik et al., 2013; Turner et al., 2014).

Proteomic analyses revealed high expression levels for a subset of TBDTs. However, it has been shown that high levels of expression were not always correlated with increased fitness *in vivo* (Turner et al., 2014). Therefore, the contribution of these TBDTs was investigated *in vivo*. Based on our expression data, series of TBDTs mutants were generated and further tested in the developed intranasal model. In contrast to previous studies, which all employed single-strain infections (Takase et al., 2000b; Minandri et al., 2016; Damron et al., 2016), we used mixed infections to assess mutant fitness in presence of a competing wild-type strain, a scenario more closely mimicking emergence of resistant clones among wild-type bacteria.

In vivo competition assays revealed the dominant role of the endogenous siderophore system pyoverdine *in vivo*. Inactivation of the pyoverdine TBDT or the pyoverdine system (both transporter and synthesis of pyoverdine) (-PVD) led to a significant drop in fitness. Pyoverdine is *P. aeruginosa* siderophore with the highest affinity to iron and its transporter FpvA is involved in CSS, which induces the expression of several virulence factors (Llamas et al., 2014; Hoegy et al., 2014). Therefore, the inactivation of the pyoverdine system might affect both the iron acquisition and the virulence of *P. aeruginosa in vivo* as reported by previous studies (Takase et al., 2000a; Turner et al., 2014; Lopez-Medina et al., 2015; Minandri et al., 2016; Granato et al., 2016).

The inactivation of both pyoverdine and pyochelin systems (-PVD-PCH) did not contribute to a fitness reduction, indicating that pyochelin was not compensating for iron acquisition in our model. This was consistent with studies in *P. aeruginosa* that showed that pyochelin was less important than pyoverdine in immunocompromized mice (Takase et al., 2000a). *Burkholderia cenocepacia*, a similar respiratory pathogen to *P. aeruginosa*, produces two siderophores, ornibactin, which shares high similarity with pyoverdine, and pyochelin. Interestingly, it was shown that *B. cenocepacia* relied mostly on ornibactin for iron acquisition *in vivo* (Visser et al., 2004). On the other hand, *B. cenocepacia* ferripyochelin was shown to induce increased virulence (Sokol and Woods, 1988) through formation of superoxide and hydrogen peroxide, increasing damages to the endothelial cells (Britigan et al., 1997; Coffman et al., 1990), consistent with *P. aeruginosa* pyochelin involvement in lung inflammation (Coffman et al., 1990).

The third endogenous siderophore nicotianamine was reported to have an important role for iron acquisition in artificial lung condition (Gi et al., 2014). The inactivation of the nicotianamine system (-NIC) did not affect *P. aeruginosa* growth in our intranasal model, however the inactivation of the three systems (-PVD-PCH-NIC) decreased the fitness of the strain, suggesting a contributing role of nicotianamine in iron acquisition in the absence of pyoverdine. Nicotianamine presents serious advantages for *P. aeruginosa* in the low-oxygen lung environment since the siderophore binds ferrous iron with high affinity (Wirén et al., 1999). Additional inactivation of a potential fourth endogenous siderophore system (-SidX: PA14_54940-PA14_54960) or the inner membrane ferrous iron sensor FeoB did not further affect the fitness of the *P. aeruginosa* (Seyedmohammad et al., 2016).

The heme transporter PhuR and HasR have been to shown to play an important role in iron acquisition via heme *in vivo* in the absence of the siderophore systems (Takase et al., 2000a; Damron et al., 2016). In CF patients, *P. aeruginosa* has been shown to swtich to heme utilization during chronic infection (Nguyen et al., 2014; Marvig et al., 2014). Contradicting data have been reported in pneumonia mouse models for heme TBDTs (Damron et al., 2016; Minandri et al., 2016). Indeed in the study of Damron and coworkers, a single deletion of *hasR* reduced considerably the fitness of PAO1 (Damron et al., 2016), while in Minandri and coworkers' study, the double mutant Δ*phuR*Δ*hasR* exhibited the same fitness as wild-type PAO1 (Minandri et al., 2016). Both mutants carried functional siderophore systems, which might skewed the contribution of heme TBDTs in iron acquisition. In our settings, inactivation of heme TBDTs had no contribution to *P. aeruginosa* fitness *in vivo* in two models of infection, i.e. pneumonia and septicemia, however inactivation of heme together with the endogenous siderophore systems (-PVD-PCH-NIC-heme) reduced the fitness to the level of (-PVD-PCH-NIC) fitness. Our data suggested thus that heme TBDTs are dispensable *in vivo*, at least in our *in vivo* settings.

Based on our expression data, we inactivated most of the TBDTs expressed in animal samples. This led to Δ25, a mutant lacking 25 TBDTs that includes the heme TBDTs, the non-iron metal TBDTs (except for BtuB, the cobalamine transporter) and most of the xenosiderophore TBDTs. This strain showed no fitness change compared to wild-type bacteria in the intranasal model, which was not surprising since it carried a functional pyoverdine system. However, additional inactivation of these siderophore systems decreased the fitness of the strain to the fitness of (-PVD-PCH-NIC), highlighting again the predominant role of pyoverdine *in vivo*.

Moreover, the loss of the xenosiderophore transporters CirA and OptL did not affect the fitness of Δ25, contrary to what was suggested (Skurnik et al., 2013). Interestingly, Δ25 fitness, which missed the ferrichrome transporter FiuA, was not consistent with Lee and coworkers study, where the single mutant Δ*fiuA* led to decrease in growth and virulence

through overproduction of the protease elastase *in vivo* (Lee et al., 2016). Deletion of *fiuA* might impair the acquisition of ferrichrome, but a second transporter FoxA has been described to compensate for ferrichrome uptake (Hannauer et al., 2010). In addition, pyoverdine has a higher affinity for iron and therefore might competes successfully against ferrichrome. Therefore, the *in vivo* phenotype of Δ*fiuA* might be associated mainly to the increased production of the elastase (Lee et al., 2016). Elastase was shown to release iron from transferrin (Wolz et al., 1994) and to reduce pro-inflammatory responses under physiological conditions (Van Der Plas et al., 2016). However, the connection between elastase and FiuA needs to be further demonstrated, since no complementation experiment was mentioned to confirm the phenotype of Δ*fiuA* (Lee et al., 2016).

Together, these data suggested that *P. aeruginosa* primarily used its high-affinity siderophore pyoverdine for iron scavenging, whereas uptake capabilities for its other endogenous siderophores, xenosiderophores, heme-associated substrates and possibly copper and zinc uptake were all dispensable for *in vivo* fitness in an intranasal model. Most reported studies employed the less virulent strain PAO1 and single TBDT-deletion mutants, which might not fully represent the *in vivo* relevance of transport systems because of the overlapping substrate spectra (Cornelis and Dingemans, 2013).

The role of siderophore in iron acquisition has been widely studied. However, it seems clear that the siderophores plan an important role in virulence (Meyer et al., 1996; Cassat and Skaar, 2013; Kirienko et al., 2015). However this function as virulence factors remains poorly studied.

7.6 Opportunities for the Trojan horse approach

In order to find successful Trojan-horse-based conjugate, we should investigate which are the essential substrates and their associated TBDT required for growth of *P. aeruginosa in vivo*. Together with previous studies, our data revealed a major role for pyoverdine and its associated receptor FpvA *in vivo*, which significantly affected *P. aeruginosa* fitness *in vivo* (Takase et al., 2000a; Turner et al., 2014; Lopez-Medina et al., 2015; Minandri et al., 2016; Granato et al., 2016). Such a candidate is ideal because it leaves the bacteria few options to survive, either the bacteria inactivate the transporter reducing its fitness and are cleared by the host immune system, or they keep the transporter and are subject to the antibacterial activity of the Trojan horse compounds. However, pyoverdine based compounds development presents hurdles due to the complex chemistry of the pyoverdine molecule structure. To date, the pyoverdine based compounds were developed by hemisynthesis (Mislin and Schalk, 2014), which might lead to difficulties in the industrial up-scaling process of the drug. Moreover, pyoverdine is specific to *Pseudomonas* species and the different types of pyoverdine are even specific to *Pseudomonas* strains, reducing

the spectrum of treatable pathogens of pyoverdine-based compounds (Briskot et al., 1986; Meyer et al., 1997).

Pyoverdine-based compounds would not be effective against installed *Pseudomonas* infections such as in CF patients. Indeed, several studies have shown that over the course of *P. aeruginosa* infections in the lungs of CF patients, there was an accumulation of pyoverdine-deficient mutants (Martin et al., 2011; De Vos et al., 2001; Smith et al., 2006; Konings et al., 2013; Dettman et al., 2013; Bianconi et al., 2015). In the absence of pyoverdine, nicotianamine and its related transporter OptC would be an ideal alternative for Trojan horse. Nicotianamine has been shown to play an important role in artificial lung conditions (Gi et al., 2014) and our data highlighted its contributing role in the absence of pyoverdine *in vivo*. The structure of nicotianamine is much less complex than pyoverdine, encouraging promising developmental options for Trojan horse-based conjugates. Moreover, nicotianamine and related molecules seem to be conserved in several pathogens (Ghssein et al., 2016), which could extend the spectrum of treatable pathogens to more than *Pseudomonas* species. More research is therefore needed to unravel the mechanisms of biosynthesis, secretion and uptake of nicotianamine in *P. aeruginosa* to guide rational the developement of nicotianamine based drugs.

Despite contradictory data in the literature (Bielecki et al., 2013; Damron et al., 2016; Minandri et al., 2016) and our *in vivo* data, heme could also be considered as an alternative for the Trojan horse strategy. In other models, heme transporters appeared relevant *in vivo* as secondary transporters for iron uptake when *P. aeruginosa* was not relying on its endogenous siderophores (Konings et al., 2013; Nguyen et al., 2014; Damron et al., 2016). Moreover, our expression data showed the abundance of heme transporters in all the conditions tested. Non-iron metalloporphyrins, such as gallium-porphyrin complexes, are a family of antibacterial compounds of therapeutic potential using the Trojan horse approach (Stojiljkovic et al., 1999; Anzaldi and Skaar, 2010; Hijazi et al., 2017). These compounds presented several advantages because heme transporters are conserved among several bacteria (Wandersman and Stojiljkovic, 2000), and could therefore reach a broad spectrum of pathogens. In addition, this redundancy in heme-related TBDTs would decrease the risk of development of resistance against heme-mimetics. Careful *in vivo* studies must be undertaken to assess the toxicity of such compounds because they could actually interfere with the host heme and jeopardize the host innate immune system (Anzaldi and Skaar, 2010; Schulz et al., 2012).

Xenosiderophore TBDTs, including PiuA and PirA, showed low contribution to *in vivo* fitness of *P. aeruginosa*. However, several studies showed that the siderophore-antibiotic conjugates induce the expression of the transporter (Gasser et al., 2016), suggesting that these conjugates have antibacterial potential despite low abundance and scattered expression of these transporters in different conditions. In order to develop efficient

conjugates, we should target TBDTs with overlapping substrate spectra to minimize the risk of antibiotic resistance by facile inactivation of TBDT. Constant vigilance and basic research on the processes associated with bacterial virulence and transport will continue to aid the development of novel and effective therapeutics.

7.7 Implications of simple porins and efflux pumps in antibiotics transport

7.7.1 Simple porins have a crucial role in nutrient uptake

Simple porins are open water filled channels that allow diffusion of molecules, such as sugars, amino acids, phosphates and cations (Hancock and Brinkman, 2002). They have been shown to be involved in antibiotic uptake. *P. aeruginosa* UCBPP-PA14 encodes 40 simple porins (Winsor et al., 2016). Among them, the most studied transporters belong to the OprD family (Hancock and Brinkman, 2002), which transports basic amino acids and derivatives but also carbapenems (Ochs et al., 1999a; Ochs et al., 1999b). One mechanism of resistance to carbapenems is the inactivation of OprD, which decreases carbapenems transport (Ochs et al., 1999b; Pirnay et al., 2002). Therefore, it is often assumed that the *P. aeruginosa* outer membrane simple porins crucially determine antibiotic translocation and efficacy. However, except for OprD, there is no clear evidence that other simple porins are involved in antibiotic uptake.

We thus applied the same approach than for the TBDTs. We used targeted proteomics to determine the abundance of simple porins *in vivo*. In contrast to the expression levels of TBDTs, the data revealed a constant expression of a subset of simple porins (OprF, OprD, FadL, OprG, OprQ, OprE) under the same *in vivo* conditions than for TBDTs, i.e. rodents samples and human patients samples. *In vivo* expression correlated with *in vitro* expression, suggesting that this subset of simple porins could be involved in the transport of essential nutrients. As a result, we assessed the functional relevance of simple porins by generating series of single and multiple gene deletions. A porin-free mutant Δ40 was generated. However, none of the simple porins mutants, except for oprD, were affected in MIC studies. Δ40 showed the same susceptibility as Δ*oprD* for carbapanems, suggesting that the simple porins have a limited contribution to antibiotic uptake. Interestingly, Δ40 growth was affected on minimal media with single carbon source, indicating a role of simple porins in nutrient uptake. This results was further motivated by the decrease of *in vivo* fitness of Δ40.

Similar expression levels of simple porins *in vivo* and *in vitro* could mean that simple porins enable transport of essential nutrients, however their substrate profile need to be further investigated. It also surprising that *P. aeruginosa* expresses so many simple porins and finally uses 12 of them. The overexpression of these cryptic porins showed

an increase in susceptibility for several antibiotics, therefore they might be exploited as antibiotic transport systems.

7.7.2 Efflux pumps have a limited contribution to antibiotics resistance in clinical isolates

Efflux pumps are multicomponent protein complexes that are used by bacteria to secrete waste, toxins and antibiotics (Hancock and Brinkman, 2002). The resistance-nodulation-division (RND) superfamily are efflux pump exporters that mediate active efflux of small molecules including many antibiotics (Hancock and Brinkman, 2002). They are associated with significant clinical antibiotic resistance in clinical isolates (Sun et al., 2014; Blair et al., 2015). However the direct connection between RND pumps expression and resistance has not been shown yet.

We developed a method to generate rapid deletion of efflux pumps in diverse clinical *P. aeruginosa* and ESBL *E. coli* isolates. We targeted the outer membrane channel of the major pumps: OprM for *P. aeruginosa* and TolC for *E. coli* (Li et al., 1995). Despite the deletions of the major efflux pumps in the isolates, the mutants remained resistant to antibiotics and no compensation mechanism by other major efflux pumps could be observed, indicating the presence of potent resistance mechanisms, alternative to efflux pumps overexpression. This data suggested thus a limited contribution of efflux pumps to the antibiotic resistance of the clinical isolates. Overexpression of efflux pumps might have an important role in the switch from susceptibility to resistance phenotype of an isolate, in helping this isolate to adapt to the antibiotic pressure (Poole, 2007). However, once the resistance is acquired, the efflux pumps are thought to intend housekeeping functions unrelated to drug export and resistance (Poole, 2007). This could explain why the efflux pumps mutants are poorly, or not at all, affected by the loss of functional efflux pumps. This limited contribution of efflux pumps also question the relevance of efflux pumps inhibitors, which have been of interest these last years (Puzari and Chetia, 2017). Understanding the mechanisms of efflux pumps induction could provide insight in *P. aeruginosa* adaptation *in vivo* and could prevent development of resistance upon antibiotic pressure.

8 Conclusion

Antimicrobial resistance is a serious public health threat worldwide. Developing new antibiotics is a considerable challenge because of the rapid emergence of resistance in bacteria. The outer membrane of Gram-negative pathogen plays a crucial role as the first line of bacterial defence against antibiotics. The opportunistic pathogen *P. aeruginosa* is intrinsically resistant to many antibiotics partly due to its large number of porins and efflux pumps that enable the pathogen to have a tight control control over influx and efflux across the outer membrane. Therefore, getting antibiotics through the outer membrane is a difficult task. So far, the Trojan horse approach is the most advanced strategy to circumvent this issue. In a Trojan horse approach, a toxic compound is efficiently transported across the outer membrane via endogenous bacterial active transporters (TBDTs), by hijacking essential substrate for *P. aeruginosa* growth *in vivo*. However the Trojan horse approach is failing when *P. aeruginosa* develops resistance by facile inactivation of the TBDT(s) involved in the process. In order to prevent the rapid development of resistance, transport capabilities and substrate specifities of *P. aeruginosa* need to be seriously investigated *in vivo*. Indeed, mimetics of substrates, found essential for the growth of *P. aeruginosa in vivo*, should be targeted. By this means, the substrate mimetic would then be actively transported via one or several endogenous TBDTs, getting around the vigilance of *P. aeruginosa* and increasing intracellular antimicrobial concentration. Inactivation of the involved TBDT(s) would contribute to the fitness reduction of the pathogen *in vivo* and would lower the risk of resistance development.

By combining advanced targeted proteomics and *in vivo* competition assays, we were able to quantify the abundance of TBDTs *in vivo* and assess their contribution to fitness *in vivo*. Overall, our data suggested that *P. aeruginosa* mainly used its high-affinity siderophore pyoverdine for iron scavenging, whereas uptake capabilities for its other endogenous siderophores, xenosiderophores, heme-associated substrates and possibly copper and zinc uptake were all dispensable for *in vivo*. However, pyoverdine is not a good candidate for Trojan horse strategy due to its complex chemistry and its reduced spectrum of treatable pathogens. Another potential candidate would be nicotianamine, because it can bind a wide range of metals and seems to have significant role in the lung, especially in absence of pyoverdine such as in CF patients lungs. Despite their low contribution *in vivo*, heme and xenosiderophores mimetics would be potential candidates, since their presence induce the expression of the associated TBDTs. Targeting substrate with redundant transport capabilities might also lower the risk of resistance development.

Understanding the host microenvironment is essential for the development of *in vitro* media. Our data from preclinical and human patients provide benchmarks for developing *in vitro* assays and animal models, that mimic better transport capabilities during infection. Deeper knowledge of *P. aeruginosa* phenotypes *in vivo* is thus essential to guide rational development of antimicrobials.

The requirement for iron has created an ongoing battle between hosts and pathogens. Free iron is already limited in the bloodstream of hosts. In addition, bacterial infections trigger the innate immune response, which sequesters iron even further. Pathogens such as *P. aeruginosa* secrete siderophores to scavenge iron from the host. The role of siderophore in iron acquisition is therefore extensively investigated. However, siderophores, such as pyoverdine and pyochelin, seem to play a key role in virulence, but this function remains poorly studied. Given the importance of siderophores as virulence factors, greater insight into the contribution of siderophores to virulence is needed.

References

Abbaspour, N., R. Hurrell, and R. Kelishadi (2014). „Review on iron and its importance for human health“. In: *Journal of Research in Medical Sciences* 19.2.

Aebersold, R. and M. Mann (2003). „Mass spectrometry-based proteomics“. In: *Nature* 422.6928, pp. 198–207.

Amaral, L. et al. (2014). „Efflux pumps of Gram-negative bacteria: what they do, how they do it, with what and how to deal with them“. In: *Frontiers in pharmacology* 4, p. 168.

Andersen, S. B. et al. (2015). „Long-term social dynamics drive loss of function in pathogenic bacteria“. In: *Proceedings of the National Academy of Sciences* 112.34, pp. 10756–10761.

Ankenbauer, R. G. and H. N. Quan (1994). „FptA, the Fe (III)-pyochelin receptor of Pseudomonas aeruginosa: a phenolate siderophore receptor homologous to hydroxamate siderophore receptors.“ In: *Journal of bacteriology* 176.2, pp. 307–319.

Anzaldi, L. L. and E. P. Skaar (2010). „Overcoming the heme paradox: heme toxicity and tolerance in bacterial pathogens“. In: *Infection and immunity* 78.12, pp. 4977–4989.

Askoura, M. et al. (2011). „Efflux pump inhibitors (EPIs) as new antimicrobial agents against Pseudomonas aeruginosa“. In: *Libyan Journal of Medicine* 6.1.

Balasubramanian, D. et al. (2012). „A dynamic and intricate regulatory network determines Pseudomonas aeruginosa virulence“. In: *Nucleic acids research*, gks1039.

Balibar, C. J. and M. Grabowicz (2016). „Mutant alleles of lptD increase the permeability of Pseudomonas aeruginosa and define determinants of intrinsic resistance to antibiotics“. In: *Antimicrobial agents and chemotherapy* 60.2, pp. 845–854.

Banin, E. et al. (2008). „The potential of desferrioxamine-gallium as an anti-Pseudomonas therapeutic agent“. In: *Proceedings of the National Academy of Sciences* 105.43, pp. 16761–16766.

Barbier, M. et al. (2014). „From the environment to the host: re-wiring of the transcriptome of Pseudomonas aeruginosa from 22 C to 37 C“. In: *PloS one* 9.2, e89941.

Basilea reports 2016 half-year results. http://www.basilea.com/News-and-Media/Basilea-reports-2016-half-year-results-CRESEMBA-launched-in-key-European-markets/af0d2479-4963-6f53-99b2-85dae0ce489b/. Accessed: 2017-04-01.

Baslé, A. et al. (2006). „Crystal structure of osmoporin OmpC from E. coli at 2.0 Å“. In: *Journal of molecular biology* 362.5, pp. 933–942.

Baumgart, A. M. K., M. A. Molinari, and A. C. de Oliveira Silveira (2010). „Prevalence of carbapenem resistant Pseudomonas aeruginosa and Acinetobacter baumannii in highcomplexity hospital“. In: *The Brazilian Journal of Infectious Diseases* 14.5, pp. 433–436.

Beare, P. A. et al. (2003). „Siderophore-mediated cell signalling in Pseudomonas aeruginosa: divergent pathways regulate virulence factor production and siderophore receptor synthesis“. In: *Molecular microbiology* 47.1, pp. 195–207.

Beneš, I et al. (1983). „Metal complex formation by nicotianamine, a possible phytosiderophore“. In: *Cellular and Molecular Life Sciences* 39.3, pp. 261–262.

Benz, G. et al. (1982). „Konstitution der Desferriform der Albomycine δ1, δ2, ε“. In: *Angewandte Chemie International Edition in English* 21.S7, pp. 1322–1335.

Berg, B. van den (2012). „Structural basis for outer membrane sugar uptake in pseudomonads“. In: *Journal of Biological Chemistry* 287.49, pp. 41044–41052.

Bianconi, I. et al. (2015). „Comparative genomics and biological characterization of sequential Pseudomonas aeruginosa isolates from persistent airways infection“. In: *BMC genomics* 16.1, p. 1105.

Bickel, H et al. (1960). „On iron-containing growth factors, sideramines, and their antagonists, the iron-containing antibiotics, sideromycins“. In: *Experientia* 16, pp. 129–133.

Bickel, H et al. (1965). „Constitution of ferrimycin A1.“ In: *Antimicrobial agents and chemotherapy* 5, p. 951.

Bielecki, P. et al. (2008). „Towards understanding Pseudomonas aeruginosa burn wound infections by profiling gene expression“. In: *Biotechnology letters* 30.5, pp. 777–790.

Bielecki, P. et al. (2011). „In-vivo expression profiling of Pseudomonas aeruginosa infections reveals niche-specific and strain-independent transcriptional programs“. In: *PLoS One* 6.9, e24235.

Bielecki, P. et al. (2013). „Ex vivo transcriptional profiling reveals a common set of genes important for the adaptation of Pseudomonas aeruginosa to chronically infected host sites“. In: *Environmental microbiology* 15.2, pp. 570–587.

Blair, J. M. et al. (2015). „Molecular mechanisms of antibiotic resistance“. In: *Nature Reviews Microbiology* 13.1, pp. 42–51.

Blanco, P. et al. (2016). „Bacterial multidrug efflux pumps: much more than antibiotic resistance determinants“. In: *Microorganisms* 4.1, p. 14.

Brandel, J. et al. (2012). „Pyochelin, a siderophore of Pseudomonas aeruginosa: physicochemical characterization of the iron (III), copper (II) and zinc (II) complexes“. In: *Dalton transactions* 41.9, pp. 2820–2834.

Braud, A. et al. (2009). „The Pseudomonas aeruginosa pyochelin-iron uptake pathway and its metal specificity“. In: *Journal of bacteriology* 191.11, pp. 3517–3525.

Brillet, K. et al. (2012). „An ABC transporter with two periplasmic binding proteins involved in iron acquisition in Pseudomonas aeruginosa“. In: *ACS chemical biology* 7.12, pp. 2036–2045.

Briskot, G, K Taraz, and H Budzikiewicz (1986). „PYOVERDINE TYPE SIDEROPHORES FROM PSEUDOMONAS-AERUGINOSA“. In: *ZEITSCHRIFT FUR NATURFORSCHUNG CA JOURNAL OF BIOSCIENCES* 41.5-6, pp. 497–506.

Britigan, B. E., G. T. Rasmussen, and C. D. Cox (1994). „Pseudomonas siderophore pyochelin enhances neutrophil-mediated endothelial cell injury“. In: *American Journal of Physiology-Lung Cellular and Molecular Physiology* 266.2, pp. L192–L198.

Britigan, B. E., G. T. Rasmussen, and C. D. Cox (1997). „Augmentation of oxidant injury to human pulmonary epithelial cells by the Pseudomonas aeruginosa siderophore pyochelin.“ In: *Infection and immunity* 65.3, pp. 1071–1076.

Bryant, C. E. and T. P. Monie (2012). „Mice, men and the relatives: cross-species studies underpin innate immunity“. In: *Open biology* 2.4, p. 120015.

Caille, O., C. Rossier, and K. Perron (2007). „A copper-activated two-component system interacts with zinc and imipenem resistance in Pseudomonas aeruginosa“. In: *Journal of bacteriology* 189.13, pp. 4561–4568.

Callahan, D. L. et al. (2007). „Relationships of nicotianamine and other amino acids with nickel, zinc and iron in Thlaspi hyperaccumulators“. In: *New Phytologist* 176.4, pp. 836–848.

Carvalho, C. C. de and P. Fernandes (2014). „Siderophores as “Trojan Horses”: tackling multidrug resistance?“ In: *Frontiers in microbiology* 5, p. 290.

Casabona, M. G. et al. (2013). „Proteomic characterization of Pseudomonas aeruginosa PAO1 inner membrane“. In: *Proteomics* 13.16, pp. 2419–2423.

Cassat, J. E. and E. P. Skaar (2013). „Iron in infection and immunity“. In: *Cell host & microbe* 13.5, pp. 509–519.

Charretier, Y. and J. Schrenzel (2016). „Mass spectrometry methods for predicting antibiotic resistance“. In: *PROTEOMICS-Clinical Applications*.

Charretier, Y. et al. (2015). „Label-free SRM-based relative quantification of antibiotic resistance mechanisms in Pseudomonas aeruginosa clinical isolates“. In: *Frontiers in microbiology* 6, p. 81.

Chaturvedi, K. S. and J. P. Henderson (2014). „Pathogenic adaptations to host-derived antibacterial copper“. In:

Chen, H. et al. (2008). „The Pseudomonas aeruginosa multidrug efflux regulator MexR uses an oxidation-sensing mechanism“. In: *Proceedings of the National Academy of Sciences* 105.36, pp. 13586–13591.

Chirumamilla, R. R., R Marchant, and P Nigam (2001). „Captopril and its synthesis from chiral intermediates“. In: *Journal of Chemical Technology and Biotechnology* 76.2, pp. 123–127.

Cho, Y.-E. et al. (2007). „Cellular Zn depletion by metal ion chelators (TPEN, DTPA and chelex resin) and its application to osteoblastic MC3T3-E1 cells“. In: *Nutrition research and practice* 1.1, pp. 29–35.

Choi, D.-S. et al. (2011). „Proteomic analysis of outer membrane vesicles derived from Pseudomonas aeruginosa“. In: *Proteomics* 11.16, pp. 3424–3429.

Chuanchuen, R. et al. (2005). „Substrate-dependent utilization of OprM or OpmH by the Pseudomonas aeruginosa MexJK efflux pump“. In: *Antimicrobial agents and chemotherapy* 49.5, pp. 2133–2136.

Coffman, T. J. et al. (1990). „Possible role of bacterial siderophores in inflammation. Iron bound to the Pseudomonas siderophore pyochelin can function as a hydroxyl radical catalyst.“ In: *Journal of Clinical Investigation* 86.4, p. 1030.

Cohen, G. N. (2011). *Microbial biochemistry*. Vol. 500. Springer.

Cole, S. J. et al. (2014). „Catheter-associated urinary tract infection by Pseudomonas aeruginosa is mediated by exopolysaccharide-independent biofilms“. In: *Infection and immunity* 82.5, pp. 2048–2058.

Cope, L. D. et al. (1994). „The 100 kDa haem: haemopexin-binding protein of Haemophilus Influenzae: structure and localization“. In: *Molecular microbiology* 13.5, pp. 863–873.

Cornelis, P. and S. C. Andrews (2010). *Iron uptake and homeostasis in microorganisms*. Horizon Scientific Press.

Cornelis, P. and J. Dingemans (2013). „Pseudomonas aeruginosa adapts its iron uptake strategies in function of the type of infections“. In:

Cowan, S. et al. (1992). „Crystal structures explain functional properties of two E. coli porins.“ In: *Nature* 358.6389, p. 727.

Crosa, J. H. and C. T. Walsh (2002). „Genetics and assembly line enzymology of siderophore biosynthesis in bacteria“. In: *Microbiology and molecular biology reviews* 66.2, pp. 223–249.

Cuív, P. Ó. et al. (2004). „Identification of rhtX and fptX, novel genes encoding proteins that show homology and function in the utilization of the siderophores rhizobactin 1021 by Sinorhizobium meliloti and pyochelin by Pseudomonas aeruginosa, respectively“. In: *Journal of bacteriology* 186.10, pp. 2996–3005.

Cuív, P. Ó., P. Clarke, and M. O'Connell (2006). „Identification and characterization of an iron-regulated gene, chtA, required for the utilization of the xenosiderophores aerobactin, rhizobactin 1021 and schizokinen by Pseudomonas aeruginosa“. In: *Microbiology* 152.4, pp. 945–954.

Cunrath, O., V. A. Geoffroy, and I. J. Schalk (2015). „Metallome of Pseudomonas aeruginosa: a role for siderophores“. In: *Environmental microbiology*.

Curie, C. et al. (2009). „Metal movement within the plant: contribution of nicotianamine and yellow stripe 1-like transporters“. In: *Annals of botany* 103.1, pp. 1–11.

Damron, F. H. et al. (2016). „Dual-seq transcriptomics reveals the battle for iron during Pseudomonas aeruginosa acute murine pneumonia“. In: *Scientific Reports* 6.

De Lorenzo, V and A. Pugsley (1985). „Microcin E492, a low-molecular-weight peptide antibiotic which causes depolarization of the Escherichia coli cytoplasmic membrane.“ In: *Antimicrobial agents and chemotherapy* 27.4, pp. 666–669.

De Vos, D. et al. (2001). „Study of pyoverdine type and production by Pseudomonas aeruginosa isolated from cystic fibrosis patients: prevalence of type II pyoverdine isolates and accumulation of pyoverdine-negative mutations“. In: *Archives of microbiology* 175.5, pp. 384–388.

Dean, C. R. and K. Poole (1993). „Cloning and characterization of the ferric enterobactin receptor gene (pfeA) of Pseudomonas aeruginosa.“ In: *Journal of bacteriology* 175.2, pp. 317–324.

Delcour, A. H. (2009). „Outer membrane permeability and antibiotic resistance“. In: *Biochimica et Biophysica Acta (BBA)-Proteins and Proteomics* 1794.5, pp. 808–816.

Destoumieux-Garzón, D. et al. (2006). „Parasitism of iron-siderophore receptors of Escherichia coli by the siderophore-peptide microcin E492m and its unmodified counterpart“. In: *Biometals* 19.2, pp. 181–191.

Dettman, J. R. et al. (2013). „Evolutionary genomics of epidemic and nonepidemic strains of Pseudomonas aeruginosa“. In: *Proceedings of the National Academy of Sciences* 110.52, pp. 21065–21070.

Dever, L. A. and T. S. Dermody (1991). „Mechanisms of bacterial resistance to antibiotics“. In: *Archives of internal medicine* 151.5, pp. 886–895.

Dickson, R. P. and G. B. Huffnagle (2015). „The lung microbiome: new principles for respiratory bacteriology in health and disease“. In: *PLoS Pathog* 11.7, e1004923.

Domon, B. and R. Aebersold (2010). „Options and considerations when selecting a quantitative proteomics strategy“. In: *Nature biotechnology* 28.7, pp. 710–721.

D'Orazio, M. et al. (2015). „The capability of Pseudomonas aeruginosa to recruit zinc under conditions of limited metal availability is affected by inactivation of the ZnuABC transporter“. In: *Metallomics* 7.6, pp. 1023–1035.

Dumas, Z., A. Ross-Gillespie, and R. Kümmerli (2013). „Switching between apparently redundant iron-uptake mechanisms benefits bacteria in changeable environments“. In: *Proceedings of the Royal Society of London B: Biological Sciences* 280.1764, p. 20131055.

ECDC. (2017). *Antimicrobial resistance surveillance in Europe 2015*. Annual Report of the European Antimicrobial Resistance Surveillance Network (EARS-Net), Stockholm.

Elias, S., E. Degtyar, and E. Banin (2011). „FvbA is required for vibriobactin utilization in Pseudomonas aeruginosa“. In: *Microbiology* 157.7, pp. 2172–2180.

Eren, E. et al. (2013a). „Toward understanding the outer membrane uptake of small molecules by Pseudomonas aeruginosa“. In: *Journal of Biological Chemistry* 288.17, pp. 12042–12053.

Eren, E. et al. (2013b). „Toward understanding the outer membrane uptake of small molecules by Pseudomonas aeruginosa“. In: *Journal of Biological Chemistry* 288.17, pp. 12042–12053.

Evans, J. C. and H. Segal (2007). „A novel insertion sequence, ISPA26, in oprD of Pseudomonas aeruginosa is associated with carbapenem resistance“. In: *Antimicrobial agents and chemotherapy* 51.10, pp. 3776–3777.

Evans, K. and K. Poole (1999). „The MexA-MexB-OprM multidrug efflux system of Pseudomonas aeruginosa is growth-phase regulated“. In: *FEMS microbiology letters* 173.1, pp. 35–39.

Fardeau, S. et al. (2014). „Synthesis and antibacterial activity of catecholate–ciprofloxacin conjugates“. In: *Bioorganic & medicinal chemistry* 22.15, pp. 4049–4060.

Fernández, L. and R. E. Hancock (2012). „Adaptive and mutational resistance: role of porins and efflux pumps in drug resistance“. In: *Clinical microbiology reviews* 25.4, pp. 661–681.

Finking, R. and M. A. Marahiel (2004). „Biosynthesis of nonribosomal peptides 1“. In: *Annu. Rev. Microbiol.* 58, pp. 453–488.

Frangipani, E. et al. (2008). „Adaptation of aerobically growing Pseudomonas aeruginosa to copper starvation“. In: *Journal of bacteriology* 190.20, pp. 6706–6717.

Gaille, C., P. Kast, and D. Haas (2002). „Salicylate biosynthesis in Pseudomonas aeruginosa Purification and characterization of PchB, a novel bifunctional enzyme displaying isochorismate pyruvate-lyase and chorismate mutase activities“. In: *Journal of Biological Chemistry* 277.24, pp. 21768–21775.

Gaille, C., C. Reimmann, and D. Haas (2003). „Isochorismate synthase (PchA), the first and rate-limiting enzyme in salicylate biosynthesis of Pseudomonas aeruginosa“. In: *Journal of Biological Chemistry* 278.19, pp. 16893–16898.

Galdiero, S. et al. (2012). „Microbe-host interactions: structure and role of Gram-negative bacterial porins.“ In: *Current protein & peptide science* 13, pp. 843–54.

Ganne, G et al. (2017a). „IIron release from the siderophore pyoverdine in Pseudomonas aeruginosa involves three new actors FpvC, FpvG and FpvH.“ In: *ACS chemical biology*.

Ganne, G. et al. (2017b). „Iron Release from the Siderophore Pyoverdine in Pseudomonas aeruginosa Involves Three New Actors: FpvC, FpvG, and FpvH“. In: *ACS Chemical Biology*.

Gasser, V. et al. (2015). „Cellular organization of siderophore biosynthesis in Pseudomonas aeruginosa: evidence for siderosomes“. In: *Journal of inorganic biochemistry* 148, pp. 27–34.

Gasser, V. et al. (2016). „Catechol siderophores repress the pyochelin pathway and activate the enterobactin pathway in Pseudomonas aeruginosa: an opportunity for siderophore–antibiotic conjugates development“. In: *Environmental microbiology*.

Ge, L. and S. Y. Seah (2006). „Heterologous expression, purification, and characterization of an L-ornithine N5-hydroxylase involved in pyoverdine siderophore biosynthesis in Pseudomonas aeruginosa“. In: *Journal of bacteriology* 188.20, pp. 7205–7210.

Gensberg, K., K. Hughes, and A. W. Smith (1992). „Siderophore-specific induction of iron uptake in Pseudomonas aeruginosa“. In: *Microbiology* 138.11, pp. 2381–2387.

Ghosh, M. and M. J. Miller (1996). „Synthesis and in vitro antibacterial activity of spermidine-based mixed catechol-and hydroxamate-containing siderophore—Vancomycin conjugates“. In: *Bioorganic & medicinal chemistry* 4.1, pp. 43–48.

Ghssein, G. et al. (2016). „Biosynthesis of a broad-spectrum nicotianamine-like metallophore in Staphylococcus aureus“. In: *Science* 352.6289, pp. 1105–1109.

Ghysels, B. et al. (2004). „FpvB, an alternative type I ferripyoverdine receptor of Pseudomonas aeruginosa“. In: *Microbiology* 150.6, pp. 1671–1680.

Ghysels, B. et al. (2005). „The Pseudomonas aeruginosa pirA gene encodes a second receptor for ferrienterobactin and synthetic catecholate analogues“. In: *FEMS microbiology letters* 246.2, pp. 167–174.

Gi, M. et al. (2014). „A novel siderophore system is essential for the growth of Pseudomonas aeruginosa in airway mucus.“ In: *Scientific reports* 5, pp. 14644–14644.

Glatter, T., E. Ahrne, and A. Schmidt (2015). „Comparison of different sample preparation protocols reveals lysis buffer-specific extraction biases in Gram-negative bacteria and human cells“. In: *Journal of proteome research* 14.11, pp. 4472–4485.

Górska, A., A. Sloderbach, and M. P. Marszałł (2014). „Siderophore–drug complexes: potential medicinal applications of the ‘Trojan horse’strategy“. In: *Trends in pharmacological sciences* 35.9, pp. 442–449.

Gotoh, N. et al. (1998). „Characterization of the MexC-MexD-OprJ multidrug efflux system in ΔmexA-mexB-oprM mutants of Pseudomonas aeruginosa“. In: *Antimicrobial agents and chemotherapy* 42.8, pp. 1938–1943.

Granato, E. T. et al. (2016). „Do bacterial “virulence factors” always increase virulence? A meta-analysis of pyoverdine production in pseudomonas aeruginosa as a test case“. In: *Frontiers in Microbiology* 7.

Greenwald, J. et al. (2007). „Real Time Fluorescent Resonance Energy Transfer Visualization of Ferric Pyoverdine Uptake in Pseudomonas aeruginosa A ROLE FOR FERROUS IRON“. In: *Journal of Biological Chemistry* 282.5, pp. 2987–2995.

Greenwald, J. et al. (2009). „FpvA bound to non-cognate pyoverdines: molecular basis of siderophore recognition by an iron transporter“. In: *Molecular microbiology* 72.5, pp. 1246–1259.

Group, E. J. W. et al. (2009). „The bacterial challenge: time to react“. In: *EMEA/576176*, pp. 13–42.

Gudmundsdottir, A et al. (1989). „Point mutations in a conserved region (TonB box) of Escherichia coli outer membrane protein BtuB affect vitamin B12 transport.“ In: *Journal of bacteriology* 171.12, pp. 6526–6533.

Guillon, L. et al. (2013). „Deciphering protein dynamics of the siderophore pyoverdine pathway in Pseudomonas aeruginosa“. In: *PloS one* 8.10, e79111.

Guina, T. et al. (2003). „Proteomic analysis of Pseudomonas aeruginosa grown under magnesium limitation“. In: *Journal of the American Society for Mass Spectrometry* 14.7, pp. 742–751.

Gupta, C. K. and B. Singh (2017). „Uninhibited biosynthesis and release of phytosiderophores in the presence of heavy metal (HM) favors HM remediation“. In: *Environmental Science and Pollution Research*, pp. 1–10.

Haley, P. J. (2003). „Species differences in the structure and function of the immune system“. In: *Toxicology* 188.1, pp. 49–71.

Hancock, R. (1987). „Role of porins in outer membrane permeability.“ In: *Journal of bacteriology* 169.3, p. 929.

Hancock, R. E. and F. S. Brinkman (2002). „Function of Pseudomonas porins in uptake and efflux“. In: *Annual Reviews in Microbiology* 56.1, pp. 17–38.

Hannauer, M. et al. (2010). „The ferrichrome uptake pathway in Pseudomonas aeruginosa involves an iron release mechanism with acylation of the siderophore and recycling of the modified desferrichrome“. In: *Journal of bacteriology* 192.5, pp. 1212–1220.

Hannauer, M. et al. (2012a). „Biosynthesis of the pyoverdine siderophore of Pseudomonas aeruginosa involves precursors with a myristic or a myristoleic acid chain“. In: *FEBS letters* 586.1, pp. 96–101.

Hannauer, M. et al. (2012b). „The PvdRT-OpmQ efflux pump controls the metal selectivity of the iron uptake pathway mediated by the siderophore pyoverdine in Pseudomonas aeruginosa“. In: *Environmental microbiology* 14.7, pp. 1696–1708.

Hare, N. J. et al. (2011). „Proteomics of Pseudomonas aeruginosa Australian epidemic strain 1 (AES-1) cultured under conditions mimicking the cystic fibrosis lung reveals increased iron acquisition via the siderophore pyochelin“. In: *Journal of proteome research* 11.2, pp. 776–795.

Hare, N. J. et al. (2012). „Proteomic profiling of Pseudomonas aeruginosa AES-1R, PAO1 and PA14 reveals potential virulence determinants associated with a transmissible cystic fibrosis-associated strain“. In: *BMC microbiology* 12.1, p. 16.

Harmer, C. et al. (2013). „Modulation of gene expression by Pseudomonas aeruginosa during chronic infection in the adult cystic fibrosis lung“. In: *Microbiology* 159.11, pp. 2354–2363.

Harrison, E. M. et al. (2010). „Pathogenicity islands PAPI-1 and PAPI-2 contribute individually and synergistically to the virulence of Pseudomonas aeruginosa strain PA14“. In: *Infection and immunity* 78.4, pp. 1437–1446.

Hartmann, A., H.-P. FIEDLER, and V. Braun (1979). „Uptake and Conversion of the Antibiotic Albomycin by Escherichia coli K-12“. In: *The FEBS Journal* 99.3, pp. 517–524.

Hayashi, A. and K. Kimoto (2007). „Nicotianamine preferentially inhibits angiotensin I-converting enzyme“. In: *Journal of nutritional science and vitaminology* 53.4, pp. 331–336.

He, J. et al. (2004). „The broad host range pathogen Pseudomonas aeruginosa strain PA14 carries two pathogenicity islands harboring plant and animal virulence genes“. In: *Proceedings of the National Academy of Sciences of the United States of America* 101.8, pp. 2530–2535.

Hearn, E. M. et al. (2009). „Transmembrane passage of hydrophobic compounds through a protein channel wall“. In: *Nature* 458.7236, pp. 367–370.

Heinisch, L. et al. (2002). „Highly antibacterial active aminoacyl penicillin conjugates with acylated bis-catecholate siderophores based on secondary diamino acids and related compounds“. In: *Journal of medicinal chemistry* 45.14, pp. 3032–3040.

Hell, R. and U. W. Stephan (2003). „Iron uptake, trafficking and homeostasis in plants“. In: *Planta* 216.4, pp. 541–551.

Hennard, C. et al. (2001). „Synthesis and Activities of Pyoverdin- Quinolone Adducts: A Prospective Approach to a Specific Therapy Against Pseudomonas a eruginosa“. In: *Journal of medicinal chemistry* 44.13, pp. 2139–2151.

Hibbing, M. E. et al. (2010). „Bacterial competition: surviving and thriving in the microbial jungle“. In: *Nature Reviews Microbiology* 8.1, pp. 15–25.

Hider, R. C. and X. Kong (2010). „Chemistry and biology of siderophores“. In: *Natural product reports* 27.5, pp. 637–657.

Higgins, M. K. et al. (2004). „Structure of the periplasmic component of a bacterial drug efflux pump“. In: *Proceedings of the National Academy of Sciences of the United States of America* 101.27, pp. 9994–9999.

Hijazi, S., P. Visca, and E. Frangipani (2017). „Gallium-protoporphyrin IX inhibits Pseudomonas aeruginosa growth by targeting cytochromes“. In: *Frontiers in Cellular and Infection Microbiology* 7.

Hilker, R. et al. (2015). „Interclonal gradient of virulence in the Pseudomonas aeruginosa pangenome from disease and environment“. In: *Environmental microbiology* 17.1, pp. 29–46.

Hirakata, Y. et al. (2009). „Efflux pump inhibitors reduce the invasiveness of Pseudomonas aeruginosa“. In: *International journal of antimicrobial agents* 34.4, pp. 343–346.

Hmelo, L. R. et al. (2015). „Precision-engineering the Pseudomonas aeruginosa genome with two-step allelic exchange“. In: *Nature protocols* 10.11, pp. 1820–1841.

Hoegy, F., G. L. Mislin, and I. J. Schalk (2014). „Pyoverdine and pyochelin measurements“. In: *Pseudomonas Methods and Protocols*, pp. 293–301.

Hood, M. I. and E. P. Skaar (2012). „Nutritional immunity: transition metals at the pathogen–host interface“. In: *Nature Reviews Microbiology* 10.8, pp. 525–537.

Hraiech, S., F. Brégeon, and J.-M. Rolain (2015). „Bacteriophage-based therapy in cystic fibrosis-associated Pseudomonas aeruginosa infections: rationale and current status“. In: *Drug design, development and therapy* 9, p. 3653.

Hudson-Shore, M. (2016). „Statistics of Scientific Procedures on Living Animals Great Britain 2015-highlighting an ongoing upward trend in animal use and missed opportunities.“ In: *Alternatives to laboratory animals: ATLA* 44.6, p. 569.

Humphrey, W., A. Dalke, and K. Schulten (1996). „VMD: visual molecular dynamics“. In: *Journal of molecular graphics* 14.1, pp. 33–38.

Hunter, R. C. et al. (2013). „Ferrous iron is a significant component of bioavailable iron in cystic fibrosis airways“. In: *MBio* 4.4, e00557–13.

Imperi, F. and P. Visca (2013). „Subcellular localization of the pyoverdine biogenesis machinery of Pseudomonas aeruginosa: A membrane-associated “siderosome”“. In: *FEBS letters* 587.21, pp. 3387–3391.

Imperi, F., F. Tiburzi, and P. Visca (2009). „Molecular basis of pyoverdine siderophore recycling in Pseudomonas aeruginosa“. In: *Proceedings of the National Academy of Sciences* 106.48, pp. 20440–20445.

Imperi, F. et al. (2013). „Repurposing the antimycotic drug flucytosine for suppression of Pseudomonas aeruginosa pathogenicity“. In: *Proceedings of the National Academy of Sciences* 110.18, pp. 7458–7463.

Ito, A. et al. (2016). „Siderophore cephalosporin cefiderocol utilizes ferric iron transporter systems for antibacterial activity against Pseudomonas aeruginosa“. In: *Antimicrobial Agents and Chemotherapy*.

Jarolim, P. et al. (1990). „Effect of hemoglobin oxidation products on the stability of red cell membrane skeletons and the associations of skeletal proteins: correlation with a release of hemin“. In: *Blood* 76.10, pp. 2125–2131.

Ji, C., P. A. Miller, and M. J. Miller (2012). „Iron transport-mediated drug delivery: practical syntheses and in vitro antibacterial studies of tris-catecholate siderophore–aminopenicillin conjugates reveals selectively potent antipseudomonal activity“. In: *Journal of the American Chemical Society* 134.24, pp. 9898–9901.

Jiricny, N. et al. (2014). „Loss of social behaviours in populations of Pseudomonas aeruginosa infecting lungs of patients with cystic fibrosis“. In: *PloS one* 9.1, e83124.

Johnstone, T. C. and E. M. Nolan (2015). „Beyond iron: non-classical biological functions of bacterial siderophores“. In: *Dalton Transactions* 44.14, pp. 6320–6339.

Jones, A. M. and M. C. Wildermuth (2011). „The phytopathogen Pseudomonas syringae pv. tomato DC3000 has three high-affinity iron-scavenging systems functional under iron limitation conditions but dispensable for pathogenesis“. In: *Journal of bacteriology* 193.11, pp. 2767–2775.

Kadner, R. (1990). „Vitamin B12 transport in Escherichia coli: energy coupling between membranes“. In: *Molecular microbiology* 4.12, pp. 2027–2033.

Kahlmeter, G et al. (2006). „European Committee on Antimicrobial Susceptibility Testing (EUCAST) technical notes on antimicrobial susceptibility testing“. In: *Clinical Microbiology and Infection* 12.6, pp. 501–503.

Kaur, A. P., I. B. Lansky, and A. Wilks (2009). „The role of the cytoplasmic heme-binding protein (PhuS) of Pseudomonas aeruginosa in intracellular heme trafficking and iron homeostasis“. In: *Journal of Biological Chemistry* 284.1, pp. 56–66.

Keseler, I. M. et al. (2013). „EcoCyc: fusing model organism databases with systems biology“. In: *Nucleic acids research* 41.D1, pp. D605–D612.

Kim, A. et al. (2015a). „Pharmacodynamic profiling of a siderophore-conjugated monocarbam in Pseudomonas aeruginosa: assessing the risk for resistance and attenuated efficacy“. In: *Antimicrobial agents and chemotherapy* 59.12, pp. 7743–7752.

Kim, H.-J. et al. (2015b). „Quantitative profiling of protein tyrosine kinases in human cancer cell lines by multiplexed parallel reaction monitoring assays“. In: *Molecular & Cellular Proteomics*, mcp–O115.

Kim, Y. J. et al. (2015c). „Quantification of SAA1 and SAA2 in lung cancer plasma using the isotype-specific PRM assays“. In: *Proteomics* 15.18, pp. 3116–3125.

King, C. D. et al. (2017). „Dataset of proteomics analysis of aging C. elegans exposed to Pseudomonas aeruginosa strain PA01“. In: *Data in Brief* 11, pp. 245–251.

Kinzel, O and H Budzikiewicz (1999). „Synthesis and biological evaluation of a pyoverdin-β-lactam conjugate: a new type of arginine-specific cross-linking in aqueous solution“. In: *The Journal of peptide research* 53.6, pp. 618–625.

Kinzel, O. et al. (1998). „The synthesis and antibacterial activity of two pyoverdin-ampicillin conjugates, entering Pseudomonas aeruginosa via the pyoverdin-mediated iron uptake pathway“. In: *The Journal of antibiotics* 51.5, pp. 499–507.

Kirienko, N. V., F. M. Ausubel, and G. Ruvkun (2015). „Mitophagy confers resistance to siderophore-mediated killing by Pseudomonas aeruginosa“. In: *Proceedings of the National Academy of Sciences* 112.6, pp. 1821–1826.

Koebnik, R., K. P. Locher, and P. Van Gelder (2000). „Structure and function of bacterial outer membrane proteins: barrels in a nutshell“. In: *Molecular microbiology* 37.2, pp. 239–253.

Kohira, N. et al. (2016). „In vitro antimicrobial activity of a siderophore cephalosporin, S-649266, against Enterobacteriaceae clinical isolates, including carbapenem-resistant strains“. In: *Antimicrobial agents and chemotherapy* 60.2, pp. 729–734.

Köhler, T. et al. (1996). „Multidrug efflux in intrinsic resistance to trimethoprim and sulfamethoxazole in Pseudomonas aeruginosa.“ In: *Antimicrobial agents and chemotherapy* 40.10, pp. 2288–2290.

Köhler, T. et al. (1999). „Characterization of MexT, the regulator of the MexE-MexF-OprN multidrug efflux system of Pseudomonas aeruginosa“. In: *Journal of Bacteriology* 181.20, pp. 6300–6305.

Konings, A. F. et al. (2013). „Pseudomonas aeruginosa uses multiple pathways to acquire iron during chronic infection in cystic fibrosis lungs“. In: *Infection and immunity* 81.8, pp. 2697–2704.

Kramer, A., I. Schwebke, and G. Kampf (2006). „How long do nosocomial pathogens persist on inanimate surfaces? A systematic review“. In: *BMC infectious diseases* 6.1, p. 130.

Krebs, H. (1950). „Chemical composition of blood plasma and serum“. In: *Annual review of biochemistry* 19.1, pp. 409–430.

Kukavica-Ibrulj, I and R. Levesque (2008). „Animal models of chronic lung infection with Pseudomonas aeruginosa: useful tools for cystic fibrosis studies“. In: *Laboratory animals* 42.4, pp. 389–412.

Lamont, I. L. et al. (2002). „Siderophore-mediated signaling regulates virulence factor production in Pseudomonas aeruginosa“. In: *Proceedings of the National Academy of Sciences* 99.10, pp. 7072–7077.

Lansky, I. B. et al. (2006). „The cytoplasmic heme-binding protein (PhuS) from the heme uptake system of Pseudomonas aeruginosa is an intracellular heme-trafficking protein to the δ-regioselective heme oxygenase“. In: *Journal of Biological Chemistry* 281.19, pp. 13652–13662.

Lassek, C. et al. (2015). „A metaproteomics approach to elucidate host and pathogen protein expression during catheter-associated urinary tract infections (CAUTIs)“. In: *Molecular & Cellular Proteomics* 14.4, pp. 989–1008.

Leal, T. et al. (2016). „Azithromycin attenuates Pseudomonas-induced lung inflammation by targeting bacterial proteins secreted in the cultured medium“. In: *Frontiers in immunology* 7.

Lee, D. G. et al. (2006). „Genomic analysis reveals that Pseudomonas aeruginosa virulence is combinatorial“. In: *Genome Biology Article R90 Genome Biology Genome Biology* 7.10.

Lee, K. et al. (2016). „The ferrichrome receptor A as a new target for Pseudomonas aeruginosa virulence attenuation“. In: *FEMS microbiology letters* 363.11, fnw104.

Leoni, L. et al. (1996). „Iron-regulated transcription of the pvdA gene in Pseudomonas aeruginosa: effect of Fur and PvdS on promoter activity.“ In: *Journal of bacteriology* 178.8, pp. 2299–2313.

Lesur, A. et al. (2015). „Screening protein isoforms predictive for cancer using immunoaffinity capture and fast LC-MS in PRM mode“. In: *PROTEOMICS-Clinical Applications* 9.7-8, pp. 695–705.

Létoffé, S. et al. (1999). „Interactions of HasA, a bacterial haemophore, with haemoglobin and with its outer membrane receptor HasR“. In: *Molecular microbiology* 33.3, pp. 546–555.

Létoffé, S. et al. (2001). „Haemophore-mediated bacterial haem transport: evidence for a common or overlapping site for haem-free and haem-loaded haemophore on its specific outer membrane receptor“. In: *Molecular microbiology* 41.2, pp. 439–450.

Létoffé, S., P. Delepelaire, and C. Wandersman (2004). „Free and hemophore-bound heme acquisitions through the outer membrane receptor HasR have different requirements for the TonB-ExbB-ExbD complex“. In: *Journal of bacteriology* 186.13, pp. 4067–4074.

Li, X.-Z., H. Nikaido, and K. Poole (1995). „Role of mexA-mexB-oprM in antibiotic efflux in Pseudomonas aeruginosa.“ In: *Antimicrobial agents and chemotherapy* 39.9, pp. 1948–1953.

Li, X.-Z. et al. (1998). „β-Lactamase inhibitors are substrates for the multidrug efflux pumps of Pseudomonas aeruginosa“. In: *Antimicrobial agents and chemotherapy* 42.2, pp. 399–403.

Li, X.-Z., N. Barré, and K. Poole (2000). „Influence of the MexA-MexB-OprM multidrug efflux system on expression of the MexC-MexD-OprJ and MexE-MexF-OprN multidrug efflux systems in Pseudomonas aeruginosa“. In: *Journal of Antimicrobial Chemotherapy* 46.6, pp. 885–893.

Lister, P. D., D. J. Wolter, and N. D. Hanson (2009). „Antibacterial-resistant Pseudomonas aeruginosa: clinical impact and complex regulation of chromosomally encoded resistance mechanisms“. In: *Clinical microbiology reviews* 22.4, pp. 582–610.

Liu, Q. et al. (2015). „Influence of carbapenem resistance on mortality of patients with Pseudomonas aeruginosa infection: a meta-analysis“. In: *Scientific reports* 5.

Livermore, D. M. (2009). „Has the era of untreatable infections arrived?“ In: *Journal of Antimicrobial Chemotherapy* 64.suppl 1, pp. i29–i36.

Llamas, M. A. et al. (2006). „The heterologous siderophores ferrioxamine B and ferrichrome activate signaling pathways in Pseudomonas aeruginosa“. In: *Journal of bacteriology* 188.5, pp. 1882–1891.

Llamas, M. A. et al. (2008). „Characterization of five novel Pseudomonas aeruginosa cell-surface signalling systems“. In: *Molecular microbiology* 67.2, pp. 458–472.

Llamas, M. a. et al. (2014). „Cell-surface signaling in Pseudomonas: Stress responses, iron transport, and pathogenicity“. In: *FEMS Microbiology Reviews* 38, pp. 569–597.

Lopez-Medina, E. et al. (2015). „Candida albicans inhibits Pseudomonas aeruginosa virulence through suppression of pyochelin and pyoverdine biosynthesis“. In: *PLoS Pathog* 11.8, e1005129.

Luján, A. M., P. Gómez, and A. Buckling (2015). „Siderophore cooperation of the bacterium Pseudomonas fluorescens in soil“. In: *Biology letters* 11.2, p. 20140934.

Majka, G. et al. (2013). „A high-throughput method for the quantification of iron saturation in lactoferrin preparations“. In: *Analytical and bioanalytical chemistry* 405.15, pp. 5191–5200.

Marshall, B. et al. (2009). „Citrate-mediated iron uptake in Pseudomonas aeruginosa: involvement of the citrate-inducible FecA receptor and the FeoB ferrous iron transporter“. In: *Microbiology* 155.1, pp. 305–315.

Martin, L. W. et al. (2011). „Pseudomonas siderophores in the sputum of patients with cystic fibrosis“. In: *Biometals* 24.6, pp. 1059–1067.

Marvig, R. L. et al. (2014). „Within-host evolution of Pseudomonas aeruginosa reveals adaptation toward iron acquisition from hemoglobin“. In: *MBio* 5.3, e00966–14.

Masi, M. et al. (2013). „Structure, function and regulation of outer membrane proteins involved in drug transport in Enterobactericeae: the OmpF/C–TolC case“. In: *The open microbiology journal* 7.1.

Masuda, N. et al. (1996). „Quantitative correlation between susceptibility and OprJ production in NfxB mutants of Pseudomonas aeruginosa.“ In: *Antimicrobial agents and chemotherapy* 40.4, pp. 909–913.

Masuda, N. et al. (2000). „Contribution of the MexX-MexY-OprM efflux system to intrinsic resistance in Pseudomonas aeruginosa“. In: *Antimicrobial agents and chemotherapy* 44.9, pp. 2242–2246.

Masuda, N. et al. (2001). „Hypersusceptibility of the Pseudomonas aeruginosa nfxB mutant to β-lactams due to reduced expression of the AmpC β-lactamase“. In: *Antimicrobial agents and chemotherapy* 45.4, pp. 1284–1286.

Matsuo, Y. et al. (2004). „MexZ-mediated regulation of mexXY multidrug efflux pump expression in Pseudomonas aeruginosa by binding on the mexZ-mexX intergenic DNA“. In: *FEMS microbiology letters* 238.1, pp. 23–28.

McHugh, J. P. et al. (2003). „Global iron-dependent gene regulation in Escherichia coli: a new mechanism for iron homeostasis“. In: *Journal of Biological Chemistry*.

McMorran, B. J. et al. (2001). „Involvement of a transformylase enzyme in siderophore synthesis in Pseudomonas aeruginosa“. In: *Microbiology* 147.6, pp. 1517–1524.

McPhee, J. B. et al. (2009). „The major outer membrane protein OprG of Pseudomonas aeruginosa contributes to cytotoxicity and forms an anaerobically regulated, cation-selective channel“. In: *FEMS microbiology letters* 296.2, pp. 241–247.

McPherson, C. J. et al. (2012a). „Clinically relevant Gram-negative resistance mechanisms have no effect on the efficacy of MC-1, a novel siderophore-conjugated monocarbam“. In: *Antimicrobial agents and chemotherapy* 56.12, pp. 6334–6342.

McPherson, C. J. et al. (2012b). „Clinically relevant Gram-negative resistance mechanisms have no effect on the efficacy of MC-1, a novel siderophore-conjugated monocarbam". In: *Antimicrobial Agents and Chemotherapy* 56.12, pp. 6334–6342.

Mercier, K. A. et al. (2009). „Structure and function of Pseudomonas aeruginosa protein PA1324 (21–170)". In: *Protein Science* 18.3, pp. 606–618.

Mesaros, N. et al. (2007). „Pseudomonas aeruginosa: resistance and therapeutic options at the turn of the new millennium". In: *Clinical microbiology and infection* 13.6, pp. 560–578.

Mestas, J. and C. C. Hughes (2004). „Of mice and not men: differences between mouse and human immunology". In: *The Journal of Immunology* 172.5, pp. 2731–2738.

Meyer, J.-M. et al. (1996). „Pyoverdin is essential for virulence of Pseudomonas aeruginosa." In: *Infection and immunity* 64.2, pp. 518–523.

Meyer, J.-M. et al. (1997). „Use of siderophores to type pseudomonads: the three Pseudomonas aeruginosa pyoverdine systems". In: *Microbiology* 143.1, pp. 35–43.

Michéa-Hamzehpour, M. et al. (1997). „Characterization of MexE–MexF–OprN, a positively regulated multidrug efflux system of Pseudomonas aeruginosa". In: *Molecular microbiology* 23.2, pp. 345–354.

Miethke, M. and M. A. Marahiel (2007). „Siderophore-based iron acquisition and pathogen control". In: *Microbiology and Molecular Biology Reviews* 71.3, pp. 413–451.

Mikkelsen, H., R. McMullan, and A. Filloux (2011). „The Pseudomonas aeruginosa reference strain PA14 displays increased virulence due to a mutation in ladS". In: *PLoS One* 6.12, e29113.

Miller, M. A. et al. (2012). „Visualization of murine intranasal dosing efficiency using luminescent Francisella tularensis: effect of instillation volume and form of anesthesia". In: *PLoS One* 7.2, e31359.

Minandri, F. et al. (2016). „Role of iron uptake systems in Pseudomonas aeruginosa virulence and airway infection". In: *Infection and immunity* 84.8, pp. 2324–2335.

Mine, T. et al. (1999). „Expression in Escherichia coli of a new multidrug efflux pump, MexXY, from Pseudomonas aeruginosa". In: *Antimicrobial Agents and Chemotherapy* 43.2, pp. 415–417.

Mislin, G. L. a. and I. J. Schalk (2014). „Siderophore-dependent iron uptake systems as gates for antibiotic Trojan horse strategies against Pseudomonas aeruginosa." In: *Metallomics : integrated biometal science* 6.3, pp. 408–20.

Möllmann, U. et al. (2009). „Siderophores as drug delivery agents: application of the "Trojan Horse" strategy". In: *Biometals* 22.4, pp. 615–624.

Morita, Y. et al. (2001). „Construction of a series of mutants lacking all of the four major mex operons for multidrug efflux pumps or possessing each one of the operons from Pseudomonas aeruginosa PAO1: MexCD-OprJ is an inducible pump". In: *FEMS microbiology letters* 202.1, pp. 139–143.

Moriwaki, Y. et al. (2011). „Molecular basis of recognition of antibacterial porphyrins by heme-transporter IsdH-NEAT3 of Staphylococcus aureus“. In: *Biochemistry* 50.34, pp. 7311–7320.

Moynié, L. et al. (2017). „Structure and function of the PiuA and PirA siderophore-drug receptors from Pseudomonas aeruginosa and Acinetobacter baumannii“. In: *Antimicrobial Agents and Chemotherapy*, AAC–02531.

Muller, C., P. Plésiat, and K. Jeannot (2011). „A two-component regulatory system interconnects resistance to polymyxins, aminoglycosides, fluoroquinolones, and β-lactams in Pseudomonas aeruginosa“. In: *Antimicrobial agents and chemotherapy* 55.3, pp. 1211–1221.

Nadal-Jimenez, P. et al. (2014). „PvdP is a tyrosinase that drives maturation of the pyoverdine chromophore in Pseudomonas aeruginosa“. In: *Journal of bacteriology* 196.14, pp. 2681–2690.

Nairn, B. L. et al. (2017). „Fluorescence high-throughput screening for inhibitors of TonB action“. In: *Journal of Bacteriology*, JB–00889.

Nestorovich, E. M. et al. (2006). „Pseudomonas aeruginosa porin OprF properties of the channel“. In: *Journal of Biological Chemistry* 281.24, pp. 16230–16237.

Neumann, W., A. Gulati, and E. M. Nolan (2017). „Metal homeostasis in infectious disease: recent advances in bacterial metallophores and the human metal-withholding response“. In: *Current Opinion in Chemical Biology* 37, pp. 10–18.

Nguyen, A. T. et al. (2014). „Adaptation of iron homeostasis pathways by a Pseudomonas aeruginosa pyoverdine mutant in the cystic fibrosis lung“. In: *Journal of bacteriology* 196.12, pp. 2265–2276.

Nikaido, H. and R. Hancock (2012). „Outer membrane permeability of Pseudomonas aeruginosa“. In: *The bacteria* 10, pp. 145–93.

Nikel, P. I., E. Martínez-García, and V. De Lorenzo (2014). „Biotechnological domestication of pseudomonads using synthetic biology“. In: *Nature Reviews Microbiology* 12.5, pp. 368–379.

Njoroge, J. and V. Sperandio (2009). „Jamming bacterial communication: new approaches for the treatment of infectious diseases“. In: *EMBO molecular medicine* 1.4, pp. 201–210.

Noinaj, N. et al. (2010). „TonB-dependent transporters: regulation, structure, and function“. In: *Annual review of microbiology* 64, pp. 43–60.

Nolan, E. M. and C. T. Walsh (2008). „Investigations of the MceIJ-catalyzed posttranslational modification of the microcin E492 C-terminus: linkage of ribosomal and nonribosomal peptides to form “trojan horse” antibiotics“. In: *Biochemistry* 47.35, pp. 9289–9299.

Noma, M, M Noguchi, and E Tamaki (1971). „A new amino acid, nicotianamine, from tobacco leaves“. In: *Tetrahedron Letters* 12.22, pp. 2017–2020.

Obritsch, M. D. et al. (2005). „Nosocomial infections due to multidrug-resistant Pseudomonas aeruginosa: epidemiology and treatment options“. In: *Pharmacotherapy: The Journal of Human Pharmacology and Drug Therapy* 25.10, pp. 1353–1364.

Ochs, M. M. et al. (1999a). „Amino acid-mediated induction of the basic amino acid-specific outer membrane porin OprD from Pseudomonas aeruginosa“. In: *Journal of bacteriology* 181.17, pp. 5426–5432.

Ochs, M. M. et al. (1999b). „Negative regulation of the Pseudomonas aeruginosa outer membrane porin OprD selective for imipenem and basic amino acids“. In: *Antimicrobial agents and chemotherapy* 43.5, pp. 1085–1090.

Ochsner, U. A. and M. L. Vasil (1996). „Gene repression by the ferric uptake regulator in Pseudomonas aeruginosa: cycle selection of iron-regulated genes“. In: *Proceedings of the National Academy of Sciences* 93.9, pp. 4409–4414.

Ochsner, U. A., Z. Johnson, and M. L. Vasil (2000). „Genetics and regulation of two distinct haem-uptake systems, phu and has, in Pseudomonas aeruginosa“. In: *Microbiology* 146.1, pp. 185–198.

Ochsner, U. A. et al. (2002). „GeneChip® expression analysis of the iron starvation response in Pseudomonas aeruginosa: identification of novel pyoverdine biosynthesis genes“. In: *Molecular microbiology* 45.5, pp. 1277–1287.

Oglesby-Sherrouse, A. G. and M. L. Vasil (2010). „Characterization of a heme-regulated non-coding RNA encoded by the prrF locus of Pseudomonas aeruginosa“. In: *PLoS One* 5.4, e9930.

Olczak, T. et al. (2012). „Gallium (III), cobalt (III) and copper (II) protoporphyrin IX exhibit antimicrobial activity against Porphyromonas gingivalis by reducing planktonic and biofilm growth and invasion of host epithelial cells“. In: *Archives of microbiology* 194.8, pp. 719–724.

Olesky, M. et al. (2006). „Porin-mediated antibiotic resistance in Neisseria gonorrhoeae: ion, solute, and antibiotic permeation through PIB proteins with penB mutations“. In: *Journal of bacteriology* 188.7, pp. 2300–2308.

Ouidir, T. et al. (2015). „Proteomic profiling of lysine acetylation in Pseudomonas aeruginosa reveals the diversity of acetylated proteins“. In: *Proteomics* 15.13, pp. 2152–2157.

Page, M. G. (2013). „Siderophore conjugates“. In: *Annals of the New York Academy of Sciences* 1277.1, pp. 115–126.

Page, M. G., C. Dantier, and E. Desarbre (2010). „In vitro properties of BAL30072, a novel siderophore sulfactam with activity against multiresistant gram-negative bacilli“. In: *Antimicrobial agents and chemotherapy* 54.6, pp. 2291–2302.

Palmer, K. L. et al. (2005). „Cystic fibrosis sputum supports growth and cues key aspects of Pseudomonas aeruginosa physiology“. In: *Journal of bacteriology* 187.15, pp. 5267–5277.

Parrow, N. L., R. E. Fleming, and M. F. Minnick (2013). „Sequestration and scavenging of iron in infection“. In: *Infection and immunity* 81.10, pp. 3503–3514.

Paulen, A. et al. (2015). „Synthesis and antibiotic activity of oxazolidinone–catechol conjugates against Pseudomonas aeruginosa“. In: *Org. Biomol. Chem.* 13.47, pp. 11567–11579.

Pederick, V. G. et al. (2015). „ZnuA and zinc homeostasis in Pseudomonas aeruginosa“. In: *Scientific reports* 5, p. 13139.

Peng, J. et al. (2017). „Pseudomonas aeruginosa develops Ciprofloxacin resistance from low to high level with distinctive proteome changes“. In: *Journal of Proteomics* 152, pp. 75–87.

Perron, K. et al. (2004). „CzcR-CzcS, a two-component system involved in heavy metal and carbapenem resistance in Pseudomonas aeruginosa“. In: *Journal of Biological Chemistry* 279.10, pp. 8761–8768.

Peterson, A. C. et al. (2012). „Parallel reaction monitoring for high resolution and high mass accuracy quantitative, targeted proteomics“. In: *Molecular & Cellular Proteomics* 11.11, pp. 1475–1488.

Pirnay, J.-P. et al. (2002). „Analysis of the Pseudomonas aeruginosa oprD gene from clinical and environmental isolates“. In: *Environmental microbiology* 4.12, pp. 872–882.

Pishchany, G. and E. P. Skaar (2012). „Taste for blood: hemoglobin as a nutrient source for pathogens“. In: *PLoS Pathog* 8.3, e1002535.

Poole, K. (2002). „Outer membranes and efflux: the path to multidrug resistance in Gram-negative bacteria“. In: *Current pharmaceutical biotechnology* 3.2, pp. 77–98.

– (2007). „Efflux pumps as antimicrobial resistance mechanisms“. In: *Annals of medicine* 39.3, pp. 162–176.

Poole, K. and R. Srikumar (2001). „Multidrug efflux in Pseudomonas aeruginosa components, mechanisms and clinical significance“. In: *Current topics in medicinal chemistry* 1.1, pp. 59–71.

Poole, K., D. E. Heinrichs, and S. Neshat (1993). „Cloning and sequence analysis of an EnvCD homologue in Pseudomonas aeruginosa: regulation by iron and possible involvement in the secretion of the siderophore pyoverdine“. In: *Molecular microbiology* 10.3, pp. 529–544.

Poole, K. et al. (1996). „Overexpression of the mexC–mexD–oprJ efflux operon in nfxB-type multidrug-resistant strains of Pseudomonas aeruginosa“. In: *Molecular microbiology* 21.4, pp. 713–725.

Poras, H. et al. (1998). „Synthesis and in vitro antibacterial activity of catechol-spiramycin conjugates“. In: *The Journal of antibiotics* 51.8, pp. 786–794.

Priebe, G. P. and J. B. Goldberg (2014). „Vaccines for Pseudomonas aeruginosa: a long and winding road“. In: *Expert review of vaccines* 13.4, pp. 507–519.

Psychogios, N. et al. (2011). „The human serum metabolome“. In: *PloS one* 6.2, e16957.

Puzari, M. and P. Chetia (2017). „RND efflux pump mediated antibiotic resistance in Gram-negative bacteria Escherichia coli and Pseudomonas aeruginosa: a major issue worldwide“. In: *World Journal of Microbiology and Biotechnology* 33.2, p. 24.

Quintero-Gutiérrez, A. G. et al. (2008). „Bioavailability of heme iron in biscuit filling using piglets as an animal model for humans“. In: *Int J Biol Sci* 4.1, pp. 58–62.

Rahme, L. G. et al. (1995). „Common virulence factors for bacterial pathogenicity in plants and animals“. In: *Science* 268.5219, p. 1899.

Rahme, L. G. et al. (2000). „Plants and animals share functionally common bacterial virulence factors“. In: *Proceedings of the National Academy of Sciences* 97.16, pp. 8815–8821.

Rawling, E. G., F. S. Brinkman, and R. E. Hancock (1998). „Roles of the carboxy-terminal half of Pseudomonas aeruginosa major outer membrane protein OprF in cell shape, growth in low-osmolarity medium, and peptidoglycan association“. In: *Journal of bacteriology* 180.14, pp. 3556–3562.

Raymond, K. N., E. A. Dertz, and S. S. Kim (2003). „Enterobactin: an archetype for microbial iron transport“. In: *Proceedings of the National Academy of Sciences* 100.7, pp. 3584–3588.

Reales-Calderón, J. A. et al. (2015). „Quantitative proteomics unravels that the post-transcriptional regulator Crc modulates the generation of vesicles and secreted virulence determinants of Pseudomonas aeruginosa“. In: *Journal of proteomics* 127, pp. 352–364.

Reimmann, C. (2012). „Inner-membrane transporters for the siderophores pyochelin in Pseudomonas aeruginosa and enantio-pyochelin in Pseudomonas fluorescens display different enantioselectivities“. In: *Microbiology* 158.5, pp. 1317–1324.

Rice, L. B. (2008). „Federal funding for the study of antimicrobial resistance in nosocomial pathogens: no ESKAPE“. In: *Journal of Infectious Diseases* 197.8, pp. 1079–1081.

Ringel, M. T., G. Dräger, and T. Brüser (2016). „PvdN Enzyme Catalyzes a Periplasmic Pyoverdine Modification“. In: *Journal of Biological Chemistry* 291.46, pp. 23929–23938.

Rosenberg, E. Y. et al. (2003). „Bile salts and fatty acids induce the expression of Escherichia coli AcrAB multidrug efflux pump through their interaction with Rob regulatory protein“. In: *Molecular microbiology* 48.6, pp. 1609–1619.

Ruiz, J. (2003). „Mechanisms of resistance to quinolones: target alterations, decreased accumulation and DNA gyrase protection“. In: *Journal of Antimicrobial Chemotherapy* 51.5, pp. 1109–1117.

Sabharwal, N. et al. (2014). „Molecular detection of virulence genes as markers in Pseudomonas aeruginosa isolated from urinary tract infections“. In: *International journal of molecular epidemiology and genetics* 5.3, p. 125.

Sakyo, S. et al. (2006). „Potency of carbapenems for the prevention of carbapenem-resistant mutants of Pseudomonas aeruginosa“. In: *J Antibiot* 59.4, pp. 220–8.

Schalk, I. J. and O. Cunrath (2016). „An overview of the biological metal uptake pathways in Pseudomonas aeruginosa“. In: *Environmental Microbiology* 18.10, pp. 3227–3246.

Schalk, I. J. and L. Guillon (2013). „Pyoverdine biosynthesis and secretion in Pseudomonas aeruginosa: Implications for metal homeostasis“. In: *Environmental Microbiology* 15.6, pp. 1661–1673.

Schalk, I. J. et al. (1999). „Copurification of the FpvA ferric pyoverdin receptor of Pseudomonas aeruginosa with its iron-free ligand: implications for siderophore-mediated iron transport“. In: *Biochemistry* 38.29, pp. 9357–9365.

Schalk, I. J., M. A. Abdallah, and F. Pattus (2002). „Recycling of pyoverdin on the FpvA receptor after ferric pyoverdin uptake and dissociation in Pseudomonas aeruginosa“. In: *Biochemistry* 41.5, pp. 1663–1671.

Schalk, I. J., W. W. Yue, and S. K. Buchanan (2004). „Recognition of iron-free siderophores by TonB-dependent iron transporters“. In: *Molecular microbiology* 54.1, pp. 14–22.

Schalk, I. J., M. Hannauer, and A. Braud (2011). „New roles for bacterial siderophores in metal transport and tolerance“. In: *Environmental microbiology* 13.11, pp. 2844–2854.

Schauer, K., D. A. Rodionov, and H. de Reuse (2008). „New substrates for TonB-dependent transport: do we only see the ‘tip of the iceberg’?“ In: *Trends in biochemical sciences* 33.7, pp. 330–338.

Schmitt, T. H., W. Frezzatti, and S. Schreier (1993). „Hemin-induced lipid membrane disorder and increased permeability: a molecular model for the mechanism of cell lysis“. In: *Archives of Biochemistry and Biophysics* 307.1, pp. 96–103.

Schulz, S. et al. (2015). „Elucidation of sigma factor-associated networks in Pseudomonas aeruginosa reveals a modular architecture with limited and function-specific crosstalk“. In: *PLoS Pathog* 11.3, e1004744.

Schulz, S. et al. (2012). „Metalloporphyrins–an update“. In: *The role of bile pigments in health and disease: effects on cell signaling, cytotoxicity and cytoprotection*, p. 95.

Schweizer, H. P. (2003). „Efflux as a mechanism of resistance to antimicrobials in Pseudomonas aeruginosa and related bacteria: unanswered questions“. In: *Genet Mol Res* 2.1, pp. 48–62.

Serino, L. et al. (1995). „Structural genes for salicylate biosynthesis from chorismate in Pseudomonas aeruginosa“. In: *Molecular and General Genetics MGG* 249.2, pp. 217–228.

Serino, L. et al. (1997). „Biosynthesis of pyochelin and dihydroaeruginoic acid requires the iron-regulated pchDCBA operon in Pseudomonas aeruginosa.“ In: *Journal of bacteriology* 179.1, pp. 248–257.

Seyedmohammad, S. et al. (2016). „Structural model of FeoB, the iron transporter from Pseudomonas aeruginosa, predicts a cysteine lined, GTP-gated pore“. In: *Bioscience reports* 36.2, e00322.

Shi, T. et al. (2012). „Advancing the sensitivity of selected reaction monitoring-based targeted quantitative proteomics“. In: *Proteomics* 12.8, pp. 1074–1092.

Shi, T. et al. (2016). „Advances in targeted proteomics and applications to biomedical research“. In: *Proteomics* 16.15-16, pp. 2160–2182.

Skaar, E. P. (2010). „The battle for iron between bacterial pathogens and their vertebrate hosts“. In: *PLoS Pathog* 6.8, e1000949.

Skurnik, D. et al. (2013). „A comprehensive analysis of in vitro and in vivo genetic fitness of Pseudomonas aeruginosa using high-throughput sequencing of transposon libraries“. In: *PLoS Pathog* 9.9, e1003582.

Smith, A. D. and A. Wilks (2015). „Differential contributions of the outer membrane receptors PhuR and HasR to heme acquisition in Pseudomonas aeruginosa“. In: *Journal of Biological Chemistry* 290.12, pp. 7756–7766.

Smith, E. E. et al. (2006). „Genetic adaptation by Pseudomonas aeruginosa to the airways of cystic fibrosis patients“. In: *Proceedings of the National Academy of Sciences* 103.22, pp. 8487–8492.

Sokol, P. A. and D. E. Woods (1988). „Effect of pyochelin on Pseudomonas cepacia respiratory infections“. In: *Microbial pathogenesis* 5.3, pp. 197–205.

Son, M. S. et al. (2007). „In vivo evidence of Pseudomonas aeruginosa nutrient acquisition and pathogenesis in the lungs of cystic fibrosis patients“. In: *Infection and immunity* 75.11, pp. 5313–5324.

Soufi, Y. and B. Soufi (2016). „Mass spectrometry-based bacterial proteomics: focus on dermatologic microbial pathogens“. In: *Frontiers in microbiology* 7.

Srikumar, R. et al. (1998). „Expression of Pseudomonas aeruginosaMultidrug Efflux Pumps MexA-MexB-OprM and MexC-MexD-OprJ in a Multidrug-Sensitive Escherichia coli Strain“. In: *Antimicrobial agents and chemotherapy* 42.1, pp. 65–71.

Stephan, U. W. et al. (1996). „The nicotianamine molecule is made-to-measure for complexation of metal micronutrients in plants“. In: *Biometals* 9.1, pp. 84–90.

Stojiljkovic, I and K Hantke (1992). „Hemin uptake system of Yersinia enterocolitica: similarities with other TonB-dependent systems in gram-negative bacteria.“ In: *The EMBO journal* 11.12, p. 4359.

Stojiljkovic, I., V. Kumar, and N. Srinivasan (1999). „Non-iron metalloporphyrins: potent antibacterial compounds that exploit haem/Hb uptake systems of pathogenic bacteria“. In: *Molecular microbiology* 31.2, pp. 429–442.

Stover, C. et al. (2000). „Complete genome sequence of Pseudomonas aeruginosa PAO1, an opportunistic pathogen“. In: *Nature* 406.6799, pp. 959–964.

Sugawara, E. et al. (2006). „Pseudomonas aeruginosa porin OprF exists in two different conformations“. In: *Journal of Biological Chemistry* 281.24, pp. 16220–16229.

Sun, J., Z. Deng, and A. Yan (2014). „Bacterial multidrug efflux pumps: mechanisms, physiology and pharmacological exploitations“. In: *Biochemical and biophysical research communications* 453.2, pp. 254–267.

Takase, H. et al. (2000a). „Impact of Siderophore Production on Pseudomonas aeruginosa Infections in Immunosuppressed Mice“. In: *Infection and immunity* 68.4, pp. 1834–1839.

– (2000b). „Requirement of the Pseudomonas aeruginosa tonB gene for high-affinity iron acquisition and infection“. In: *Infection and immunity* 68.8, pp. 4498–4504.

Tamber, S. and R. E. Hancock (2006). „Involvement of two related porins, OprD and OpdP, in the uptake of arginine by Pseudomonas aeruginosa“. In: *FEMS microbiology letters* 260.1, pp. 23–29.

Tängdén, T. (2014). „Combination antibiotic therapy for multidrug-resistant Gram-negative bacteria“. In: *Upsala journal of medical sciences* 119.2, pp. 149–153.

Thomas, S. N. et al. (2015). „Multiplexed targeted mass spectrometry-based assays for the quantification of N-linked glycosite-containing peptides in serum“. In: *Analytical chemistry* 87.21, pp. 10830–10838.

Thomas, X. et al. (2004). „Siderophore peptide, a new type of post-translationally modified antibacterial peptide with potent activity“. In: *Journal of Biological Chemistry* 279.27, pp. 28233–28242.

Tiburzi, F., F. Imperi, and P. Visca (2008). „Intracellular levels and activity of PvdS, the major iron starvation sigma factor of Pseudomonas aeruginosa“. In: *Molecular microbiology* 67.1, pp. 213–227.

Tillotson, G. S. (2016). „Trojan Horse Antibiotics—A Novel Way to Circumvent Gram-Negative Bacterial Resistance?“ In: *Infectious diseases* 9, p. 45.

Tomaras, A. P. et al. (2013). „Adaptation-based resistance to siderophore-conjugated antibacterial agents by Pseudomonas aeruginosa“. In: *Antimicrobial Agents and Chemotherapy*.

Tong, Y. and M. Guo (2007). „Cloning and characterization of a novel periplasmic heme-transport protein from the human pathogen Pseudomonas aeruginosa“. In: *JBIC Journal of Biological Inorganic Chemistry* 12.6, pp. 735–750.

– (2009). „Bacterial heme-transport proteins and their heme-coordination modes“. In: *Archives of biochemistry and biophysics* 481.1, pp. 1–15.

Touw, D. S., D. R. Patel, and B. Van Den Berg (2010). „The crystal structure of OprG from Pseudomonas aeruginosa, a potential channel for transport of hydrophobic molecules across the outer membrane“. In: *PLoS One* 5.11, e15016.

Toyofuku, M. et al. (2012). „Identification of proteins associated with the Pseudomonas aeruginosa biofilm extracellular matrix“. In: *Journal of proteome research* 11.10, pp. 4906–4915.

Trias, J and H Nikaido (1990a). „Outer membrane protein D2 catalyzes facilitated diffusion of carbapenems and penems through the outer membrane of Pseudomonas aeruginosa.“ In: *Antimicrobial Agents and Chemotherapy* 34.1, pp. 52–57.

– (1990b). „Protein D2 channel of the Pseudomonas aeruginosa outer membrane has a binding site for basic amino acids and peptides.“ In: *Journal of Biological Chemistry* 265.26, pp. 15680–15684.

Tsuji, A. et al. (1982). „The Effects of Temperature and pH on the Growth of Eight Enteric and Nine Glucose Non-Fermenting Species of Gram-Negative Rods“. In: *Microbiology and immunology* 26.1, pp. 15–24.

Tsukiura, H et al. (1964). „Danomycin, a new antibiotic.“ In: *The Journal of antibiotics* 17, p. 39.

Turner, K. H. et al. (2014). „Requirements for Pseudomonas aeruginosa acute burn and chronic surgical wound infection“. In: *PLoS Genet* 10.7, e1004518.

Tyrrell, J. and M. Callaghan (2016). „Iron acquisition in the cystic fibrosis lung and potential for novel therapeutic strategies“. In: *Microbiology* 162.2, pp. 191–205.

Usuda, K. et al. (2009). „Genetically engineered rice containing larger amounts of nicotianamine to enhance the antihypertensive effect“. In: *Plant biotechnology journal* 7.1, pp. 87–95.

Van Delden, C., M. G. Page, and T. Köhler (2013). „Involvement of Fe uptake systems and AmpC β-lactamase in susceptibility to the siderophore monosulfactam BAL30072 in Pseudomonas aeruginosa“. In: *Antimicrobial agents and chemotherapy* 57.5, pp. 2095–2102.

Van Der Plas, M. J. et al. (2016). „Pseudomonas aeruginosa elastase cleaves a C-terminal peptide from human thrombin that inhibits host inflammatory responses“. In: *Nature communications* 7.

Vandenende, C. S., M. Vlasschaert, and S. Y. Seah (2004). „Functional characterization of an aminotransferase required for pyoverdine siderophore biosynthesis in Pseudomonas aeruginosa PAO1“. In: *Journal of bacteriology* 186.17, pp. 5596–5602.

Venter, H. et al. (2015). „RND-type drug efflux pumps from Gram-negative bacteria: Molecular mechanism and inhibition“. In: *Frontiers in Microbiology* 6.APR, pp. 1–11.

Vértesy, L. et al. (1995). „Salmycin A–D, Antibiotika aus Streptomyces violaceus, DSM 8286, mit Siderophor-Aminoglycosid-Struktur“. In: *Helvetica Chimica Acta* 78.1, pp. 46–60.

Visca, P., F. Imperi, and I. L. Lamont (2007). „Pyoverdine siderophores: from biogenesis to biosignificance“. In: *Trends in microbiology* 15.1, pp. 22–30.

Visser, M. et al. (2004). „Importance of the ornibactin and pyochelin siderophore transport systems in Burkholderia cenocepacia lung infections“. In: *Infection and immunity* 72.5, pp. 2850–2857.

Walker, E. L. and B. M. Waters (2011). „The role of transition metal homeostasis in plant seed development“. In: *Current opinion in plant biology* 14.3, pp. 318–324.

Walsh, C. T. et al. (1990). „Molecular studies on enzymes in chorismate metabolism and the enterobactin biosynthetic pathway“. In: *Chemical Reviews* 90.7, pp. 1105–1129.

Wandersman, C. and I. Stojiljkovic (2000). „Bacterial heme sources: the role of heme, hemoprotein receptors and hemophores“. In: *Current opinion in microbiology* 3.2, pp. 215–220.

Wang, Y. et al. (2011). „Phenazine-1-carboxylic acid promotes bacterial biofilm development via ferrous iron acquisition“. In: *Journal of bacteriology* 193.14, pp. 3606–3617.

Welte, W. et al. (1995). „Structure and function of the porin channel“. In: *Kidney international* 48.4, pp. 930–940.

Westritschnig, K. et al. (2014). „A randomized, placebo-controlled phase I study assessing the safety and immunogenicity of a Pseudomonas aeruginosa hybrid outer membrane protein OprF/I vaccine (IC43) in healthy volunteers“. In: *Human vaccines & immunotherapeutics* 10.1, pp. 170–183.

Whiteside, S. A. et al. (2015). „The microbiome of the urinary tract [mdash] a role beyond infection“. In: *Nature Reviews Urology* 12.2, pp. 81–90.

WICKSTRÖM, C. et al. (1998). „MUC5B is a major gel-forming, oligomeric mucin from human salivary gland, respiratory tract and endocervix: identification of glycoforms and C-terminal cleavage“. In: *Biochemical Journal* 334.3, pp. 685–693.

Wiehlmann, L. et al. (2007). „Population structure of Pseudomonas aeruginosa“. In: *Proceedings of the National Academy of Sciences* 104.19, pp. 8101–8106.

Winsor, G. L. et al. (2016). „Enhanced annotations and features for comparing thousands of Pseudomonas genomes in the Pseudomonas genome database“. In: *Nucleic acids research* 44.D1, pp. D646–D653.

Wirén, N. von et al. (1999). „Nicotianamine chelates both FeIII and FeII. Implications for metal transport in plants“. In: *Plant Physiology* 119.3, pp. 1107–1114.

Wolter, D. (2008a). „Discordance Between Imipenem (IPM) Resistance and oprD Expression in a Pseudomonas aeruginosa (PA) Overexpressing mexEF-oprN (EFN)“. In: *46th Annual Meeting*. Idsa.

– (2008b). „MexT-Associated Downregulation of oprD in Pseudomonas aeruginosa (PA) Involves Inhibition of Transcription Initiation“. In: *46th Annual Meeting*. Idsa.

Wolter, D. J., N. D. Hanson, and P. D. Lister (2004). „Insertional inactivation of oprD in clinical isolates of Pseudomonas aeruginosa leading to carbapenem resistance“. In: *FEMS microbiology letters* 236.1, pp. 137–143.

– (2005). „AmpC and OprD are not involved in the mechanism of imipenem hypersusceptibility among Pseudomonas aeruginosa isolates overexpressing the mexCD-oprJ efflux pump“. In: *Antimicrobial agents and chemotherapy* 49.11, pp. 4763–4766.

Wolz, C. et al. (1994). „Iron release from transferrin by pyoverdin and elastase from Pseudomonas aeruginosa.“ In: *Infection and immunity* 62.9, pp. 4021–4027.

Worlitzsch, D. et al. (2002). „Effects of reduced mucus oxygen concentration in airway Pseudomonas infections of cystic fibrosis patients“. In: *The Journal of clinical investigation* 109.3, pp. 317–325.

Wurtzel, O. et al. (2012). „The single-nucleotide resolution transcriptome of Pseudomonas aeruginosa grown in body temperature“. In: *Plos pathog* 8.9, e1002945.

Xiao, R. and W. S. Kisaalita (1997). „Iron acquisition from transferrin and lactoferrin by Pseudomonas aeruginosa pyoverdin“. In: *Microbiology* 143.7, pp. 2509–2515.

Yeterian, E. et al. (2010a). „An efflux pump is required for siderophore recycling by Pseudomonas aeruginosa“. In: *Environmental microbiology reports* 2.3, pp. 412–418.

Yeterian, E. et al. (2010b). „Synthesis of the siderophore pyoverdine in Pseudomonas aeruginosa involves a periplasmic maturation“. In: *Amino acids* 38.5, pp. 1447–1459.

Yoneyama, H. and T. Nakae (1996). „Protein C (OprC) of the outer membrane of Pseudomonas aeruginosa is a copper-regulated channel protein“. In: *Microbiology* 142.8, pp. 2137–2144.

Yoon, S. S. et al. (2002). „Pseudomonas aeruginosa anaerobic respiration in biofilms: relationships to cystic fibrosis pathogenesis“. In: *Developmental cell* 3.4, pp. 593–603.

Zhou, M.-L. et al. (2013). „Nicotianamine synthase gene family as central components in heavy metal and phytohormone response in maize“. In: *Functional & integrative genomics* 13.2, pp. 229–239.

Webpage

BD (2017). *223050 Casamino Acids BD*. URL: http://www.bd.com/ds/productCenter/223050.asp (visited on Mar. 27, 2017).

PAMELA SAINT AUGUSTE

French ● June 9th, 1990
3 Allée Louis Cristin ● 1196 Gland ● Switzerland
+41(0)79 192 38 59 ● pamela.stauguste@gmail.com
www.linkedin.com/in/pamela-saintauguste

Enthusiastic researcher with an EPF training in Chemistry and Infectious Diseases, I benefit from a wide international experience in public speaking and visual communication. I'm a creative team player with experience in leadership and medical affairs gathered during my current position at Procter and Gamble. Stepping out of my comfort zone doesn't scare me.

PROFESSIONAL EXPERIENCE

Medical & Technical Affairs Europe Leader – Procter and Gamble Since Apr 2017
Cold and Flu category - Personal Healthcare International *Geneva, CH*

- Claims substantiation assessment based on internal and external scientific literature
- Key Opinion Leaders Strategy development and execution;
- Regional and local claim/copy clearance process owner and trainer

Research Assistant – Infection Biology, Prof. Bumann – Biozentrum 2013-2017
European Innovative Medicine Initiatives, New Drugs 4 Bad Bugs, Translocation *Basel, CH*
Goal: Investigate the functions of *P. aeruginosa* active transporters during rodent/human infections

- Optimization of several strategies for gene deletion, mouse infection model and proteomics;
- Establishment of collaborations with industrial partners and European groups within IMI consortium;
- Development of strong conceptual and oral communication skills at international conferences;
- Supervision of a master project on the *in vitro* characterization of *P. aeruginosa* active transporters.

Junior Research Assistant – Intern in Drug Development – Merck KGaA Sep - Mar 2013
Physico-chemical characterization of solid-states group, Alex Becker *Darmstadt, DE*
Goal: Assessed in-silico approaches for better anti-cancer drug design

- Assessment of different software to optimize in silico screening of potential API co-crystals;
- Improvement in-house drug development pipeline by implementing the best in-silico solutions.

Trainee in System Biology – EPFL Jan - Aug 2012
Laboratory of Computational Systems Biotechnology, Prof. Hatzimanikatis *Lausanne, CH*
Goal: Explored of sugar and lipid metabolism by exploiting the in-house algorithm BNICE

- Semester project grade: 6/6, extended by trainee position;
- Utilization of in-house algorithm to predict metabolic reactions in *E. Coli*;
- Construction of metabolic network in *E. Coli*, focus on sugar and lipid metabolisms.

EDUCATION

PhD in Microbiology – Infection Biology, Biozentrum 2017
Basel, CH

MCC Summer Academy: Business beyond borders – Mathias Corvinus Collegium 2016
Business in International Relations, International Strategic Management and Marketing *Budapest, HU*

Master in Molecular and Biological Chemistry – EPFL 2013
Specialization in Computational chemistry *Lausanne, CH*
Grenier Prize for best EPFL master thesis

Bachelor in Chemistry and Chemical Engineering – EPFL 2011
Specialization in Computational chemistry *Lausanne, CH*

Prize and Honors

Selected candidate for **Keep-in-Touch Program** – by **McKinsey & Company** 2016
Selected candidate for **Novartis International Biocamp** – by **Novartis** 2016
European TRANSLOCATION for four years PhD project – **IMI, New Drug 4 Bad Bugs** 2013
Grenier Prize for Best EPFL Master Thesis – **EPFL, Fondation William Grenier** 2013

Extracurricular Activities

Marketing and Public Relations co-chair – Healthcare Business Women's Association (HBA) 2016

- Lead and implement Basel HBA marketing and communication efforts;
- Provide recommendations and insights on the overall marketing and communications strategy;
- Liaise with HBA EU Director of Marketing and PR to align on strategies, objectives and tactics as well as share best practices.

Manager of Microbiology Blockkurs week – Biozentrum 2015-2016

- Team management (10 supervisors and 30-45 students);
- Course planning: fitting 4 experiments in a week;
- Creating the script of the course: from design to edition;
- Student evaluation: >95% satisfied. Rated as 2nd best Blockkurs week, two times in a raw.

Organizing Committee President Global Village 2016 – AIESEC Basel Fall 2015

- Team leader of newly created Project department at AIESEC Basel;
- Team management (5 persons);
- Event conception and initiation: Global Village to promote intercultural exchange at Basel University.

Manager of Academic Matters at ADEC, Association of Chemistry EPFL Students 2011-2012

- Guidance on undergraduate administration;
- Mediator between chemistry department and students.

Student Representative at the Basic Sciences Faculty Board, EPFL 2011-2012

- Advice and voting on strategic faculty decisions;
- Mediator between Basic sciences faculty and students.

Head of Entertainment and Sports at AGEPoly, General Association of EPFL Students 2010-2012

- Part of AGEPoly Board: frequent meeting with ETH Board, industrial partners and students;
- Team management (20 persons): mobilise and motivate people to help along the year;
- Event management: 5 external parties, 3 on-campus events. Budget from 1K-50K CHF per event;
- Leading recruitment campaign for new team members;
- Creating event promotion materials (event logo, posters and flyers).

Professional Training in Communication

Conflict Management workshop 2016
3 Oral and Visual Communication courses 2014-2016
Tutor and teaching assistant for several courses in Chemistry and Biology at university level 2012-2016
Details on request.

Additional Skills

Languages

- **French** (Native),
- **English** (Fluent C2),
- **German** (Basic A2),
- Spanish (Basic A1),
- Tamil (Conversational)

Computer skills

- Adobe Illustrator
- Latex
- HTML
- R

Personal interests

- Strong passion for design of visual communication materials: participation in online logo/posters/flyers design contests.
- Enjoy travelling around the world to experience different cultures, food and challenges